Structural studies of bk and jc polyomaviruses interactions with their receptors

Marie Sorin

THESE DE DOCTORAT DE

NANTES UNIVERSITE
EBERHARD KARLS UNIVERSITÄT TÜBINGEN

ECOLE DOCTORALE N° 605
Biologie Santé
Spécialité : Virologie, Biochimie

Par
Marie SORIN

STRUCTURAL STUDIES OF BK AND JC POLYOMAVIRUS INTERACTIONS WITH THEIR RECEPTORS

Thèse présentée et soutenue à Nantes, le 15.09.2022
Unités de recherche :
Center for Research in Transplantation and Translational Immunology – UMR1064, Nantes Université
Interfakultäres Institut für Biochemie, Eberhard Karls Universität Tübingen

Rapporteurs avant soutenance :

Ute KRENGEL	Professeur – University of Oslo
Marija BACKOVIC	Chargée de recherche, HDR – Institut Pasteur, Paris

Composition du Jury :

Président :	Antoine TOUZE	Professeur – Université de Tours
Examinateurs :	Ute KRENGEL	Professeur – University of Oslo
	Marija BACKOVIC	Chargée de recherche, HDR – Institut Pasteur, Paris
	Morgane SOLIS.	Maître de conférences des universités & Praticien Hospitalier – Hôpitaux de Strasbourg, Université de Strasbourg
	Antoine TOUZE	Professeur – Université de Tours
Dir. de thèse :	Dorian MCILROY	Maître de conférences des universités, HDR – Nantes Université
Co-dir. de thèse :	Thilo STEHLE	Professeur - Eberhard Karls Universität Tübingen

Acknowledgments

First, I would like to sincerely thank my PhD defense committee: Prof. Ute Krengel, Dr. Marija Backovic, Prof. Antoine Touze and Dr. Morgane Solis for accepting to read and evaluate my work as well as being present for my PhD defense.

I also want to thank again Prof. Antoine Touze but also Dr. Cyrille Grandjean for following my work during the past 3 years, as part of my thesis committee members and for your advices and suggestions.

I moslty enjoyed my time as a PhD student. The past 3 years were exciting but also quite challenging, especially when you do a co-supervised PhD in two different countries during a pandemic!
But I absolutely do no regrets that choice and I am very happy and grateful that I was able to do my PhD like that: in between two labs, with two supervisors and in between two countries. I was able to gain a lot of professional and personal experiences.

Thus, I would like to thank first Dr. Dorian McIlroy. I am very grateful to have you as one of my supervisors. It started by a short internship in first year of master's degree and then it was "do you want to go to Germany for your second-year master's degree internship?". Thank you for trusting me and believing that I would be able to learn structural biology and work on this amazing project that became my main PhD project and a publication. I am very grateful for your guidance during those 3 and more years. I really learn a lot from you whether it was about experimental techniques or about how to communicate my work. I will try to remember all of your advises and tips for the future.
I am also very grateful toward Prof. Thilo Stehle for being my other supervisor. Thank you for accepting me in your lab for my master's degree internship even though I had no structural biology background. I was able to learn so much during this internship and I still learnt a lot during my PhD. So, thank you for your trust and your guidance during those years.
Both Dorian and Thilo have always been available when I needed their support and guidance, and I am very grateful for that because juggling between one place to another was not always easy for me but also for them.

I would like to thank also, for their work and involvement in the different projects, our collaborators at Glycoscience Laboratory, Imperial College, for the glycan array screening, at Université de Lilles, for the mass spectroscopy, from the Service d'Anatomie et Cytologie Pathologie of CHU Nantes, for the biopsies and the plateform IMPACT for the SPR measurements.

Thank you to Team 1 of CR2TI for listening, giving feedbacks and advises after my presentations. A special thanks to the Viro team: Khanh, Eléa, Cécile, Flora, Louise,

Simon, Frank, and Céline for being very supportive and for the interesting discussions about my work during our meetings.
In this team, I want to deliver a special thanks to both Cécile and Flora for being amazing supporters of my work. Thank you for listening to my worries and doubts, for being encouraging, sharing your great mood and for the other personal talks we had during those years!
A final thanks to Khanh who helped me a lot during those years and was always ready to show me something or answer my questions!

Thank you to the Stehle's team of the IFIB for also being very helpful and for their advises during my time in the lab. Thank you for welcoming me when you had no idea who I was and what I was doing here. I ended up staying a bit more than 5 months! Thanks also for putting up with my inability to speak German.
Special thanks to the Polyomavirus gang: Nils, Jasmine, Niklas and Christina for their help and nice discussions.
But also, Aleks who was the only non-German when I started and who became a great friend!
I am grateful to Georg, who with Thilo allowed me to participate in X-ray crystallography lectures and thought me about it.

During my multiple stays in Germany, I always managed to go back to the same WG and I was very grateful for that. So big thanks to my roommates: Rebecca, Martina, Nathanael, Anne, Christopher, Sören, Lara and Julian. I had great times there despite the pandemic. I enjoyed our cooking night, our game night and all the nice stuff we did together!
Special thanks to Rebecca who accepted me in this WG 3 years ago!

J'aimerais particulièrement remercier cette team d'amis : étudiants en master qui ont fini thésards au CR2TI : Céline, Sita, Florian et Thomas, et qui a su rendre ses journées de thèse plus agréables que ce soit via leur aide pour des manips ou autres, via les pauses déjeuners ou goûters et les nombreuses activités hors labo !

Merci aussi à Maissa, Ella, Bérangère, Anaïs, Eléa et tous ceux avec qui j'ai pu partager le bureau. Merci pour les discussions plus qu'intéressantes qu'elles aient pu être scientifiques ou non. Merci pour ce rituel de goûter et la bonne ambiance !

Merci au gang des hippocampes : Camille, Eléonore et Séverine, des amies de longues dates maintenant qui, malgré les différents chemins que nous ayons pris depuis le lycée, m'ont toujours soutenu !

Merci aussi à Cy, Blob et Marine pour leur soutien : après avoir survécu à la prépa, qui l'eut cru, j'ai survécu à une thèse ! En particulier, merci à Cy, ça me manquera ce

partage constant de nos aventures et anecdotes de PhD au quotidien. J'espère que ça continuera en postdoc ;)

Pour finir, j'aimerais bien sûr remercier ma famille pour leur soutien constant. Merci Papa, qui tente encore de comprendre ce que je fais malgré tous ces chiffres et abréviations. Merci à Maman qui m'a toujours poussé à faire les études que je voulais pour faire un métier que j'aime ! Merci à Élisa d'avoir supporté cette période intense de ma vie, même si je t'ai laissé des périodes de répits pendant mes séjours en Allemagne ;) et bien sûr merci au best baby bro, Baptiste ! Merci aussi aux autres membres de ma famille qui m'ont toujours montré leur soutien et leur intérêt pour ce que je fais !

En espérant n'oublier personne, merci encore !

Financial support:
I would like to thank the Université Franco-Allemande as well as the Deutscher Akademischer Austauschdienst (DAAD) for their financial support during my co-supervised thesis.

Table of content

List of figures

List of tables

List of abbreviations

5-HT: 5-Hydroxytryptamine
AAV: Adeno-Associated Virus
AAVR: Adeno-Associated Virus Receptor
AdV: Adenovirus
AIDS: Acquired Imunnodeficiency Syndrome
ART: Antiretroviral Therapy
BGG: β-galactosylated glycan
BKPyV: BK Polyomavirus
BKPyVAN: BK Polyomavirus Associated Nephropathy
BSA: Bovine Serum Albumine
cART: combination Antiretroviral Therapy
CHS: cholesteryl hemisuccinate
CNS: Central Nervous System
CS: Chondroitin Sulphate
CSF: Cerebrospinal Fluid
CT: Computed Tomography
CTL: Cytotoxic T Lymphocyte
DC: Dendritic Cell
DDM: n-dodecyl-β-D-maltoside
DNA: DesoxyriboNucleic Acid
ELISA: Enzyme-Linked Immunosorbent Assay
EM: Electron Microscopy
ER: Endopplasmic Reticulum
ERAD: Endoplasmic Reticulum Associated Degradation
GAG: Glycosaminoglycan
GCN: Granule Cell Neuronopathy
HC: Hemorrhagic Cystitis
hCMV: human Cytomegalovirus
HIV: Human Immunodefficiency Virus
HLA: Human Leucocyte Antigen
HRP: Haptoglobin Related Protein
HPV: Human Papillomavirus
HPyV: Human Polyomavirus
HS: Heperan Sulphate
HSC: Hematopoietic Stem Cell
HSLB: High Salt Lysis Buffer
IARC: International Agency for Research on Cancer
ICTV: International Committee on Virus Taxonomy
IFN: Interferon
IRIS: Imuune Reconstitution Inflammatory SyndromeIVIG: Intravenous Immunoglobulin
JCPyV: JC Polyomavirus
JCPyVAN : JC Polyomavirus Associated Nephropathy
kbp: kilo base pair
KIPyV: Karolinska Institute Polyomavirus
KIR: Killer cell Immunoglobulin like Receptor
LIPyV: Lyon IARC Polyomavirus
LSLB: Low Salt Lysis Buffer
LSTc: lactoseries tetrasaccharide c
LTAg: Large Tumour Antigen
mAb: monoclonal Antibody
MCPyV: Merkel Cell Polyomavirus
MHC I: Major Histocompatibility I
miRNA: micro–Ribonucleic Acid
MOI: Multiplicity of Infection

MPyV: Murine Polyomavirus
MRI: Magnetic Resonance Imaging
MS: Multiple Sclerosis
mTOR: mammalian Target Of Rapamycin
MWPyV: Malawi Polyomavirus
NCCR: Non-Coding Control Region
NGS: Next-Generation Sequencing
NJPyV: New Jersey Polyomavirus
NK: Natural Killer
NLS: Nuclear Localisaiton Sequence
nm: nanometer
ORF: Open Reading Frame
ORI: Origin of Replication
PCR: Polymerase Chain Reaction
PDI: Protein Disulfide Isomerase
PML: Progressive Multifocal Leukoencephalopathy
PMSF: Phenylmethylsulfonyl Fluoride
PyV: Polyomavirus
PyVAN: Polyoamvirus Associated Nephropathy
Rb: Retinoblastoma
RCA: Rolling Circle Amplification
RNA: Ribonucleic Acid
RPTEC: Renal Proximal Tubule Epithelial Cell
RU: Response Unit
SDS-PAGE: sodium dodecylsulfate polyacrylamide gel electrophoresis
SEC: Size-Exclusion Chromatography
SLN: sialyllactosamine
SLPyV: St Louis Polyoamvirus
SNP: Single Nucleotide Polymorphism
SPR: Surface Plasmon Resonance
stAg: small tumour antigen
SV40: Simian Virus 40
TF: Transcription Factor
TMB: 3,3',5,5''-Tetramethylbenzidine
TNF: Tumour Necrosis Factor
truncTAg: truncated tumour antigen
TSPyV: Trichodysplasia Spinulosa Polyomavirus
ULBP3: UL16 Binding Protein 3
VLP: Virus Like Particle
VP: Viral Protein
WT: Wild-Type
WUPyV: Washington University Polyomavirus

Introduction

1. Discovery of Human Polyomaviruses

In 1953, Gross discovered that cell-free filtrates from leukemic mice were, in addition to leukaemia, causing fibrosarcomas after injection in newborn mice (Gross, 1951). It was only later, in 1958, that Stewart's work described the agent responsible for the formation of solid tumours as a DNA virus ubiquitously present in mice, which is now known as the Murine polyomavirus (MPyV) (Stewart et al., 1958). Hence, the name Polyomavirus comes from the Greek: poly – multiple and oma – tumours which refers to the pathology initially associated with the virus.

In 1960, the first primate polyomavirus was identified in African green monkey kidney cells as simian virus 40 (SV40) by Sweet and Hilleman (Sweet & Hilleman, 1960). Like MPyV, SV40 was also described to induce tumours in new born hamsters or multimammate mice (genus *Mastomys*).

Polyomaviruses are non-enveloped double stranded circular DNA viruses, and since the discovery of MPyV and SV40, a total of 117 polyomaviruses have been detected in vertebrate hosts, including humans. The first two human polyomaviruses: BK and JC polyomaviruses (BKPyV, JCPyV) were identified in 1971. BKPyV (**Figure 1**) was isolated from a urine sample of a kidney transplant patient while JCPyV was detected in a patient's brain suffering from Progressive Multifocal Leukoencephalopathy (PML) (Padgett et al., 1971; Gardner, 1973).

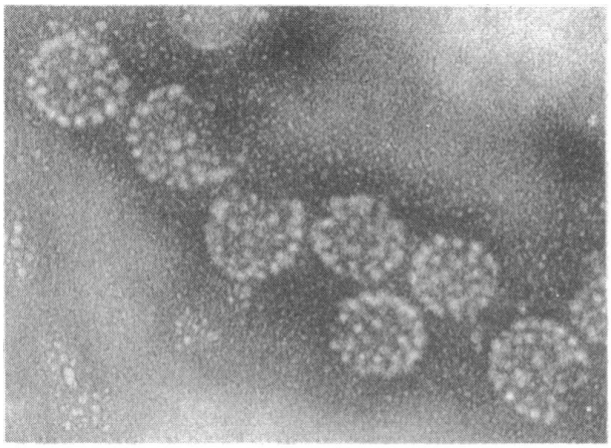

Figure 1 - BK polyomavirus particles found in patient urine samples, observed with electron microscope (x240 000) (Coleman et al., 1973)

From 2007, with the improvement of technologies in sequencing and increased sensitivity due to techniques such as rolling circle amplification (RCA), it was possible to discover several more HPyV (**Figure 2**). The third and fourth HPyV were isolated from nasopharyngeal tissues and carry the name of the research institutes where they were identified: Karolinska Institute polyomavirus (KIPyV) and Washington University polyomavirus (WUPyV) (Allander et al., 2007; Gaynor et al., 2007). In 2008, Merkel Cell polyomavirus (MCPyV) was discovered and named according to its involvement in Merkel cell carcinoma (Feng et al., 2008). MCPyV is the only known oncogenic HPyV.

The three following polyomaviruses were found mostly in skin tissues and were named according to the order of their discovery (HPyV6 and HPyV7) while TSPyV derives its name from its identification in the rare skin disease trichodysplasia spinulosa (Schowalter et al., 2010; van der Meijden et al., 2010). Also found in skin tissues, HPyV9 was, in addition, detected in blood and urine samples of kidney transplant recipients (Scuda et al., 2011). In 2012, HPyV10 and HPyV11, respectively known as Malawi (MWPyV) and St Louis polyomaviruses (SLPyV), were found in stool samples as well as in condyloma for MWPyV (Buck et al., 2012; Foulongne et al., 2012; Siebrasse et al., 2012; Lim et al., 2013). Then, HPyV12 was identified from a liver sample, in 2013, while HPyV13, or New Jersey polyomavirus (NJPyV), was identified from a muscle biopsy of a pancreatic transplant recipient (Korup et al., 2013; Mishra et al., 2014). Finally, in 2017, Lyon IARC polyomavirus (LIPyV) was identified from skin and oral samples as the 14th human polyomavirus (Gheit et al., 2017).

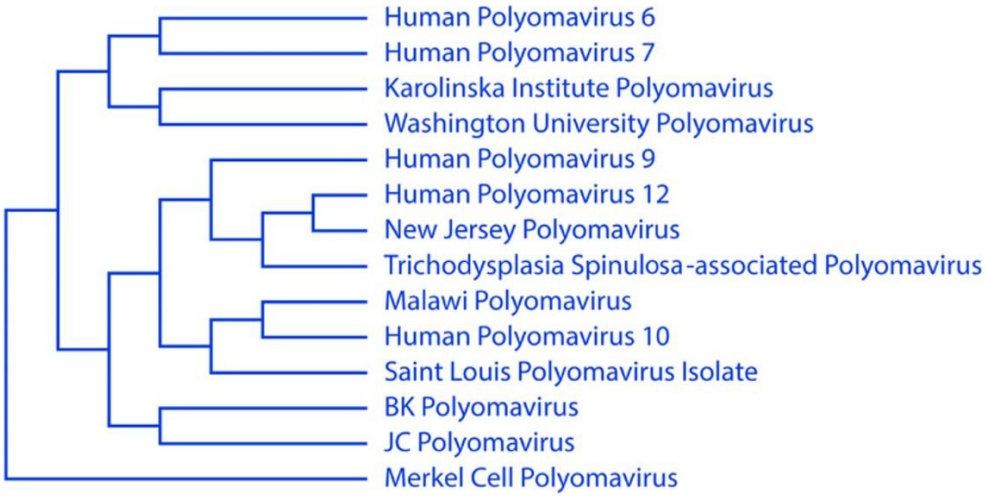

Figure 2 - Phylogenetic tree representing the 14 discovered HPyV (Ambalathingal et al., 2017)

Recently, only 12 out of the 14 polyomaviruses found in human samples were confirmed to have humans as host (ICTV Report Consortium, 2019). HPyV12 initially found in human skin is, in fact, able to naturally infect shrews and is not described as a HPyV anymore (Gedvilaite et al., 2017). Similarly, Lyon IARC polyomavirus, first identified in human samples, was also characterised in cat faeces samples suggesting that it may be a feline, rather than a human, virus (Fahsbender et al., 2019; Kamminga et al., 2019; Y. Li et al., 2021).

2. Taxonomy of Human Polyomaviruses

Historically, polyomaviruses and papillomaviruses were considered to be genus-level clades (Polyomavirus and Papillomavirus) that were grouped together in the Papovaviridae family. This family was abolished in 1999, and the polyomaviruses and papillomaviruses were re-classified as distinct virus families, the Polyomaviridae and Papillomaviridae. More recently, the International Committee on Virus Taxonomy (ICTV) has proposed several higher-level taxonomic groupings, including the class Papovaviricetes, which includes both families of Polyomaviridae and Papillomaviridae (https://talk.ictvonline.org/taxonomy/).

The Polyomaviridae family is divided into six genera, named after the 6 first letters of the Greek alphabet, and numbers 117 different polyomavirus species. The classification of the virus species in the different genera is determined by analyses of the large tumour antigen (LTAg) sequences (Calvignac-Spencer et al., 2016). Human polyomaviruses are found in three Polyomaviridae genera. The Alphapolyomavirus genus includes the skin-associated human viruses MCPyV and TSPyV, while the most studied human polyomaviruses BKPyV and JCPyV are found in the Betapolyomavirus genus along with KIPyV and WUPyV. Finally, the Deltapolyomavirus genus is composed of HPyV6 and HPyV7 found in human skin, as well as MWPyV and SLPyV detected in gastrointestinal tract (https://talk.ictvonline.org/taxonomy/). Alternative species-level designations, summarised in **Table 1**, also exist for HPyV, though it remains to be seen whether the binomial species names proposed by the ICTV in 2021 will be adopted by the virology community.

Genus	Common name	2015-2019 ICTV nomenclature	2021 ICTV proposal
Alphapolyomavirus	MCPyV	HPyV5	*Alphapolyomavirus quintihominis*
	TSPyV	HPyV8	*A. octihominis*
	HPyV9	HPyV9	*A. nonihominis*
	NJPyV	HPyV13	*A. terdecihominis*
Betapolyomavirus	BKPyV	HPyV1	*Betapolyomavirus hominis*
	JCPyV	HPyV2	*B. secuhominis*
	KIPyV	HPyV3	*B. tertihominis*
	WUPyV	HPyV4	*B. quartihominis*
Deltapolyomavirus	HPyV6	HPyV6	*Deltapolyomavirus sextihominis*
	HPyV7	HPyV7	*D. septihominis*
	MWPyV	HPyV10	*D. decihominis*
	SLPyV	HPyV11	*D. undecihominis*

Table 1 - Current and proposed HPyV species nomenclature.

2.1. BKPyV genotypes and subgroups

BKPyV strains can be divided into four genotypes: I, II, III and IV which were first differentiated through serological methods (Knowles et al., 1989; Knowles, 2001) and then refined through analysis of PCR-amplified VP1, capsid protein, sequences (Jin al., 1993a; Jin et al., 1993b). These studies were able to identify that the main differences between the genotypes were found in a specific region of the VP1 protein spanning amino acids 61 to 83 (**Table 2**), known as the typing region. This segment of the VP1protein comprises the BC-loop region on the outer face of the virus capsid that was subsequently found to be involved in receptor binding (Liddington et al., 1991).

Amino acid n°	60	61	62	63	64	65	66	67	68	69	70	71	72	73	74	75	76	77	78	79	80	81	82	83	84	85
Genotype I	D	E	N	L	R	G	F	S	L	K	L	S	A	E	N	D	F	S	S	D	S	P	E	R	K	M
Genotype II	D	**N**	**D**	L	R	G	**Y**	S	L	K	L	**T**	A	E	N	**A**	F	**D**	S	D	S	P	**D**	**K**	K	M
Genotype III	D	**D**	**H**	L	R	G	**Y**	S	**Q**	**H**	L	**T**	A	E	N	**A**	F	**D**	S	D	S	P	**D**	**K**	K	M
Genotype IV	D	**N**	**D**	L	R	G	**Y**	S	L	**R**	L	**T**	A	E	**T**	**A**	F	**D**	S	D	S	P	**D**	R	K	M

Table 2 - BC-loop sequences in the 4 different genotypes.

Single Nucleotide Polymorphisms (SNPs) in the VP1 typing region sequences were then used to determine the different genotypes. Genotype I was found to be the most widespread genotype with a prevalence in all human populations, followed by genotype IV, found in both Asian and European populations, while genotypes II and III were only found sporadically (Jin, 1993; Jin et al., 1993b,1995; Di Taranto et al., 1997; Carr et al., 2006; Nishimoto et al., 2006; Zheng et al., 2007; Thongprayoon et al., 2019). Based on DNA variations, genotypes I and IV were divided into subgroups (Takasaka et al., 2004; Ikegaya et al., 2006; Nishimoto et al., 2006, 2007; Zheng et al., 2007; Zhong et al., 2009). For genotype I, four subgroups were defined and associated to different human populations, where subgroup Ia is found in African populations, Ib-1 in Southeast Asians, Ib-2 in Europeans and West Asians and Ic in Northeast Asians (Takasaka et al., 2004; Nishimoto et al., 2006; Zheng et al., 2007). For genotype IV, six subgroups were defined: IVa1, IVa2, IVb1, IVb2, IVc1 and IVc2, with all of them associated to East Asians populations expect IVc2, which is found in European and Northern Asian populations (Nishimoto et al., 2007; Zhong et al., 2009). Analysis of both VP1 and LTAg sequences proved to show the same phylogenetic tree with the distinct genotypes and subgroups with an improved robustness compared to analysis of only VP1 sequences variability (Luo et al., 2009). More recently, the correspondence between BKPyV genotypes and neutralising serotypes wasconfirmed using pseudotype virus particles (Pastrana et al., 2012, 2013).

2.2. JCPyV genotypes and subgroups

Depending on the non-coding control region (NCCR) rearrangement (archetype or rearranged) in its genome, JCPyV was initially classified in two groups: I and II (Walker and Frisque, 1986). Later, a classification composed of three groups: A, B and C was suggested based on the nucleotide differences observed in the genome of

JCPyV (Yogo et al., 1991; Guo et al., 1996). Those studies also established that type A of JCPyV was identified mostly in Europe, while Type B was found mainly in Asia and African and Type C localised in West Africa. A total of 18 genotypes were then established based on the sequence variations found in the IG region (Guo et al., 1996; Sugimoto et al., 1997; Ryschkewitsch et al., 2000; Jobes et al., 2001; Yanagihara et al., 2002). This region of 610 bp starts in position 2131 in the VP1 gene and stops at position 2740 in the LTAg gene (Ault & Stoner, 1992). Combined with whole-genome analysis, JCPyV genotypes phylogeny can be built (**Figure 3**) (Sugimoto et al., 2002). Ancestral JCPyV would have diverged into three superclusters: A, B and C. A would have split into 3 genotypes, EU-a, -b and -c, found in Europe and Mediterranean areas with 2 subgroups within EU-a: SK occurring in Northern Japan and Arc in Arctic areas of Northern America and Northeast Siberia. Type B first split would have generated the Af2 genotype found in African and West and South Asia, followed by a second split giving B1-c, a genotype found in Europe. Then multiple splits of this type B group would have led to genotypes found in Asia, like B2, and Oceania, like 8A (**Figure 3**). In contrast, type C only contains genotype Af1 found in West and Central Africa (Yogo et al., 2004). The subtypes identified by Sugimoto et al. were mostly confirmed by subsequent studies, but re-designated as genotypes 1 to 9, with genotypes 1, 4 and 9 corresponding to supergroup A, genotype 6 corresponding to type C, and the remaining genotypes 2, 3, 5, 7 and 8 making up supergroup B.

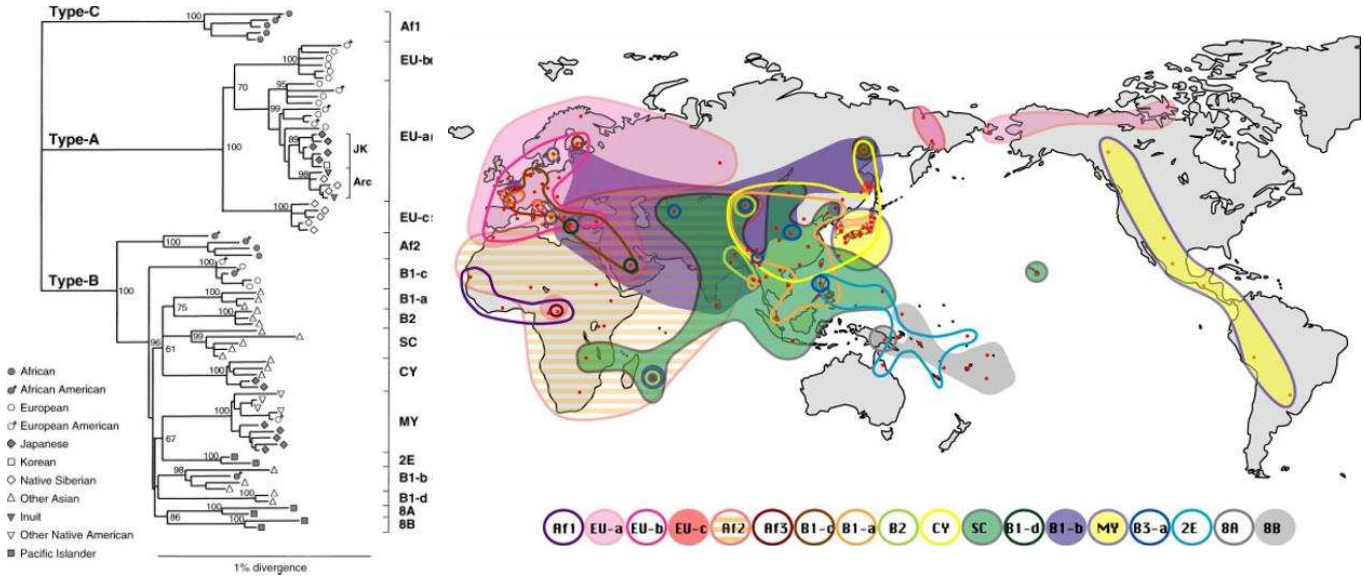

Figure 3 - Phylogenetic tree of JCPyV genotypes and distributions of those genotypes across the world (Yogo et al., 2004).

A more detailed picture has emerged from an analysis of 431 complete and 701 partial JCPyV genome sequences, which concluded that JCPyV has an ancient origin, and has co-evolved with human populations for more than 200 000 years. Surprisingly, the European/Siberian JCPyV sequences (genotypes 1, 4 and 9), and not the African genotype 6 have a basal position in JCPyV phylogeny (Forni et al., 2020). The authors of the study discussed three possible explanations for this discrepancy: extinction of one or more ancestral African JCPyV lineage; existence of an as yet unsampled basal African JCPyV lineage; introduction of genotypes 1, 4 and 6 from archaic hominins (Denisovans or Neanderthals) when modern humans migrated into Europe/Siberia.

3. Human Polyomaviruses structure

3.1. Viral capsid

Polyomaviruses are non-enveloped icosahedral viruses with a 40-45 nm diameter capsid. This capsid is composed of 72 pentamers of the major capsid protein VP1 arranged in T = 7d symmetry (**Figure 4A**) and each pentamer is internally linked to either one VP2 or VP3 protein, forming a capsomer.

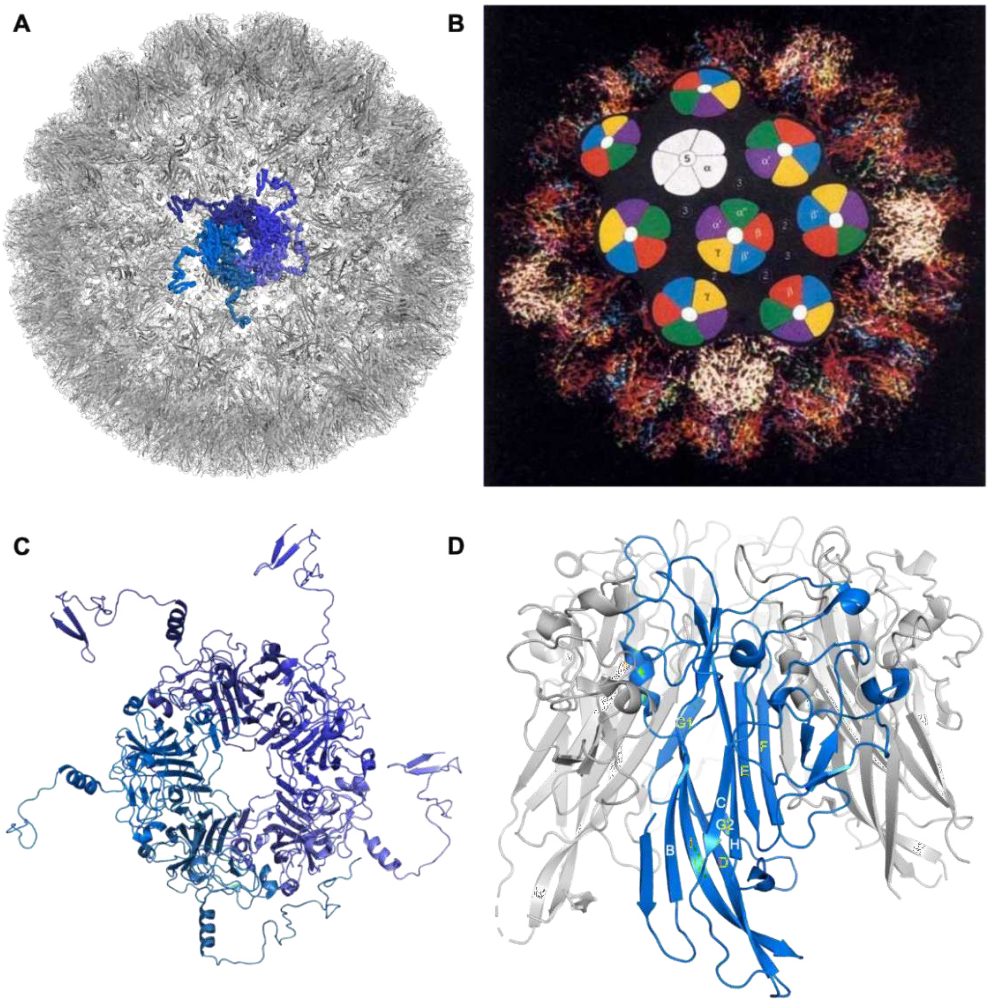

Figure 4 - Capsid structure of polyomaviruses. (A) BKPyV capsid (PDB ID: 6ESB) represented in grey except for highlighted pentamer with VP1 monomers displayed as ribbons in different shades of blue. (B) Capsid structure of SV40. The strict pentamer is represented in white while the local capsomers are in colours. The six VP1 conformation are labelled α', α'', β, β', γ, α and icosahedral symmetry axes are numbered 5, 3 and 2 (Liddington et al., 1991) (C) Top view of BKPyV VP1 pentamers displayed as cartoon colored in different shades of blue for each subunit. (D) Side view of BKPyV VP1 pentamer displayed as cartoon with VP1 monomer highlighted in blue. Figures (A), (C) and (D) were made with Pymol.

T = 7d symmetry can be defined by the presence of twelve strict VP1 pentamers at the 5-fold axes of the icosahedral capsid which are surrounded by 60 local capsomers. There are five possible VP1 conformations from a local capsomer as well as one from an adjacent strict pentamer, respectively annotated α', α'', β, β', γ and α. These conformations lead to interpentameric interactions: a 3-fold axis between VP1 monomers α, α' and α''; a first 2-fold axis involving monomers β and β' and finally a second 2-fold axis between monomers γ and α (**Figure 4B**). Taken together, those 6 VP1 conformations, and by applying a 60-fold icosahedral symmetry, are sufficient to generate the entire viral capsid. Capsomers interact tightly with each other thanks to the invading VP1 C-terminal arm coming diametrically from the capsomer core to interact with adjacent capsomers. Multiple disulphide bonds are also found. And they are important to maintain inter and intrapentameric interactions.

All VP1 pentamers, either from the strict pentamers or the local capsomers, share the same β-sandwich jelly roll fold core structure (**Figure 4C & D**). This topology is given by the presence in each VP1 monomer of many β -strand B to I, named in alphabetical order starting from the N-terminus, linked by extensive loops. Each VP1 pentamer is associated internally with one other capsid protein VP2 or VP3 encapsulating viral DNA wrapped around host cell-derived histones (Belnap et al., 1996; Liddington et al., 1991; Stehle et al., 1996; Stehle, 1997; Neu et al., 2013; Hurdiss et al., 2018; Bayer et al., 2020).

3.2. Viral genome

Polyomaviruses have a circular double stranded DNA genome, of ~5 kbp. Their genome can be divided into 3 functional regions: the non-coding control region (NCCR), the early gene and late gene regions (**Figure 5**).

The NCCR is an important regulatory region of around 400 bp divided in different sections. This region contains essential sequences for replication with the origin of replication (ORI) as well as promoter, enhancer, and transcription factor sequences for efficient bidirectional transcription of the viral genes. This region differs from one HPyV to another regarding the sequences, number, and positions of the different viral LTAg and host cell transcription factor-binding sites (Ajuh et al., 2018). Rearrangements of archetype NCCR have been described in BKPyV, JCPyV, HPyV7 and HPyV9 and

showed that most of those variant forms increased the expression of the early gene region, as well as enhancing viral replication and cytopathology (Gosert et al., 2008; Ferenczy et al., 2012; Hirsch et al., 2013a; Ajuh et al., 2018).

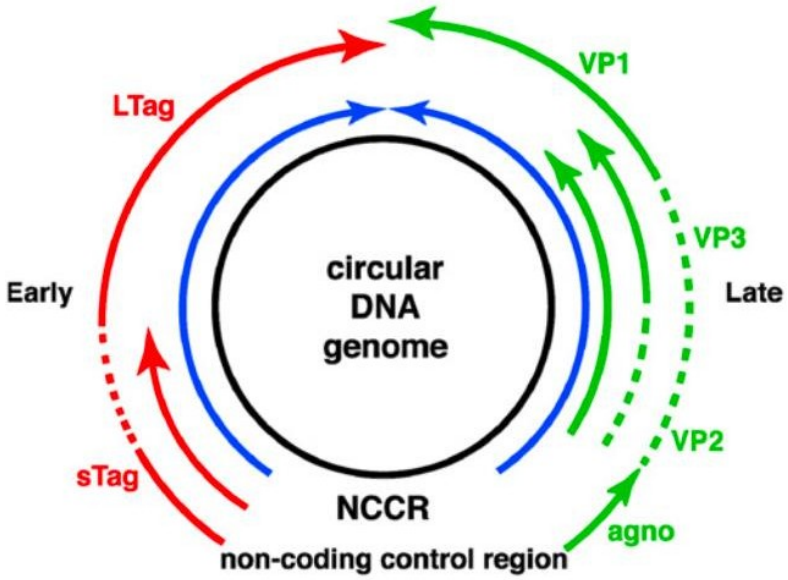

Figure 5 - Representation of HPyV circular genome: double stranded DNA is represented in black, the primary transcript of early and late regions in blue, the spliced transcripts of early regions in red and late regions in green (open reading frame (ORF), solid line and introns, dotted line) (Dalianis & Hirsch, 2013).

The early gene region essentially encodes for the non-structural proteins: large and small tumour antigens (LTAg, stAg) through alternative splicing. Some polyomaviruses encode for more tumours antigens, like BKVyP and MCPyV with truncated T Ag (truncTAg) or JCyPV with alternatively spliced T' antigens (Decaprio & Garcea, 2013; Hirsch et al., 2013a; Hirsch al., 2013b). Polyomavirus LTAg are known to be essential for viral DNA replication, transcription and virion assembly as well as being able to interact with multiple cellular pathways including proliferation, cell death and the inflammatory response (An et al., 2012). On the other hand, stAg is thought to be directly involved in the activation of the cell cycle progression to S phase (Khalili et al., 2008).

The late gene region encodes for the structural proteins VP1, VP2 and VP3. Two mRNA are generated through alternative splicing, one encoding for both VP2 and VP3 and the other one for VP1. As the first initiation codon, AUG, is not in optimal context for initiation, both proteins from the same mRNA can be translated. These proteins assemble in the nucleus of the host cell to form new virions. *Betapolyomaviruses*, including BKPyV and JCPyV, also encode for another small structural protein called

agnoprotein with its coding region being upstream of the VP1 orf on the same mRNA (Okada et al., 2001; Rinaldo et al., 1998). For both BKPyV and JCPyV, the agnoprotein appears to be essential for the efficient release of infectious viral particles (Okada et al., 2001; Panou et al., 2018).

The genomes of BKPyV, JCPyV and MCPyV also encode for micro-RNAs (miRNAs) in their late region which inhibit LTAg expression, leading to downregulation of viral replication at the late stage of infection (Seo et al., 2008, 2009; S. Lee et al., 2011; Broekema & Imperiale, 2013; Tian et al., 2014; Zou & Imperiale, 2021). In addition to their ability to regulate viral replication, miRNAs have been shown or predicted to target host cellular proteins (Bauman et al., 2011; S. Lee et al., 2011). Indeed, identical miRNAs from both BKPyV and JCPyV were found to target the immune response. They can downregulate expression of ULBP3, a stress-mediated ligand of the killer receptor NKG2D, which consequently allows escape from recognition by NK or CD8+ T cells (Bauman et al., 2011).

4. Polyomavirus life cycle

HPyV life cycle (**Figure 6**) starts when viruses interact with their receptors (1) at the surface of the host cell which triggers internalisation; (2) either by caveolin-, for BKPyV, or by clathrin-dependent, for JCPyVendocytosis. (3) Viral particles are transported either to the endosome, for BKPyV, orthe early endosome for JCPyV, and then to the endoplasmic reticulum. (4) There, virus undergoes partial uncoating revealing VP2 and VP3 on the capsid. (5) Then, partially uncoated viruses leave the ER potentially through ERAD complex. (6) Viral genome is then transported to the nucleus where (7) early-gene expression leads to production of the different T antigens. (8) Viral genome is replicated. (9) Then, late-gene expression allows production of the structural proteins: VP1/2/3 as well as agnoprotein. (10) New virions are formed with the structural proteins and newly replicated genome which can then be released in a non-lytic manner (11) or through cell lysis (12).

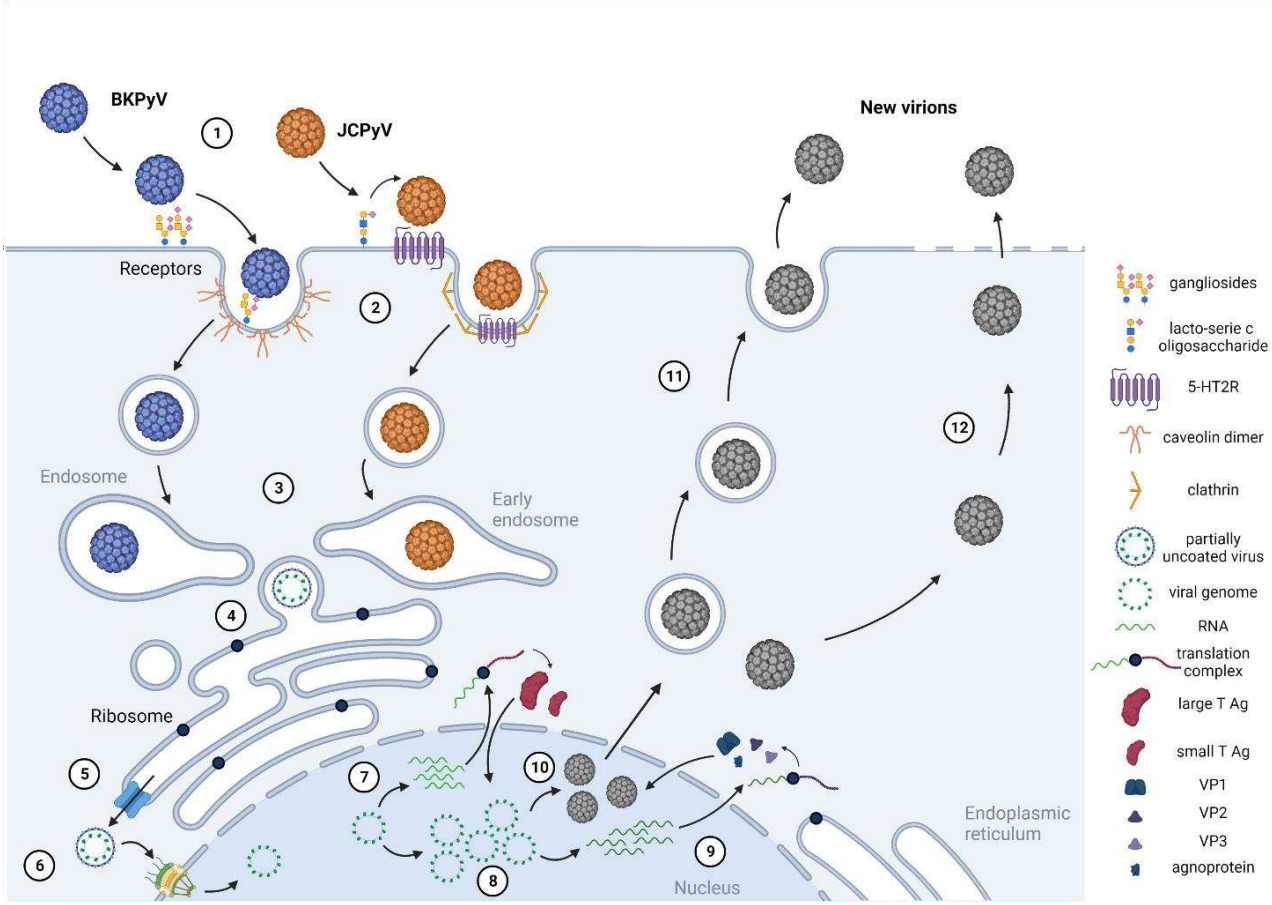

Figure 6 - Replication cycle of polyomavirus. Figure was made with Biorender.

4.1. Polyomaviruses mainly use sialylated glycans for entry

HPyV are known to have a limited host range and cell tropism and many polyomaviruses can attach to sialylated glycans at the cell surface: the gangliosides. Gangliosides are glycosphingolipids that can carry one or multiple sialic acids (N-acetylneuraminic acid (Neu5Ac), in humans). Sialic acids are linked to galactose residues by an α2,3-linkage. And they can be connected to each other by an α2,8-linkage. The name of the gangliosides follows the nomenclature of L. Svennerholm where G = ganglio and L = lacto, the letters: A = 0, M = 1, D = 2, T = 3, Q = 4, P = 5, H = 6 and S = 7 indicate the number of sialic acids and a number, not higher than 5, indirectly refers to the neutral sugars in the structure. For example, GM1 is from the ganglio series, contains one sialic acid and (5 - “1” = 4) neutral sugars. Sometimes the name is followed by a small letter: a, b or c meaning that those gangliosides belong the series of the same name where a-series is for glycans carrying one sialic acid on the first galactose, b-series is for two sialic acids and c-series three. The o-series groups gangliosides do not carry any sialic acid on their first galactose and, therefore, should not be named with a small letter, however, o-series GM1b and GD1c are the exceptions (**Figure 7**) (Kolter, 2012; Svennerholm, 1964).

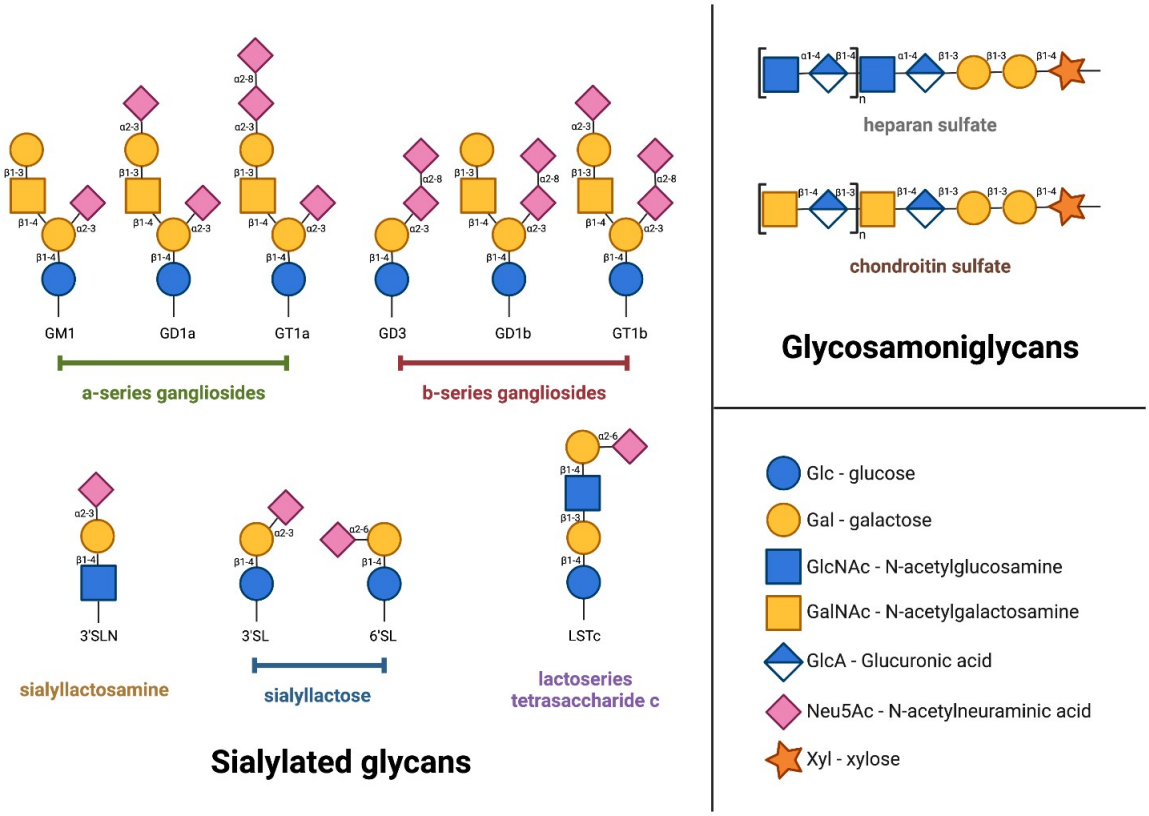

Figure 7 - Structures of different glycans

To enter the host cell, BKPyV was first shown to interact with GT1b and GD1b gangliosides and later, with all b-series gangliosides through their di-sialic acid motif (Low et al., 2006; Neu et al., 2013). In fact, the crystal structure of BKPyV VP1 pentamers with GD3 reveals five binding sites on the top of the pentamers, one for each VP1 molecule. The di-sialic acid part of GD3 interacts with multiple residues found in three loops (BC-, HI- and DE-loops) of a single VP1 monomer and one loop from each of the neighbouring monomers (BC- and DE-loops) (Neu et al., 2013) (**Figure 8**). Like BKPyV, MCPyV can interact with GT1b but also GD1a (Erickson et al., 2009; Neu et al., 2012). Structural studies revealed that the HI-, BC- and DE-loops of MCPyV VP1 bind to the single sialic acid found on the second galactose of GD1a which is also present in the structure of GT1b (Neu et al., 2012) (**Figure 8**).

JCPyV is known to attach sialylated glycosphingolipids, specifically the lactoseries tetrasaccharide c (LSTc) where a single sialic acid is bound in α2,6 to the second galactose. Like for BKPyV and MCPyV, the receptor binds on the top of the VP1 pentamer with five possible binding sites, one per monomer. Again, for this binding, the BC-, HI- and DE-loops of a single VP1 monomer are involved as well as the BC-

loop of the neighbouring monomer. In this case, not only the sialic acid makes contact to the VP1 residues but also the N-acetylglucosamine (GlcNAc) found upstream in the LSTc structure (Neu et al., 2010) (**Figure 8**).

As for JCPyV, HPyV9 binding to its receptors involves BC-, HI- and DE-loops from a single VP1 monomer and the BC-loop of the neighbouring monomer. However, HPyV9 was found to attach α2,3-linked sialyllactosamine (3'SLN) where a single sialic acid connects to the sugar compounds through α2,3 linkage (Khan et al., 2014) (**Figure 8**).

For the more recently discovered NJPyV, binding to α2,3 linked sialyllactose structure was described. This kind of structure is usually found on complex glycans like gangliosides. For this polyomavirus, the binding pocket differs slightly from the other previously described PyV capsid sialic acid binding pockets, since only the HI- and BC-loops of a single monomer are involved in the binding (Ströh et al., 2020) (**Figure 8**).

Regarding TSPyV, a single sialic acid moiety was found to bind the VP1 pentamers quite differently as it was seen for most polyomaviruses. Indeed, the Neu5Ac is solely bound by the second part of the BC-loop in the VP1 monomer and by the DE-loop coming from the neighbouring monomer. This study clearly showed that only the sialic acid structure is observed to bind the VP1 proteins and concluded that TSPyV can interact with both α2,3 and α2,6-linked sialylated glycans (Ströh et al., 2015) (**Figure 8**).

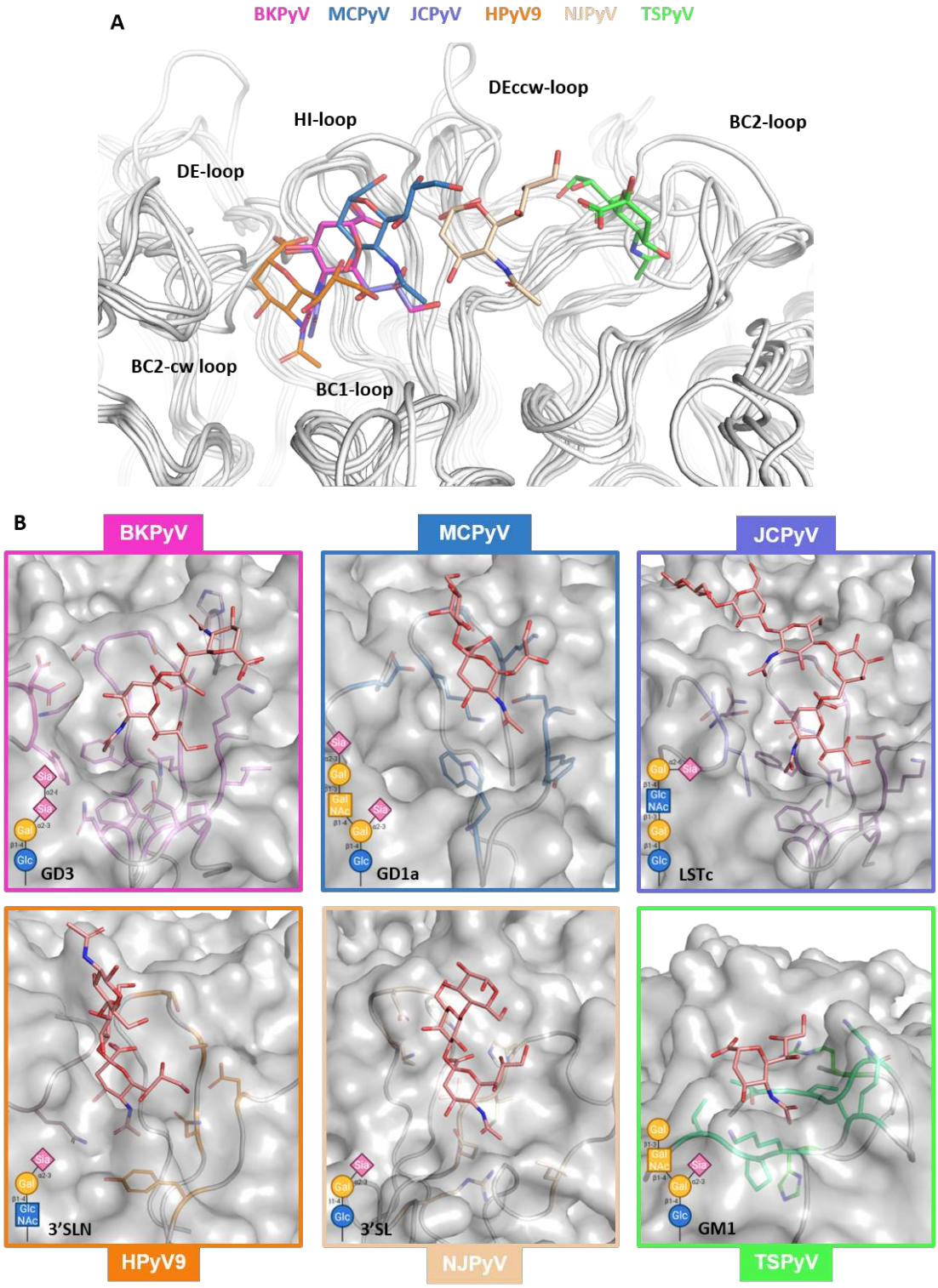

Figure 8 - Sialic acid binding sites among HPyV. (A) Superposition of all HPyV structure in interaction with sialic acid, represented as coloured sticks, focusing on the binding site. (B) Binding site with sialylated glycans for each HPyV structures: BKPyV in interaction with GD3 (4MJ0), MCPyV in interaction with GD1a (4FMJ), JCPyV in interaction with LSTc (3NXD), HPyV9 in interaction with 3'SLN (4POS), NJPyV in interaction with 3'SL (6Y5Y) and TSPyV in interaction with GM1 (4U60), with amino acids involved in binding shown as coloured sticks and ligands as light pink sticks *(*Neu et al., 2010, 2012, 2013; Khan et al., 2014; Ströh et al., 2015, 2020). Figures were made using Pymol, except schemes of glycans which were done using Biorender.

On the other hand, studies on both HPyV6 and HPyV7 showed that neither of them can bind sialylated glycans. Indeed, on a structural level, the HI-loop of their VP1 monomer is much more extended than that found in the previously discussed HPyV. Moreover, this loop conformation seemed to block the sialic acid binding pockets (Stroh et al., 2014) (**Figure 9**). No clear receptors have yet been described for these two HPyVs.

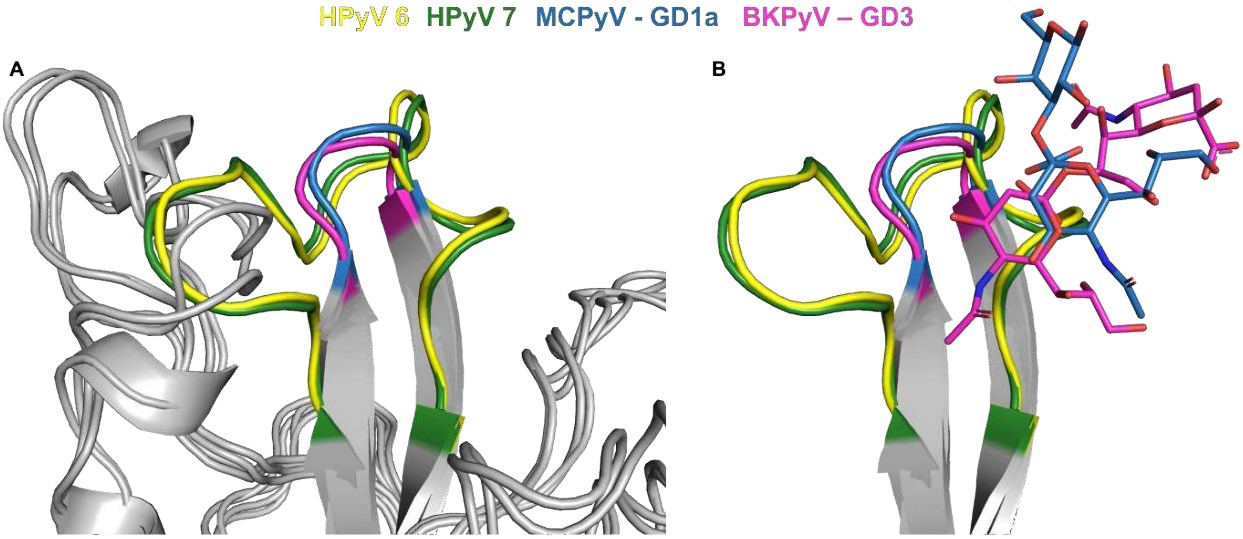

Figure 9 - Comparison of HI loop orientation in HPyV6 (4CPG), HPyV7 (4CPH), MCPyV (4FMJ) and BKPyV (4MJ0). (A) Superposition of VP1 monomer with HI loop in colour: yellow for HPyV6, dark green for HPyV7, dark blue for MCPyV and pink for BKPyV. (B) Focus on the HI loops of the different HPyVs with ligands of MCPyV and BKPyV shown as sticks in dark blue and pink, respectively. Figures were made with Pymol.

While for most polyomaviruses, interactions with sialylated glycans are thought to be sufficient for virus entry into host cells, some polyomaviruses show additional binding to non-sialylated glycans like glycosaminoglycans. GAGs are long linear polysaccharides carrying negative charges that can be sulphated like heparin sulphate (HS) and chondroitin sulphate (CS) (Gandhi & Mancera, 2008) (**Figure 7**). Merkel Cell polyomavirus was shown to primarily bind HS and CS GAGs before engaging with gangliosides to enter cells (Schowalter et al., 2010; Bayer et al., 2020). Another study also hinted toward JCPyV and BKPyV being capable of interacting with GAGs (Geoghegan et al., 2017). Moreover, a cryo-EM study tried to solve the BKPyV capsid in interaction with heparin. However, despite observing difference density in between the capsomers and on top of them, it can not be clearly associated with the presence of heparin (Hurdiss et al., 2018; Sorin et al., 2021).

In addition to its binding to glycans, JCPyV is believed to interact with a secondary protein receptor, which has been identified as the seven-transmembrane domain type-2 5-hydroxytryptamine, or serotonin, receptors 5-HT2A, 5-HT2B, and 5-HT2C. Thus, LSTc would serve as an attachment receptor for JCPyV and the 5-HT2 receptors as entry receptors (Elphick, 2004; Assetta et al., 2013, 2019).
Other non-human polyomaviruses have been shown to interact with protein receptors as well as glycans like SV40 and MPyV. For SV40, the major histocompatibility class I molecules (MHC I) serve as an attachment receptor and GM1 gangliosides as entry receptors while for MPyV, the α4β1 integrin is used as a post-attachment receptor in addition to gangliosides (Caruso et al., 2003; Toscano & de Haan, 2018). Thus, this shows that a two-receptor entry mechanism can be used by polyomaviruses with involvement of gangliosides mostly as the entry receptor.

After binding at the plasma membrane, most polyomaviruses are known to enter cells by caveolin-endocytosis (Eash et al., 2004). Nevertheless, JCPyV enters through clathrin-dependent endocytosis which is thought to be due to the 5-HT2 receptors, since they are known to trigger this type of endocytosis (Pho et al., 2000; Elphick, 2004; Assetta et al., 2019). Finally, BKPyV was observed to also enter human tubule renal epithelial cells through independent caveolin- and clathrin-mediated endocytosis (Zhao et al., 2016).

4.2. Intercellular trafficking

Transported in vesicles, the polyomavirus virions first enter the endolysosome and then are redirected to the endoplasmic reticulum (ER) (Eash et al., 2004; Gilbert & Benjamin, 2004; Qian et al., 2009). While this pathway is thought to be similar for the different polyomaviruses using sialylated glycans to enter cell, JCPyV by entering through clathrin endocytosis is first transported to early endosomes and then retrogradely through caveolin-1 vesicles to the ER (Querbes et al., 2006; Nelson et al., 2012, 2013; Becker et al., 2019).
Once in the ER, the virions undergo partial decapsidation. ER protein disulphide isomerases (PDI) can reduce the disulphide bonds that hold VP1 pentamers closely attached, as well as unravelling their C-terminal domain, leading to exposure of

VP2/VP3 on the exterior of viral particle (Jiang et al., 2009; Nelson et al., 2012, 2013). Although the mechanism is not well understood, partially decapsidated particles are then transported to the cytosol probably with the help of ER-associated degradation (ERAD) components (Inoue & Tsai, 2013). Through recognition of nuclear localisation sequences (NLS) found on the C-terminus of VP2 and VP3 proteins, viral particles are transported to the nucleus by the α and β1 importins which interact with nuclear pore complexes (Bennett et al., 2015; Qu et al., 2004).

4.3. Viral transcription and replication

Once in the nucleus, replication as well as viral gene expression occur. Viral gene transcription is initiated by binding of host-cell transcription factors (TF) to the NCCR. For JCPyV, multiple cellular TFs are described to be involved in viral gene transcription regulation by binding the enhancer elements in the NCCR. Some TFs, like Tst-1, YB-1 or AP-1 stimulate viral early and late gene transcriptions. However, other TFs, like C/EBPβ or SRSF1, have been described for their repressive activities. Interestingly, cellular TFs are also important determinants of cell tropism like for JCPyV where Tst-1 is the key TF for controlling transcription and is specifically expressed in myelinated glial cells (Yang & You, 2020). Similarly, as JCPyV, cellular TFs, like p53, YY1 and NF-1, can repress BKPyV gene expression while other TFs, like Spr1 or Ets1 repress early transcription. Whereas TF like p65 can stimulate the viral early promoter and, in synergy with C/ERPβ, induce viral gene expression. Finally, NFAT was shown to have both an activation and repressive effect on viral gene expression by interacting with either c-Jun or p65 (Bethge et al., 2015; Yang & You, 2020).

LTAg is also particularly involved in transcriptional control. A lot of studies on SV40 have highlighted that LTAg inhibits early transcription to favour late transcription. LTAg can interact with TF AP-2, to prevent its binding to viral DNA, but also with viral DNA directly at the ORI to inhibit initiation of early transcription. LTAg can also act as TF by binding NCCR to promote late gene expression. Extended studies have also been done on JCPyV LTAg which is also involved in inhibition of early transcription. Indeed, LTAg was found to interact with cellular TF, YB-1, to inhibit early transcription but this interaction also induces late transcription (Yang & You, 2020). For BKPyV,

distribution of SP1 binding sites in NCCR has been shown to play an essential role in the initial balance between early and late gene transcription (Bethge et al., 2015). Moreover, biopsies from patients with BKPyV associated nephropathy (BKPyVAN) showed that cells at early stage of infection are LTAg +/VP1 - while cells at late stage are LTAg +/VP1 + or LTAg -/VP1 +, indicating that a similar transcription regulation occurs in BKPyV as the one described in JCPyV and SV40 (Seemayer et al., 2008). LTAg binding to the ORI is known to induce DNA unfolding and recruitment of host cell machinery like topoisomerase I and DNA polymerases (Swenson et al., 1996; Tikhanovich & Nasheuer, 2010; Harrison et al., 2011; Wang et al., 2012). Finally, LTAg can interact with the cell cycle machinery including p53 and pRb to push cell cycle progression and prevent apoptosis (Harris et al., 1996, 1998; Tyagarajan & Frisque, 2006; Seamone et al., 2010).

For JCPyV and BKPyV, stAg was shown to interact with Rb proteins as well as protein phosphatase 2A, which seems to contribute to cell cycle progression (Bollag et al., 2010; Helle et al., 2017). While for MCPyV, stAg seems to interact with the mTOR pathway, and along with LTAg, drives tumorigenesis (Shuda et al., 2011).

4.4. Virus assembly and release

Individual VP1 and VP2/3 proteins associate in the cytosol to form capsomers, which are then transported to the nucleus through VP1 NLS sequence (Shishido-Hara et al., 2000; Helle et al., 2017). There, the newly replicated viral genome is encapsidated into new virions. The rich calcium environment is essential for capsid formation and interpentameric disulphide bonds help stabilise the overall virion structures (Haynes et al., 1993; Chen et al., 2001). The release mechanism of newly formed viral particles is thought to occur mostly through lytic release but also, for JCPyV and BKPyV, in a non-lytic manner possibly involving the secretion of exosomes containing multiple virus particles (Low et al., 2004; Suzuki et al., 2010; Evans et al., 2015; Morris-Love et al., 2019; Handala et al., 2020).

The main function of the agnoprotein, expressed by *Betapolyomaviruses*, appears to be to enhance virion release from infected cells. Different mechanisms have been described by different groups, with agnoprotein reported to be essential for the formation of infectious JCPyV and SV40 particles in the nucleus, for BKPyV virion

export from the nucleus, and possibly also acting directly as a viroporin, facilitating virion release at the plasma membrane (Sariyer et al., 2008; Suzuki et al., 2010, 2012; Panou et al., 2018).

5. Pathogenicity of BKPyV & JCPyV

5.1. Epidemiology, transmission and latency

BKPyV and JCPyV are opportunistic viruses with seroprevalences above 80%, for BKPyV, and around 30-70%, for JCPyV, in worldwide adult populations (Egli et al., 2009; Knowles et al., 2003).

BKPyV primo infection occurs during the first year of life once maternal antibodies wane while JCPyV primo infection happens in late childhood (Knowles, 2001; Wollebo et al., 2015). For both viruses, the first infection is mostly asymptomatic and can sometimes be associated with mild respiratory symptoms (Mäntyjärvi et al., 1973; Shah et al., 1973; Goudsmit et al., 1982; Wollebo et al., 2015).

The transmission mode of these viruses is not yet clearly identified. Detection of viral DNA in oropharyngeal tissues and saliva, for BKPyV, suggests transmission via oropharyngeal route (Goudsmit et al., 1982; Monaco et al., 1998; L. K. Jeffers et al., 2009; Comar et al., 2010). BKPyV and JCPyV were also detected in urban sewage suggesting a faecal-oral transmission inside the family or with close relatives or in less frequent cases because of polluted water sources (Bofill-Mas et al., 2000). Other less frequent routes have been documented like transplacental transmission, blood transfusion or organ transplantation, especially kidney graft (Andrews et al., 1988; Boldorini et al., 2011; Haghighi et al., 2019).

After infection, both viruses are known to persist in many different tissues. BKPyV and JCPyV are known to be latent in the renal-urinary tract, especially in kidneys, where virus reactivation can be detected mainly in urine of immunocompromised but also at low viral loads in healthy individuals (Heritage et al., 1981; Chesters et al., 1982; Polo et al., 2004; Egli et al., 2009). For JCPyV there is some evidence for the presence of the virus in lymphoid tissues and brain (Perez-Liz et al., 2008; Tan et al., 2009; Tan & Koralnik, 2010; Bayliss et al., 2011). JCPyV was also reported to be found in bone marrow but recent virome study done with NGS contradicts this (Tan et al., 2009; Toppinen et al., 2021).

However, the mechanism of viral latency is still not clearly understood for BKPyV, JCPyV, or indeed any HPyV. It could be that the virus still exhibits persistent low-level

viral replication, or that it enters a state of true latency with no viral replication and expression. Intermittent switching between these two states is also a possibility.

5.2. BKPyV associated diseases

BKPyV reactivates in immunocompromised contexts like transplantation, clinical acquired immunodeficiency syndrome (AIDS) or in the context of myeloablative cancer treatments. Immunosuppressive therapy, particularly in the case of kidney transplantation can lead to BKPyV reactivation causing diseases such as nephropathy (BKPyVAN) or ureteric stenosis, and in this case, the engrafted organ introduces the virus into the recipient. On the other hand, haemorrhagic cystitis caused by BKPyV during the aplasic phase after hematopoietic stem cell (HSC) graft occurs due to reactivation of the endogenous virus already present in the recipient. Other sites of reactivation have been described with less frequent occurrences.

5.2.1. BKPyV associated nephropathy (BKPyVAN)

In kidney graft recipients, usual symptoms of active viral replication are presence of virus in the urine, viruria, and in the blood, viremia. Around 60% of kidney recipients have viruria and in 10-30% of cases, progression to viremia can be seen. In 1-10 % kidney recipients, this infection can lead to BKPyVAN which can greatly impact the kidney function and sometimes cause graft loss (Hirsch et al., 2013b; Mengel, 2017; Sharma & Zachariah, 2020). Usually, patients with viremia higher than 10^4 cp/ml and/or viruria higher than 10^7 cp/ml, present a high risk of BKPyVAN (Hirsch, et al., 2013b).

BKPyVAN is a tubule-interstitial nephropathy that most often develops within 12 to 24 months after kidney graft. Infection starts with viral replication detectable in urine through viruria. Then, prolonged uncontrolled high viral replication in the kidney induces lysis of epithelial cells as well as denudation of the basal membrane due to the viral cytopathic effect. This leads to the release of virus in blood but also tubular fluid infiltration in the interstitium causing interstitial fibrosis and tubular atrophy (Randhawa et al., 1999; Mazalrey et al., 2015; Furmaga et al., 2021). Some of these effects can be irreversible leading to kidney graft dysfunction and sometimes graft loss (Ramos et al., 2002; Wadei et al., 2006). The risk factors to develop BKPyVAN are

dependent on the donor, the recipient, the virus and the graft (Hirsch et al., 2013b; Mazalrey et al., 2015; Ambalathingal et al., 2017; Tan et al., 2019; Wunderink et al., 2019) (**Figure 10**). BKPyVAN can also be found very rarely in non-kidney transplanted patients (Limaye et al., 2005).

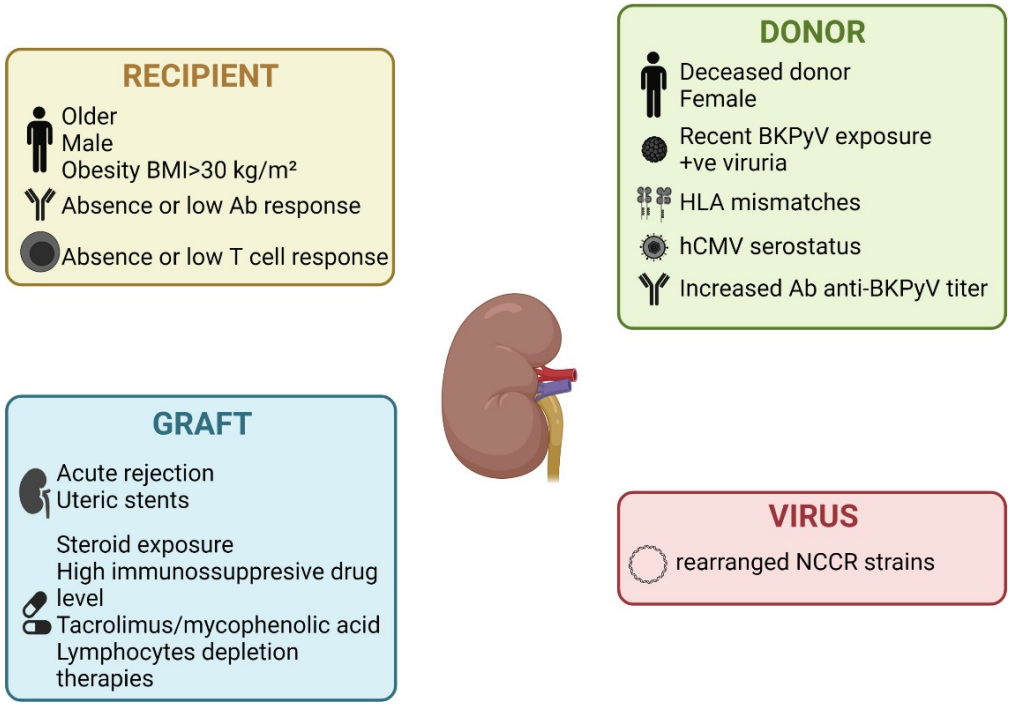

Figure 10 - Risk factors associated with BKPyVAN (inspired by Hirsch et al., 2013b; Mazalrey et al., 2015; Ambalathingal et al., 2017). Figure was made with Biorender.

5.2.2. Ureteric stenosis

Ureteric stenosis was associated with the first isolation of BKPyV, in 1973, from a kidney graft recipient (Gardner, 1973). This pathology can be found in adult and paediatric kidney recipients as well as HSC graft recipients (Mazalrey et al., 2015). However, ureteric stenosis is no longer frequently diagnosed, which could be due to improved surgical techniques and the routine use of ureteral stents (Hirsch & Steiger, 2003).

5.2.3. Haemorrhagic cystitis

Haemorrhagic cystitis (HC) associated with BKPyV was first detected in the 1980s with high viral load of BKPyV in the urine of HSC graft recipients (Arthur et al., 1986) . Patients with HC can have symptoms of dysuria, urination urgency, urination

frequency, pain and various degrees of haematuria. In severe cases, blood clot formation can be seen in the bladder resulting in kidney failure. BKPyV associated HC usually occurs at a late stage, > 2 months after HSC graft, in 5-15% of patients. In this patient population, HC can also develop due to drug toxicity of other viral infections like human cytomegalovirus (hCMV) or adenovirus (Hirsch, 2002; Dropulic & Jones, 2008). However, only around one-half of HSC recipients with BKPyV viruria developed HC. The pathogenesis of BKPyV is thought to occur in three steps. First, induction therapies for graft cause lesions of the urothelial mucosa. Second, HSC graft pre-conditioning eliminates the host antiviral response, and thus favours BKPyV reactivation and replication which leads to detection of the virus in the urine. Finally, hematopoietic reconstruction will re-establish an anti-BKPyV immunity and trigger an immune response that can lead to consequent mucosal damage and haemorrhage (Leung et al., 2005).

5.2.4. Other BKPyV associated diseases

In a strong immunosuppressive context, BKPyV has been associated with a variety of other diseases. BKPyV has been identified as the cause of meningoencephalitis in HIV/AIDS patients with manifestations of BKPyV replication in many other organs (Hirsch & Steiger, 2003). The virus was also detected in cerebrospinal fluid (CSF) of children suspected of encephalitis and adults suspected of meningitis and/or encephalitis (Behzad-Behbahani et al., 2003a; 2003b). Another particular case where BKPyV was also detected in the CSF of a kidney graft recipient suggested progressive multifocal leukoencephalopathy (PML) (Hix et al., 2004). In AIDS patients, BKPyV reactivation has been found to cause, in rare cases, pneumonitis, salivary gland diseases and retinitis (Vallbracht et al., 1993; Hedquist et al., 1999; Cubukcu-Dimopulo et al., 2000; Jeffers & Webster-Cyriaque, 2011; Burger-Calderon et al., 2014).

5.3. JCPyV associated diseases

JCPyV reactivates mostly in strongly immunocompromised states caused by AIDS, lymphoproliferative disorders, immunomodulatory therapies and sometimes kidney transplantation. The major pathology caused by JCPyV reactivation is

progressive multifocal leukoencephalopathy (PML), but other rare diseases found in the brain as well as nephropathy can be associated with JCPyV infections.

5.3.1. Progressive multifocal leukoencephalopathy (PML)

The first described cases of PML were in 1958 in patients presenting Hodgkin's disease or chronic lymphocytic leukaemia (Åström et al., 1958). Due to immunosuppression, JCPyV reactivates in the brain, more specifically in oligodendrocytes and astrocytes. Lysis of these cells due to infection leads to demyelination of the white matter in the central nervous system (CNS) and to extensive axonal dysfunction which can result in neuron loss (Ferenczy et al., 2012) (**Figure 11A & 12A**). Thus, this disease was called PML with "progressive" meaning that the disease progressively evolves to a worse state leaving irreversible brain damage, "multifocal" standing for JCPyV reactivation occurring in different part of the brain and "leukoencephalopathy" for the damage caused in the white brain matter. Clinical manifestations can be cognitive dysfunction, visual symptoms, motor weakness, speech disturbance, appendicular or gait ataxia as well as less frequently, headaches, seizures, and sensory loss. Symptoms can be dependent on the localisation of the demyelination lesions (Berger & Khalili, 2011). PML is potentially fatal, but restoration of immune response seemed to improve survival (Atkinson & Atwood, 2020).

PML was a rare disease until the mid-1980s when AIDS epidemic started (Holman et al., 1998). Since then, PML was most frequently diagnosed in this population with 2-5% of AIDS infected individuals developing the disease (Tan & Koralnik, 2010). However, introduction of highly active antiretroviral therapy (HAART), by targeting HIV and thus preserving immune function, strongly decreased the number of AIDS-related PML (Christensen et al., 2010) . The recent development of immunomodulatory drugs, especially use of monoclonal antibodies (mAbs), to treat autoimmune disorders created a new population of PML-susceptible individuals. Monoclonal antibodies are used to target specific immune factors to block their function. Natalizumab targets infiltration of leukocytes in an inflammatory context. This monoclonal antibody is usually used to treat multiple sclerosis (MS) and Crohn's disease and has been associated with PML cases in those patients. Efalizumab, an antibody specific for CD11a which prevents lymphocyte activation, proliferation, and migration, was used

to treat psoriasis but was withdrawn from the market in 2009 after the diagnosis of PML cases in treated patients. Finally, rituximab, known to target CD20+ B lymphocytes, is commonly used to treat non-Hodgkin lymphoma but also lupus, MS and in some cases rheumatoid arthritis and was also associated with PML cases in that patient population (Tan & Koralnik, 2010).

Almost all cases of PML are either associated with lymphoproliferative disorders, AIDS or immunomodulatory therapies. Only rare cases of PML were reported in other contexts like pregnancy, hepatitis cirrhosis, renal failure, dementia, dermatomyositis or in individuals without any specific diagnosis (Gheuens et al., 2010).

5.3.2. Granule Cell Neuronopathy (GCN)

JCPyV was also found to infect granule cell neurons in the cerebellum where granule cells appear to have hypochromatic and enlarged nuclei (**Figure 11B**). Death of these cells leads to cerebellar dysfunction like incoordination, gait ataxia and dysarthria (Tan & Koralnik, 2010). The first cases of this disease were found in 5%of PML patients before the HIV epidemic (Richardson & Webster, 1983). Then, it was also found associated to PML in AIDS patients, but also in HIV-positive and HIV-negative patients without PML (Pasquier et al., 2003; Tyler, 2003; Koralnik et al., 2005; Hecht et al., 2007; Granot et al., 2009). Thus, GCN can develop on its own or in association with PML.

5.3.3. Others JCPyV associated pathologies in the brain

In rare cases, JCPyV can also infect the grey matter and cause encephalitis (Blake et al., 1992; Wüthrich et al., 2009) (**Figure 11D**). Meningitis has also been found to be caused by JCPyV in both immunosuppressed and immunocompetent individuals (Tan & Koralnik, 2010; Viallard et al., 2005).

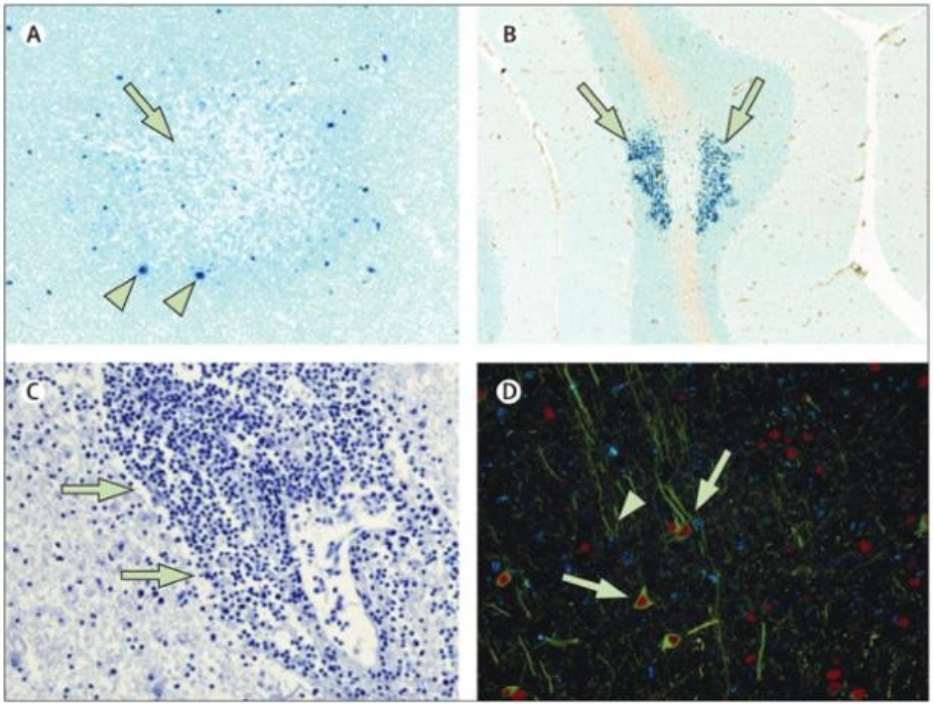

Figure 11 - Histological spectrum of JCV infection of the central nervous system. (A) Classic PML: demyelinating lesion of the white matter (arrow) surrounded by multiple JCV-infected glial cells (arrowheads). (B) JCV GCN: JCV infection of granule cell neurons (arrows). (C) PML-IRIS: marked lymphocytes penetrating the perivascular region (arrows). (D) JCV encephalopathy: JCV infected (arrow) hemispheric cortical neurons (arrowhead) (Tan & Koralnik, 2010).

5.3.4. JCPyV associated nephropathy (JCPyVAN)

In contrast to BKPyV, JCPyV associated nephropathy is rare and found in less than 1% of kidney graft recipients, although it can still cause graft dysfunction and loss. Compared to BKPyV, JCPyV reactivation does not induce high viremia despite patients having high viruria. Moreover, histologically, JCPyV seems to induce fewer cytopathic effects than BKPyV in kidney graft recipients with nephropathy (Drachenberg et al., 2007).

5.3.5. Immune reconstitution inflammatory syndrome (IRIS)

This syndrome is usually triggered by restoration of immunity after immunosuppression that can be due to HIV/AIDS, lymphoproliferative disorders, transplantation, immunomodulatory therapies and so on. The development of IRIS

depends on how fast the immunity is restored: the shorter the period is, the more likely IRIS is to occur (Harypursat et al., 2020). Associated with PML, IRIS often leads to high morbidity and mortality due to the intense immune response that usually results in tissue damage and amplification of the injury (**Figure 11C & 12C**). In PML-IRIS, patients have fewer JCPyV infected cells, but a higher number of infiltrating immune T and B cells compared to patients with PML only (Bauer et al., 2015). Killing of infected cells, particularly oligodendrocytes, by virus-specific cytotoxic T-lymphocytes (CTL) will increase the injury and exacerbate the pathology.

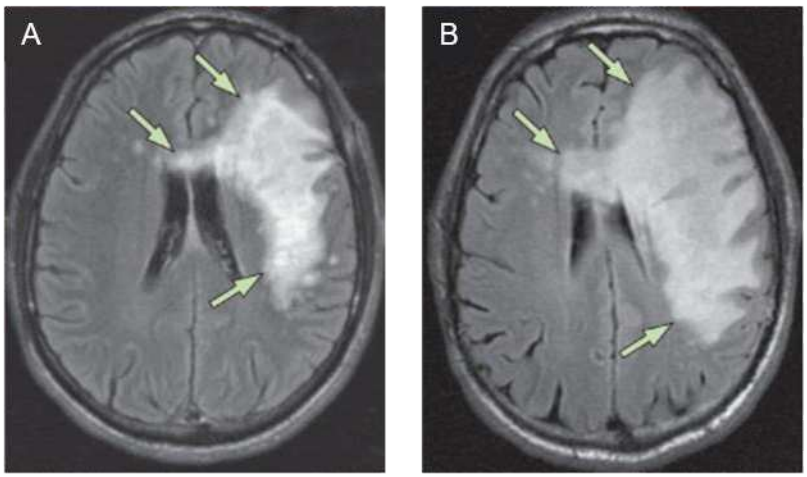

Figure 12 - PML-IRIS in an HIV+ patient. (A) PML lesion in AIDS patient before initiation of antiretroviral therapy (ART) (B) IRIS-PML with enlarged lesion 2.5 months after initiation of ART, after IRIS was treated with ART discontinuation for 2 weeks (Tan & Koralnik, 2010).

5.4. Oncogenicity of BKPyV & JCPyV

BKPyV and JCyPV tumour antigens are known to interact with many cell factors involved in the cell cycle progression and apoptosis, such as pRB proteins, making these viruses potentially oncogenic. Moreover, they have also been associated with induction of cancers in rodents, including sarcomas and brain tumours (zur Hausen, 2008). Different mechanisms have been proposed to contribute to cancer development following BKPyV or JCPyV infection. Firstly, a direct “driver” role where non-lytic infection leads to continuous expression of tumour antigens (LTAg and stAg) in all cancer cells. This is also the case for MCPyV, in which integration of the virus genome leads to expression of a truncated form of TAg that transforms the host cell. Secondly, a “hit-and-run” mechanism has been proposed, in which expression of viral

genes would participate in the initiation of the oncogenic transformation only. Actually, a recent study showed that a potential “hit-and-run” mechanism where BKPyV reactivation induces elevated levels of APOBECA and B proteins leading to APOBEC-induced damage in the urothelial genome. Thus, this study suggested that BKPyV reactivation should be considered a risk factor for bladder cancer (Baker et al., 2022). Furthermore, BKPyV and JCPyV could also have a “passenger” role where the virus can actively replicate but is not involved in the malignancy. Finally, the last role could be “innocent by-stander” where the virus is found actively replicating in cells near the cancerous site (Dalianis & Hirsch, 2013).

Due to being a hotspot of BKPyV reactivation, some case reports have described tumours in the urothelium and renal tubule tumours in kidney graft recipients associated with BKPyV, though most tumours of the urinary tract do not contain BKPyV genetic material (Alexiev et al., 2013; Papadimitriou et al., 2016; Loria et al., 2022). Similarly, JCPyV has been reported to be associated with many brain cancers, as gliomas, oligoastrocytomas, glioblastomas and medulloblastomas, due to its reactivation in this tissue. However, a large study showed very few positive samples for JCPyV DNA in those cancers (Rollison et al., 2005).

BKPyV and JCPyV have also been reported to be involved in other tumours: like prostates, lymphoma, colorectal cancer and more. However, the initial observations have not been replicated thus making these evidences not convincing (Bergh et al., 2007; Abend et al., 2009; Maginnis & Atwood, 2009; Martinez-Fierro et al., 2010; Hirsch et al., 2013a; Anzivino et al., 2015; Levican et al., 2018; Sarvari et al., 2018; Shen et al., 2021). Thus, the causative role of BKPyV and JCPyV in cancer remains to be proven. However, despite the lack of evidence of carcinogenesis in humans but sufficient evidence in experimental animals, BKPyV and JCPyV are classified as “possibly carcinogenic to humans” by the International Agency of Research on Cancer (Bouvard et al., 2012).

5.5. Immune responses

5.5.1. Innate immune response

The most important innate antiviral immune mediator is interferon (IFN) response. Type I and type II IFN induces an antiviral state in epithelial cells that blocks

polyomavirus replication (Assetta et al., 2016; Fiore et al., 2020; Wilson et al., 2011). Interestingly, BKPyV infected endothelial cells, but not renal tubular epithelial cells, express IFN-β (An et al., 2019; de Kort et al., 2017). Similarly, although DC bound and internalised BKPyV VLP and infectious particles, this did not result in DC activation or IFN secretion (Sikorski et al., 2021). Taken together, these findings indicate that endothelial cells rather than RPTEC or DC, may spark the initial innate response to BKPyV infection. Moreover, for JCPyV, type I IFN responses were shown to block infection in human foetal glial cells (Co et al., 2007; Verma et al., 2006). However, a recent study also highlighted that JCPyV stAg was an antagonist of IFN induction by targeting the RIG-I mediated innate immune pathway (Chiang et al., 2021).

5.5.2. Humoral response

Primo-infection by BKPyV and JCPyV, usually during childhood, induces production of specific neutralising antibodies with antibodies being present in more than 80% of individuals by young adulthood, for BKPyV and for around 30-60% of the worldwide population for JCPyV, and contrary to BKPyV, the different JCPyV genotypes constitute only a single serotype (Egli et al., 2009; Knowles et al., 2003). However, antibodies alone do not provide protection against BKPyV and JCPyV reactivation and diseases. Indeed, seronegative kidney recipients do not have a higher risk of BKPyV viremia compared to seropositive recipients. However, several studies have revealed the importance of the titre of BKPyV-specific antibodies at the time of graft for subsequent BKPyV viremia. Bohl et al. found that mean pre-transplant ELISA titres were lower in patients who subsequently developed viremia and the same association was found by Solis et al. who measured neutralising titres in a pseudotype assay (Bohl et al., 2008; Solis et al., 2018). Furthermore, when kidneys from donors with high anti-BKPyV titres, presumably indicating recent BKPyV replication in the donor, were transplanted into receivers with low anti-BKPyV titres, this resulted in a 10-fold higher risk of BKPyV viremia (Wunderink et al., 2017). Finally, persistent BKPyV viremia refractory to modulation of immunosuppressive therapy was found to be associated with the accumulation of neutralisation escape mutations in VP1, indicating that the antibody response exerts selection pressure on the virus in kidney recipients (McIlroy et al., 2020; Peretti et al., 2018).

For JCPyV, high levels of specific antibodies were detected in both HIV-positive and HIV-negative patients with PML indicating that the humoral response is not sufficient to prevent JCPyV reactivation (Giudici et al., 2000; Weber et al., 2001). On the other hand, the VP1 mutations that characterise PML-associated JCPyV have been associated with escape from neutralisation by cognate serum (Jelcic et al., 2016; Ray et al., 2015).

5.5.3. Cellular response

In the case of BKPyV infection, both specific CD4+ and CD8+ T-cells can be found in healthy individuals and kidney graft recipients but CD4+ T-cell responses seem to be the most predominant, triggering expression of IFN-γ, tumour necrosis factor (TNF) and granzyme B (Weist et al., 2014, 2015). In fact, polyfunctional T cells were found more frequently in patients with rapidly controlled viral replication compared to those with persistent infection, suggesting protective effects of polyfunctional T-cells (Trydzenskaya et al., 2011). Moreover, the CD4+ T-cell response was shown to mainly target VP1 while LTAg triggers CD8+ T-cells response (Binggeli et al., 2007). Interestingly, apparent CTL escape mutations have been identified in LTAg sequences curated in sequence databases, while whole BKPyV genome sequences from patients showed a significant enrichment of non-synonymous mutations in HLA-C epitopes (Domingo-Calap et al., 2018; Leuzinger et al., 2020). Both these observations are consistent with a significant antiviral function of BKPyV-specific T-cells in kidney recipients, despite their quantitatively low levels. Due to the high level of homology between BKPyV and JCPyV, prior infection by JCPyV can induce T-cell response that can cross-protect from BKPyV-associated diseases and vice versa (Krymskaya et al., 2005).

The importance of the cellular immune response in the control of JCPyV reactivation is illustrated by the observation that both Natalizumab treated MS patients and HIV+ patients have an increased risk of developing PML. MS patients taking Natalizumab have a decreased presence of lymphocytes, mostly CD19+ B-cells and CD4+ T-cells, in the CNS, due to Natalizumab's targeting of CD49d which is an important factor for the migration of these cells into the CNS. Moreover, the loss of this CD49d forces CD4+ T-cells to use different entry pathways that can alter and impact their function.

Thus, it creates an environment where the cellular response is impaired making it difficult to clear JCPyV infection and leading to potential development of PML for these patients (Mills & Mao-Draayer, 2018). In the context of AIDS, CD4+ T-cell lymphocytopenia was associated with PML (Berger et al., 1998; Marzocchetti et al., 2009). Moreover, JCPyV-specific CD4+ T-cells have been detected in the blood of PML survivors correlating with clearance of JCPyV infection (Gasnault et al., 2003).

Overall, it appears that the antibody response on its own is not enough to control persistent latent infection, which most likely relies on the induction of stable antiviral memory T cell response (Ambalathingal et al., 2017).

5.6. Diagnosis

5.6.1. Diagnosis of BKPyV infection

Real-time quantitative Polymerase Chain Reaction (PCR) is the most widely used technique for diagnosis of BKPyV infection by detection of viral DNA in urine (viruria) and blood (viremia). After transplant, screening for viral DNA should be done monthly for 3 to 6 months and then every three months during the first-year post transplantation (KDIGO Transplant Work Group, 2009). While BKPyVAN diagnosis can not be made through viruria, high levels, > 10^7 cp/mL, can be an early indication of viremia (Randhawa et al., 2004). In case of high levels of viruria, DNA screening in plasma should be performed monthly, and in patients with prolonged viremia higher than 10^4 cp/mL, a diagnosis of “presumptive BKPyVAN" can be made. However, only histological diagnosis through biopsy can validate the assumption of BKPyVAN (Hirsch et al., 2013b).

BKPyV reactivation can also be assessed by detection of urinary decoy cells which are large basophilic cells containing enlarged nuclei with ground glass appearance and a central inclusion body (Hirsch et al., 2013b). The “Polyomavirus-haufen” test can be used to predict BKPyVAN by identifying aggregates (= “haufen” in German) of BKPyV particles in urine samples due to high viral replication (Singh et al., 2009). Despite the high correlation between the “Polyomavirus-haufen” test and biopsy results, its reliance on electron microscopy means that this test cannot be routinely used in the clinical setting (Nickeleit et al., 2021a).

However, renal biopsies must be done to definitively establish a BKPyVAN diagnosis. In 2018, the Banff Working Group published a morphological classification scheme for BKPyVAN. Through histological analysis of renal biopsies, BKPyVAN severity is evaluated and classified in three classes according to the interstitial fibrosis level, given by Banff ci score, and the polyomavirus replication level, called pvl. Class 1 corresponds to the early infection with active viral replication with few infected cells and little or no fibrosis. While for class 2 and 3, clear tissue damage, like tubular atrophy or fibrosis, can be seen with clear evidence of polyomavirus replication (**Figure 13**). Biopsies are stained with haematoxylin and eosin and an antibody targeting SV40 LTAg, known to cross-react with BKPyV and JCPyV LTAg, is used for polyomavirus detection (Nickeleit et al., 2018; 2021b).

Polyomavirus nephropathy classes					
Class I		Class II		Class III	
pvl	Banff ci score	pvl	Banff ci score	pvl	Banff ci score
1	0-1	1	2-3	–	–
–	–	2	0-3	–	–
–	–	3	0-1	3	2-3

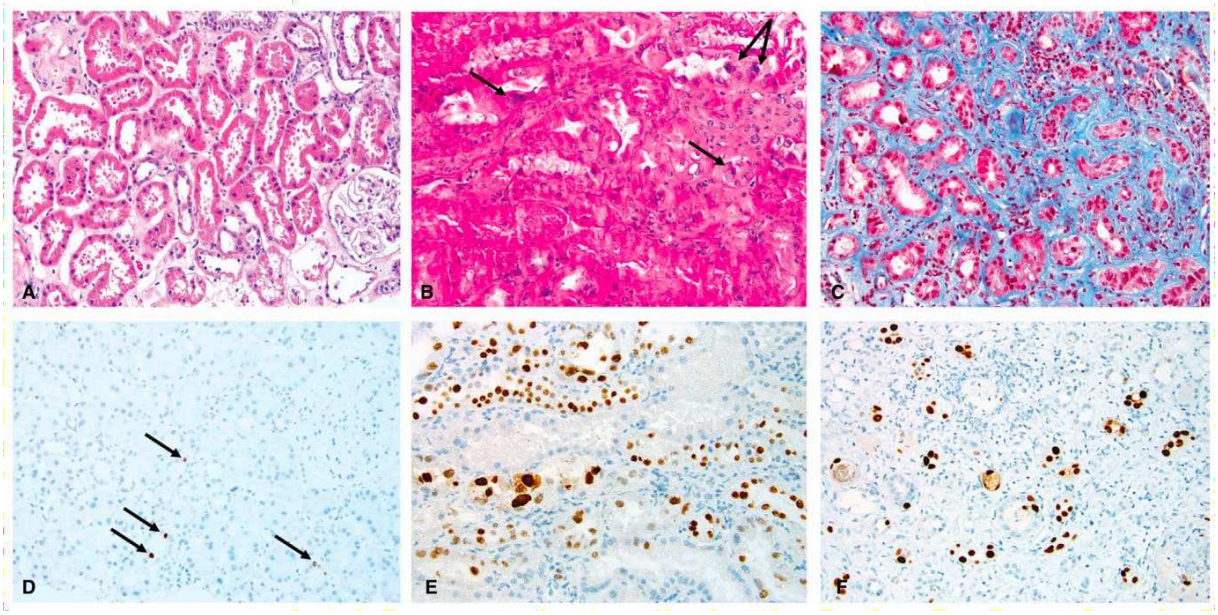

Figure 13 - Different classes of BKPyVAN. Table presenting the different BKPyVAN classes. Histology of polyomavirus nephropathy (BKPyVAN) disease classes. Class 1 (A/D): Renal cortex with no significant changes with evidence of polyomavirus replication (arrows in D). Biopsy scores: pvl = 1 & ci = 0. Class 2 (B/E): Tubules with nuclear viral inclusion bodies (arrows in B). Biospy scores: pvl: 3 & ci: 1. Class 3 (C/F): Evidence of diffuse fibrosis and tubular atrophy and polyomavirus replication. Biospy score: pvl: 3, ci: 3. (Nickeleit et al., 2021b)

5.6.2. Diagnosis of JCPyV infection

The gold standard for PML diagnosis used to be brain biopsy with histological identification of PML lesions (Koralnik, 2006). However, brain biopsies are associated with significant risks, leading to the diagnosis of PML currently depending on both imaging (MRI or CT) and detection of JCPyV DNA in the CSF by PCR. Cerebral imaging of PML patients can be variable but most have multifocal lesions with frontal or parieto-occipital localizations (Adang & Berger, 2015). Like for PML, GCN is also diagnosed through both imaging and JCPyV DNA detection. However, cerebralimages show atrophic areas with no lesions in the white matter (Koralnik et al., 2005). For the few reported cases of meningitis and encephalopathy associated with JCPyV, the diagnosis was based on clinical symptoms and detection of JCPyV DNA in CSF (Hirsch et al., 2013a). Finally, JCPyVAN is diagnosed usually by the presence of high viruria and through kidney biopsy. Both techniques are used to confirm the diagnosis since antibodies used for histology cross-react with both BKPyV and JCPyV LTAg, whereas qPCR is species-specific. Thus, JCPyVAN can be one cause of PyVAN without BKPyVAN viremia (Drachenberg et al., 2004).

5.7. Therapeutic strategies

Modulation of the immunosuppressive treatments is the standard therapeutic strategy and is applied as a curative treatment when BKPyVAN is histologically diagnosed or as pre-emptive treatment when viremia is higher than 10^4 cp/ml without biopsy confirmation. Immunosuppressive treatments after kidney graft are usually composed of three drugs: inhibitor of lymphocyte proliferation (mycophenolic acid), corticosteroids and a calcineurin inhibitor (tacrolimus or cyclosporine). In most cases, corticosteroids are either reduced or discontinued and one of the other drugs is reduced by 50%. If infection persists, the other drug is reduced or a remaining one is stopped. In more severe cases, some drugs can be replaced by another as well as decreasing doses (Hirsch et al., 2013b). Similar strategy is applied for JCPyVAN (Drachenberg et al., 2007). In case of PML, for HIV-positive patients, combination antiretroviral therapy (cART) improves the outcome of PML but still half of patients suffer from disability caused by PML or die from it (Hirsch et al., 2013a). For PML patients under monoclonal antibody therapy, withdrawal of the treatment allows

clearance of the virus but can trigger IRIS in patients (Tan & Koralnik, 2010). Corticosteroids, by their ability to control excessive immune response, are used in PML-IRIS patients with clear neurologic degradation. Finally, for JCPyV associated-GCN, meningitis or encephalitis, the therapeutic strategies are similar to those used for PML, that is reduction of immunosuppressive treatment or using cART in HIV-positive patients (Tan & Koralnik, 2010).

Many other therapeutic strategies have been tested against BKPyV and JCPyV or are in the process of being developed. A summary of them and their efficiency can be found in the following table.

Therapy		Virus/Disease	Efficiency	Clinical trials	Studies
Antivirals	Cidofovir/Brincidofovir	BKPyVAN	Good potential when combined with reduction of immunosuppression	No	(Ambalathingal et al., 2017)
	Cidofovir	PML	No survival benefit or improvement of PML-related disability on HIV+ patients	Yes	(De Luca et al., 2001, 2008; Gasnault et al., 2001)
Antibiotics	Fluoroquinolone	BKPyVAN	Efficient in vitro No effect in vivo	Yes	(Knoll et al., 2014; Lee et al., 2014)
	Mefloquine	PML	Efficient in vitro No effect in vivo	Yes	(Brickelmaier et al., 2009; Clifford et al., 2013)
Antimetabolic drug: cytarabine		PML	Stabilise PML in HIV- patient with leukemia or lymphoma	No	(Aksamit, 2001; Hou and Major, 1998)
			No survival benefit for HIV+ patients	Yes	(De Luca et al., 1999; Hall et al., 1998)
Maraviroc: CCR5 chemokine receptor inhibitor		PML	No clear positive effect	No	(Bernard-Valnet et al., 2021)
Mirtazapine: serotonin receptor blocker		PML	No clear positive effect	No	(Cettomai and McArthur, 2009; Verma et al., 2007)
Intravenous immunoglobulins (IVIG)		BKPyVAN	Antiviral efficacy when combined with reduction of immunosuppression	No	(Chan et al., 2020; Kable et al., 2017; Vu et al., 2015)
Broadly neutralising monoclonal antibodies		BKPyVAN	In clinical development		(Lindner et al., 2019) NCT05358106 & NCT04294472
Virus-Like Particles (VLPs) + IL-7		PML	PML stabilisation & decreased of JCPyV viral load	No	(Sospedra et al., 2014)
Antiviral T cell therapy		BKPyVAN & HC	Promising result with viral clearance	Ongoing	(Nelson et al., 2021) NCT04293042
		PML	Promising result with long-term survival	No	(Bernard-Valnet et al., 2021)
Immune checkpoint inhibitors		PML	No or low benefit	No	(Bernard-Valnet et al., 2021)
Recombinant human IL-7		PML	Encouraging results but development of IRIS	No	(Bernard-Valnet et al., 2021)

Table 3 - Therapeutic strategies against BKPyV and JCPyV

Research objectives

My work essentially focuses on studying interactions of BKPyV and JCPyV with their receptors, on a functional and structural level. By combining both approaches, I was able to characterise and understand more about host-virus interactions.

Three projects will be developed in this manuscript. My first project focuses on characterising the tropism and structure of different patient-derived variants of BKPyV. The second has similar objectives but focuses on the four BKPyV genotypes. Finally, my third project aimed to characterise the interaction of the JCPyV capsid with its protein receptor: the serotonin receptor 5HT2RB.

Project A: patient derived BKPyV variants tropism and structure

In kidney transplant recipients BKPyV poses a particular problem, as latent or low-level infection in the graft can reactivate after the transplant and lead to nephropathy and in extreme cases to loss of the graft. In Nantes University Hospital, we have a cohort of kidney graft recipients that have shown the accumulation of mutations in the VP1 protein of BKPyV in the context of persistent high viruria and viremia. These mutations are mostly localised in the BC-loop region of VP1, and the most frequent virus genotypes in the cohort are Ib2 and IVc2. Previous work done in the Nantes' team sequenced the different variants found in patients and preliminary analysis showed diverse infection profiles on two renal cell lines compared to the wild-type (WT) BKPyV (McIlroy et al., 2020), suggesting that the VP1 variants observed in patients could impact virus tropism. Thus, the primary aim of my doctoral thesis was to understand how the mutations in the VP1 protein could influence interactions between the virus capsid and ganglioside receptors and resolve the crystal structure of selected VP1 variants.

Project B: BKPyV genotypes tropism and structure

BKPyV can be divided in four genotypes with gI being the most prevalent in the European population followed by gIV, while gII and III are found sporadically. Most differences between genotypes are found in the BC-loop, and one previous study suggested that tropism of the genotypes could be different, based on the hemagglutinating properties of BKPyV VLPs of different genotypes (Pastrana et al., 2013). Thus, similarly to my first project, our aim was to characterise the structures of the different genotypes and find out if tropism was different between them. As part of a collaboration, my work in this project was to solve the structure of gIVc2 BKPyV VP1 pentamer and perform functional studies to clarify the sialic acid-dependency of the different genotypes.

Project C: Characterisation of JCPyV interaction with 5HT2RB

JCPyV is also an opportunistic virus and in immunocompromised patients can lead to progressive multifocal leukoencephalopathy. JCPyV is known to infect oligodendrocytes through the lacto-series c oligosaccharides which serves as attachment receptors (Neu et al., 2010). The serotonin receptors: the 5-hydroxytryptamine receptors (HT) of the 2nd family A, B and C have been identified as entry receptors for JCPyV (Assetta et al., 2019; Elphick, 2004). However, no clear characterisation of this interaction has been yet published. Thus, the aim of this project was to characterise the interaction of JCPyV with 5-HT2RB through binding assays and structural methods. Characterisation of this interaction would be a first for a polyomavirus and a protein receptor.

Research results

Before starting to present the results of the different projects, I want to clarify the implication of the different collaborators. The different glycan array studies were done by the Glycoscience Laboratory at Imperial College in London. I provided the different His-tag VP1 pentamers and there, the team made the binding assays and analysis. This work involved Dr. Antonio Di Maio, Dr. Lisete M. Silva, Dr. Ten Feizi, Dr. Wengang Chai and Dr. Yan Liu from the Glycoscience laboratory. For mass spectrometry, we collaborated with Clément Delannoy and Dr. Yann Guerardel of Université de Lilles. They performed the study on the two renal cell lines to characterise the ganglioside composition of the cell membranes which appears in the pre-print. The different patient biopsy results, also presented in the pre-print, were provided by Karine Renaudin-Autin from the “Service d'Anatomie et Cytologie Pathologique” of Nantes University Hospital. During his internship, Domenic Ebert performed N-Q variant VP1 pentamer purification and helped in solving the structure of this variant. Ngoc-Khanh Nguyen helped by producing and purifying some of the PSVs and VLPs used in this project. Franck Halary was involved in the different discussion and building of this project as well as Céline Bressollette-Bodin who is also responsible for the kidney recipient cohort from where the BKPyV variants were found and studied.

JCPyV VP1 encoding baculovirus was kindly provided by Prof. Antoine Touzé of Université de Tours. 5HT2RB encoding pFastbac and baculovirus as well as detailed purification protocol was kindly provided by Dr. Daniel Wacker of Icahn School of Medicine at Mount Sinai. The SPR measurements were done at the platform IMPACT by Mike Maillasson.

The rest of the data presented were the result of my work. I performed protein expression and purification (Pentamers, VLPs, PSVs, receptors), X-ray crystallisation, data processing and model building of the different structures presented in this manuscript. For the functional studies, I did all in cell binding and infectivity assays and ELISA. Concerning the pre-print that will be presented in the next pages, I initially wrote the first draft of this publication which was then corrected by Dorian McIlroy and Thilo Stehle. Collaborators involved in this project for glycan array screening and mass spectrometry wrote their own part in material and methods and generate some figures (Figure 1B, Figure 2A, B and C, Suppl. Figure 2 and 3).

The different structures obtained through x-ray crystallography are listed in the following table:

VP1 pentamers	Submission
gI BKPyV E73Q	Submitted. PDB ID: 8AGO
gI BKPyV VQQ	Submitted. PDB ID: 8AH0
gI BKPyV E73A	Submitted. PDB ID: 8AGH
gI BKPyV N-Q	Submitted. PDB ID: 8AH1
gIV BKPyV WT	Not submitted yet
gIV BKPyV E73K	Not submitted yet
gIV BKPyV D77N	Not submitted yet
gIV BKPyV K-N	Not submitted yet

Table 4 - Solved VP1 pentamer structures

Project A: patient derived BKPyV variants tropism and structure

The aim of this project is to understand how the mutations found in patients' BKPyV can influence the tropism and the structure of the virus. I studied different variants and part of those results led to the following publication.

1. Paper: Structural and functional analysis of natural capsid variants reveals sialic-acid independent entry of BK polyomavirus

bioRxiv posts many COVID19-related papers. A reminder: they have not been formally peer-reviewed and should not guide health-related behavior or be reported in the press as conclusive.

New Results

Follow this preprint

Structural and functional analysis of natural capsid variants reveals sialic-acid independent entry of BK polyomavirus

M.N. Sorin, A. Di Maio, L.M. Silva, D. Ebert, C. Delannoy, N.-K. Nguyen, Y. Guerardel, W. Chai, F. Halary, K. Renaudin-Autain, Y. Liu, C. Bressollette-Bodin, T. Stehle, D. McIlroy

doi: https://doi.org/10.1101/2022.07.13.499703

Structural and functional analysis of natural capsid variants reveals sialic-acid independent entry of BK polyomavirus

Authors: **M.N. Sorin[1,2]**, A. Di Maio[3], L.M. Silva[3], D. Ebert[2], C. Delannoy[4], N.-K. Nguyen[1], Y. Guerardel[4,5], W. Chai[3], F. Halary[1], K. Renaudin-Autain[6], Y. Liu[3], C. Bressollette-Bodin[1,7,8], T. Stehle[2], D. McIlroy[1,9]

1. Nantes Université, CHU Nantes, INSERM, Center for Research in Transplantation and Translational Immunology, UMR 1064, F-44000 Nantes, France
2. Interfaculty Institute of Biochemistry, University of Tübingen, Germany
3. Glycoscience Laboratory, Department of Metabolism, Digestion and Reproduction, Imperial College London, London, United Kingdom
4. Université de Lille, CNRS, UMR 8576 – UGSF - Unité de Glycobiologie Structurale et Fonctionnelle, F-59000 Lille, France
5. Institute for Glyco-core Research (iGCORE), Gifu University, Gifu, Japan
6. CHU Nantes Service d'Anatomie et Cytologie Pathologique, Medical, Nantes, France
7. CHU Nantes Laboratoire de Virologie, Nantes, France
8. Faculté de Médecine, Nantes Université, Nantes, France 9. Faculté des Sciences et des Techniques, Nantes Université, Nantes, France

1.1. Abstract

BK Polyomavirus (BKPyV) is an opportunistic pathogen that causes nephropathy in kidney transplant recipients. The BKPyV major capsid protein, VP1, engages gangliosides, lipid-linked sialylated glycans at the cell surface, to gain entry into cells. Here, we characterise the influence of VP1 mutations observed in patients with persistent post-transplant BKPyV replication on ganglioside binding, VP1 protein structure, and the tropism of the virus in two renal cell lines: 293TT and immortalised renal tubular epithelial (RS) cells. Infectious entry of single mutants E73Q, E73A and the triple mutant A72V-E73Q-E82Q (VQQ) remained sialic acid-dependent. These three variants acquired binding to a-series gangliosides, including GD1a, although only E73Q was able to infect GD1a-supplemented LNCaP or GM95 cells. Crystal structures of the three mutants showed a clear shift of the BC2 loop in mutants E73A and VQQ that correlated with the inability of these VP1 variants to infect ganglioside complemented cells. On the other hand, the double mutant K69N-E82Q lost the ability to bind sialic acid, with the K69N mutation leading to a steric clash which precludes sialic acid binding. Nevertheless, this mutant retained significant infectivity in 293TT cells that was not dependent on heparan sulphate proteoglycans, implying that an unknown sialic acid-independent entry receptor for BKPyV exists.

1.2. Introduction

BK Polyomavirus (BKPyV) is a small non-enveloped double stranded DNA virus with an icosahedral capsid formed by 72 capsomers, where a capsomer is an association of a pentamer of the VP1 protein linked internally to a single copy of either the VP2 or the VP3 proteins. BKPyV is known to interact with the urothelium and kidney epithelium through the gangliosides GT1b and GD1b but also via other b-series gangliosides (Shinohara et al., 1993; Low et al., 2006; Neu et al., 2013), which are glycosphingolipids carrying one or multiple sialic acids. The crystal structure of a BKPyV VP1 pentamer in interaction with GD3, shows that multiple loops at the surface of the VP1 form a pocket that directly interacts with the α2,8-disialic acid motif of the b-series gangliosides (Neu et al., 2013).

BKPyV is an opportunistic virus with a prevalence of 80% in the worldwide population (Knowles et al., 2003; Egli et al., 2009). Usually, infections occur asymptomatically during childhood and then lead to latency in kidneys. Active viral replication appears to be suppressed by the host, because in immunosuppressive contexts like solid organ or hematopoietic stem cell transplants, BKPyV can reactivate (Hirsch and Steiger, 2003; Hirsch, 2005). This is a particular issue in the case of kidney transplant, where replication in the engrafted kidney results in the secretion of BKPyV in urine (viruria) and the presence of BKPyV DNA in the blood (DNAemia). These parameters are followed clinically as non-invasive markers to evaluate the state of the infection in the graft. Viruria higher than 10^7 cp/mL and DNAemia greater than 10^4 cp/mL are associated with BKPyV-associated nephropathy (BKPyVAN), that must be confirmed through biopsy (Hirsch et al., 2013; Nickeleit et al., 1999). Persistent and uncontrolled BKPyV replication can lead to kidney graft dysfunction and ultimately loss of the graft (Ramos et al., 2002; Drachenberg et al., 2007; Viscount et al., 2007). Usually, the therapeutic strategy is to re-establish the host immune response against BKPyV by modulating the immunosuppressive treatments without endangering the graft (Babel et al, 2011). However, for approximately 25% of BKPyVAN patients, high-level BKPyV replication persists (Nickeleit et al., 2018) despite immunosuppressive treatment modulation, and these are the patients with the highest risk of subsequent graft loss (Nickeleit et al., 2021). Persistent high-level BKPyVAN (Randhawa et al., 2002) or DNAemia is accompanied by the accumulation of mutations in the VP1 capsid protein which cluster around the sialic-acid binding pocket (McIlroy et al., 2020).

These mutations appear to be caused by viral genome editing by host APOBEC3 enzymes and lead to neutralisation escape (Peretti et al., 2018), a model in which host innate immune responses supply the mutations that are then selected by the adaptive response. In previous work, we found that VP1 mutations also modified the infectivity of pseudotyped particles, suggesting that neutralisation escape mutations could also modify BKPyV tropism (McIlroy et al., 2020).

In this study, we focus on four variant forms of the VP1 protein coming from three kidney recipients who experienced persistent BKPyV replication after graft despite immunosuppressive treatment modulation. Viruses sampled sequentially from these patients accumulated multiple mutations in the BC-loop region of the VP1 protein, which is involved in the direct interaction of the virus with sialic acids. The BC-loop can be divided in two parts: BC1 and BC2 loops where each part faces in different directions (Neu et al., 2013). Through both functional assays and structural studies, we investigated how these mutations influence both the tropism and the structure of BKPyV and were able to reveal the involvement of a sialic-acid independent receptor in BKPyV infection.

1.3. Materials & Methods

Patients and clinical samples

Patients in the present study were transplanted between 2011 and 2014 and had previously been included in a prospective observational study approved by the local ethics committee and declared to the French Commission Nationale de l'Informatique et des Libertés (CNIL, n°1600141). All patients gave informed consent authorising the use of archived urine samples, blood samples and biopsies forresearch protocols. Anonymised clinical and biological data for these patients were extracted from the hospital databases. BKPyV VP1 mutations occurring in these patients have been previously described (McIlroy et al., 2020). PyVAN was documented by immunohistochemical staining with mouse monoclonal anti-SV40 T Antigen (clone PAb416, Sigma Aldrich - Saint-Quentin-Fallavier France) diluted 1: 50 with polymer-based EnVision FLEX detection system (Dako K8021, les Ulis - France) utilising onboard Dako Omnisautomate OMNIS (Dako, Les Ulis - France).

Protein expression and purification

VP1 pentamer were produced using plasmid pET15b expression vector encoding BKPyV VP1 mutant amino acid sequences from positions 30-300 with an N-terminal hexahistidine tag (His-tag) and a thrombin cleavage site (BioCat Gmbh). The protein was expressed in *E.coli* BL21 DE3 by IPTG induction. Proteins were purified first by nickel affinity chromatography using a 5 mL HisTrap FF crude column (Cytiva). After protein sample loading, the column was washed with 20 mM Tris pH 7.5, 250 mM NaCl, 10 mM imidazole and 10% glycerol, and proteins were eluted by applying a gradient of elution buffer composed of 20 mM Tris pH 7.5, 250 mM NaCl, 500 mM imidazole and 10% glycerol. For glycan array analysis, the His-tag was retained while for crystallisation this tag was cleaved with 10 U/mg of thrombin protease (Cytiva) for 24h at 20°C with agitation. Cleaved and uncleaved pentamers were finally purified by size-exclusion chromatography on a Superdex 200 16/600 column (Cytiva) by eluting protein with 20 mM HEPES pH 7.5 and 150 mM NaCl.

Crystallisation and structure determination

BKPyV VP1 pentamers were concentrated to 3-4 mg/mL and crystallised at 20°C by hanging drop vapour diffusion against reservoir solutions of 10-18 % PEG 3.350, 0.1 M HEPES pH 7.5, 0.1- 0.3 M LiCl (drop size 1 µL of protein/1 µL of reservoir). Crystals were harvested and cryoprotected in reservoir solution supplemented with 20 to 25 % of glycerol for several seconds before flash-freezing them in liquid nitrogen. Diffraction data were collected at the PXIII beamline of the Swiss Light Source of the Paul Scherrer Institut (Villigen, CH) and processed with XDS (Kabsch, 2010). Structures were solved using molecular replacement with Phaser (CCP4) (Winn et al., 2011) using the wild-type (WT) BKPyV VP1 structure (PDB: 4MJ1) as a model. Refinement was done using Phenix (Liebschner et al., 2019) and the model was built and adjusted in Coot (Emsley et al., 2010).

Cell culture

HEK 293TT cells, purchased from the National Cancer Institute's Developmental Therapeutics Program (Frederick, Maryland, USA), were grown in complete DMEM (ThermoFisher) containing 10% FBS (Gibco), 100 U/mL penicillin, 100 µg/mL streptomycin (Dutscher), 1x Glutamax-I (ThermoFisher) and 250 µg/mL Hygromycin B (Sigma). RS cells (Evercyte, Vienna, Austria) were grown in Optipro (ThermoFisher) containing 100 U/mL penicillin, 100 µg/mL streptomycin (Dutscher), 1x Glutamax-I (ThermoFisher). GM95 cells purchased from the RIKEN BRC cell bank were cultured in DMEM with 10% FBS (Gibco), 100 U/mL penicillin, 100 µg/mL streptomycin, and 1x Glutamax-I (ThermoFisher), and LNCaP cells were grown in RPMI medium supplemented with 10% FBS (Gibco) 100 U/mL penicillin, 100 µg/mL streptomycin (Dutscher), and 1x Glutamax-I (ThermoFisher). Cells were maintained at 37°C in a humidified 5% CO2 incubator and passaged at confluence by trypsinisation for 10 minutes with 1x TrypLE Express (ThermoFisher).

VLP production

BKPyV virus-like particles (VLPs) were prepared following the protocols developed by the Buck lab with slight modifications (Pastrana et al., 2012). Briefly, 1.10^7 HEK 293TT cells were seeded in a 75 cm^2 flask in DMEM 10% FBS without antibiotics, then transfected using Lipofectamine 2000 reagent (ThermoFisher)

according to manufacturer's instructions. A total of 36 µg VP1 plasmid DNA was mixed with 1.5 mL of Opti-MEM I (ThermoFisher). 72 µL of Lipofectamine 2000 was diluted in 1.5 mL of Opti-MEM I and incubated for 5 min at room temperature prior to mixing with the diluted plasmid DNA. After 20 min at room temperature, 3 mL of DNA-Lipofectamine complexes were added to each flask containing pre-prepared 293TT cells.

Cells were harvested 48h post transfection by trypsinisation and washed once in PBS then resuspended in one pellet volume ("v" µL) of PBS, then mixed with 0.4v µL of 25 U/mL type V Neuraminidase (Sigma). After 15 min at 37°C, 0.125v µL of 10% Triton X-100 (Sigma) was added to lyse cells for 15 min at 37°C. The pH of the lysate was adjusted by addition of 0.075v µL of 1M ammonium sulphate, or sodium bicarbonate if VLPs were to be fluorescence-labelled before ultracentrifugation, then 1 µL of 250 U/µL Pierce Nuclease (Pierce) was added to degrade free DNA. After 3h at 37°C, lysates were adjusted to 0.8M NaCl, incubated on ice for 10 min and centrifuged at 5000g for 5 min at 4°C. Supernatant was transferred to a new tube and pellet was resuspended in 2 pellet volumes of PBS 0.8M NaCl, then centrifuged. The second supernatant was combined with the first, then pooled supernatant was re-clarified by centrifuging. Cleared lysate from a T75 flask was labelled with 50 µg Alexa Fluor 647 succinimidyl ester (ThermoFisher Ref A20006) for 1 hour at room temperature. Labelled or unlabelled lysate was layered onto an Optiprep 27%/33%/39% gradient (Sigma) prepared in DPBS/0.8M NaCl, then centrifuged at 175 000 g at 4°Covernight in a Sw55TI rotor (Beckman). For labelled VLPs, visible bands were harvested directly, while for unlabelled VLPs, tubes were punctured with a 25G syringe needle, and ten fractions of each gradient were collected into 1.5 mL microcentrifuge tubes. 6.5 µL of each fraction was kept for SDS-PAGE to verify VP1 purity and determine peak fractions for pooling, then PBS 5% bovine serum albumin (BSA) was added to each fraction to a final concentration of 0.1% BSA as a stabilising agent. Peak VP1 fractions were pooled, then the VP1 concentration of each VLP stock was quantified by migrating 5µL on SDS-PAGE, then quantifying the VP1 band by densitometry using a standard curve constructed from a series of 5-fold dilutions of BSA starting at 5 µg/well.

Pseudovirus production

BKPyV and HPV16 pseudovirus (PSV) particles were prepared following the protocols developed by the Buck lab with slight modifications (Pastrana et al., 2012). Briefly, cell preparation and transfection were performed similarly to BKPyV VLP production. However, instead of transfecting only VP1 plasmid, a total of 36 µg plasmid DNA consisting of 16 µg VP1 plasmid, 4 µg ph2b, 8 µg ph3b and 8 µg pEGFP-N1 was transfected into 293TT cells. 48h after transfection, producer cells were collected by trypsinisation. The pellet was washed once in cold PBS then resuspended in 800 µL hypotonic lysis buffer containing 25 mM Sodium Citrate pH 6.0, 1 mM $CaCl_2$, 1 mM $MgCl_2$ and 5mM KCl. Cells were subjected to sonication in a Bioruptor Plus device (Diagenode) for 10 minutes at 4°C with 5 cycles of 1 min ON / 1 min OFF. Type V neuraminidase (Sigma) was added to a final concentration of 1 U/mL and incubated for 30 min at 37°C. 100 µL of 1M HEPES buffer pH 7.4 (ThermoFisher) was added to neutralise the pH, then 1 µL of 250 U/µL Pierce Nuclease (Pierce) was added before incubation for 2 hours at 37°C. The lysate was clarified by centrifuging twice at 5000 g for 5 min at 4°C and PSV was purified in an Optiprep gradient as described for VLP production. After ultracentrifugation and fraction collection, 8 µL of each fraction was removed for qPCR and the peak fractions were pooled, aliquoted and stored at -80°C for use in neutralisation assays.

For quantification of pEGFP-N1 plasmid, 5 µL of each fraction was mixed with 5 µL of proteinase K (stock of 2 mg/mL) and 40 µL of sterile water. This solution was incubated at 55°C for 60 min followed by 95°C for 10 min. Then, 1 µL of the solution was used for qPCR using Applied Biosystems 2x SYBR Green Mix (Applied Biosystems). Primers were CMV-F 5'-CGC AAA TGG GCG GTA GGC GTG-3' and pEGFP-N1-R 5'-GTC CAG CTC GAC CAG GAT G-3'. Thermal cycling was initiated with a first denaturation step at 95°C for 10 min, followed by 35 cycles of 95°C for 15 sec and 55°C for 40 sec. Standard curves were constructed using serial dilutions from 10^7 to 10^2 copies of the pEGFP-N1 plasmid per tube.

AAV2-GFP vector was prepared by the Nantes Université CPV core facility (https://sfrsante.univ-nantes.fr/en/technological-facilities/biotherapies/cpv-core-facility).

Ganglioside supplementation

LNCaP cells were seeded at 4.10^5 cells/well in a 12-well Falcon plate for binding experiments and at 10^4 cells/well in 96-well Falcon plate for infectivity experiments.

Gangliosides GM1, GT1b, GD1b, GD1a, GT1a and GD3 (Matreya) were dissolved in chloroform/methanol/water (2:1:0.1) at 1 mg/mL and stored at -20°C. For supplementation, gangliosides in their storage solution were diluted to desired concentration in RPMI containing 20 mM HEPES, 100 U/mL of penicillin, 100 µg/mL of streptomycin and 1x Glutamax-I. Then, ganglioside solutions were sonicated 4*30s and put in open Eppendorf tubes for 3h at 37°C to allow evaporation of chloroform and methanol. Ganglioside solution was then added to cells at a final concentration of 5 µM and incubated at 37°C for 18h. Culture medium contained 1% FBS during supplementation.

For VLP binding, after ganglioside incorporation, cells were detached with trypsin/EDTA for 15 min at 37°C. Cells were seeded at 25 µL per well in a 96-well V-bottom plate and incubated for 30 min at 4°C with the different BKPyV VLPs coupled with Alexa Fluor 647. After staining, cells were washed with PBS containing 0.5% FBS by centrifuging at 2 000 rpm for 1 min, 3 times. Fluorescence was measured with a Canto II flow cytometer (Becton Dickinson).

For infectivity assays, after ganglioside supplementation, cells were washed twice with complete medium, then PSVs were inoculated. Infection was observed after 5 days by measuring GFP fluorescence with a Cellomics ArrayScan HCS reader (Thermo Scientific). The percentage of GFP+ cells was calculated using Cellomics Scan software with identical settings for all wells analysed in a single experiment. For visualisation, GFP and Hoechst fluorescence contrast was enhanced across all wells in a plate in Cellomics View software, then images of representative fields exported as .png files.

Enzymatic removal of sialic acid and glycosaminoglycans

293TT cells were seeded at 4.10^5 cells/well in a 12-well Falcon plate for binding experiments and at 10^4 cells/well in 96-well Falcon plate for infectivity experiments. 293TT cells were treated for 1h at 37°C, with 0.5U/mL of Neuraminidase V from *Clostridium perfringens* (Sigma N2876) in DMEM + 20 mM HEPES + 0.1% BSA or without Neuraminidase V for control conditions. The VLP binding protocol was the

same as previously described. For infectivity, cells were inoculated with different PSVs for 3 hours and then washed 3 times with complete medium before incubation for 72-96 hours at 37°C.

For glycosaminoglycan (GAG) removal, heparinase I/III (H2519-H8891, Merck) or chondroitinase ABC (C2905, Merck) were applied to 293TT cells for 2h in digestion medium (20 mM HEPES, pH 7.5, 150 mM NaCl, 4 mM $CaCl_2$ and 0.1% BSA) at 37°C. Cells were then used for infectivity assays as described for neuraminidase infectivity experiments.

Inhibition assays with GAGs

293TT cells were incubated with 100 µg/mL of heparin (H4784, Merck) or chondroitin sulphate A/C (C4384, Merk), followed by inoculation with PSVs. Infection was observed after 48h by measuring GFP fluorescence with Cellomics ArrayScan HCS reader (Micropicell, SFR Bonamy). HPV 16 and AVV 2 PSVs carrying eGFP plasmid were used as positive controls.

Glycan array screening

The binding specificities of the his-tagged recombinant BKPyV VP1s were analysed in the neoglycolipid (NGL)-based microarray system (Liu et al., 2012). Two versions of microarrays were used: (1) ganglioside-focused arrays featuring 26 glycolipid and NGL probes (Fig 2A-C), and (2) broad spectrum screening microarrays of 672 sequence-defined lipid-linked glycan probes, of mammalian and non-mammalian type essentially as previously described (McAllister et al., 2020). The glycan probes included in the screening arrays and their sequences are given in Supplemental Table 2. Details of the preparation of the glycan probes and the generation of the microarrays are in Supplementary Glycan Microarray Document (Supplemental Table 3) in accordance with the MIRAGE (Minimum Information Required for A Glycomics Experiment) guidelines for reporting of glycan microarray-based data (Liu et al., 2017). The microarray analyses were performed essentially as described (Khan et al., 2014; Neu et al., 2013). In brief, after blocking the slides for 1h with HBS buffer (10 mM HEPES, pH 7.4, 150 mM NaCl) containing 0.33% (w/v) blocker Casein (Pierce), 0.3% (w/v) BSA (Sigma) and 5 mM CaCl2, the microarrays were overlaid with the VP1 proteins for 90 minutes as protein-antibody complexes that

were prepared by preincubating VP1 with mouse monoclonal anti-polyhistidine and biotinylated anti-mouse IgG antibodies (both from Sigma) at a ratio of 4:2:1 (by weight) and diluted in the blocking solution to provide a final VP1 concentration of 150 µg/mL. Binding was detected with Alexa Fluor-647-labelled streptavidin (Molecular Probes) at 1 µg/mL for 30 minutes. Unless otherwise specified, all steps were carried out at ambient temperature. Imaging and data analysis are described in the Supplementary MIRAGE document (Supplemental Table 3).

Glycolipid extraction and purification

HEK-293-TT and RS cells were detached from T75 flasks and washed twice with PBS. 5.10^6 cells were lyophilized and extracted twice with $CHCl_3/CH_3OH$ (2:1, v/v) and once with $CHCl_3/CH_3OH$ (1:2, v/v) using intermediary centrifugations at 2500g for 20 min. The combined supernatants were dried under a nitrogen stream, subjected to mild saponification in 0.1 M NaOH in $CHCl_3/CH_3OH$ (1:1, v/v) at 37 °C for 2 h and evaporated to dryness. The samples were reconstituted in CH_3OH/0.1% TFA in water (1:1, v/v) and applied to a reverse phase C18 cartridge (Waters, Milford, MA, USA) on a Interchim® SPE 6.25ws WorkStation. Reverse phase cartridge was equilibrated in the same solvent. After washing with CH_3OH/0.1% TFA in water (1:1, v/v), GSL were eluted with CH_3OH, $CHCl_3/CH_3OH$ (1:1, v/v) and $CHCl_3/CH_3OH$ (2:1, v/v). The elution fraction was dried under a nitrogen stream prior to structural analysis.

Mass spectrometry analysis of GSL

Isolated glycosphingolipids were permethylated by the sodium hydroxide/DMSO slurry methods (Khoo and Yu, 2010) at room temperature for 2h under agitation. The derivatization was stopped by addition of water and the permethylated glycans were extracted in $CHCl_3$ and washed at least seven times with water. Permethylated glycosphingolipids were analysed by a MALDI-QIT-TOF Shimadzu AXIMA Resonance mass spectrometer (Shimadzu Europe, Manchester, UK) in the positive mode. Samples were prepared by mixing directly on the target 1 µL of glycosphingolipid sample, solubilized in CHCl3, with superDHB matrix solution (10 mg/mL dissolved in $CHCl_3/CH_3OH$ (1:1, v/v)) and spotted on the MALDI target. The “mid mode” for a mass range of m/z 1000–3000 was used for scanning and laser

power was set to 100, with 2 shots at each of the 200 locations within the circular sample spot.

Statistics

Significant differences seen in the different experiments were calculated through one-way ANOVA followed by Dunnet's test where one condition per experiment was used as a control group; **** $p<0.0001$, *** $p<0.001$, ** $p<0.01$, * $p<0.05$. All tests were performed using GraphPad Prism 8.

1.4. Results

VP1 variants show differing infectious profiles compared to the wild-type strain

To investigate the effect of VP1 mutations on BKPyV tropism, we selected BC-loop mutations previously identified in three patients from the Nantes University Hospital KTx cohort with persistent DNAemia caused by subtype Ib2 BKPyV (Supplemental Figure 1). Pseudoviruses carrying the following VP1 variant proteins were generated: the double mutant K69N E82Q (N-Q) from patient 3.4; the E73Q mutant and the triple mutant A72V E73Q E82Q (VQQ) from patient 3.5; and the E73A mutant observed in patient 3.9. Cell lines 293TT and RS were used to test the infectivity of all variant pseudoviruses as well as wild-type subtype Ib2 pseudovirus. These cell lines were chosen for their kidney origin and their expression of SV40 TAg for amplification of reporter gene expression. In 293TT cells, the E73Q variant was as infectious as the WT while E73A and N-Q variants showed 3-fold lower infectivity and VQQ variant was barely infectious (Fig 1A). In RS cells, the VQQ variant had equivalent, or slightly higher infectivity than WT, depending on the experiment, while infectivity of the E73A variant was slightly lower than WT. The strongest differences were observed for the N-Q variant, which was almost non-infectious in this cell line, and the E73Q variant, which showed five to ten-fold higher infectivity compared to the WT (Fig 1B).

To gain insights into the basis of the different infectious profiles that we observed of WT and variant pseudoviruses we characterised the ganglioside profiles of the 293TT and RS cell lines by mass spectrometry following organic extraction of cell membrane components. Analysis was performed by a combination of MALDI-QIT-TOF-MS and MS/MS of permethylated glycosphingolipids to establish the cellular profiles and the sequence of individual components. Both cell lines were shown to contain monosialylated GM2 and GM3 a-series gangliosides along with neutral globosides. In addition, RS cells, but not 293TT cells, specifically expressed b-series disialylated gangliosides GD2 and GD3 carrying Sia-Sia epitopes as well as lower proportions of the a-series ganglioside GD1a substituted by a single sialic acid on both internal and external Gal residues (Fig 1C). Finally, RS cells exhibited the uncommon disialylated Globo-series ganglioside DSGb5.

From these observations and knowing that the mutations are found in the BC-loop, which is directly involved in ganglioside binding, we sought to characterise their effects on glycan binding specificity.

N-Q variant infection is sialic acid-independent

Since polyomaviruses are known to interact with sialylated glycans, we tested whether the infectivity of mutant pseudoviruses was also sialic-acid dependent by infecting cells treated with type-V neuraminidase, which removes terminal α-2,3- α-2,6- and α-2,8-linked sialic acid residues (Fig 1D & E). VQQ variant infection was only performed in RS cells while N-Q variant only in 293TT because of the weak infectious capacity of each variant for the other cell line. However, E73Q and E73A variant infectivity was tested in both cell lines. In RS cells, WT, E73Q, VQQ and E73A BKPyV infectivity was significantly decreased by the removal of sialic acid, leading to a remaining infection of around 15% for WT and E73A PSVs, 50% for VQQ and 40% for E73Q PSVs. In 293TT cells, the ability of WT BKPyV to infect was also impacted by the lack of sialic acid on the cell surface with only around 10% of remaining infection for WT and E73A, and around 20% for the E73Q variant. However, the N-Q variant maintained its ability to infect 293TT cells after sialic acid removal, indicating that its infection occurs in a sialic acid-independent manner. Indeed, its infectious ability was even enhanced by sialic acid removal. Thus, another receptor must be involved to support N-Q variant infection in 293TT cells.

Variants have distinct glycan binding profiles compared to WT

BKPyV is known to use the gangliosides GD1b and GT1b as entry receptors (Low et al, 2006) but is also able to infect cells through other b-series gangliosides (Neu et al, 2013). Gangliosides of the b-series are characterised by their two sialic acids (with an α2-8-linkage) attached to the first galactose of the carbohydrate chain via α2-3-sialyl linkage as in GD3 and GD1b. This disialyl moiety interacts directly with the BKPyV capsid. To assess the binding profile of the BKPyV variants, purified variant and WT genotype I VP1 pentamers were used for glycan array screening with a ganglioside-focused array comprising 26 ganglioside-related probes, glycolipids and ganglio-oligosaccharide NGLs (Fig 2A-C). The microarray analysis revealed different binding profiles for theVP1 variants compared to WT VP1 pentamers. The WT BKPyV

binding was consistent with previously published data where signal was detected for GT1b and GD1b probes (Neu et al, 2013). A broader profile was observed for the E73A, E73Q, and VQQ variants, comprising binding signals for GD1a, GT1a, and GQ1b, as well as NGL probes GM1b-DH and GD1a-DH in addition to GT1b and GD1b. The structural difference for a-series compared to b-series gangliosides is that they carry a single sialic acid α2-3-linked to the on the first galactose from the reducing end of the carbohydrate chain (Fig 2C). These data indicate that mutations at the E73 residue of the VP1 protein led to less specific and broader binding, including gangliosides of both band a-series. The overall binding intensities for the two variants with E to Q mutation at position 73, E73Q and VQQ, were higher compared to the E73A and the WT VP1s. For the double N-Q mutant, negligible or no significant binding was observed to any of the probes included in the glycan array indicating the loss of ability to bind to sialylated glycan moieties of gangliosides for the N-Q mutant.

The five VP1 proteins were further analysed in a broad-spectrum glycan screening array encompassing 672 sequence-defined lipid-linked oligosaccharide probes, representing the major types of mammalian glycans found on glycoproteins (N-linked and O-linked), glycolipids, and proteoglycans, as well as those derived from polysaccharides of bacteria, fungi, and plant origins (Supplemental Fig 2 and Supplemental Table 2). In overall agreement with findings in the ganglioside-focused arrays, the WT, the single and the triple mutant VP1s (E73A, E73Q, and VQQ) showed binding to sialyl glycans but not to the over 400 neutral and sulphated glycan probes that do not contain sialic acids. With the repertoire of sialyl glycans included in the screening array it is clear that the E73Q and VQQ variants acquired the ability to bind to a broader range of sialyl glycans, beyond ganglioside sequences, with enhanced signal intensities compared to the WT VP1 (Supplemental Table 2). The E73A showed a binding pattern similar to that of the WT VP1 except for the additional binding to the a-series ganglioside GD1a and the NGL probe GM1b-DH observed in the focused array. Binding was not detected with the N-Q double mutant VP1 to any sialylated or non-sialylated glycans included in the screening arrays. It remains possible that carbohydrate ligands for the N-Q mutant exist but were not included in the arrayed probe library.

To corroborate the glycan array results, cellular binding assays were performed on LNCaP cells supplemented with a panel of gangliosides (GM1, GD3, GD1b, GT1b, GD1a and GT1a) with fluorescent WT, VQQ and N-Q VLPs (Fig 2D-E). WT VLPs

bound to cells supplemented with GD1b and GT1b, consistent with the known role of these gangliosides as BKPyV receptors. VQQ VLPs were able to bind all gangliosides tested except GM1, confirming the glycan array data. Stronger binding was seen for both GD1b and GT1b followed by GD1a and GT1a and then weak binding to cells supplemented with GD3 (Fig 2D-E). Also consistent with the glycan array results, N-Q VLPs did not bind any of the tested gangliosides (Fig 2D-E).

Gangliosides are not sufficient to support VQQ variant infection

To determine whether binding of the different gangliosides by WT, VQQ, E73Q and E73A variant VP1 can lead to infection, we performed infectivity assays on LNCaP and GM95 cells supplemented with gangliosides. As expected, infection was seen for WT in cells supplemented with GD1b, but also for E73Q and E73A PSVs under the same condition, and infection was also seen for E73Q when cells were supplemented with GD1a in both LNCaP and GM95 cells (Fig 2F). The ability of the E73Q variant to infect cells supplemented with GD1a was consistent with its increased infectivity in RS cells, which carried GD1a gangliosides. Surprisingly, no infection was observed for VQQ in any supplementation condition, despite its ability to bind GD1b, GD1a, and other gangliosides on the surface of cells. Hence, ganglioside binding was not sufficient for infection with VQQ variant PSV. Finally, as predicted, no infection was seen in any supplementation condition for the N-Q variant, confirming that gangliosides are not used by this variant for infectious entry (Fig 2G).

Mutations at VP1 positions 72 and 73 can lead to BC-loop flipping

To understand the impact of the mutations on the VP1 protein structure, variant structures were solved through X-ray crystallography. The single mutants E73Q, E73A, and triple mutant VQQ VP1 pentamer structures were solved at 1.85, 1.89 and 1.8 Å (Table 1). All variant VP1 pentamer structures were globally similar to the WT VP1 pentamer with a doughnut-shaped ring composed of a central pore surrounded by five VP1 monomers in five-fold symmetry. Like the WT structure, the monomers have a β-sandwich fold with jelly-roll topology. The eight β-strands (B, I, D, G and C,H, E, F) are linked by extensive loops, exposed at the surface of the protein (Fig 3A- B).

The E73Q pentamer structure was almost identical to that of the WT (r.m.s.d. of 0.5 Å), whereas the E73A mutant presenting an alanine in the same position, showed some structural changes (r.m.s.d of 1.3 Å). Indeed, a shift of the BC2-loop, which includes the E73A mutation, was clearly seen for two monomers out of the five (Fig 3C). However, two monomers retained the WT loop conformation while the last monomer seemed to have a state where both conformations are superimposed. Thus, this mutation to alanine induces a more flexible conformation for the loop compared to the WT and the E73Q single mutant. Interestingly, while the E73Q mutation on its own did not induce any structural changes, when combined with A72V, as seen in the VQQ variant, the second part of the BC-loop was switched (r.m.s.d of 1.5Å) in a similar manner to that seen in the E73A variant (Fig 3C). However, in the case of the VQQ variant, the modified orientation of the BC-loop was observed in all five VP1 monomers, not just in the two monomers seen in E73A. This suggests that mutations at position 73 on their own may not be enough to induce a clear structural change in the loop orientation, which only occurs if mutations in this position are combined with the A72V mutation at the neighbouring amino acid.

However, structural changes seen in the VQQ variant are not directly involved in the ganglioside interaction. As previously described, the double sialic part of the b-series gangliosides interacts with the BC1-loop, not the BC2-loop, as well as HI- and DE-loops (Neu et al, 2013). Thus, the structure of the VQQ variant is consistent with its ability to bind gangliosides.

K69N mutation in N-Q variant induces loss of interaction with sialic acids.

The structure of the N-Q variant VP1 pentamer was also solved at 2.01 Å (Table 1). Like the other variants, the N-Q VP1 pentamer structure was very similar to the WT VP1 pentamer (Fig 4A-B). Although no major change was observed in the backbone orientation of the BC-loop that carried the K69N and E82Q mutations, the mutation from lysine to asparagine at position 69 induced significant changes (Fig 4C). Lysine 69 is involved directly with the double sialic acid part of the b-series gangliosides by making van der Waals, salt bridge and hydrogen bond interactions through its side chain, and its replacement by asparagine leads to loss of those interactions (Fig 4D). Moreover, if gangliosides were to bind the pentamer in the same way, the asparagine

side chain would be orientated too close (1.3 Å) to the hydroxyl group on C8 of the second sialic acid, leading to a steric clash between the sialic acid and the asparagine.

WT and N-Q BKPyV do not interact with GAGs

Despite losing its ability to bind sialic acid, the N-Q variant remains infectious in the 293TT cell line, indicating that another receptor is used by this variant to enter these cells. Merkel Cell Polyomavirus (MCPyV) is known to interact with both sialylated and non-sialylated glycans for infection. Like BKPyV, MCPyV can interact with gangliosides as attachment receptors, but also heparan sulphate (HS) or chondroitin sulphate (CS) glycosaminoglycans (GAGs), as entry receptors (Schowalter et al., 2011). To test whether the BKPyV N-Q variant could interact with GAGs as an alternative entry receptor, heparin and chondroitin sulphate A/C were added to 293TT cells before and during the infection experiments. Pre-incubation with heparin effectively blocked infectious entry of HPV16 and AAV2, which are both known to use GAGs as entry receptors, whereas pre-incubation with chondroitin sulphate significantly reduced infectious entry of HPV16 (Fig 5A). In contrast, neither heparin, nor chondroitin sulphate had any effect on WT or N-Q BKPyV infectivity (Fig 5). To further confirm that GAGs are not receptors for N-Q variant capsids, 293TT cells were treated with heparinase I/III or chondroitinase ABC to remove heparan sulphate or chondroitin sulphate from the cell surface. Infection by both WT and N-Q PSVs was not inhibited by the enzyme treatment (Fig 5B).

1.5. Discussion

In this functional and structural study, we show that mutations in the BC-loop of the VP1 protein that occur in KTx recipients impact the ganglioside binding specificity of the BKPyV capsid, and we describe two very different functional patterns, illustrated by the VQQ and N-Q variants.

The N-Q variant has lost the ability to interact with sialic acids due to the mutation of lysine 69 to asparagine. In a previous study, mutation of the same lysine to serine induced a change of tropism from b-series gangliosides to GM1, known to be an SV40 receptor (Neu et al., 2013). This emphasises the essential role that amino acid 69 seems to play in the interaction with gangliosides. Pseudotypes carrying N-Q VP1 had reduced infectivity in both RS and 293TT cells, but the remaining infectivity in 293TT cells was entirely sialic-acid independent, and in fact increased after neuraminidase treatment, suggesting that an alternative receptor is involved in infectious entry of the N-Q variant. Our first candidates were the heparan sulphate and chondroitin sulphate GAGs, since it has been reported that MCPyV (Schowalter et al, 2011) and mutant JCPyV and BKPyV pseudotypes can use GAGs for infectious entry (Geoghagan et al. 2017). However, neither the addition of excess heparin or chondroitin sulphate nor the removal of HS or CS GAGs from 293TT cells had any effect on the infectivity of WT or N-Q BKPyV. Furthermore, none of the BKPyV VP1 variants bound to any of the glycosaminoglycan oligosaccharides presented on the broad spectrum glycan array. We therefore tentatively conclude that an as yet uncharacterized receptor is involved in the infectious entry of the N-Q BKPyV variant.

Mutations at VP1 residue 73 had two distinct effects on VP1 structure: first, loss of charge at the capsid surface on the lip of the sialic acid binding site, seen in the E73A, E73Q and VQQ variants; and secondly, a conformational flip of the BC2-loop with the orientation of amino acids 73 and 74 significantly shifted. Mutation of the initial glutamic acid at position 73 to glutamine in the E73Q variant did not modify the orientation of the BC-loop, while its mutation to alanine, in E73A, revealed the flexibility of this part of the BC loop. In the E73A variant crystal structure, two VP1 monomers kept their initial BC-loop conformation, two monomers had an alternative orientation of the loop, and the last monomer appeared to have both conformational states of the BC2-loop superposed. In the crystal structure of the VQQ variant, all five monomers showed the alternative, “flipped” conformation. Thus, we concluded that on its own,

mutation of amino acid 73 does not induce a stable conformational change of the loop, which requires a second mutation at position 72. The requirement for the A72V mutation in order to stabilise the alternative orientation of BC-loop region 73-75 explains the previously reported statistical association of the A72V mutation with E73 mutations in patient samples (McIlroy et al., 2020), and is consistent with the sequential appearance of VP1 mutations, first at position 73, then followed by A72V, that were seen in patients 3.5 and 3.9 (Figure S1).

Variants E73A, E73Q and VQQ all showed broader ganglioside binding (Figure 2A), indicating that negative charge at residue 73 may restrict WT BKPyV VP1 binding to b-series gangliosides, and that removing this charge is sufficient to allow binding to a-series gangliosides. On the other hand, only variant E73Q showed strongly enhanced infectivity in RS cells which, as shown by mass spectrometry, carried the GD1a ganglioside, and only variant E73Q was able to infect LNCaP and GM95 cells supplemented with GD1a. Similarly, in 293TT cells, E73Q retained infectivity equivalent to that of WT VP1, whereas both VQQ and E73A showed significantly reduced infectivity. Therefore, flipping of the BC2-loop, and not loss of negative charge at position 73, was correlated with loss of infectivity in 293TT cells. This led us to a model in which the two different structural effects of VP1 mutations at position 73 have opposite effects on infectivity: loss of charge increases infectivity, by broadening ganglioside binding, whereas BC-loop flipping reduces infectivity. These two effects explain the infectivity patterns that were observed for the different VP1 variants. In RS cells, the ability to use GD1a as an entry receptor results in the strongly increased infectivity of the E73Q variant, whereas for E73A and VQQ, enhanced ganglioside binding was balanced by a loss of infectivity due to BC-loop flipping, leading to near-WT infectivity for both variants. In 293TT cells, although the infectivity of WT, E73Q and E73A variants was sialic acid dependent, this was not due to gangliosides, since neither a- nor b-series gangliosides were present on 293TT cells (Figure 1C). Therefore, the infectivity of E73Q was not increased relative to wild type, and the negative impact of BC-loop flipping on the infectivity of E73A and VQQ variants was not compensated by increased ganglioside binding. One previous report described sialic acid dependent infection by BKPyV that was strongly impacted by tunicamycin, an inhibitor of N-linked protein glycosylation, leading the authors to conclude that an N-linked glycoprotein, rather than a ganglioside, was an entry receptor for BKPyV (Dugan et al., 2005). A receptor of this type could be involved in infectious entry in

293TT cells. In the broad-spectrum glycan screening arrays, indeed there was binding with various intensities to sialyl glycans beyond ganglioside sequences (Supplemental Table 2). These could be followed up further in future structural and functional studies. Overall, the N-Q and VQQ variants appeared to be almost mirror images of each other. The N-Q variant lost all ganglioside-binding activity but retained infectivity in293TT cells through a sialic-acid independent pathway, whereas VQQ showed enhanced ganglioside binding, but almost completely lost infectivity in 293TT cells. One plausible explanation of these observations is that the VQQ variant may have lost the ability to interact with the unknown entry receptor employed by the N-Q variant to infect 293TT cells, and that this interaction is required, in addition to sialic acid binding, for infectious entry (Figure 6). This would explain why binding and infectivity were uncoupled for the VQQ variant in both 293TT cells and ganglioside-supplemented LNCaP and GM95 cells. If this is correct, then the WT orientation of the BC-loop residues 73-74 must be critical for the interaction of the BKPyV capsid with this putative receptor.

What are the mutational and selective pressures that drive the emergence of these mutations in patients? As previously noted, the E73Q and E82Q mutations we analysed occur at optimal APOBEC3A/B editing sites (Peretti et al., 2018), however, although both the A72V and K69N mutations involve cytosine deamination, they are located in the trinucleotide context GCT, which is not an APOBEC3A/B target site. In addition, the E73A mutation involved a T>G transversion. These observations imply that additional mutagenic processes, independent of APOBEC3A/B, occur in KTx recipients. Once they arise, BC-loop mutations conferring neutralisation escape appear to be selected by the host humoral response, (Peretti et al., 2018; McIlroy et al., 2020), which explains why variants with reduced infectivity relative to WT can rise to dominance in a given individual's viral population. In terms of tissue tropism, although patient 3.4 underwent transplantectomy, due to deteriorating graft function, at 49 months post-transplant, BKPyV-infected cells could not be clearly identified in kidney tissue at this time (Supplemental Figure 1A). In contrast, PyVAN was clearly diagnosed in patient 3.9 at a time when the viral population was predominantly WT (Supplemental Figure 1C), whereas graft function was stable, with no biopsies taken, after the patient's second graft, when the E73A mutation dominated the viral population. Biopsies were not available for patient 3.5 at time points when the VQQ variant was documented, although the graft was still functional, without PyVAN at 70

months post-graft. These observations are consistent with the reduced in vitro infectivity of the VQQ and N-Q variants and suggest that BKPyV carrying the K69N mutation had an attenuated phenotype in vivo.

Our study has some important limitations, in particular the description of the structural and functional impact of BKPyV VP1 mutations remains incomplete because additional VP1 mutations accumulated in patients 3.4, 3.5 and 3.9 over time. In patient 3.5, K69M and D75N were added to the VQQ variant, and in patient 3.4 D60N and A72V were added to N-Q. However, we were unable to express the M69 V72 Q73 N75 Q82 and the N60 N69 V72 Q82 mutants as either crystallisable VP1 pentamers, VLPs or high-titre pseudotypes. It was therefore not possible to determine whether subsequent mutations induced more radical changes in virus tropism, or on the contrary, compensated for the deleterious effects on infectivity that we document in the VQQ and N-Q variants. Moreover, we were not able to generate structural data from crystals of the VQQ variant complexed with GD1a ganglioside, so the details of this molecular interaction remain to be determined. Nevertheless, the identification of a naturally occurring “sialic acid blind” VP1 variant does allow us to conclude that a sialic acid independent entry receptor for BKPyV, relevant for in vivo infection, must exist.

1.6. Acknowledgements

This work was supported by grants from the Agence Nationale de la Recherche (BKNAB ANR-17-CE17-0003), the Université Franco-Allemande (CT-12-20), the German Research Foundation DFG Research Unit FOR2327 ViroCarb, and the Wellcome Trust Biomedical Resource Grants (WT099197/Z/12/Z, 108430/Z/15/Z and 218304/Z/19/Z). The March of Dimes Prematurity Research Center grant 22-FY18-82 provided partial financial support to the Imperial College Glycosciences Laboratory. The sequence-defined glycan microarrays contain many saccharides provided by collaborators whom we thank as well as Professor Ten Feizi and other members of the Glycosciences Laboratory for their contribution in the establishment of the neoglycolipid-based microarray system. YL is grateful to Professor Barbara Mulloy and for the excellent facilities provided by Tom Frenkiel and his team (UK MRC Biomedical NMR Centre at the Francis Crick Institute) for conducting the NMR analysis of oligosaccharides for the Carbohydrate Microarray Facility over the years. For microscopy, we acknowledge the IBISA MicroPICell facility (Biogenouest), member of the national infrastructure France-Bioimaging supported by the Agence Nationale de la Recherche (ANR-10-INBS-04). TS is grateful for beam time at the Swiss Light Source (Villigen, Switzerland).

1.7. References

Drachenberg, C.B., Hirsch, H.H., Papadimitriou, J.C., Gosert, R., Wali, R.K., Munivenkatappa, R., Nogueira, J., Cangro, C.B., Haririan, A., Mendley, S., et al. (2007).Polyomavirus BK versus JC replication and nephropathy in renal transplant recipients: a prospective evaluation. Transplantation *84*, 323–330. https://doi.org/10.1097/01.tp.0000269706.59977.a5.

Dugan, A.S., Eash, S., and Atwood, W.J. (2005). An N-linked glycoprotein with alpha(2,3)-linked sialic acid is a receptor for BK virus. J. Virol. *79*, 14442–14445. https://doi.org/10.1128/jvi.79.22.14442-14445.2005.

Egli, A., Infanti, L., Dumoulin, A., Buser, A., Samaridis, J., Stebler, C., Gosert, R., and Hirsch, H.H. (2009). Prevalence of polyomavirus BK and JC infection and replication in400 healthy blood donors. J. Infect. Dis. *199*, 837–846. https://doi.org/10.1086/597126.

Emsley, P., Lohkamp, B., Scott, W.G., and Cowtan, K. (2010). Features anddevelopment of Coot. Acta Crystallogr. D Biol. Crystallogr. *66*, 486–501. https://doi.org/10.1107/S0907444910007493.

Hirsch, H.H. (2005). BK virus: opportunity makes a pathogen. Clin. Infect. Dis. Off. Publ.Infect. Dis. Soc. Am. *41*, 354–360. https://doi.org/10.1086/431488.

Hirsch, H.H., and Steiger, J. (2003). Polyomavirus BK. Lancet Infect. Dis. *3*, 611–623. https://doi.org/10.1016/S1473-3099(03)00770-9.

Hirsch, H.H., Randhawa, P., and the AST Infectious Diseases Community of Practice(2013). BK Polyomavirus in Solid Organ Transplantation: BK Polyomavirus in Solid Organ Transplantation. Am. J. Transplant. *13*, 179–188. https://doi.org/10.1111/ajt.12110.

Kabsch, W. (2010). XDS. Acta Crystallogr. D Biol. Crystallogr. *66*, 125–132. https://doi.org/10.1107/S0907444909047337.

Khan, Z.M., Liu, Y., Neu, U., Gilbert, M., Ehlers, B., Feizi, T., and Stehle, T. (2014). Crystallographic and Glycan Microarray Analysis of Human Polyomavirus 9 VP1 Identifies N-Glycolyl Neuraminic Acid as a Receptor Candidate. J. Virol. *88*, 6100–6111. https://doi.org/10.1128/JVI.03455-13.

Khoo, K.-H., and Yu, S.-Y. (2010). Chapter One - Mass Spectrometric Analysis of Sulfated N- and O-Glycans. In Methods in Enzymology, M. Fukuda, ed. (AcademicPress), pp. 3–26.

Knowles, W.A., Pipkin, P., Andrews, N., Vyse, A., Minor, P., Brown, D.W.G., and Miller, E. (2003). Population-based study of antibody to the human polyomaviruses BKV andJCV and the simian polyomavirus SV40. J. Med. Virol. *71*, 115–123. https://doi.org/10.1002/jmv.10450.

Liebschner, D., Afonine, P.V., Baker, M.L., Bunkóczi, G., Chen, V.B., Croll, T.I., Hintze,B., Hung, L.W., Jain, S., McCoy, A.J., et al. (2019). Macromolecular structure determination using X-rays, neutrons and electrons: recent developments in Phenix.
Acta Crystallogr. Sect. Struct. Biol. *75*, 861–877.https://doi.org/10.1107/S2059798319011471.

Liu, Y., Childs, R.A., Palma, A.S., Campanero-Rhodes, M.A., Stoll, M.S., Chai, W., and Feizi, T. (2012). Neoglycolipid-based oligosaccharide microarray system: preparation ofNGLs and their noncovalent immobilization on nitrocellulose-coated glass slides for microarray analyses. Methods Mol. Biol. Clifton NJ *808*, 117–136. https://doi.org/10.1007/978-1-61779-373-8_8.

Liu, Y., McBride, R., Stoll, M., Palma, A.S., Silva, L., Agravat, S., Aoki-Kinoshita, K.F., Campbell, M.P., Costello, C.E., Dell, A., et al. (2017). The minimum information requiredfor a glycomics experiment (MIRAGE) project: improving the standards for reporting glycan microarray-based data. Glycobiology *27*, 280–284. https://doi.org/10.1093/glycob/cww118.

Low, J.A., Magnuson, B., Tsai, B., and Imperiale, M.J. (2006). Identification of Gangliosides GD1b and GT1b as Receptors for BK Virus. J. Virol. *80*, 1361–1366. https://doi.org/10.1128/JVI.80.3.1361-1366.2006.

McAllister, N., Liu, Y., Silva, L.M., Lentscher, A.J., Chai, W., Wu, N., Griswold, K.A., Raghunathan, K., Vang, L., Alexander, J., et al. (2020). Chikungunya Virus Strains fromEach Genetic Clade Bind Sulfated Glycosaminoglycans as Attachment Factors. J. Virol.*94*, e01500-20. https://doi.org/10.1128/JVI.01500-20.

McIlroy, D., Hönemann, M., Nguyen, N.-K., Barbier, P., Peltier, C., Rodallec, A., Halary,F., Przyrowski, E., Liebert, U., Hourmant, M., et al. (2020). Persistent BK Polyomavirus Viruria Is Associated with Accumulation of VP1 Mutations and Neutralization Escape.
Viruses *12*, 824. https://doi.org/10.3390/v12080824.

Neu, U., Allen, S.A., Blaum, B.S., Liu, Y., Frank, M., Palma, A.S., Ströh, L.J., Feizi, T., Peters, T., Atwood, W.J., et al. (2013). A Structure-Guided Mutation in the Major CapsidProtein Retargets BK Polyomavirus. PLoS Pathog. *9*, e1003688. https://doi.org/10.1371/journal.ppat.1003688.

Nickeleit, V., Singh, H.K., Randhawa, P., Drachenberg, C.B., Bhatnagar, R., Bracamonte, E., Chang, A., Chon, W.J., Dadhania, D., Davis, V.G., et al. (2018). The Banff Working Group Classification of Definitive Polyomavirus Nephropathy: MorphologicDefinitions and Clinical Correlations. J. Am. Soc. Nephrol. *29*, 680–693. https://doi.org/10.1681/ASN.2017050477.

Nickeleit, V., Singh, H.K., Dadhania, D., Cornea, V., El-Husseini, A., Castellanos, A., Davis, V.G., Waid, T., and Seshan, S.V. (2021). The 2018 Banff Working Group classification of definitive polyomavirus nephropathy: A multicenter validation study in themodern era. Am. J. Transplant. *21*, 669–680. https://doi.org/10.1111/ajt.16189.

Nickeleit, V., Hirsch, H.H., Binet, I.F., Gudat, F., Prince, O., Dalquen, P., Thiel, G., and Mihatsch, M.J. Polyomavirus Infection of Renal Allograft Recipients: From Latent Infection to Manifest Disease. J Am Soc Nephrol 10. .

Pastrana, D.V., Brennan, D.C., Çuburu, N., Storch, G.A., Viscidi, R.P., Randhawa, P.S.,and Buck, C.B. (2012). Neutralization Serotyping of BK Polyomavirus Infection in KidneyTransplant Recipients. PLoS Pathog. *8*, e1002650. https://doi.org/10.1371/journal.ppat.1002650.

Peretti, A., Geoghegan, E.M., Pastrana, D.V., Smola, S., Feld, P., Sauter, M., Lohse, S., Ramesh, M., Lim, E.S., Wang, D., et al. (2018). Characterization of BK Polyomaviruses from Kidney Transplant Recipients Suggests a Role for APOBEC3 in Driving In-Host

Virus Evolution. Cell Host Microbe *23*, 628-635.e7. https://doi.org/10.1016/j.chom.2018.04.005.

Ramos, E., Drachenberg, C.B., Papadimitriou, J.C., Hamze, O., Fink, J.C., Klassen, D.K., Drachenberg, R.C., Wiland, A., Wali, R., Cangro, C.B., et al. (2002). Clinical courseof polyoma virus nephropathy in 67 renal transplant patients. J. Am. Soc. Nephrol. JASN*13*, 2145–2151. https://doi.org/10.1097/01.asn.0000023435.07320.81.

Randhawa, P.S., Vats, A., Zygmunt, D., Swalsky, P., Scantlebury, V., Shapiro, R., and Finkelstein, S. (2002). Quantitation of viral DNA in renal allograft tissue from patients with BK virus nephropathy1: Transplantation *74*, 485–488. https://doi.org/10.1097/00007890-200208270-00009.

Schowalter, R.M., Pastrana, D.V., and Buck, C.B. (2011). Glycosaminoglycans and Sialylated Glycans Sequentially Facilitate Merkel Cell Polyomavirus Infectious Entry.PLoS Pathog. *7*, e1002161. https://doi.org/10.1371/journal.ppat.1002161.

Shinohara, T., Matsuda, M., Cheng, S.H., Marshall, J., Fujita, M., and Nagashima, K.(1993). BK virus infection of the human urinary tract. J. Med. Virol. *41*, 301–305. https://doi.org/10.1002/jmv.1890410408.

Viscount, H.B., Eid, A.J., Espy, M.J., Griffin, M.D., Thomsen, K.M., Harmsen, W.S., Razonable, R.R., and Smith, T.F. (2007). Polyomavirus polymerase chain reaction as asurrogate marker of polyomavirus-associated nephropathy. Transplantation *84*, 340– 345. https://doi.org/10.1097/01.tp.0000275205.41078.51.

Winn, M.D., Ballard, C.C., Cowtan, K.D., Dodson, E.J., Emsley, P., Evans, P.R., Keegan,R.M., Krissinel, E.B., Leslie, A.G.W., McCoy, A., et al. (2011). Overview of the CCP4 suite and current developments. Acta Crystallogr. D Biol. Crystallogr. *67*, 235–242. https://doi.org/10.1107/S0907444910045749.

1.8. Figures

Figure 1 – Patient-derived variant of BKPyV have distinct infectious profiles
(A), (B) Infectivity assays in 293TT and RS cells. Cells were inoculated with different variants or WT PSVs. Infection was characterised by quantification of GFP+ cells. Significant differences were tested through one-way ANOVA followed by Dunnett's test with "WT" condition used as the control group **** $p<0.0001$, *** $p<0.001$, ** $p<0.01$, * $p<0.05$.
Representative images of cells infected by each PSV in both cell lines are associated with each panel.
(C) Comparison of MALDI-TOF-MS profiles of permethylated glycosphingolipids from HEK-293-TT and RS cells. GSL are present as d18:1/C16:0 (Cer*) and d18:1/C24:0 (Cer**) isomers. yellow circles, galactose; blue circles, glucose; yellow squares, N-acetylgalactosamine; purple diamonds, N-acetylneuraminic acid.
(D), (E) Percentage of remaining infection by PSVs after neuraminidase treatment in 293TT and RS cells. Representative images of cells with and without neuraminidase infected with different PSVs are associated with each panel.

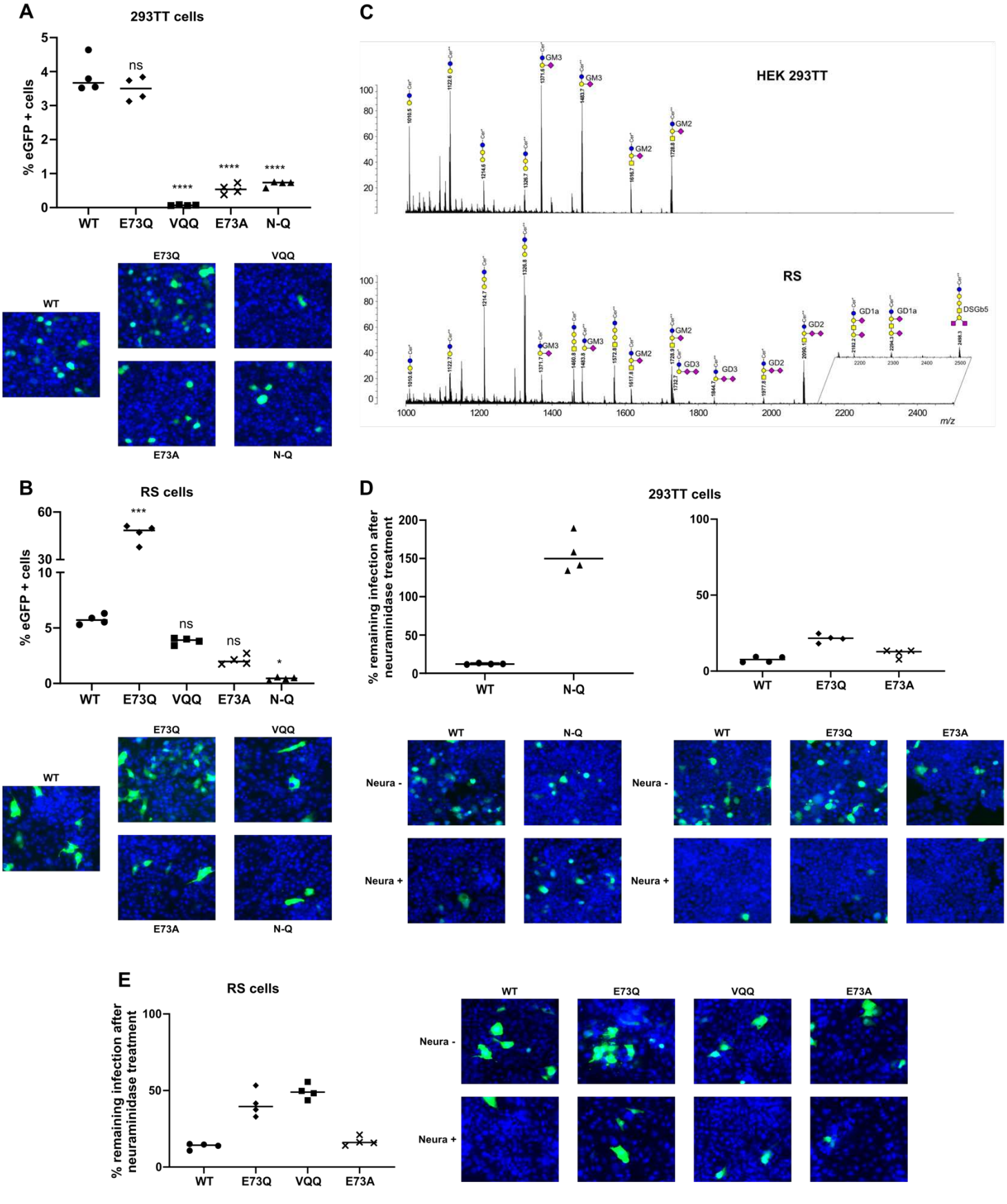
A
293TT cells
% eGFP + cells
ns
****
****
****
WT
E73Q
VQQ
E73A
N-Q
C
HEK 293TT
RS
GM3
GM2
GD3
GD2
GD1a
DSGb5
m/z
B
RS cells
% eGFP + cells
***
ns
ns
*
D
293TT cells
% remaining infection after neuraminidase treatment
Neura -
Neura +
E
RS cells
% remaining infection after neuraminidase treatment

Figure 2 – BKPyV variants have distinct glycan binding profiles

(A) Ganglioside-focused glycan microarray results shown as histogram charts of showing fluorescence intensities of binding of His-tagged BKPyV VP1s as means of duplicate spots at 5 fmol/spot. Error bars represent half of the difference between the two values.

(B) Heat maps of relative intensities and fluorescence binding scores of BKPyV VP1s (means of duplicate spots at 5 fmol/spot); 100%, the highest binding intensity in the five experiments.

(C) Sequences of oligosaccharide probes variously bound by BKPyV VP1s given as symbolic representations. Symbols used for individual monosaccharides are indicated in the key at the bottom of the panel. The full list of the 26 probes with sequences is included in Supplemental Table 3.

(D) Histograms representing fluorescent intensities of Alexa-647 variant or WT VLPs during cell-binding assays on ganglioside supplemented LNCaP cells. LNCaPs cells alone are shown in a filled grey histogram for negative control, other conditions with VLPs are represented by coloured histograms.

(E) Median fluorescence intensity comparison for binding of each VLP to LNCaP cells supplemented with different gangliosides. Significant differences were tested through one-way ANOVA followed by Dunnett's test with "no gg" condition used as the control group **** $p<0.0001$, *** $p<0.001$, ** $p<0.01$, * $p<0.05$.

(F)(G) Infectivity assays on ganglioside supplemented LNCaP or GM95 cells with different PSVs. Infection was characterised through quantification of GFP+ cell.

Research results: Project A

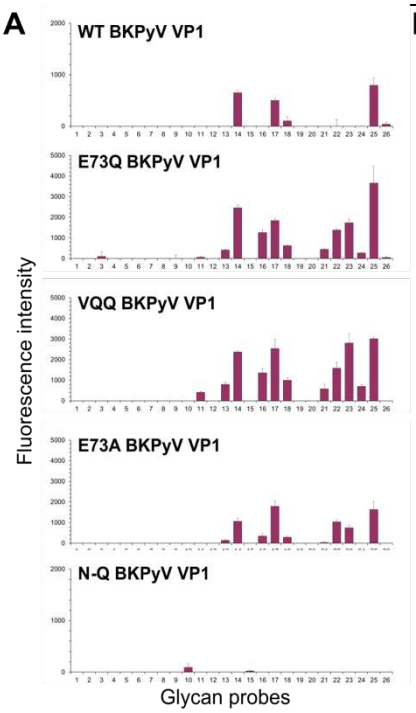

B

Pos[a]	Probe	WT Score	E73Q Score	VQQ Score	E73A Score
1	Asialo-GM2	-	-	-	-
2	Asialo-GM1	-	-	-	-
3	GM4	-	101	-	-
4	Haematoside	-	-	-	-
5	GM3	-	-	-	-
6	GM3(Gc)	-	-	-	-
7	GM1	-	-	-	-
8	GM1(Gc)	-	-	-	-
9	GM1b	-	-	-	-
10	GM2	-	-	-	-
11	GD3	-	69	414	-
12	GD2	-	-	-	-
13	GD1a	-	415	803	139
14	GD1b	652	2,460	2,375	1,065
15	GalNAc-GD1a(Ac,Gc)	-	-	-	-
16	GT1a	-	1,263	1,362	352
17	GT1b	502	1,846	2,542	1,794
18	GQ1b	105	622	1,000	291
19	Asialo-GM1-DH	-	-	-	-
20	GM1-DH	-	-	-	-
21	GM1(Gc)-DH	-	446	590	34
22	GM1b-DH	-	1,377	1,589	1,038
23	GD1a-DH	-	1,739	2,809	750
24	GD3-DH	-	271	706	-
25	GD1b-DH	796	3,665	3,013	1,633
26	GT1c-DH	42	59	-	-

Relative binding intensity: 0-10% 10-30% 30-70% 70-100%

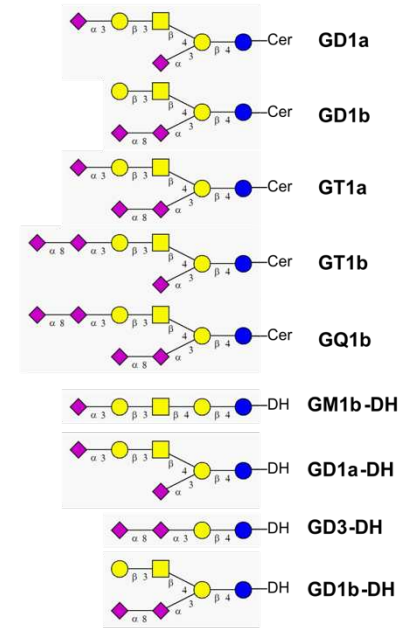

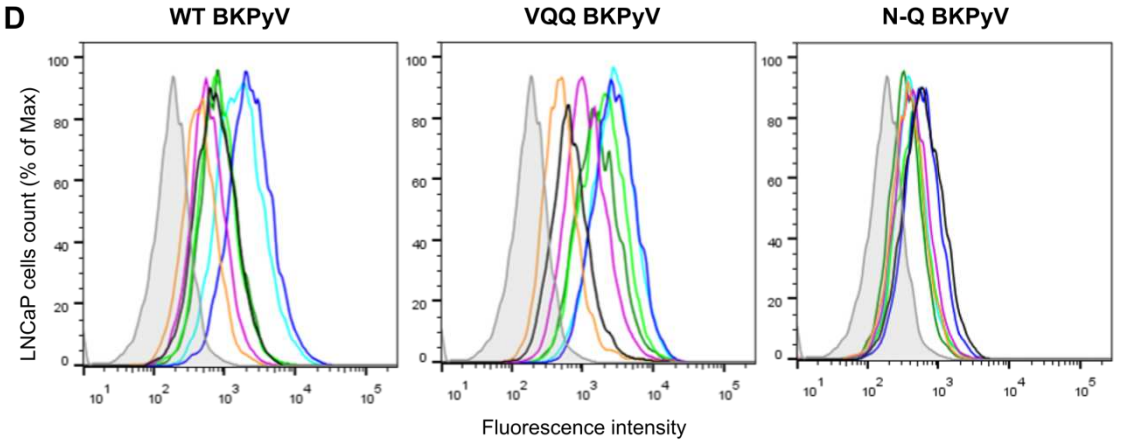

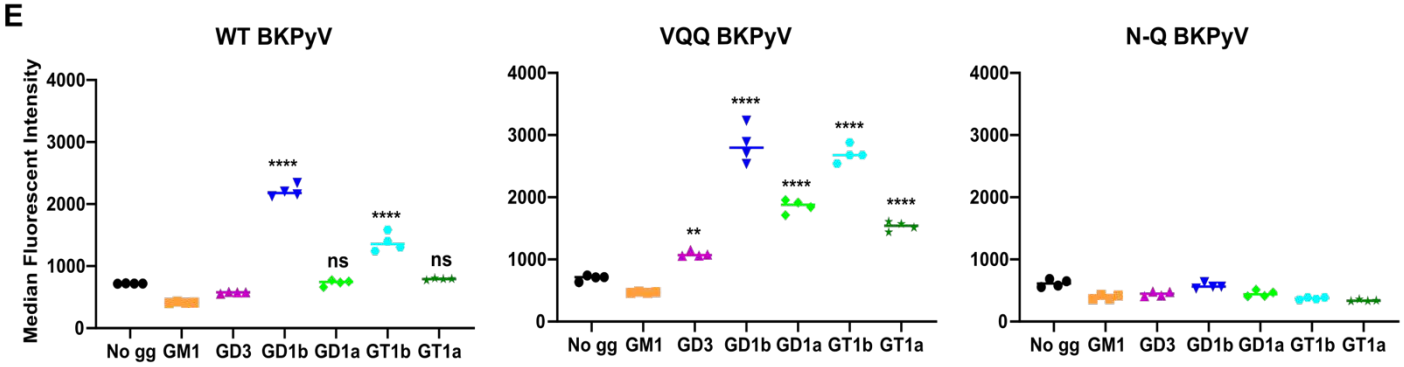

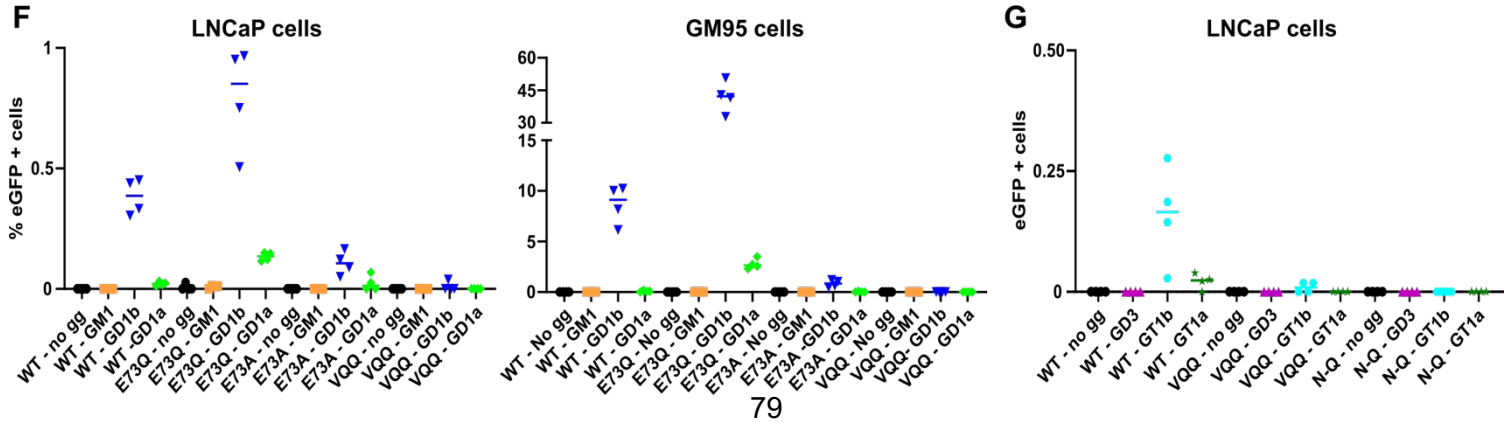

Figure 3 – Mutations of amino acids 72 and 73 lead to structural changes in the BC-loop conformation

(A) Superposition of variant E73Q, E73A and VQQ VP1 pentamer structures. One monomer for each structure is highlighted in yellow for E73Q, green for E73A and blue for VQQ.

(B) Superposition to variant VP1 pentamers with BKPyV WT VP1 pentamer in association with GD3 oligosaccharides (PD ID: 4MJ0). WT VP1 monomer is highlighted in pink and GD3 molecules are represented by yellow sticks.

(C) Zoom on the BC-loops of highlighted VP1 monomers. Amino acids 72, 73 and 82 are represented as sticks.

Figure was made with Pymol.

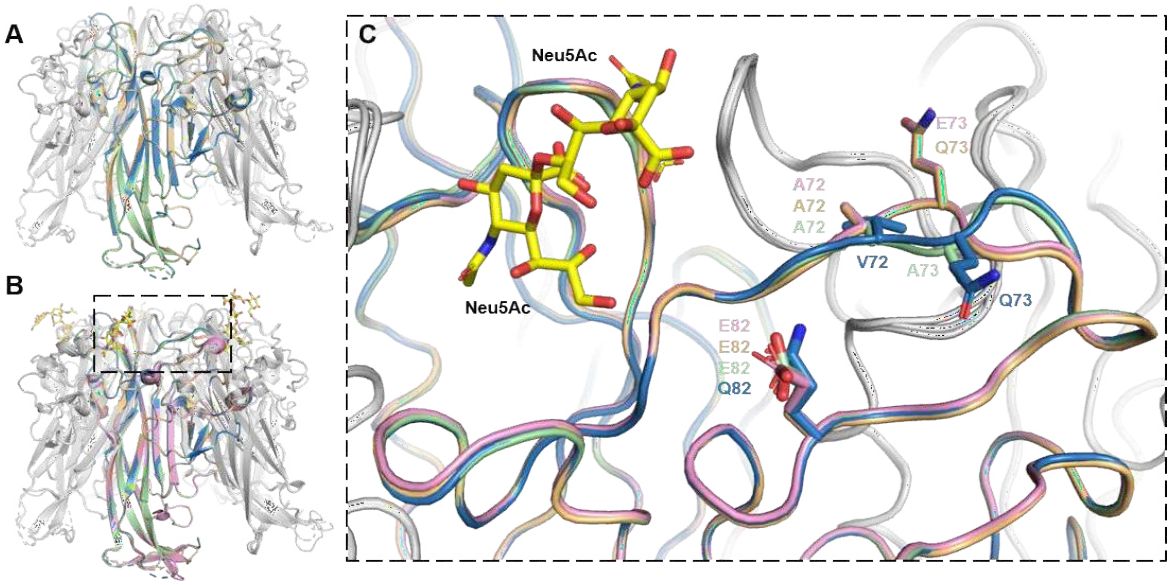

Figure 4 – Structure of N-Q VP1 pentamer

(A) Structure of N-Q VP1 pentamer. VP1 monomer is highlighted in purple.

(B) Superposition of N-Q VP1 pentamer onto WT VP1 pentamers associated with GD3 oligosaccharides (PD ID: 4MJ0). WT VP1 monomer is highlighted in pink and GD3 molecules are represented by yellow sticks.

(C) Zoom on the BC-loops of highlighted VP1 monomers. Amino acids 69 and 82 are represented as sticks.

(D) Focus on amino acids in position 69 and their interaction with Neu5Ac. Hydrogen bonds represented by black dashed lines between K69 and hydroxyl groups of Neu5Ac.

Figure was made with Pymol.

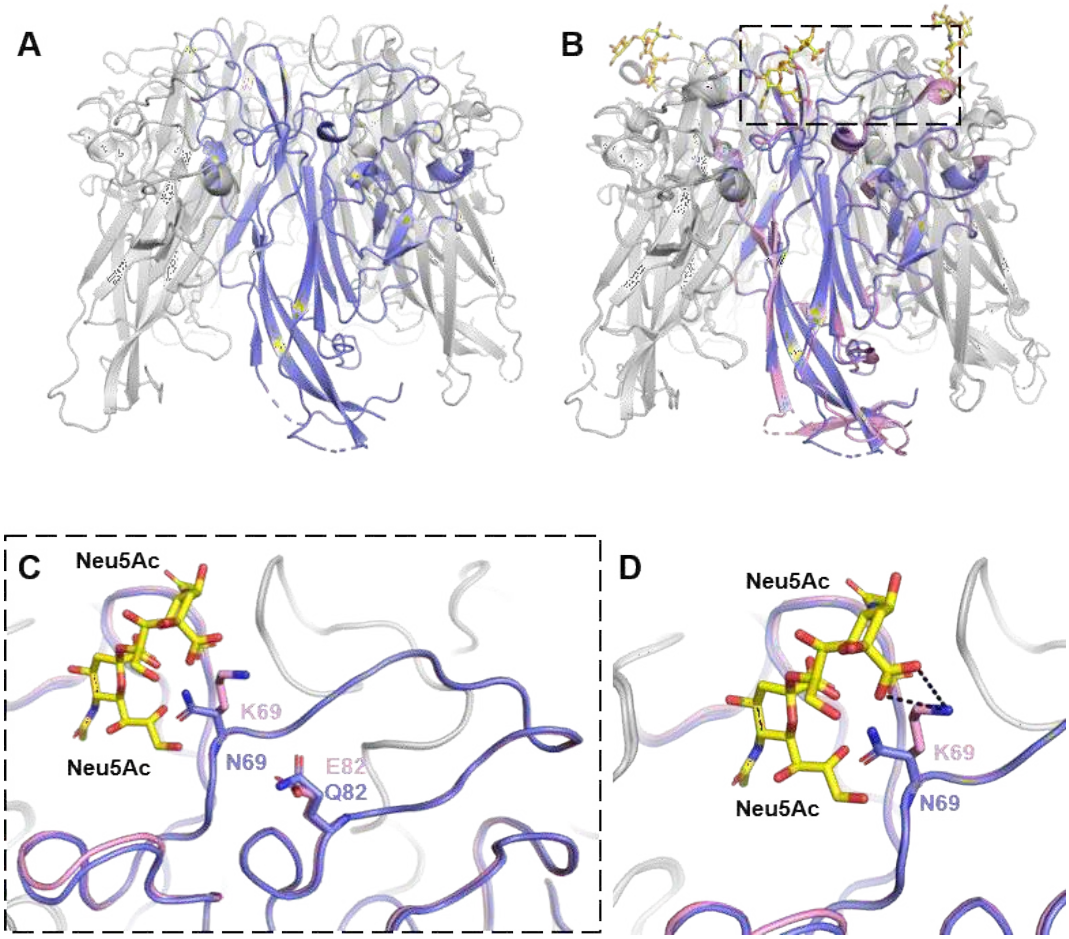

Figure 5 – N-Q does not interact with GAGs

(A) Infectivity assays in presence or not of 100 µg/ml of heparin or chondroitin sulphate A/C with BKPyV WT and N-Q PSVs. HPV 16 and AAV 2 PSVs serve as positive control. Error bars correspond to standard deviations. NT - Not tested.

(B) Infectivity assays treated or not with heparinase I/III or chondroitinase ABC with BKPyV WT and N-Q PSVs. HPV 16 and AAV 2 PSVs serve as positive control. Error bars correspond to standard deviations. NT - Not tested.

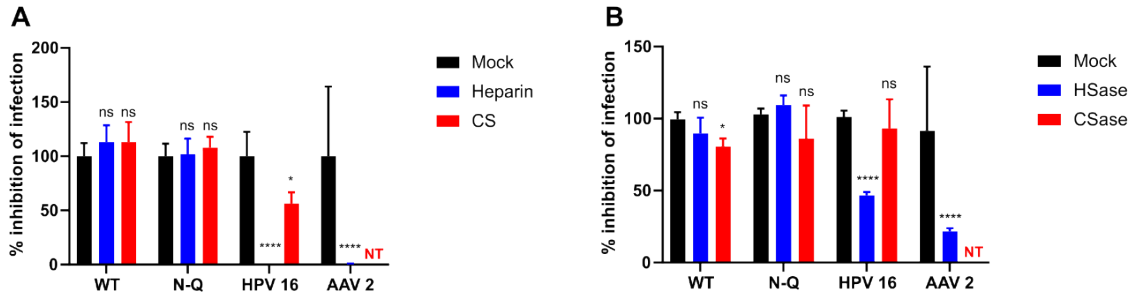

Figure 6 – Putative entry mechanisms of N-Q and VQQ variants

Figure was made with Biorender

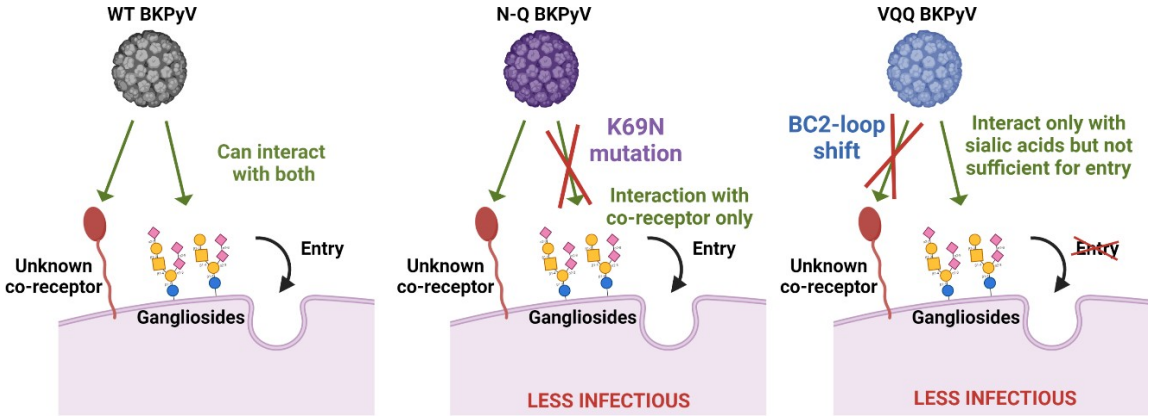

Table 1 - Data processing and refinement

Data collection	gI E73Q	gI E73A	gI A72V E73Q E82Q	gI K69N E82Q
PDB ID	8AGO	8AGH	8AH0	8AH1
Space group	P2(1)2(1)2	P2(1)2(1)2	P2(1)2(1)2	P2(1)
Unit cell length (Å)	a = 145.25 b = 153.04 c = 62.80	a = 144.49 b = 152.31 c = 62.58	a = 144.69 b = 152.60 c = 62.75	a = 60.46 b = 155.96 c = 141.32
Unit cell angle (°)	α = 90 β = 90 γ = 90	α = 90 β = 90 γ = 90	α = 90 β = 90 γ = 90	α = 90 β = 92.64 γ = 90
Pentamers/ASU	1	1	1	2
Resolution(Å)	50 - 1.85 (1.92-1.85)	50 - 1.89 (1.96-1.89)	50 - 1.80 (1.86-1.80)	50 - 2.01 (2.08-2.01)
Total reflections	1 582 082 (153 046)	1 488 272 (149 590)	1 743 972 (175 371)	1 086 928 (100 014)
Unique reflections	119 532 (11 509)	111 193 (10 995)	129 677 (12 697)	164 438 (17 100)
Rmeas (%)	17.3 (190.2)	13.2 (164.2)	14.7 (168.2)	20.8 (149.2)
Completeness (%)	99.6 (97.4)	99.9 (99.9)	99.9 (99.4)	94.8 (98.73)
CC1/2 (%)	99.9 (73.7)	99.9 (62.6)	99.9 (57.6)	99.4 (57.0)
I/σ	13.99 (1.40)	15.63 (1.72)	13.40 (1.48)	8.35 (1.29)
Refinement				
Rwork (%)	18.86	17.38	17.12	17.95
Rfree (%)	23.05	21.12	21.00	23.14
Average B factor (Å²)	31.0	33.0	29.0	31.0
RMS deviation:				
Bond lenght (Å)	0.010	0.010	0.011	0.010
Bond angle (°)	1.60	1.62	1.65	1.71
Wilson B factor (Å²)	25.8	28.6	24.6	25.9

Supplemental Table 1 – Clinical data for each patients.

Patient code	3.4	3.5	3.9
Age at KTx	64	27	56
Sex	M	M	M
Graft type	Kidney 1st graph	Kidney 1st graph	Kidney 2nd graft*
Donor	Deceased	Deceased	Living familial donor
HLA mismatches	3	4	4
Immunosuppressive drug regimen	MMF Tacrolimus	MMF Tacrolimus Corticoids	Azathioprine Tacrolimus
Log10 BKPyV glb2 neutralising titre at KTx	2.7	3.3	4.6 (before KTx 2) Serum at KTx1 not available
Log10 BKPyV glb2 neutralising titre at M12 post-KTx	4.1	5.1	4.4 (after KTx2)

*The first graft was kidney and pancreas, but the first graft ended with PyVAN.

Supplemental Table 2 - List of glycan probes in the broad spectrum glycan screening arrays, their fluorescence binding scores and relative binding intensities ('matrix') elicited with BKPyV VP1s
(Excel file: https://uncloud.univ-nantes.fr/index.php/s/GtbB9i37KSnqx7C)

Supplemental Table 3 - Supplementary glycan microarray document based on MIRAGE Glycan Microarray guidelines
(PDF file: https://uncloud.univ-nantes.fr/index.php/s/cdqfr9Ac8qyPyZd)

Supplemental Figure 1 - Left panels: Viruria, DNAemia and VP1 mutation % of NGS reads as a function of time after graft for the three kidney recipients whose VP1 variants were studied. (A) Patient 3.4; (B) Patient 3.5; (C) Patient 3.9. Right panels: SV40 TAg staining of biopsies from patients 3.4 - no significant staining; 3.5 - no significant staining; and 3.9 - focal nuclear positivity of epithelial tubular cells. Graphs were made with GraphPad Prism 8.

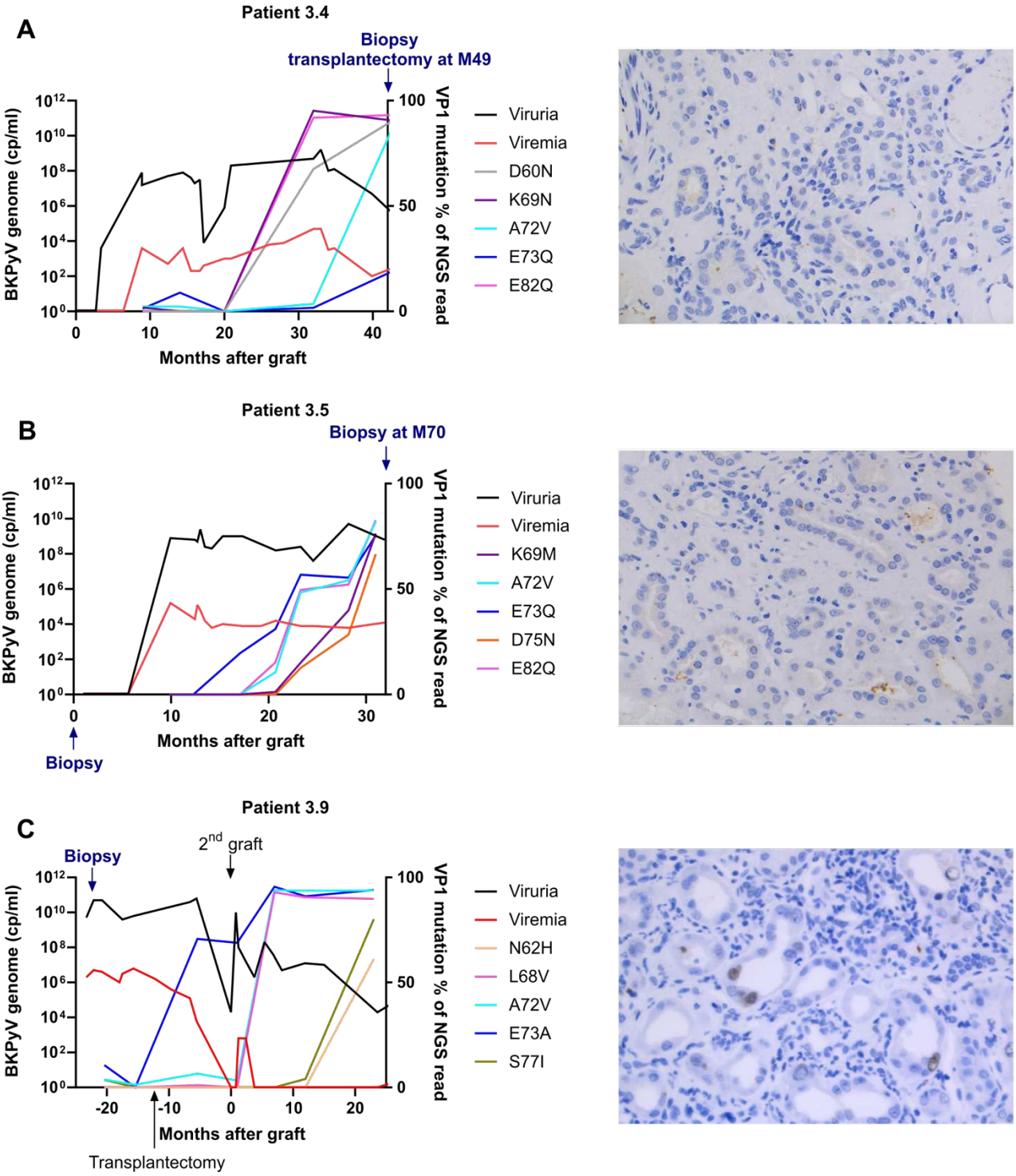

Supplemental Figure 2 - Glycan microarray screening analyses of His-tagged pentameric BKPyV VP1 proteins, WT (A), E73A mutant (B), E73Q mutant (C), VQQ mutant (D) and N-Q mutant (E). The results are the means of fluorescence intensities of duplicate spots, printed at 5 fmol per spot. The error bars represent half of the difference between the two values. In the glycan array the 672 lipid-linked probes are grouped according to sialyl linkages as annotated by the coloured panels. The list of glycan probes, their sequences and binding scores are in Supplemental Table 2.

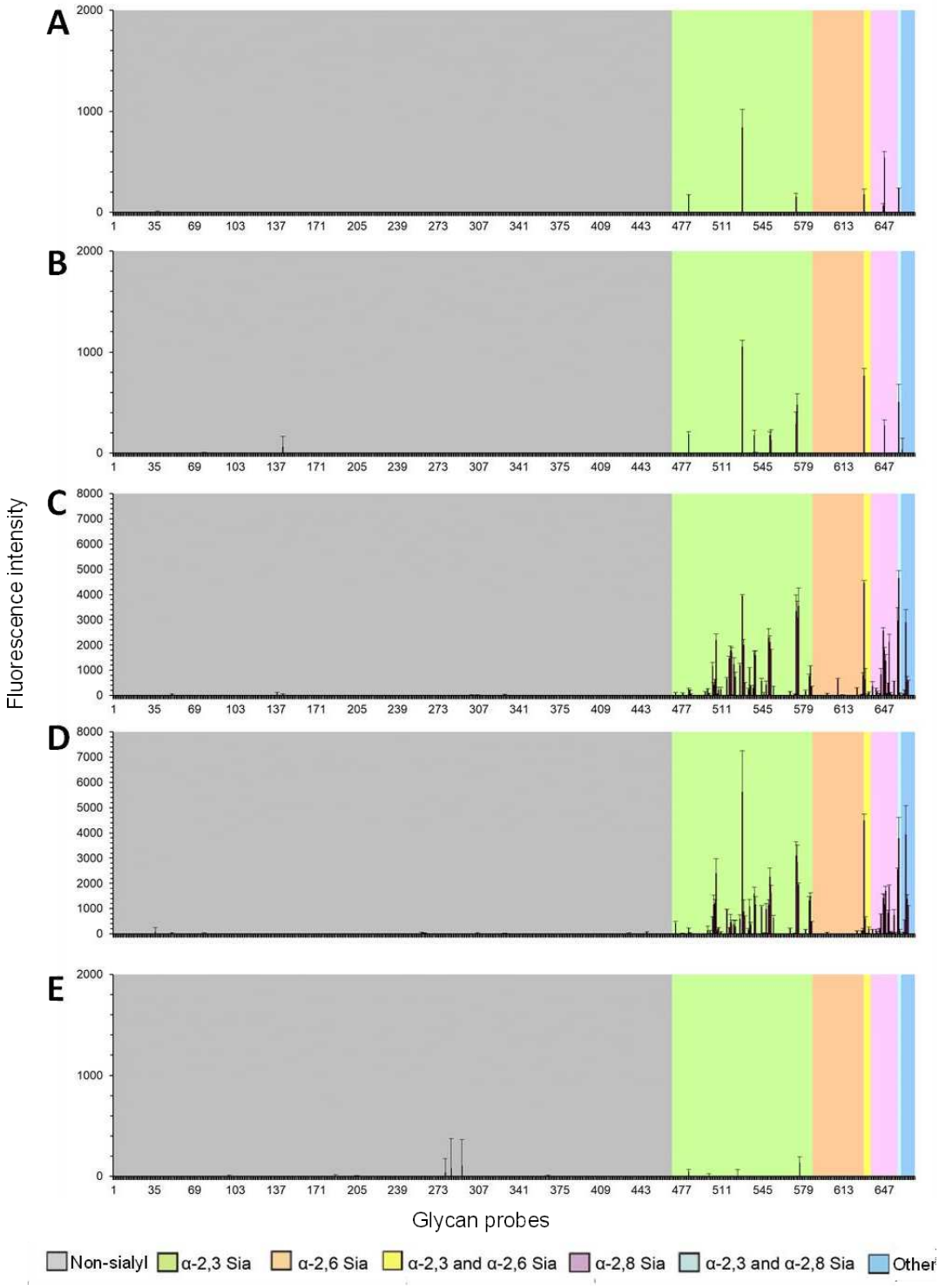

The broad glycan array screening, presented in the previous publication, also showed an interesting hit for a non-ganglioside glycan: LSTa (NeuAcα-3Galβ-3GlcNAcβ-3Galβ-4Glc) for BKPyV WT, VQQ, E73A and E73Q VP1 pentamers (**Table 5**)

Pos[a]	Probe[b]	Sequence[c]	WT BKPyV VP1		E73A BKPyV VP1		E73Q BKPyV VP1		VQQ BKPyV VP1		N-Q BKPyV VP1	
528	LSTa	NeuAcα-3Galβ-3GlcNAcβ-3Galβ-4Glc-DH	840	178	1 051	66	3 937	73	5 626	1 628	-	1

Table 5 – Glycan array screening results on a broad array for WT, E73A, E73Q, VQQ and N-Q BKPyV VP1 pentamers. Focused on LSTa probe.

2. Structural and functional analysis of other gI & gIV BKPyV variants

Other patient derived variants of gIb2 BKPyV were studied as well as variants of gIVc2 BKPyV.

A

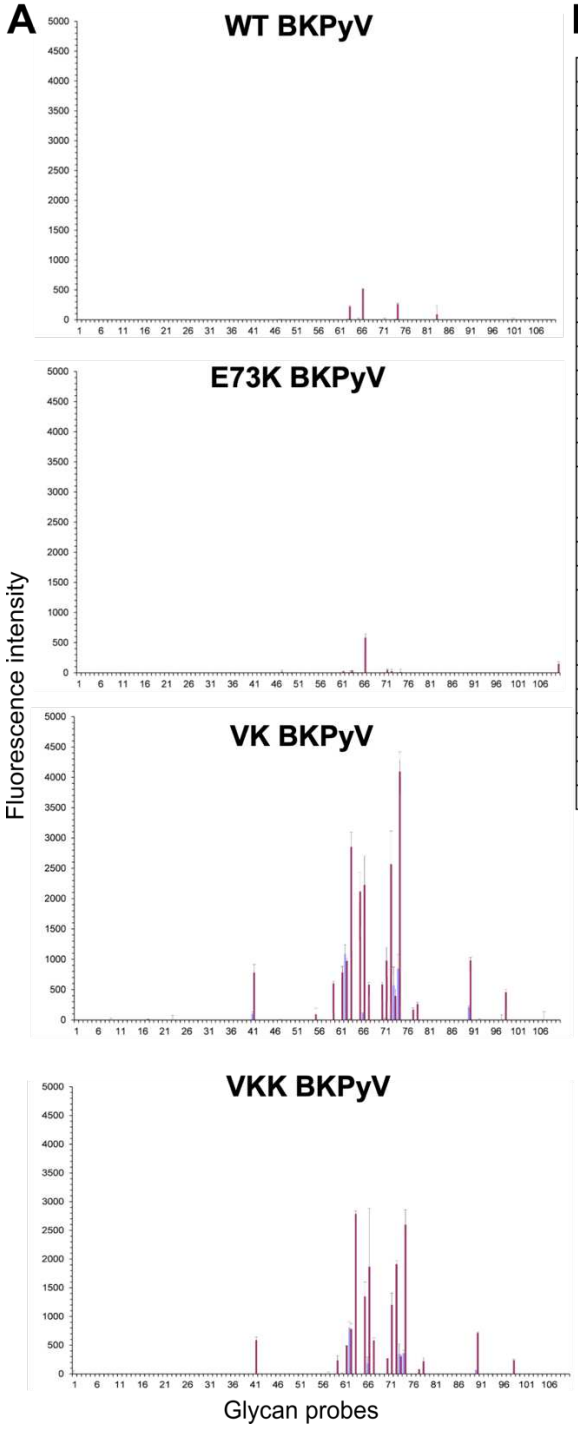

B

Position	Probe	WT BKPyV Score	E73K BKPyV Score	VK BKPyV Score	VKK BKPyV Score	MVQNQ BKPyV Score
41	LSTa	-	-	779	588	-
48	Asialo-GM2	-	-	-	-	-
49	Asialo-GM1	-	-	-	-	-
50	GM4	-	-	-	-	-
52	GM3	-	-	-	-	-
53	GM3(Gc)	-	-	-	-	-
54	GM1	-	-	-	-	-
55	GM1	-	-	94	-	-
56	GM1(Gc)	-	-	-	-	-
57	GM1b	-	-	-	-	-
58	GM2	-	-	-	-	-
59	GD3	-	-	600	235	48
60	GD2	-	-	-	-	-
61	GD1a	-	24	782	493	39
62	GD1a	-	-	977	783	46
63	GD1b	222	35	2 855	2 785	1 290
64	GalNAc-GD1a(Ac,Gc)	-	-	-	-	-
65	GT1a	10	-	2 121	1 349	137
66	GT1b	518	585	2 222	1 866	862
67	GQ1b	-	-	582	583	121
68	Asialo-GM1-Tetra	-	-	-	-	-
69	GM1-penta	-	-	-	-	-
70	GM1(Gc)-penta	-	-	585	267	-
71	GM1b-DH	8	49	980	1 204	288
72	GD1a-hexa	-	28	2 565	1 913	737
73	GD3-tetra	-	-	395	307	-
74	GD1b-DH	262	15	4 095	2 601	590
75	GT1c-DH	-	-	-	-	-

Relative binding intensity: 0-10% | 10-30% | 30-70% | 70-100%

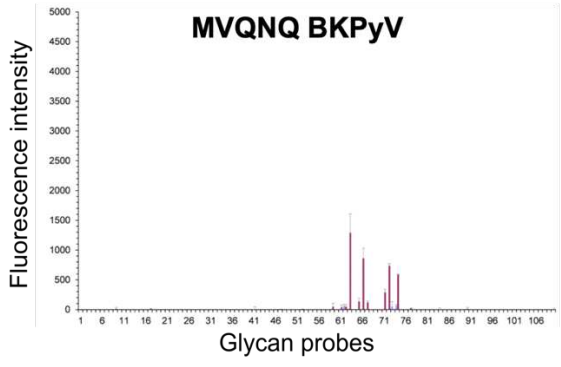

Figure 14 - Neuro-glycan and β-galactosylated glycan (BGG) array results for gI VP1 pentamer variants. (A) Diagram, for each VP1 pentamer, with average high and low fluorescent intensities for each probe. (B) Table summarising the relative binding intensity for each VP1 pentamers focusing on gangliosides.

The gIb2 K69M A72V E73Q D75N E82Q (MVQNQ) variant comes from patient 3.5 and appears at 28 months post-transplantation. In another patient (3.19) who also presented persistent viruria and viremia, a series of gI variant were also found: E73K, A72V E73K (VK) and A72V E73K E82K (VKK). As for patient 3.5, the mutations are again found at positions 72, 73 and 82. For those variants, I managed to purify stable His-tag VP1 pentamers to perform glycan array studies. Glycan array studies were again performed by the Glycoscience Laboratory at Imperial College in London. A neuro glycan β-galactosylated glycan array containing the different ganglioside probes was used. The screening showed a very similar binding profile for MVQNQ, VK, and VKK as that previously described for E73Q, E73A and VQQ. Binding to known BKPyV receptors: GT1b and GD1b is maintained and binding to other gangliosides can be seen, in particular the a-series GT1a and GD1a, but also o-series GM1b and the b- series GQ1b for VK and VKK variants. However, E73K surprisingly only showed binding to GT1b (**Figure 14**).
Other studies on those remaining variants were not performed for different reasons: time and choice to focus on the variant presented in the paper, as well as difficulty in producing VKK and MVQNQ as stable digested pentamers for crystallisation or as VLP and PSVs for functional assays.

The Nantes University Hospital kidney recipient cohort also has some patients with persistent infection presenting mutation in genotype IVc2 BKPyV. We decided to work on four variants coming from two patients: patient 2.4 who had gIVc2 E73K and gIVc2 A72V E73K (VK) variants as well as patient 3.3 with the gIVc2 D77N and R69K D77N (K-N) variants. While patient 3.3 had persistent high viruria and viremia, patient 2.4 had negative viremia but persistent high viruria over time (**Figure 15**).

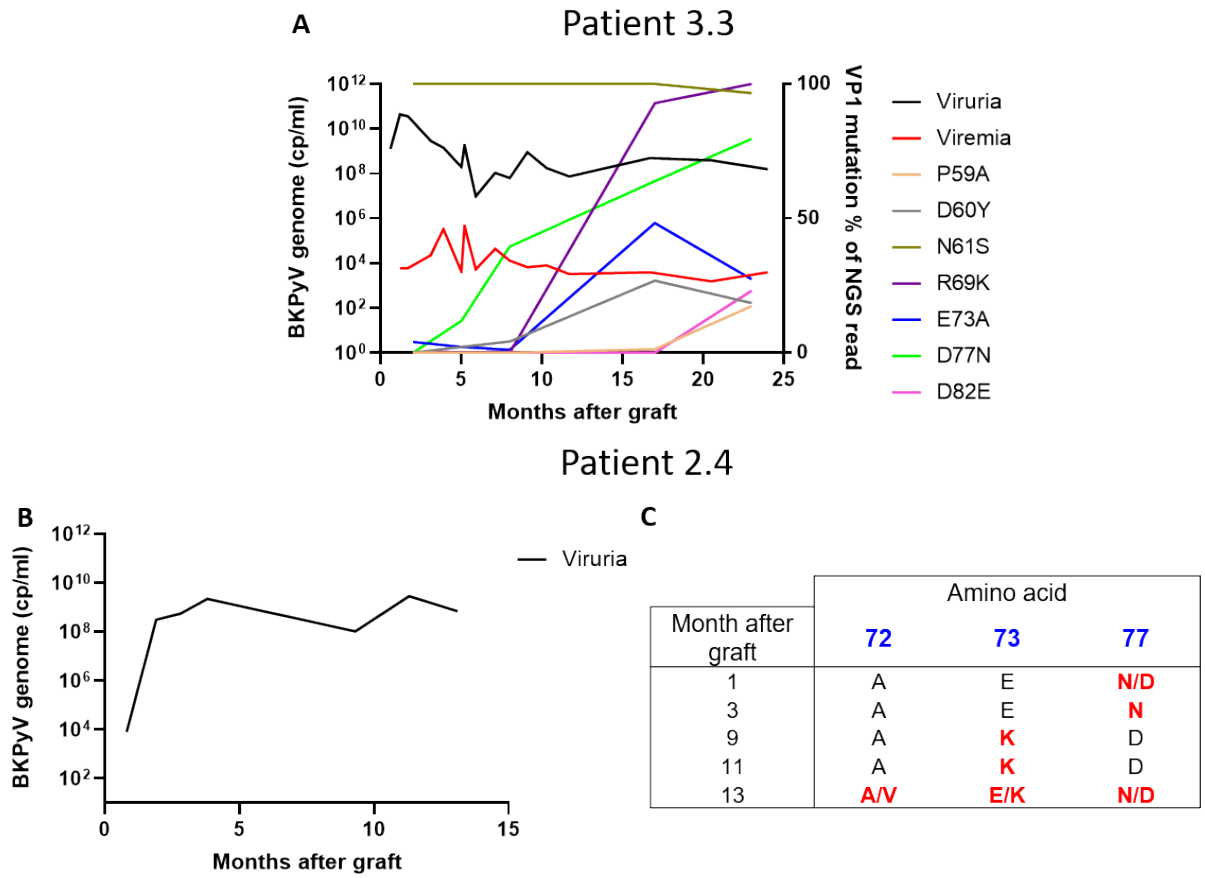

Month after graft	Amino acid 72	73	77
1	A	E	N/D
3	A	E	N
9	A	K	D
11	A	K	D
13	A/V	E/K	N/D

Figure 15 - Clinical data of patients presenting mutations of VP1 gIV BKPyV. (A) Clinical data for patient 3.3. (B) Viruria over time after graft for patient 2.4. (C) Table summarising the mutations found in BKPyV of patient 2.4 through Sanger sequencing. Graphs were made with GraphPad Prism 8.

Like for gIb2 variants, I produced and purified the different gIVc2 variants as well as gIVc2 WT His-tag VP1 pentamers for glycan array screening. The gIVc2 WT showed very weak binding in general and targeted GT1b and GM1b-DH probes. Again, for this genotype, the E73K mutation induces only binding to GT1b. For gIV VK, only GT1b was bound among the known BKPyV receptors, and we can also see binding to GM1b-DH and GD1a-DH probes. Stronger binding to the array was seen for gIVc2 D77N by targeting GD1b, GT1b and GT1a as well as weaker binding seen for GQ1b and GM1b-DH. Finally, gIVc2 K-N was found to bind the known receptors: GT1b and GD1b (**Figure 16**).

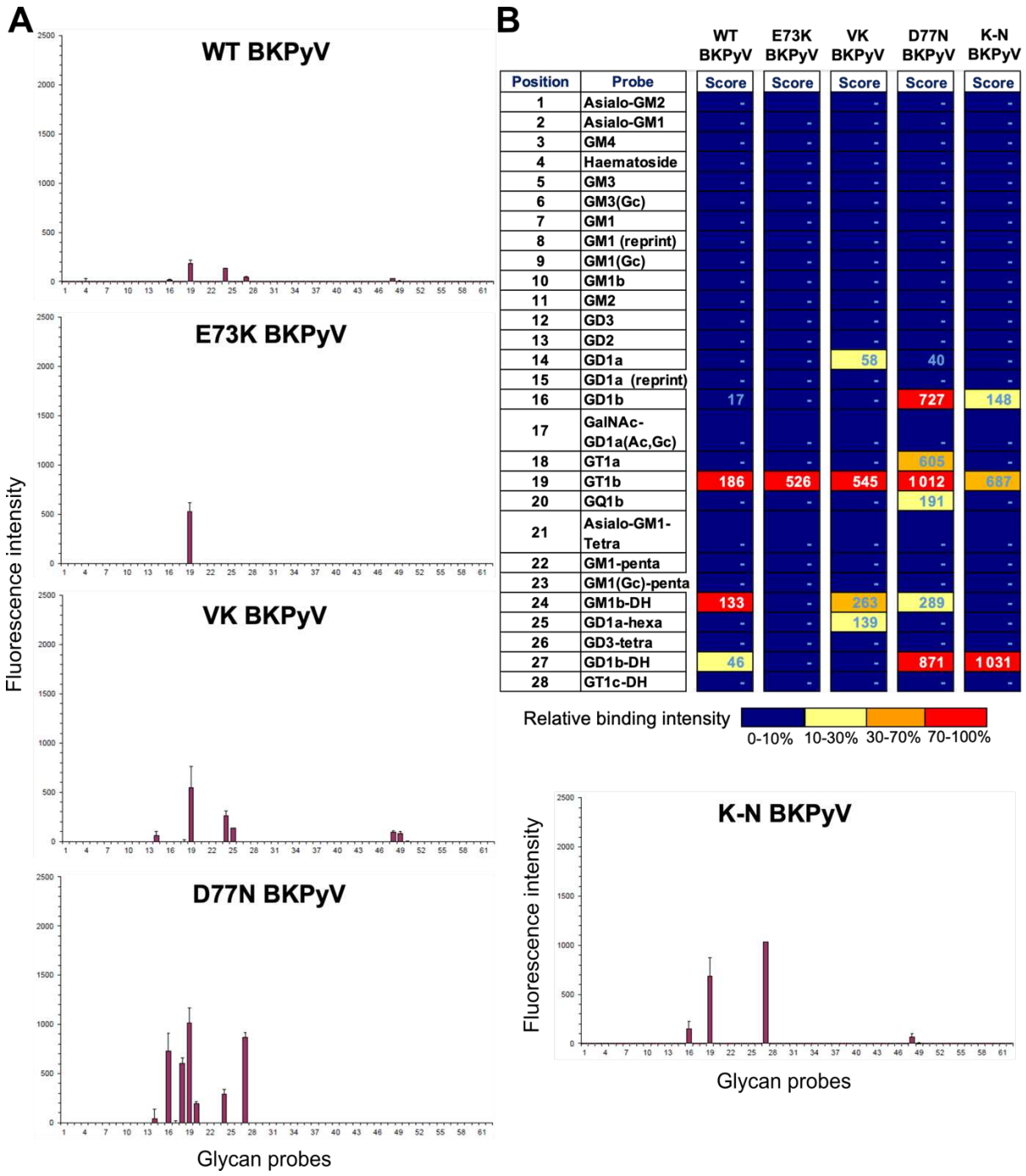

Position	Probe	WT BKPyV Score	E73K BKPyV Score	VK BKPyV Score	D77N BKPyV Score	K-N BKPyV Score
1	Asialo-GM2	-	-	-	-	-
2	Asialo-GM1	-	-	-	-	-
3	GM4	-	-	-	-	-
4	Haematoside	-	-	-	-	-
5	GM3	-	-	-	-	-
6	GM3(Gc)	-	-	-	-	-
7	GM1	-	-	-	-	-
8	GM1 (reprint)	-	-	-	-	-
9	GM1(Gc)	-	-	-	-	-
10	GM1b	-	-	-	-	-
11	GM2	-	-	-	-	-
12	GD3	-	-	-	-	-
13	GD2	-	-	-	-	-
14	GD1a	-	-	58	40	-
15	GD1a (reprint)	-	-	-	-	-
16	GD1b	17	-	-	727	148
17	GalNAc-GD1a(Ac,Gc)	-	-	-	-	-
18	GT1a	-	-	-	605	-
19	GT1b	186	526	545	1 012	687
20	GQ1b	-	-	-	191	-
21	Asialo-GM1-Tetra	-	-	-	-	-
22	GM1-penta	-	-	-	-	-
23	GM1(Gc)-penta	-	-	-	-	-
24	GM1b-DH	133	-	263	289	-
25	GD1a-hexa	-	-	139	-	-
26	GD3-tetra	-	-	-	-	-
27	GD1b-DH	46	-	-	871	1 031
28	GT1c-DH	-	-	-	-	-

Figure 16 - Neuro-glycan glycan array results for gIVc2 VP1 pentamer variants. (A) Diagram, for each VP1 pentamer, with fluorescent intensity for each probe. (B) Table summarising the relative binding intensity for each VP1 pentamers focusing on gangliosides.

I also performed cellular binding assays with labelled gIVc2 WT and K-N VLPs on supplemented LNCaP cells to confirm the glycan array results. Cells were supplemented with gangliosides GM1, GD1b, GD1a, GT1a and GD3. Only duplicates were done during this experiment. Both gIV and K-N have a similar binding pattern

(**Figure 17**). GD1b and GT1a seem to be bound preferentially followed by GD1a and GD3. These results differ from the glycan array screening. Indeed, binding of gIVc2 WT was very weak and no binding for any of the gangliosides tested here in this assay was found. While for gIVc2 K-N, glycan array results only showed GD1b and GT1b binding. Unfortunately, GT1b was not tested in this experiment as I encountered a problem of stability of the compound after long term storage.

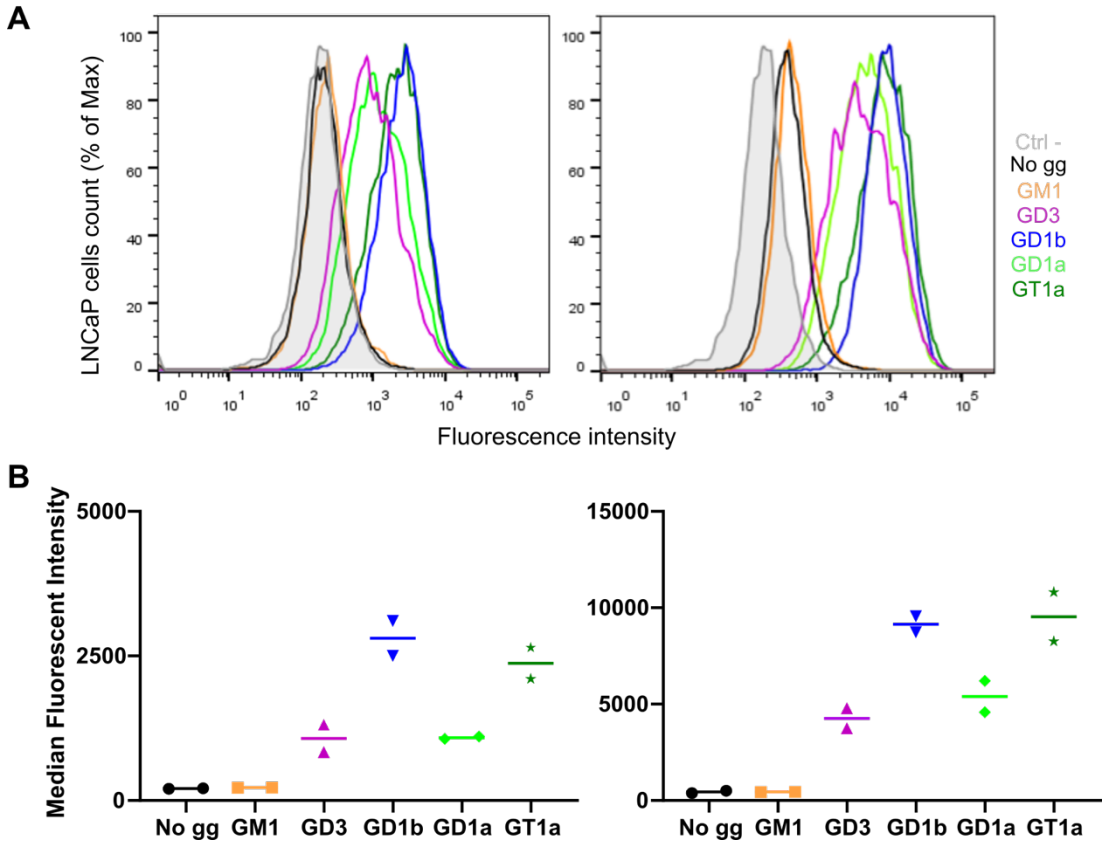

Figure 17 - Cellular binding assays with WT and K-N labelled VLPs on supplemented LNCaP cells. (A) Histograms representing fluorescent intensities of Alexa-647 WT or K-N VLPs during cell-binding assays on ganglioside supplemented LNCaP cells. LNCaP cells alone are shown in a filled grey histogram for negative control, other conditions with VLPs are represented by coloured histograms. (B) Median fluorescence intensity comparison for binding of each VLP to LNCaP cells supplemented with different gangliosides. Histograms were made with FlowJo VX and graphs with GraphPad Prism 8.

Infectivity assays were performed with gIVc2 WT and K-N PSVs in LNCaP and GM95 supplemented with either GM1, GD1b or GD1a. The same infection pattern is seen in both cell lines but GM95 cells show stronger infection. Both PSVs infect cells supplemented with GD1b and GD1a with higher infection for GD1b, which is consistent with the previous binding results. We can also see that infection is stronger with K-N PSVs (**Figure 18**).

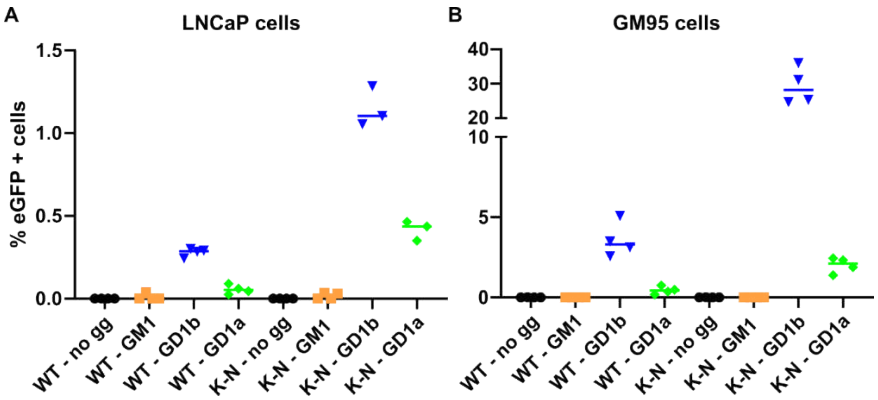

Figure 18 - Infectivity assays with WT and K-N PSVs on supplemented cell lines. Percentage of eGFP positive supplemented LNCaP (A) or GM95 (B) cells when infected with WT or K-N PSVs. Graphs were made with GraphPad Prism 8.

I also performed neuraminidase treatment on 293TT cells to confirm the sialic acid dependency of gIVc2 WT and K-N BKPyV. Binding assays showed less than 20% of remaining binding after neuraminidase treatment. For infectivity assays on neuraminidase treated 293TT cells, gIVc2 WT has a remaining infection of around 50% while K-N is at less than 30%. These results show that K-N is more dependent on sialic acid than gIVc2 WT BKPyV for infection of 293TT cells (**Figure 19**).

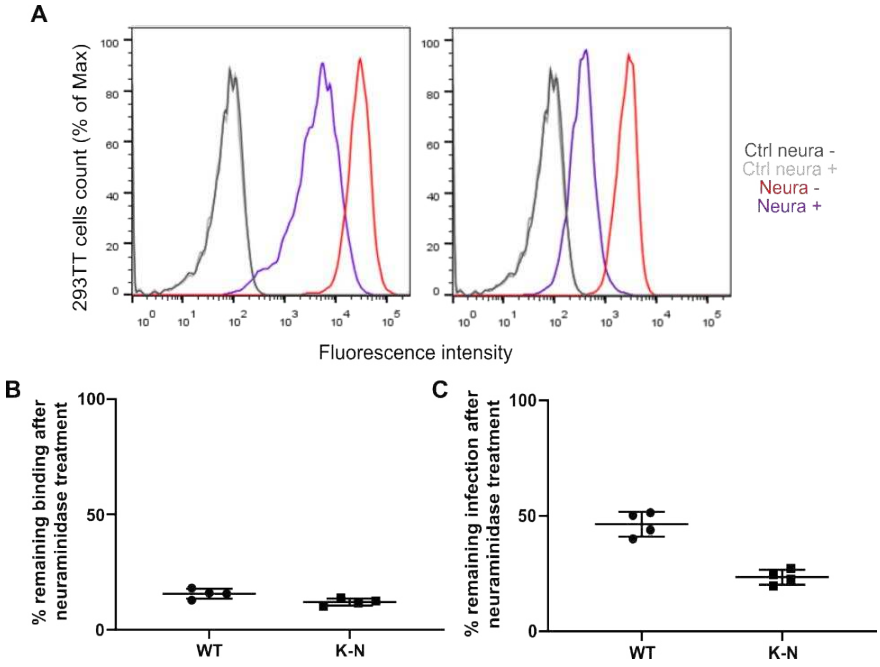

Figure 19 - Binding and infectivity assays with WT and K-N BKPyV on neuraminidase treated 293TT cells. (A) Histograms representing fluorescence intensities of Alexa- 647 WT or K-N VLPs during cell-binding assays on neuraminidase treated 293TT cells. (B) Percentage of remaining VLPs binding to cells after neuraminidase treatment. (C) Percentage of remaining infectivity with PSVs after neuraminidase treatment of 293TT cells. Histograms were made with FlowJo VX and graphs with GraphPad Prism 8.

For structural studies, I was able to express, purify and crystallise gIVc2 WT, D77N, E73K and K-N VP1 pentamers (**Table 6**).

Data collection	gIV WT	gIV E73K	gIV D77N	gIV R69K D77N
Beamline		PXIII		
Wavelength (Å)		1.000021		
Space group	P2(1)	P2(1)2(1)2	P2(1)	P2(1)
Unit cell length (Å)	a = 61.62 b = 132.73 c = 83.57	a = 149.06 b = 151.58 c = 61.92	a = 61.50 b = 142.60 c = 82.90	a = 62.38 b = 146.13 c = 152.97
Unit cell angle (°)	α = 90 β = 109.85 γ = 90	α = 90 β = 90 γ = 90	α = 90 β = 109.7 γ = 90	α = 90 β = 88.87 γ = 90
Pentamers/ASU	1	1	1	2
Resolution(Å)	50 - 1.72 (1.74-1.72)	50 - 1.89 (1.91-1.89)	50 - 2.3 (2.34-2.30)	50 - 2.70 (2.80-2.70)
Completeness (%)	96.6 (95.9)	99.6 (97.8)	99.8 (99.6)	99.9 (99.6)
Total reflections	864 593 (136 028)	1 421 489 (112 813)	411 855 (59 699)	528 689 (87 040)
Unique reflections	129 745 (20 771)	119 829 (18 562)	64 654 (9 611)	75 356 (12 077)
Rmeas (%)	18.0 (153.3)	17.6 (126.5)	20.4 (142.2)	23.2 (135.6)
CC1/2 (%)	99.6 (92.0)	99.8 (83.3)	99.4 (54.4)	99.1 (62.5)
I/σ	9.52 (1.38)	14.11 (2.27)	8.62 (1.43)	8.78 (1.44)
Refinement				
Rwork/Rfree (%)	18.93/21.85	18.38/21.13	17.29/20.44	21.04/23.33
RMS deviation:				
Bond lenghts (Å)	0.015	0.007	0.008	0.005
Bond angles (°)	1.30	1.43	1.02	0.91
Average B factor (Å²)	28.2	34.0	37.9	50
Wilson B factor (Å²)	27.7	29,7	41,3	50.4

Table 6 - Data collection and refinement

Overall structures were similar. For the BC-loop, where the mutations are found, only gIVc2 E73K presents a conformational change of the backbone structure with a switch of the loop from amino acid 72 to 74 for what it seems to be 4 out 5 monomers in the pentamer. Otherwise, the two other mutants have the same backbone structure with slight side chain differences (**Figure 20B**). If we compare the lysine 69 of gI WT and gIVc2 K-N, we can see that the lysine in the gIVc2 variant is not in the same orientation as the lysine in gI WT, with an orientation toward the sialic acid binding site (**Figure 20C**). However, out of 10 chains, I was able to build only 2 lysines in this orientation. On another chain, density seemed to show an orientation for a lysine closer to that seen in the gI WT structure. And for other chains, I was not able to build the entire side chain. Thus, it could be that the side chain orientation is quite flexible. Both gIVc2 WT and the gI N-Q variant do not have lysine in position 69 and instead have arginine or

asparagine, respectively. Compared to the asparagine orientation, the arginine side chain is not oriented toward the sialic acids and thus does not create any steric clash with them (**Figure 20D**).

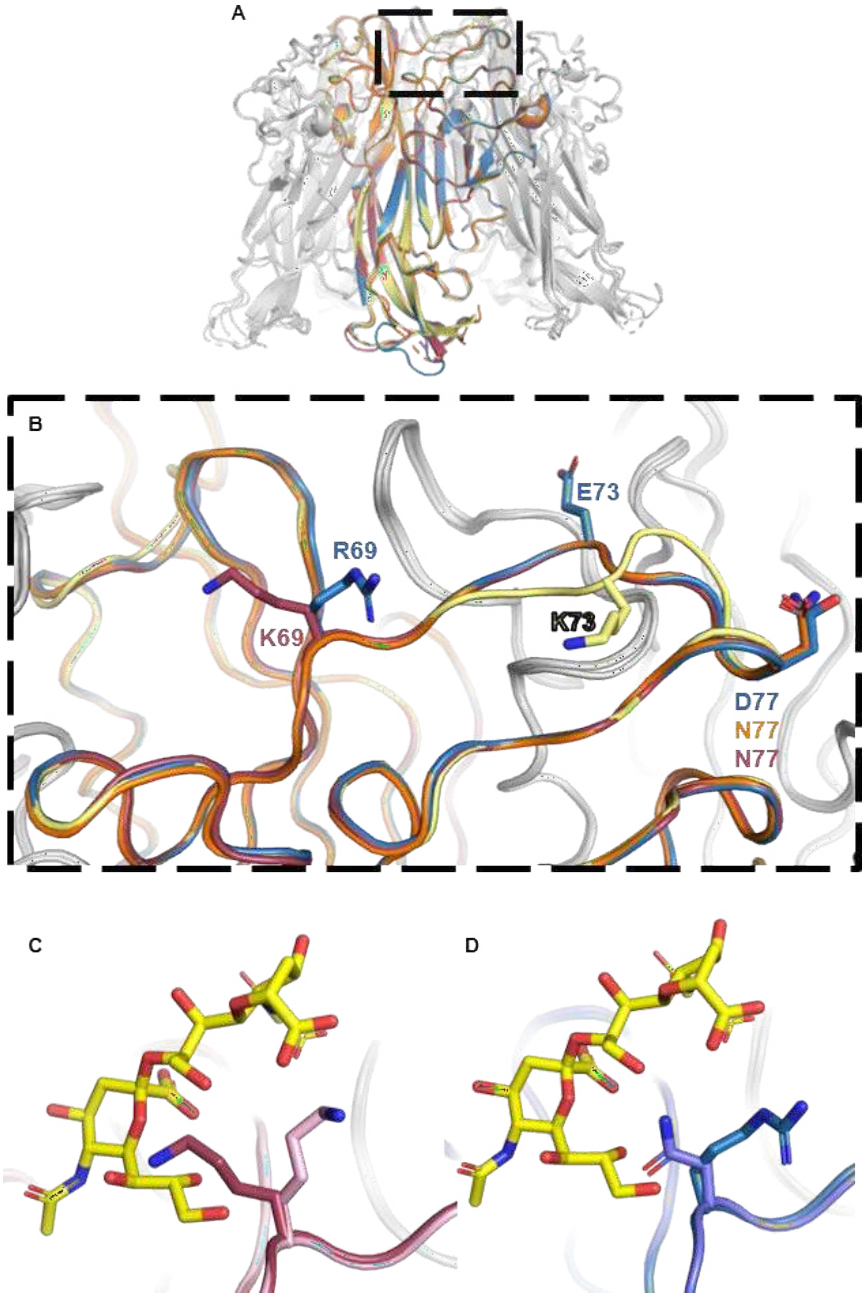

Figure 20 - Structures of gIVc2 WT and variant VP1 pentamers. (A) Superposition of gIV variant VP1 pentamer onto WT VP1 pentamers. gIV WT VP1 monomer is highlighted in blue, E73K in yellow, D77N in orange and K-N in red. (B) Zoom on the BC-loops of highlighted VP1 monomers. Amino acids 69, 73 and 77 are represented as sticks. (C) Superposition of IVc2 K-N (red) structure to gI WT (pink) structure focusing on the sialic acid (yellow) binding site (PDB ID: 4MJ0). Lysine 69 are represented as sticks. (D) Superposition of IVc2 WT (blue) structure to gI N-Q (purple) structure focusing on the sialic acid (yellow) binding site (PDB ID: 4MJ0). Amino acids 69 are represented as sticks. Figures were made with Pymol.

3. Structure quality

All structures were solved with a resolution ranging from 1.72 to 2.7Å. The variants crystallised either in a $P2_12_12_1$ symmetry with only one pentamer per asymmetric unit (ASU), or in $P2_1$ symmetry with one or two pentamers/ASU.

For all structures the N and C-terminal regions were not built entirely due to no or poor electron density. Close to the N-terminus, the region from amino acids 35 to 45 is not well resolved in general and was not entirely built in most structures. Only a few monomers had enough density to allow building of this region, however, side chains of the different amino acids were rarely built due to poor electron density. The last poorly resolved region in most structures is the CD loop from amino acids 99 to 106. Once again, this region was built only in a few monomers and side chains were usually not built due to poor density.

The E73Q variant structure presents a well resolved BC loop where the mutation can be found for the glutamine side chain as well as the backbone. For the VQQ variant structure, a loop switch can be seen in the BC loop where mutations A72V and E73Q are found. This region is also well resolved in this structure, except for the side chain of asparagine 74, which only had sufficient electron density to build the side chain in one of the five monomers. In this monomer, the glutamine 73 side chain is oriented differently compared to the WT glutamate side chain, as the loop backbone switches orientation. For the E82Q mutation, density for the side chain was clear enough to build it in each pentamer.

The E73A variant structure displays a loop orientation similar to that seen in the WT structure for monomers 1 and 2, while monomers 3 and 4 present the loop switch described for the VQQ variant structure, and monomer 5 appears to harbour both backbone conformations. For monomers 1 to 3, the backbone is quite well resolved and while side chains can be built, they are not as well resolved as they are in other parts of the structure. Monomer 4 also presents a quite well resolved backbone in this region, except for asparagine 74 where Cα does not clearly sit in electron density. Moreover, not enough density was present to build the side chains. Finally, in monomer 5, enough density was present in order to build the loop in both orientations. However, despite many refinement runs, those parts remained less well resolved compared to the other monomers, and side chains, like for asparagine 74 in monomer 4, were not built.

The BC loop of the gIV WT structure, where most mutations can be found, is well resolved and all side chains, except two arginines, were built. However, it is important to note that the orientation of the asparagine 61 in monomer 1 and of arginine 69 in monomer 2 are influenced by crystal contacts.

Regarding the gIV variants, the region with the D77N mutation is well resolved in both the single mutant D77N and the K-N double mutant. For the latter structure, the region where the K69N mutation is found is well resolved for the backbone but over 10 monomers, only two lysines were built entirely, due to lack of clear electron density for the other monomers. Finally, the single variant E73K structure has four out of five monomers showing a loop switch similar to that seen in the VQQ variant structure. The region is sufficiently well resolved to build the backbone of the protein, but density was present for the side chain in only one monomer.

Project B: BKPyV genotypes tropism and structure

For this collaborative project, the main objectives were to study the tropism of the four different BKPyV genotypes as well as their structures. I solved the structure of genotype IVc2 WT VP1 pentamer which I already presented in the previous section to compare it with the gIVc2 variant structures. However, here, if we compare it to the gI WT VP1 pentamer structure, we can see that both pentamers have the same overall structure. By looking at the BC-loop, where most sequence differences are found between genotypes, there are no conformational changes in the backbone structure. So, despite sequence polymorphism, the BC-loop structure is highly conserved between gI and gIV. However, the nature of the side chains is different, and this could have an impact on tropism (**Figure 21**).

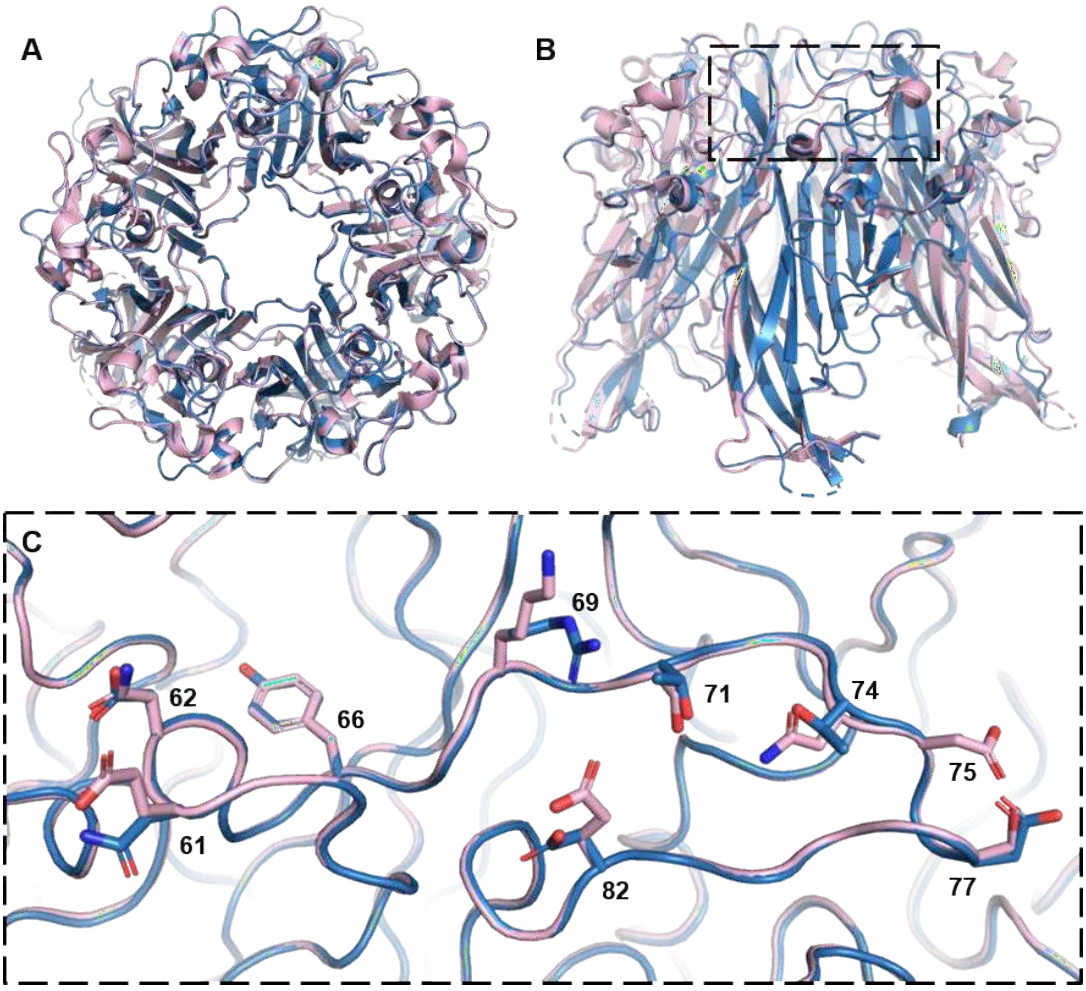

Figure 21 - Superposition of gI (pink) (PDB ID: 4MJ1) and gIVc2 (blue) WT VP1 pentamers. (A) Top-view. (B) Side-view. (C) Zoom into the BC-loop with the different amino acids shown in sticks. Figures were made with Pymol.

To test the tropism of different BKPyV genotypes, we first wanted to check if all genotypes remained sialic acid dependent for binding and infection. For that, I treated 293TT cells with neuraminidase and tested binding with labelled VLPs and infection with PSVs. For all genotypes, we were able to see that less than 15 % of VLPs can bind after neuraminidase treatment (**Figure 22A & B**). For infection, we can see that gI, gII and gIII have only around 10 % of remaining infection after neuraminidase treatment while gIV maintains around 50% of infection (**Figure 22C**). Thus, despite being highly dependent on sialic acid for binding the cells, gIVc2 still retains around 50% of its infectivity after neuraminidase treatment of target cells, indicating that another receptor could be involved in infectious entry for this genotype. The other three genotypes, however, are sialic-acid dependent for binding and infection.

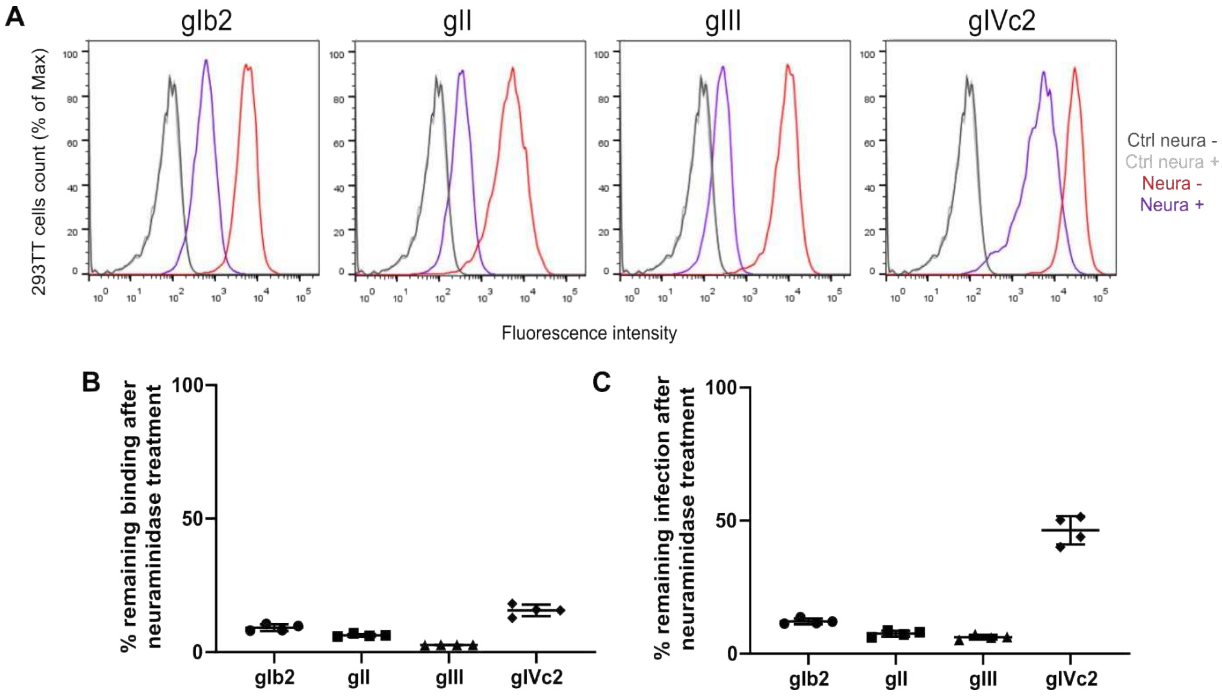

Figure 22 - Binding and infectivity assays with the different BKPyV genotypes on neuraminidase treated 293TT cells. (A) Histograms representing fluorescence intensities of Alexa-647 coupled VLPs of the four WT BKPyV genotypes in cell-binding assays on neuraminidase treated 293TT cells. (B) Percentage of remaining VLPs binding to cells after neuraminidase treatments. (C) Percentage of remaining infectivity with PSVs after neuraminidase treatment of 293TT cells. Histograms were made with FlowJo VX and graphs with GraphPad Prism 8.

Project C: Characterisation of JCPyV interaction with 5HT2RB

For this project, the aim was to characterise the interaction between JCPyV and 5HT2RB receptors. As an initial step, we aimed to test whether the interaction requires the entire capsid, meaning that the receptor interacts at the interface of multiple pentamers of VP1, or if only a pentamer would be enough. To answer this, JCPyV VP1 pentamers and VLPs were expressed and purified to test their binding to 5HT2RB. As transmembrane receptors are challenging to express and purify, I also tried to perform binding assays through ELISA with peptides representing the external loops of the 5HT2RB receptors. Ultimately, I was also able to express and purify this receptor to perform surface plasmon resonance (SPR) measurements.

1. Material & Methods

JCPyV VP1 pentamer production and purification

As for BKPyV VP1 pentamer production and purification, a pET15B expression vector was used containing the JCPyV VP1 sequence from amino acids 30 to 300 with an N-terminal hexahistidine tag and a thrombin cleavage site (BioCat Gmbh). Proteins were expressed in BL21 DE3 *E.coli* with IPTG induction. Purification was done first by nickel affinity chromatography using a 5 mL HisTrap FF crude column (Cytiva) with buffer A (50 mM Tris pH 7.5, 250 mM NaCl, 10 mM imidazole and 10 % glycerol) for wash and buffer B (20 mM Tris pH 7.5, 250 mM NaCl, 500 mM imidazole and 10% glycerol) for elution. His tags were also digested with 10U of thrombin protease (Cytiva) by mg of protein after 24 hours at 20°C with rotation. Cleaved pentamers were again purified on nickel affinity chromatography and finally by size-exclusion chromatography (SEC) with an elution buffer (20 mM HEPES pH 7.5 and 150 mM NaCl).

Cell culture

SF9 cells were grown in SF900 II medium (Gibco) with 100 U/mL of penicillin and 100 µg/mL of streptomycin (Dutscher). Cells were maintained at 27°C in a humidified incubator. Cells were either grown as suspension or adherent culture. For

adherent culture, passaging was done at confluence by using a cell scraper to detach cells.

JCPyV VLPs production and purification

Baculoviruses, kindly provided by Prof. A.Touzé (Universite de Tours), were used to produce JCPyV VLPs. Adherent SF9 cell cultures were inoculated with JCPyV VP1 baculovirus at MOI 0.01 for 5 days. Cells were harvested and resuspended in PBS with 1% of Triton-X100 and 1X of protease inhibitor cocktail at 100 µL per 10^7 cells. Then, cells were incubated 30 minutes on ice before 15 minutes of centrifugation at 10 000g and 4°C. The pellet was resuspended in PBS containing $CaCl_2$, $MgCl_2$ and 1X of proteinase inhibitor cocktail. Cells were lysed by sonication (five times with 1 min ON/ 1 min OFF). Lysate was treated with benzonase (Merck) and incubated at least 2 hours at 37°C. After centrifugation of the lysate, the supernatant was kept and transferred to Optiprep (Sigma) gradient for ultracentrifugation, as described previously for BKPyV VLP purification. Gradient tubes were punctured with a 25G syringe needle, and ten fractions were collected. SDS-PAGE was performed for each fraction to determine the peak fraction for pooling. Peak fractions were pooled, and another SDS-PAGE was performed with the BSA standard to determine the concentration of VLPs.

Production of recombinant bacmid

The sequence taken from Wacker et al., 2017 (**Figure 23**) was used to generate a pFastBac vector (BioCat Gmbh) (Wacker et al., 2017).

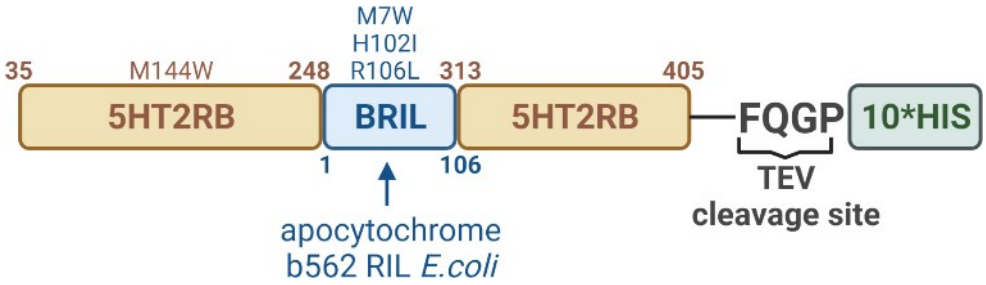

Figure 23 - 5HT2RB sequences used (Wacker et al., 2017). Figure was made with Biorender.

E.coli DH10Bac were transformed with pFastBac-5HT2RB plasmid to generate a recombinant bacmid expressing 5HT2RB. Serial dilutions of transformed bacteria were grown on selective LB-agar plates containing 50 µg/mL of kanamycin (Sigma), 7

µg/mL of gentamicin (Sigma), 10 µg/mL of tetracycline (Roth), 100 µg/mL of X-β-gal (Sigma) and 40 µg/mL of IPTG (PeqLab VWR) for 48 hours at 37°C. White colonies, containing recombinant bacmid, were picked, and streaked on selective LB-agar plates overnight at 37°C. After confirming the white phenotype of a colony, this colony was inoculated in liquid LB containing 50 ug/mL of kanamycin, 7 µg/mL of gentamicin and 10 µg/mL of tetracycline. Recombinant bacmid was extracted from bacteria by using PureLink HiPure Plasmid MaxiPrep Kit (ThermoFischer).

Production of recombinant baculovirus expressing 5HT2RB

SF9 cells were first grown without antibiotics. When cells were in log phase with a viability greater than 95%, 8.10^5 SF9 cells were seeded in each well in a 6-well plate with fresh medium without antibiotics. For transfection, Cellfectin II (ThermoFischer) was diluted in medium without antibiotics and then mixed with 1 µg of recombinant bacmid. The mixture was left for 20 minutes at room temperature and then added to cells drop by drop. Cells were incubated with bacmid for 3 to 5 hours before replacing medium with fresh medium without antibiotics. Cells were left 72 hours in culture before medium was collected. Centrifugation was applied on the medium to get rid of cells and large debris, and the cleared supernatant constituted the P0 stock of baculovirus which was stored at 4°C. This stock was amplified to P1 by infecting cells at an estimated MOI of 0.1, considering that the infectious titre of P0 is usually around 10^6 to 10^7 pfu/mL. The P1 stock was estimated at 10^7 to 10^8 pfu/mL.

Production and purification of 5HT2RB

A detailed protocol for 5HT2RB was kindly communicated by Dr Daniel Wacker (Icahn School of Medicine at Mount Sinai) (Wacker et al., 2017). 5HT2RB was expressed by infecting SF9 cells with P1 stock of recombinant baculovirus at MOI 5 for 3 days. Cells were harvested and resuspended in Low Salt Lysis Buffer (LSLB) (10 mM HEPES pH 7.5, 10 mM MgCl2 and 20 mM KCl) with 1 mM phenylmethylsulfonyl fluoride (PMSF) and transferred to a dounce homogenizer for lysis. Cells were lysed with 30 to 40 strokes, then centrifuged in a Ti70 rotor at 45 000 rpm for 30 minutes at 4°C. The pellet was resuspended in 10 mL of High Salt Lysis Buffer (HSLB) (10 mM HEPES pH 7.5, 10 mM MgCl2, 20 mM KCl and 1 M of NaCl) with 1 mM PMSF and transferred to the douncer. After 20 strokes to homogenise the membrane pellets, they were transferred again to a Ti70 rotor for 30 minutes at 45 000 rpm at 4°C. The last

two steps were repeated with HSLB without PMSF. Then, the pellet was flash frozen and stored at -80°C.

The next day, resuspension buffer (100 mM HEPES pH 7.5, 150 mM NaCl, 10 mM MgCl2 and 20 mM KCl) was added to the frozen membrane pellet for thawing. Iodoacetamide was added to the resuspended membrane pellet at final concentration of 2 mg/mL and the solution was placed at 4°C under agitation for 20 minutes. Then 2X solubilization buffer (100 mM HEPES pH7.5, 150 mM, 2/0.4 % n-dodecyl-β-D-maltoside (DDM)/cholesteryl hemisuccinate (CHS)) was added to a final concentration of 1X and incubated 2 hours at 4°C with agitation. Membrane pellets were centrifuged with a Ti70 rotor at 65 000 rpm for 20 minutes at 4°C. Supernatant was recovered, mixed with 20 mM of imidazole and 500 µl of pre-washed Talon resin (Cytiva) and incubated overnight at 4°C under agitation.

The Talon resin was then spun down and transferred to a gravity flow column. Resin was washed with two buffers: Wash buffer I (50 mM HEPES pH 7.5, 800 mM NaCl, 0.1/0.02% DDM/CHS, 20 mM imidazole and 10% glycerol) and Wash buffer II (25 mM HEPES pH 7.5, 500 mM NaCl, 0.05/0.01% DDM/CHS and 10% glycerol), and protein was eluted with elution buffer (20 mM HEPES pH 7.5, 200 mM NaCl, 0.05/0.1% DDM/CHS, 250 mM imidazole and 10% glycerol). The elution fraction was then loaded on an SD200 increase column (Cytiva) for SEC, and protein was eluted with Wash Buffer II.

ELISA with 5HT2RB peptides

Peptides corresponding to the external loops 2, 3 and 4 of 5HT2RB were purchased with biotinylated N-terminus from GeneCust (**Figure 24**). The sequences used for each peptide were based on the human 5HT2RB protein sequence found on Uniprot.

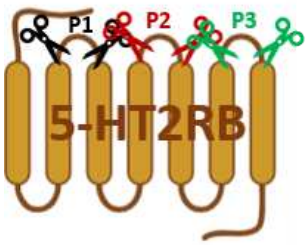

Peptide	Sequences
P1	TIMFEAMWPLPLVLCP
P2	KGIETDVDNPNNITCVLTKERFGD
P3	TLVLCDSCNQTTLQM

Figure 24 - Peptides sequences corresponding to external loop of 5HT2RB receptor. Figures was made with Biorender.

100 ng of VLPs/well were coated in 96-well plates and then washed three times with PBS with 0.05% of Tween-20. After that, wells were blocked with PBS, 0.05% Tween-20 and 5% of powdered milk for 1 hour at 37°C. After washes, serial dilutions of peptides in blocking solution were added to wells and incubated 1 hour at 4°C. Streptavidin-Horseradish Peroxidase (HPR) was then added to wells for 30 minutes after washes. To reveal binding, 3,3',5,5'- Tetramethylbenzidine (TMB) was added to each well after washes and revealing was stopped by adding H2SO4. Then, absorbance of wells was read with a Tecan plate reader at 450 nm.

Surface Plasmon Resonance

Measurements were performed on Bioacore T2000 with a CM5 sensor Chip equilibrated with Wash buffer II, at 25°C. In a first attempt, amine-coupled anti-His was immobilised on the chip in order to capture his-tag 5HT2RB. In a second trial, amine coupled 5HT2RB was immobilised directly on the chip. JCPyV and BKPyV VLPs or VP1 pentamers were used at many concentrations to detect binding to the receptor with a flow rate of 40 µL/min.

2. Results

To determine which part of the 5HT2RB external domain interacts with JCPyV capsids, I used peptides corresponding to the three external loops of the receptors in an ELISA assay. BSA, BKPyV VLPs and MuPyV VLPs were used for coating as control. Each condition was performed in triplicate (**Figure 25**).

Results were not conclusive. Peptides 1 and 2 seem to strongly bind JCPyV VLPs compared to peptide 3 but the same pattern was seen for BKPyV VLPs despite the lack of evidence that BKPyV interacts with this receptor. We can also see strong binding of peptide 1 to MuPyV which again is not known to interact with 5HT2RB. Moreover, the BSA and non-coating conditions are also showing binding by peptides 1 and 2 indicating that unspecific binding can be seen in the VLP conditions. Testing several different binding conditions and peptide concentrations did not improve the results, which remained inconclusive.

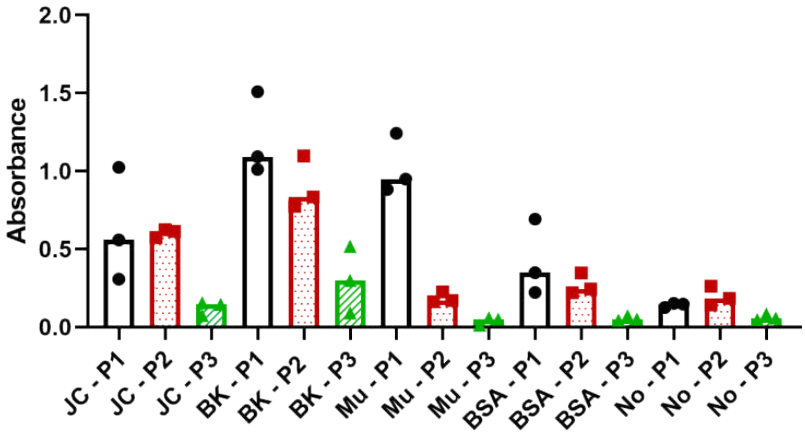

Figure 25 - Binding of HT2RB derived peptides to JCPyV VLPs. Graph was made with GraphPad Prism 8.

I initially used recombinant bacmid, kindly sent by Dr. Wacker of Icahn School of Medicine at Mount Sinai, to express the entire 5HT2RB. However, after several expression tests with SF9 cells, no receptor was expressed. Thus, I performed a PCR to check if the bacmid carried the insert gene for 5HT2RB expression by using primers for pUC/M13, flanking the insert. As suspected, PCR results showed that no insert was found in the bacmid sample (**Figure 26A**). I then decided to generate a new recombinant bacmid with the pFastbac that was also sent by Dr. Wacker. Before that, I checked the sequence by sending the plasmid for sequencing. Unfortunately, a deletion of 3 bp, initially encoding for a valine, was found toward the end of the receptor sequence (**Figure 26B**). Thus, I decided to order a new pFastBac with the correct sequence for 5HT2RB with a 10xHis Tag. From this new plasmid I was able to generate recombinant bacmid and then baculovirus stock expressing the 5HT2RB receptor.

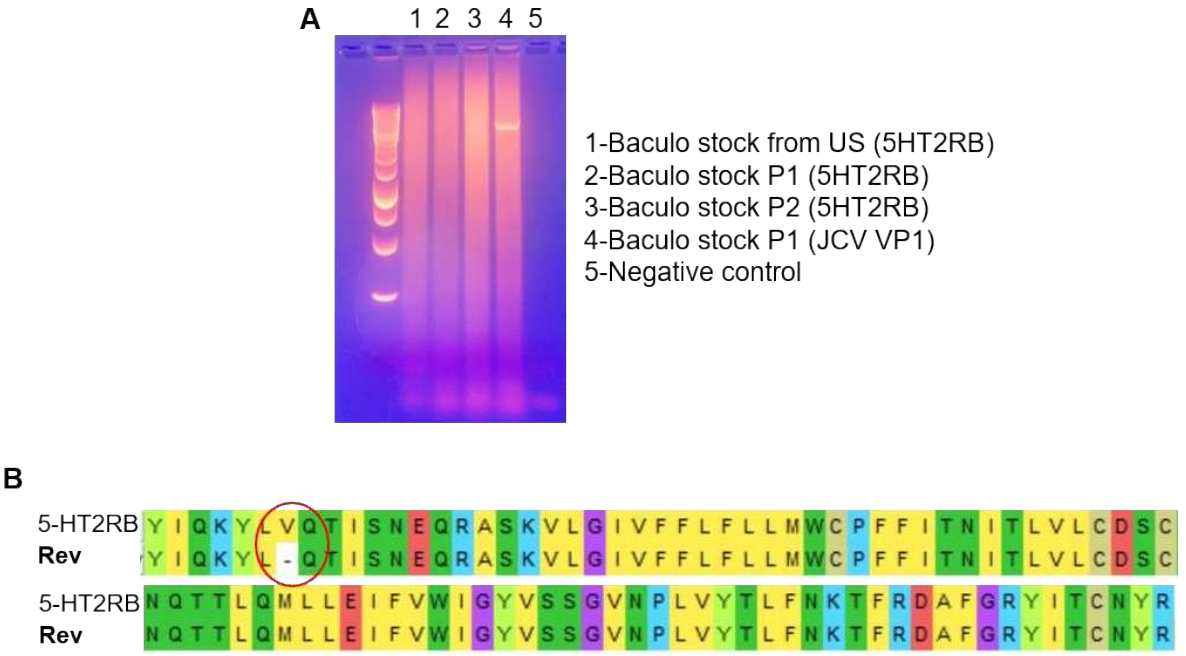

Figure 26 - Verification of baculovirus stock and pFastbac sequences. (A) Agarose gel with different baculovirus stock for 5HT2RB expression and with baculovirus encoding for JCPyV VP1 protein as positive control. (B) Alignment of 5HT2RB (top) protein sequence as reference and pFastBac plasmid sequence.

Then, I expressed and purified the entire 5HT2RB receptor to perform SPR measurements. It proved difficult to obtain a high quantity of pure, stable, solubilised 5HT2RB receptors. After several purification attempts, at the size exclusion chromatography step, I always saw a main peak eluting at around 11 mL corresponding to 450 kDa, which is above the molecular weight of a single 5HT2RB receptor (MW = 45 kDa) (**Figure 27**). However, the receptor is surrounded by detergent molecules, which makes the entire structure heavier than expected. Unfortunately, due to time constraints, I was not able to better characterise this peak and assumed that it was 5HT2RB in detergent micelle. I still was able to estimate the overall protein concentration of the SEC peak with nanodrop. Thus, I used this for SPR measurement.

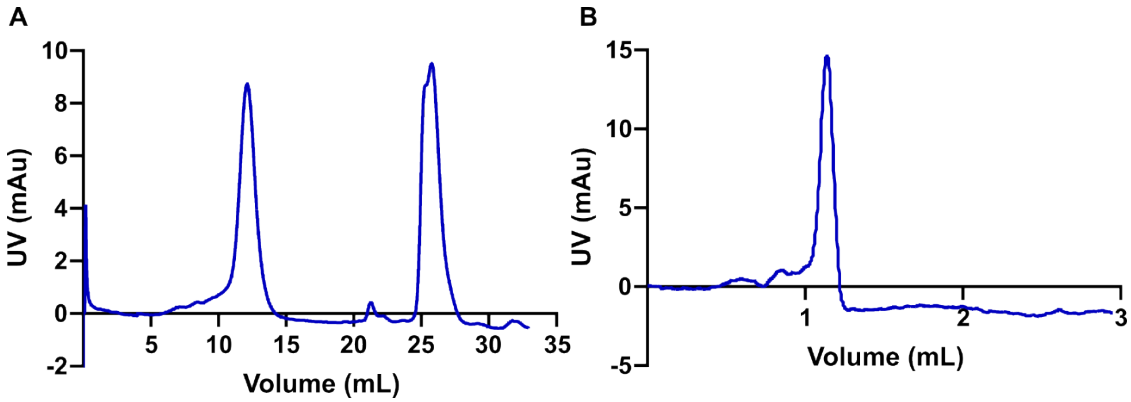

Figure 27 - Purification of 5HT2RB. (A) Size-exclusion chromatogram where 1st peak was pooled and loaded on the analytical SEC. (B) Analytical size-exclusion chromatogram. Graphs were made with GraphPad Prism 8.

Our goal was to get dissociation constant measurements between the receptor and either VLPs or VP1 pentamers of JCPyV. For that, we performed SPR measurements, with the aim to immobilise the His-tag receptor to the chip with an antibody targeting the His-tag. Unfortunately, this strategy was not successful, so the receptor was directly immobilised on the chip (**Figure 28**).

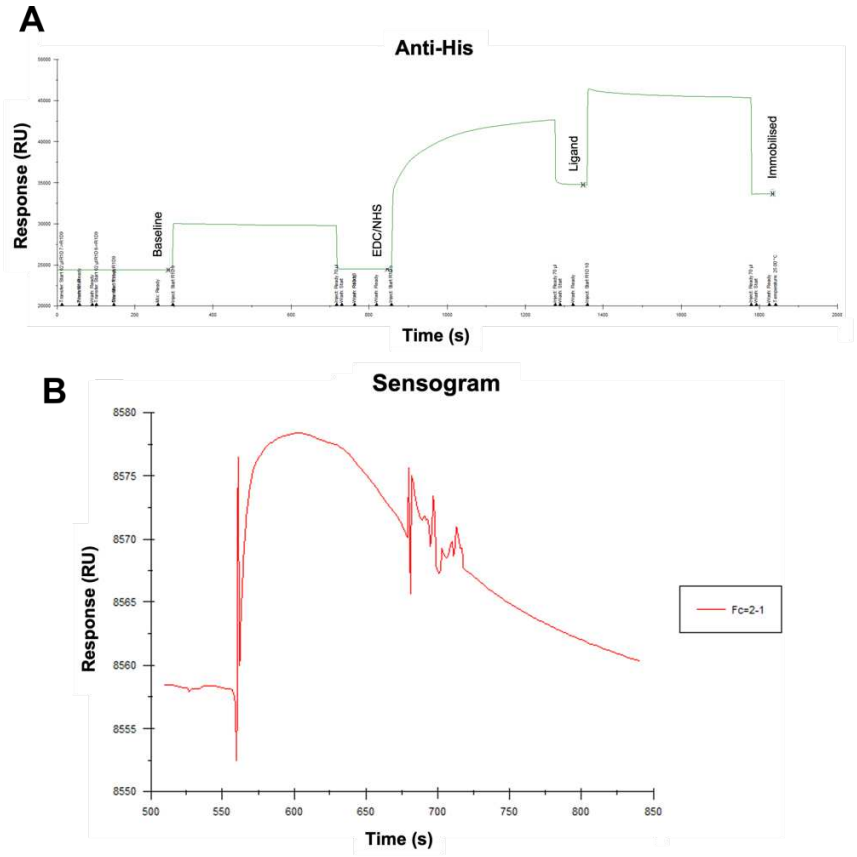

Figure 28 - Capture of 5HT2RB with immobilised anti-His. (A) immobilisation of amide anti-His with response in Response Unit (RU) according to time. (B) Capture of 5HT2RB with response in RU according to time.

After immobilisation of the receptor on the chip, JCPyV VLP and VP1 pentamer binding were tested, as well as BKPyV VLPs and VP1 pentamers as negative control. Different concentrations were tested but unfortunately no interpretable signal was obtained by the different tests (**Figure 29**). Thus, we can not conclude here on the interaction between JCPyV and 5HT2RB.

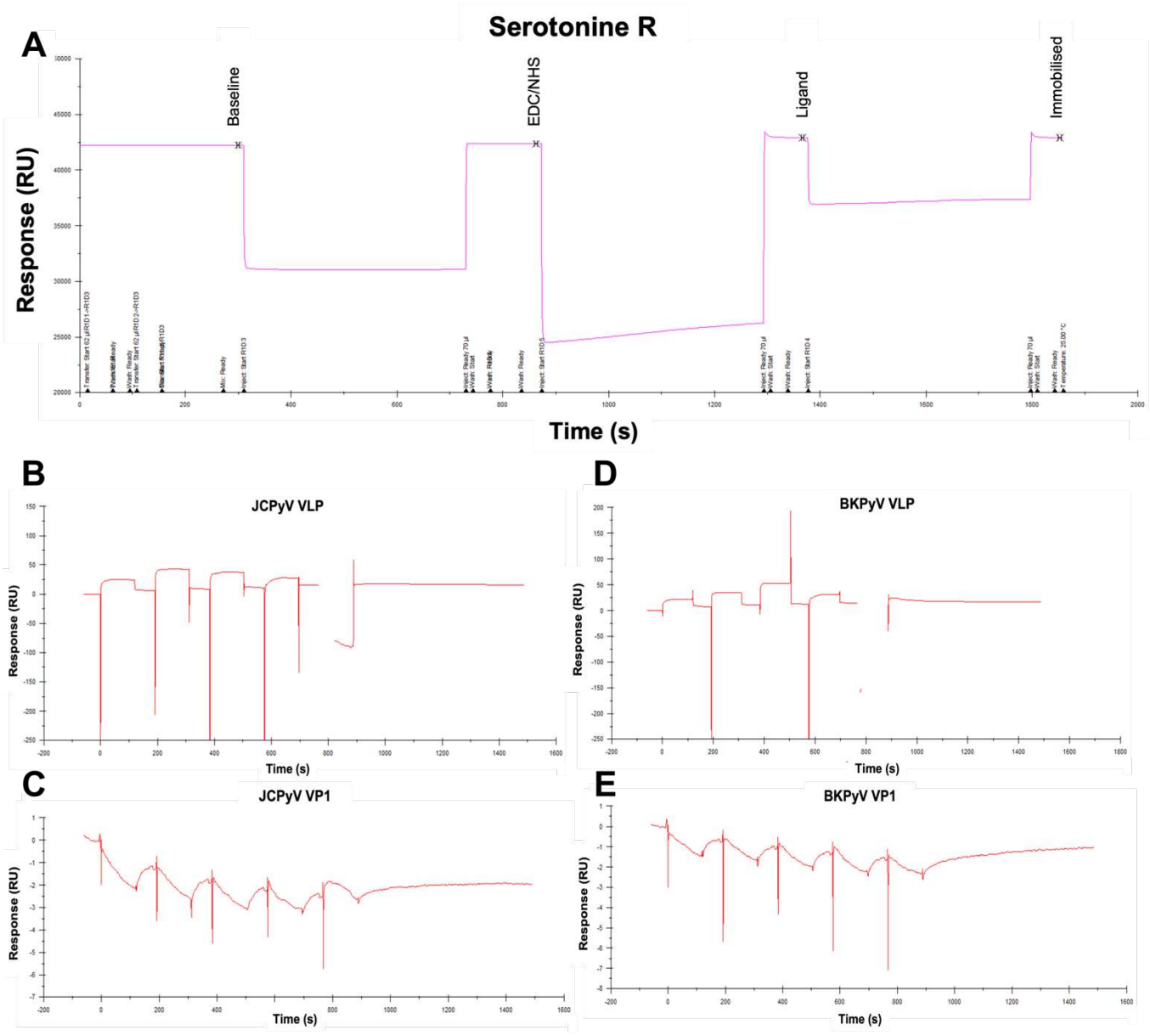

Figure 29 - Binding of different VLPs or VP1 to immobilised 5HT2RB. (A) 5HT2RB immobilisation with response in RU according to time. JCPyV VLPs (B), VP1 (C), BKPyV VLPs (D) and VP1 (E) signal with response in RU according to time.

Discussion

Project A: Patient-derived BKPyV variants

With this functional and structural study, we were able to show that mutations in the BC-loop of the VP1 protein impact ganglioside specificity of the BKPyV capsid. We were able to identify two functional entry patterns through two natural variants of BKPyV. We showed that infection of 293TT cells by the N-Q variant is not dependent on sialic acid, indicating the presence of an unknown co-receptor. The crystal structure of the N-Q variant showed that the K69N mutation was responsible for the loss of sialic acid binding. On the other hand, the VQQ variant, despite having a broader ganglioside binding spectrum than WT, loses the capacity to infect ganglioside-supplemented cells. In structural terms, the VQQ VP1 pentamer has a loop switch from amino acids 73-74, and this same structural feature was present in the E73A VP1 mutant. The BC2 loop switch correlated with the loss of infection in 293TT cells, which raises the intriguing possibility that amino acids 73-74 may be involved in the interaction with the unknown receptor used by the N-Q variant.

We tried to check if heparan sulphate or chondroitin sulphate GAGs could be involved in BKPyV entry since these GAGs, especially heparan sulphate, are found to be involved in the infectious entry of many non-enveloped viruses such as MCPyV, Human Papillomavirus (HPV), Adeno-associated Virus (AAV), enterovirus or adenovirus (Dechecchi et al., 2000; Giroglou et al., 2001; Goodfellow et al., 2001; Tuve et al., 2008; Schowalter et al., 2011; Richards et al., 2013; Huang et al., 2014; Rajan et al., 2021). Moreover, a study described by Geoghegan et al., 2017, showed that a mutant of BKPyV designed to lose binding to sialic acid required heparan sulphate for infection. However, through infectivity assays we saw that both WT and N-Q BKPyV do not seem to interact with these GAGs for infection.

Other targets we wanted to check were the AAV Receptor (AAVR), known to interact with AAV, as well as β1 integrins which, associated to different α chains, are also described as entry receptors for different non-enveloped viruses like human parvovirus B19, some rotaviruses and adenoviruses as well as MPyV (E. Li et al., 2001; Caruso et al., 2003; Weigel-Kelley et al., 2003; Arias et al., 2015; Pillay et al., 2016). Moreover, 293TT cells express both receptors at their surface (Bodary & McLean, 1990; Pillay et al., 2016). Initial infectivity assays using antibodies targeting those receptors to block

their potential interaction with BKPyV PSVs did not give clear results (**Figure 30**). To further test this hypothesis, we could also generate knock-out 293TT cells for each receptor and try to infect these cells with BKPyV N-Q variant PSVs.

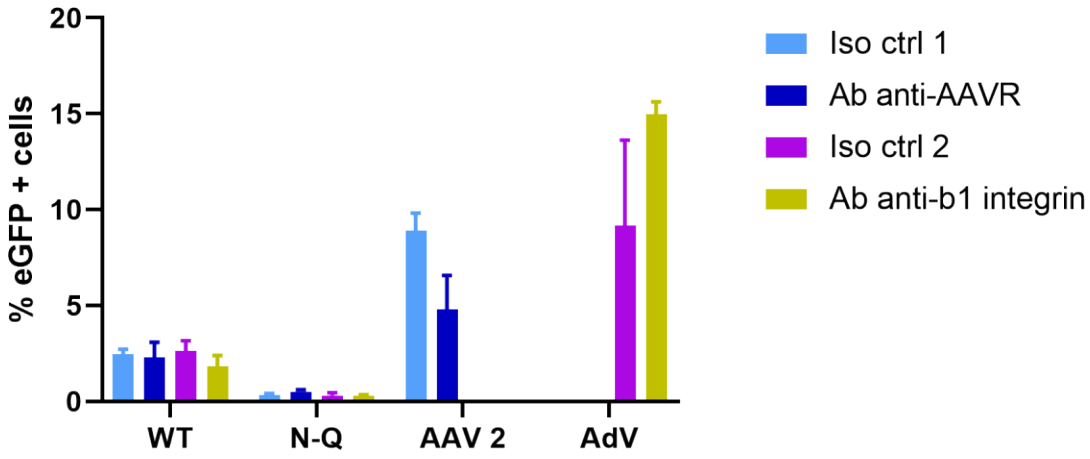

Figure 30 - Infectivity assays with blocking antibodies against AAVR or β1 integrin. Infection done with BKPyV WT and N-Q PSVs on 293TT cells. AAV2 and AdV were used as positive controls to test AAVR & β1 integrin, respectively. Graph was made with GraphPad Prism 8.

To broadly screen for the unknown receptor, we could also use a similar method to that which led to the discovery of AAVR by doing a genome-wide screening with mutagenesis in 293TT cells (Pillay et al., 2016). A library of mutant 293TT cells would have to be built by knocking-out a different non-essential gene per mutant cell, probably by CRISPR-Cas9 editing. Infection with BKPyV PSVs then would have to be performed to identify mutant cells that are not infected. After sorting these infection-resistant mutant cells, one or multiple genes important for infection can be identified with, among them, the potential new receptor. It could be that among all the different hits, genes involved in the viral internalisation and trafficking are also identified. Once a potential receptor is identified, to further confirm its involvement in BKPyV infection, reestablishment and perhaps also, overexpression of this gene in the knock-out cells could be done to check if infection by BKPyV is rescued.

Regarding the other gIb2 variants, glycan array results showed that the MVQNQ variant binds to the known receptors: GD1b and GT1b but also has weak binding to a-series GD1a and GT1a. Somehow, it seems that MVQNQ shows similar binding as

the VQQ variant but with weaker signal, which is interesting because MVQNQ replaces VQQ as the dominant variant in patient 3.5. However, we saw for VQQ that, although it had a broader binding profile, it was not able to infect cells supplemented with those same gangliosides. Thus, it would have been interesting to check if MVQNQ PSVs could infect ganglioside-supplemented cells, as we did for the VQQ variant. Moreover, on a structural level, it would have been interesting to see if the BC2 loop shift is still present. Both amino acids 69 and 75 are involved in direct interactions with the double sialic acids in the WT structure, so we could have expected a more drastic change in tropism for this variant compared to VQQ. However, we did not see many differences in binding of MVQNQ VP1 pentamers on the glycan array. Thus, K69M does not appear to induce any drastic changes in ganglioside specificity, as we described for K69N, or as was previously reported for the K69S mutation (Neu et al., 2013). Unfortunately, we were not able to express stable, crystallisable MVQNQ VP1 pentamers, VLPs or PSVs to confirm these suppositions.

The last three gIb2 variants, E73K, VK, and VKK all come from the patient 3.19 and became dominant variants one after the other. While VK and VKK variants harbour broader ganglioside binding profiles, including again both known receptors, but also a-series receptors like GD1a and GT1a, the single variant E73K seems to be specific for only GT1b, according to the glycan array screening results.
When we compared the binding profile of this single variant to the two others, E73Q and E73A (coming from two different patients) we saw that both showed broader binding profiles by targeting a- and b-series gangliosides. E73Q and E73A both lost the negative charge initially carried by E73, however for the E73K variant, the negative charge is replaced by a positive one. While we previously suggested that loss of charge was responsible for broadening the ganglioside binding, in the case of E73K, the change from negative to positive charge could have the opposite effect and may restrict the binding of this variant to only GT1b. Moreover, for gIVc2 E73K, glycan array screening results also showed specific binding to only GT1b. The crystal structure of this gIVc2 mutant revealed also that the mutation in 73 to lysine led to a loop switch similar to that seen for gIb2 E73A and VQQ (**Figure 31**).

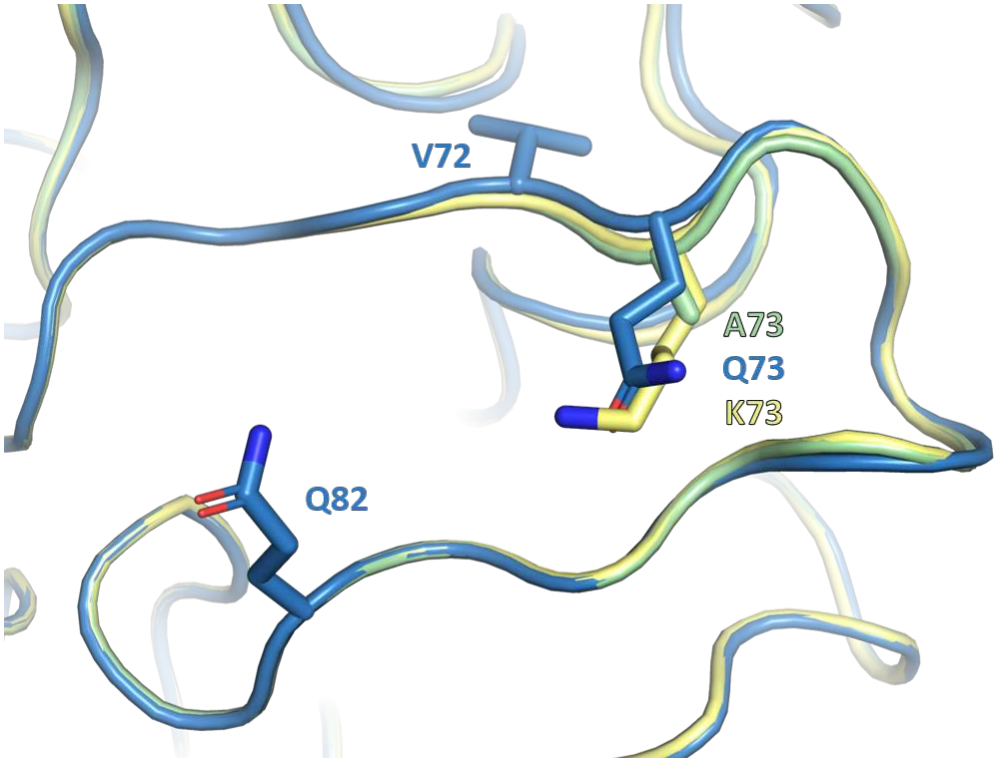

Figure 31 - Superposition of gI E73A (green), VQQ (blue) and IVc2 E73K (yellow) focusing on the BC-loop where the mutations are found. Mutated residues are represented as sticks. Figure was made with Pymol.

Thus, it further supports the view that position 73 is the main determinant of BC2 loop orientation. Moreover, this loop switch could have a similar impact on gIVc2 E73K variant infectivity to that seen for the gIb2 VQQ and E73A variants, which had strongly reduced infectivity in 293TT cells, possibly due to loss of interaction with the unknown co-receptor found on these cells. Unpublished data previously obtained at the CR2TI concerning the gIVc2 E73K variant showed that this was indeed the case (**Figure 32**).

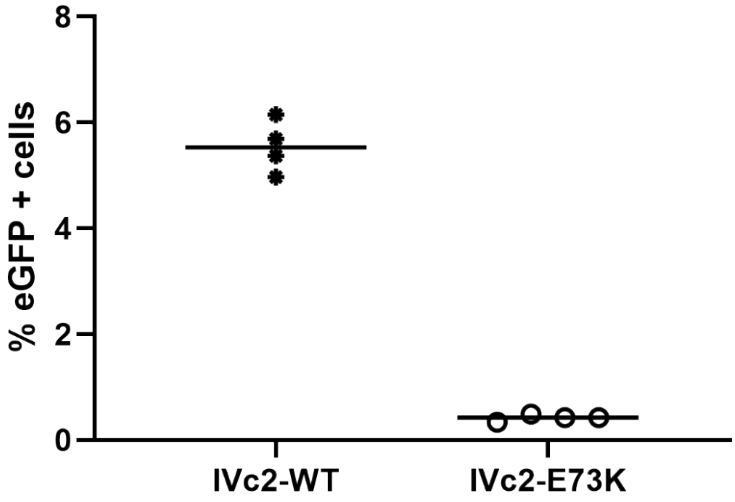

Figure 32 - Infectivity assay with IVc2 WT and E73K PSVs on 293TT cells. The graph was made with GraphPad Prism 8.

To better characterise the impact of the E73K mutation in the context of BKPyV genotypes Ib2 and IVc2, it would be interesting to perform cellular binding assays, and further infection assays as well as a structural study of gIb2 E73K to see if the same loop switch as that seen in the gIVc2 E73K structure is observed.
Another mutant VK can be found for both gIb2 and gIVc2 BKPyV. The mutations are found at position 72 and 73 which are amino acids frequently found mutated in patients. While gI VK harbours broad binding profile including a- and b-series gangliosides, gIVc2 VK show strong binding to GT1b and weaker binding to GD1a and GM1b, indicating that somehow here the genotype of BKPyV influences the gangliosides specificity.

Similarly, we can compare gIb2 and gIVc2 WT BKPyV binding profiles. For gIVc2 WT, glycan array screening shows very weak binding results while preliminary cellular binding assays highlight a broader binding profile than gIb2 WT with binding to a-series GT1a and GD1a in addition to b-series gangliosides. However, infection seemed not to be supported by GD1a but by GD1b, while infection induced through GT1b and GT1a remain to be tested. Thus, gIVc2 WT seems to bind a- and b-series gangliosides but infect only through b-series gangliosides.

Finally, the last two variants: D77N and K-N come from the same patient. Glycan array results show that the D77N variant can interact with b-series gangliosides but also a-series GT1a. While for K-N, binding is only seen for BKPyV described receptors: GT1b and GD1b. However, for this variant, preliminary cellular binding assays also showed that additional binding to GD3 and a-series GD1a and GT1a was seen. Thus, it seems that the broader binding profile seen for the D77N variant is conserved for this K-N variant, which appears later in the patient. Interestingly, we were also able to see that the K-N variant can infect through a- and b-series gangliosides: GD1a and GD1b. We could have expected a binding and infectious profile closer to that of gI WT BKPyV since the mutation 69 re-establishes the lysine found in gIb2 WT sequence, but here, the D77N mutation is also present and might be enough to broaden the binding and infectious profile of this mutant.

No co-crystallisation, soaking or docking were performed with ganglioside ligands. Superposition of the WT structure in interaction with GD3 (PD ID: 4MJ1, Neu et al.,

2013) to the different variants was done by aligning the structures in Pymol. It was performed to observe if the di-sialic motif in its conformation in the WT structure could also bind in the same conformation the variant structure. By doing this, we are assuming that the ligand would bind in the exact same conformation as when it binds the WT pentamer. However, we can not guarantee that the ligand could not bind in another conformation to the VP1 pentamers. Furthermore, all structures were compared to the structure of the gI WT VP1 pentamer in interaction with GD3 published by Neu et al, 2013. However, Hurdiss et al., 2018 also published a structure of gI WT BKPyV capsid in interaction with GT1b. For this structure, while the di-sialic acid motif binds in the same binding pocket as described in the structure of Neu et al, 2013, density can also be seen in between amino acids D60 and K84 where the other part of GT1b terminated by a single sialic acid interacts. None of the studied variants present mutations in this area, thus no comparison was made with this structure. But we could speculate that mutations of these amino acids would probably influence the interactions with GT1b and similarly structured gangliosides.

Even if further functional and structural studies are required on the last batch of variants, we were able to see that mutations occurring in the BC-loop can impact the tropism and structure of the virus. Indeed, while most mutations seemed to influence the ganglioside-specificity of BKPyV by broadening or restricting it, the gI N-Q variant stuck out by totally losing its interaction with gangliosides. Structural studies also allowed us to pinpoint the structural modifications that correlated with the variants' phenotype in terms of receptor specificity and infectivity. But mostly, with the N-Q variant, we were able to highlight the use of a sialic acid-independent pathway for infection, indicating the presence of an unknown receptor. We also suspect that WT BKPyV could interact with this unknown receptor, which would mean that BKPyV is also able to use a two-receptor entry mechanism, as is seen for some other polyomaviruses and many non-enveloped viruses.

Project B: BKPyV genotypes tropism and structure

The four BKPyV genotypes are characterised by sequence differences mostly in the BC-loop region of VP1 which, as we saw in the previous project, are important regarding sialic acid interactions. Thus, by having inter-genotype differences concentrated in this part of the VP1, it seemed logical to hypothesise that tropism could be different between the four BKPyV genotypes.

Pastrana et al., 2013, reported infection in GM95 by genotype IVc2 BKPyV independently of the presence of gangliosides GD1b and GT1b (Pastrana et al., 2013).

However, we were not able to confirm this observation, as no infection was seen for gIVc2 WT PSVs in GM95 cells without ganglioside supplementation (**Figure 18**).

Functional assays showed that binding of all genotypes to 293TT cells is sialic acid dependent. However, for infection, while gI, II and III lose almost all infectivity in these cells after neuraminidase treatment, gIV retains around 50% of its infectious capacity. Thus, this could indicate that a distinct entry pathway is used by this genotype - perhaps related to that utilised by the gIb2 N-Q variant. Functional assays on the other renal cell line: the RS cells could also be interesting to see if again gIV maintains a significant infection capacity when sialic acids are removed and if the other genotypes, especially gII and gIII, are still dependent on sialic acid for infection.

Despite this observation, gIV, like gI BKPyV can still use gangliosides for infection. Indeed, glycan array and cell binding assay results showed binding to several gangliosides including GT1b and GD1b. Infection was confirmed when LNCaP or GM95 cells were supplemented with GD1b. Thus, this indicates that gIV BKPyV remains able to use the known receptors GT1b and GD1b for infection.

For gI BKPyV, we confirmed that it can bind and infect cells via GT1b and GD1b as well as other b-series gangliosides. However, as discussed above, no such gangliosides are found on 293TT cells, indicating that another compound carrying sialic acid must be used to enter those cells. It was already suggested that an N-linked glycoprotein carrying α2-3 sialic acid was used by BKPyV to infect 293TT rather than gangliosides (Dugan et al., 2005). Moreover, results on a broad glycan array revealed binding to LSTa, which also carries α2-3 sialic acid. Thus, it could be that a glycan structure close to LSTa is present on 293TT cells and be the sialic acid compound used by gI WT for entry into these cells. More functional and structural assays should

be done to confirm this hypothesis. Moreover, this could highlight a similarity between BKPyV and JCPyV because JCPyV was shown to interact with LSTc, a lacto-series oligosaccharide similar to LSTa.

For gII and gIII, binding and infection also remain dependent on sialic acid, however it is currently not known which different sialylated glycans or glycoproteins are targeted. The structure of both gI and gIVc2 VP1 pentamers show no drastic structural changes, despite the extensive sequence variation in the BC-loop between genotypes. Binding to the double sialic acid part of the gangliosides involves BC-loop residues including amino acids at positions 62, 66, 68, 69 and 75 which can differ between genotypes (**Figure 33**). In the gI VP1 pentamer structure in interaction with GD3, amino acids 66 and 68 have van der Waals interaction with the double sialic acid part of the gangliosides, while amino acids at positions 62 and 75 of the neighbouring monomer have water-mediated hydrogen bonds. Finally, amino acid 69 makes a direct hydrogen bond with the glycerol chain of the first sialic acid and a salt bridge the carboxyl group of the second sialic acid, through its side chain.

We know that amino acid 69 is critical in the interaction of VP1 with sialic acid because a change of this amino acid can lead to loss of interaction with sialylated compounds, as seen with the gIb2 N-Q variant, or change the ganglioside specificity, as done in the Neu et al., 2013 study where mutation of lysine to serine altered ganglioside specificity to GM1 only. We saw that mutation of lysine to arginine for gIV does not seem to impact greatly the ganglioside specificity, probably due to the similar structure of both side chains as well as both being positively charged. Genotype II also carries a lysine however gIII has a histidine at this position. While histidine is also a basic amino acid like arginine and lysine, the overall structure is quite different with a shorter cyclic side chain. So, we could hypothesise that gIII may have a different ganglioside specificity compared to gI, II and IV. Mutations of the other amino acids at positions 62, 66, 68 and 75 could also potentially influence the overall binding.

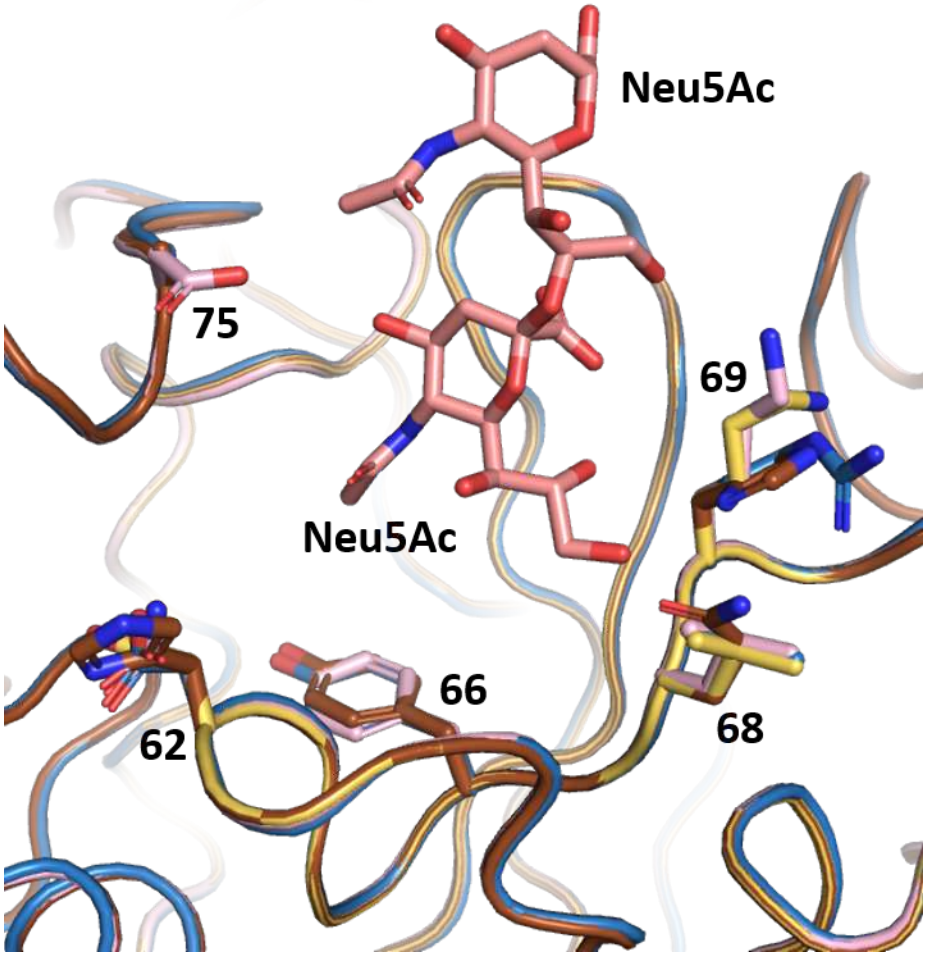

Figure 33 - Binding pocket of four genotypes of BKPyV. Structures of gI (pink) (PDB ID: 4MJ0) and IV (blue) genotypes were used while genotype II (yellow) and III (brown) were modelled in Pymol. Di-sialic acid motif is represented in pink sticks. Amino acids 62, 66, 68, 69 and 75 are shown as sticks. gI: N62, F66, L68, K69, D75; gII: D62,Y66, L68, K69, A75; gIII: H62, Y66, Q68, H69, A75 & gIV: D62, Y66, L68, R69, A75. Figure was made with Pymol.

Interestingly, genotype III BKPyV is rarely found in the population. Thus, we could hypothesise that this genotype might be interacting with a different subset of sialylated receptors less represented at the renal cell surface making it less prevalent in the worldwide population. On the other hand, its relative rarity could be simply due to the fact that it is found mainly in Africa. Most studies of BKPyV genetic polymorphism involve cohorts recruited in North America, Europe, or East Asia, and this sampling bias automatically reduces the number of gIII viruses that are reported.

To answer the receptor specificity question, glycan array screening experiments with ganglioside and broad glycan arrays are planned with gII and gIII VP1 pentamers. Thus, after a clearer definition of the binding spectrum of those genotypes, cellular

binding assays and infection assays should be done to confirm the glycan array screening results as presented here.

Similarly, as described before, all genotypes should be tested for their interactions with the putative co-receptor. This is particularly true for gIV, which retains partial infectivity after sialic acid removal in 293TT cells.

Project C: Characterisation of JCPyV interaction with 5HT2RB

A first study made on glial cells by Elphick et al, 2004, revealed that JCPyV could use G-coupled receptor: 5-HT2A receptor, a serotonin receptor, for infection. Further studies highlighted that JCPyV initially binds to the plasma membrane through glycan receptor: LSTc and confirmed that afterwards, through transient interactions, the virus interacts with 5HT2RA but also isoforms 5HT2RB and C (Assetta et al., 2013, 2019). Those receptors are used by the virus for internalisation though clathrin-dependent endocytosis. This endocytosis is thought to mainly occur by interaction of β-arrestin with intracellular loops and C-terminus of the 5HT2Rs (Assetta et al., 2019; Mayberry et al., 2019, 2021). This triggers recruitment of other proteins for endocytosis like AP-2 or clathrin, as well as activation of signalling pathways like MAPK pathway which was shown to be essential for JCPyV infection in glial cells (DuShane et al., 2018; Mayberry et al., 2019). While many studies focus on how the virus triggers internalisation through the 5HT2Rs, no studies clearly investigate how the virus interacts with the receptor. Only a study by Assetta et al., 2019, proposed that 5HT2R-dependent infection can occur without the 2nd and 3rd extracellular loop (Assetta et al., 2019). So, it could be that the virus interacts only with the first external loop, or the N-terminal domain of the receptor. Thus, our aim with this project was to further characterise the interaction of JCPyV with the serotonin receptor: 5HT2RB.

To approach these different questions, we first tried to perform binding assays through ELISA by using peptides representing the external loop sequences.

However, despite multiple trials, we encountered a lot of background unspecific binding for all experiments, and no real specific binding to VLPs was identified. No clear result was seen either because the free peptides did not adopt their native conformation, or because multiple regions of HTR2B participate in the interaction. Either of these two possibilities would explain the absence of real binding to the VLP target. We therefore abandoned this approach and commenced work on the full receptor.

Expression and purification of transmembrane receptors are notoriously challenging, but I based my work on the sequence and the purification protocol of Wacker et al., 2017. This group managed to design, express, purify and even crystallise 5HT2RB. Thus, I used the same construct as them but without the N-terminal FLAG tag and

then generated a recombinant baculovirus expressing the receptor successfully. I initially followed their protocol too, for purification but decided to add a size-exclusion step to have a purer sample. I did manage to express the receptor, however in small quantities. After multiple purifications, I always ended up with a chromatogram peak around the same molecular weight of around 450 kDa so I assumed it was the receptor associated with detergent. However, I did not have time to further characterise this compound. As I kept the His-tag, it could be multiple receptors associated together through multiple His-tag interactions. Even so, I have no possibility to affirm that the receptor, even in detergent, is in its correct conformation. Despite these doubts, I still tried to perform SPR measurements which ended up not being successful. First, we were not able to capture the receptor by the His-tag whichcould indicate that the tag is not accessible and thus, that the receptor might not be in the correct conformation. Therefore, I do think the problem is the receptor, its quantity and probably its conformation and stability.

Thus, purification of the receptor needs to be improved for this project to progress. Instead of using detergents, polymers are also sometimes used to capture the receptor in the lipid bilayer creating a more stable environment for the receptor which should stay in its initial conformation (Jamshad et al., 2015). We could also purify the receptor in a form of receptor-enriched membrane vesicle (Minic et al., 2005; Silin et al., 2006).

Characterising an affinity constant between the virus and the receptor as well as identifying whether pentamers or full capsids are required for the interaction would have been done by SPR measurement. However, characterisation of the different amino acids involved on the receptor and the virus in the interaction was planned to be done through structural studies: either with X-ray crystallography after co-crystallisation of pentamer-HTR2B complexes or cryo-EM of capsid-HTR2B complexes.

Indeed, if only one pentamer interacts with the receptor, crystallisation of VP1 pentamers of JCPyV with purified 5HT2RB receptor in lipid cubic phase could be attempted. However, if the receptor requires multiple pentamers for interaction, cryo-EM might be more suitable to get a complex of the viral particle in interaction with the receptor.

Since the attachment receptor, the lacto-series c oligosaccharide, seems to interact

on the top of the pentamer, it could be that the interaction with the external loop of 5HT2RB requires multiple pentamers interface and thus more on the side of the pentamer rather than on top. To show that, we could have also performed binding assays with labelled JCPyV VP1 pentamers or VLPs on SF9 insect cells expression 5HT2RB.

The structural basis of the interaction between HTR2B and the JCPyV capsid therefore remains to be resolved.

References

Abend, J. R., Jiang, M., & Imperiale, M. J. (2009). BK Virus and Human Cancer : Innocent until Proven Guilty. *Seminars in cancer biology*, *19*(4), 252-260. https://doi.org/10.1016/j.semcancer.2009.02.004

Adang, L., & Berger, J. (2015). Progressive Multifocal Leukoencephalopathy. *F1000Research*, *4*, F1000 Faculty Rev-1424. https://doi.org/10.12688/f1000research.7071.1

Ajuh, E. T., Wu, Z., Kraus, E., Weissbach, F. H., Bethge, T., Gosert, R., Fischer, N., & Hirsch, H. H. (2018). Novel Human Polyomavirus Noncoding Control Regions Differ in Bidirectional Gene Expression according to Host Cell, Large T-Antigen Expression, and Clinically Occurring Rearrangements. *Journal of Virology*, *92*(7). https://doi.org/10.1128/jvi.02231-17

Aksamit, A. J. (2001). Treatment of non-AIDS progressive multifocal leukoencephalopathy with cytosine arabinoside. *Journal of Neurovirology*, *7*(4), 386-390. https://doi.org/10.1080/13550280152537292

Alexiev, B. A., Randhawa, P., Vazquez Martul, E., Zeng, G., Luo, C., Ramos, E., Drachenberg, C. B., & Papadimitriou, J. C. (2013). BK virus-associated urinary bladder carcinoma in transplant recipients : Report of 2 cases, review of the literature, and proposed pathogenetic model. *Human Pathology*, *44*(5), 908-917. https://doi.org/10.1016/j.humpath.2012.09.019

Allander, T., Andreasson, K., Gupta, S., Bjerkner, A., Bogdanovic, G., Persson, M. A. A., Dalianis, T., Ramqvist, T., & Andersson, B. (2007). Identification of a Third Human Polyomavirus. *Journal of Virology*, *81*(8), 4130-4136. https://doi.org/10.1128/jvi.00028-07

Ambalathingal, G. R., Francis, R. S., Smyth, M. J., Smith, C., & Khanna, R. (2017). BK Polyomavirus : Clinical Aspects, Immune Regulation, and Emerging Therapies. *Clinical Microbiology Reviews*, *30*(2), 503-528. https://doi.org/10.1128/CMR.00074-16

An, P., Robles, M. T. S., & Pipas, J. M. (2012). Large T antigens of polyomaviruses : Amazing molecular machines. *Annual Review of Microbiology*, *66*, 213-236. https://doi.org/10.1146/annurev-micro-092611-150154

An, P., Sáenz Robles, M. T., Duray, A. M., Cantalupo, P. G., & Pipas, J. M. (2019). Human polyomavirus BKV infection of endothelial cells results in interferon pathway induction and persistence. *PLoS Pathogens*, *15*(1), e1007505. https://doi.org/10.1371/journal.ppat.1007505

Andrews, C. A., Shah, K. V., Daniel, R. W., Hirsch, M. S., & Rubin, R. H. (s. d.). *A Serological Investigation of UK Virus and JC Virus Infections in Recipients of Renal Allografts*. 6.

Anzivino, E., Rodio, D. M., Mischitelli, M., Bellizzi, A., Sciarra, A., Salciccia, S., Gentile, V., & Pietropaolo, V. (2015). High Frequency of JCV DNA Detection in Prostate Cancer Tissues. *Cancer Genomics & Proteomics*, *12*(4), 189-200.

Arias, C. F., Silva-Ayala, D., & López, S. (2015). Rotavirus Entry : A Deep Journey into the Cell with Several Exits. *Journal of Virology*, *89*(2), 890-893. https://doi.org/10.1128/JVI.01787-14

Arthur, R. R., Shah, K. V., Baust, S. J., Santos, G. W., & Saral, R. (1986). Association of BK Viruria with Hemorrhagic Cystitis in Recipients of Bone Marrow Transplants. *New England Journal of Medicine*, *315*(4), 230-234. https://doi.org/10.1056/NEJM198607243150405

Assetta, B., De Cecco, M., O'Hara, B., & Atwood, W. J. (2016). JC Polyomavirus Infection of Primary Human Renal Epithelial Cells Is Controlled by a Type I IFN-Induced Response. *mBio*, *7*(4), e00903-16. https://doi.org/10.1128/mBio.00903-16

Assetta, B., Maginnis, M. S., Gracia Ahufinger, I., Haley, S. A., Gee, G. V., Nelson, C. D. S., O'Hara, B. A., Allen Ramdial, S. A., & Atwood, W. J. (2013). 5-HT 2 Receptors Facilitate JC Polyomavirus Entry. *Journal of Virology*, *87*(24), 13490-13498. https://doi.org/10.1128/jvi.02252-13

Assetta, B., Morris-Love, J., Gee, G. V., Atkinson, A. L., O'Hara, B. A., Maginnis, M. S., Haley, S. A., & Atwood, W. J. (2019). Genetic and Functional Dissection of the Role of Individual 5-HT2 Receptors as Entry Receptors for JC Polyomavirus. *Cell Reports*, *27*(7), 1960-1966.e6. https://doi.org/10.1016/j.celrep.2019.04.067

ÅSTRÖM, K.-E., MANCALL, E. L., & RICHARDSON, E. P., JR. (1958). PROGRESSIVE MULTIFOCAL LEUKO-ENCEPHALOPATHY : A HITHERTO UNRECOGNIZED COMPLICATION O CHRONIC LYMPHATIC LEUKÆMIA AND HODGKIN'S DISEASE1. *Brain*, *81*(1), 93-111. https://doi.org/10.1093/brain/81.1.93

Atkinson, A. L., & Atwood, W. J. (2020). Fifty Years of JC Polyomavirus : A Brief Overview and Remaining Questions. *Viruses*, *12*(9), 969. https://doi.org/10.3390/v12090969

Ault, G. S., & Stoner, G. L. (1992). Two Major Types of JC Virus Defined in Progressive Multifocal Leukoencephalopathy Brain by Early and Late Coding Region DNA Sequences. *Journal of General Virology*, *73*(10), 2669-2678. https://doi.org/10.1099/0022-1317-73-10-2669

Baker, S. C., Mason, A. S., Slip, R. G., Skinner, K. T., Macdonald, A., Masood, O., Harris, R. S., Fenton, T. R., Periyasamy, M., Ali, S., & Southgate, J. (2022). Induction of APOBEC3-mediated genomic damage in urothelium implicates BK polyomavirus (BKPyV) as a hit-and-run driver for bladder cancer. *Oncogene*, *41*(15), 2139-2151. https://doi.org/10.1038/s41388-022-02235-8

Bauer, J., Gold, R., Adams, O., & Lassmann, H. (2015). Progressive multifocal leukoencephalopathy and immune reconstitution inflammatory syndrome (IRIS). *Acta Neuropathologica*, *130*(6), 751-764. https://doi.org/10.1007/s00401-015-1471-7

Bauman, Y., Nachmani, D., Vitenshtein, A., Tsukerman, P., Drayman, N., Stern-Ginossar, N., Lankry, D., Gruda, R., & Mandelboim, O. (2011). An identical miRNA of the human JC and BK polyoma viruses targets the stress-induced ligand ULBP3 to escape immune elimination. *Cell Host and Microbe*, *9*(2), 93-102. https://doi.org/10.1016/j.chom.2011.01.008

Bayer, N. J., Januliene, D., Zocher, G., Stehle, T., Moeller, A., & Blaum, B. S. (2020). Structure of Merkel Cell Polyomavirus Capsid and Interaction with Its Glycosaminoglycan Attachment Receptor. *Journal of Virology*, *94*(20), e01664-19, /jvi/94/20/JVI.01664-19.atom. https://doi.org/10.1128/JVI.01664-19

Bayliss, J., Karasoulos, T., & McLean, C. A. (2011). Frequency and Large T (LT) Sequence of JC Polyomavirus DNA in Oligodendrocytes, Astrocytes and Granular Cells in Non-PML Brain. *Brain Pathology*, *22*(3), 329-336. https://doi.org/10.1111/j.1750-3639.2011.00538.x

Becker, M., Dominguez, M., Greune, L., Soria-Martinez, L., Pfleiderer, M. M., Schowalter, R., Buck, C. B., Blaum, B. S., Schmidt, M. A., & Schelhaas, M. (2019). Infectious Entry of Merkel Cell Polyomavirus. *Journal of Virology*, *93*(6), e02004-18. https://doi.org/10.1128/JVI.02004-18

Behzad-Behbahani, A., Klapper, P., Vallely, P., & Cleator, G. (2003a). BK virus DNA in CSF of immunocompetent and immunocompromised patients. *Archives of Disease in Childhood*, *88*(2), 174-175. https://doi.org/10.1136/adc.88.2.174

Behzad-Behbahani, A., Klapper, P. E., Vallely, P. J., Cleator, G. M., & Bonington, A. (2003b). BKV-DNA and JCV-DNA in CSF ofPatients with Suspected Meningitis orEncephalitis. *Infection*, *31*(6), 374-378. https://doi.org/10.1007/s15010-003-3078-5

Belnap, D. M., Olson, N. H., Cladel, N. M., Newcomb, W. W., Brown, J. C., Kreider, J. W., Christensen, N. D., & Baker, T. S. (1996). Conserved Features in Papillomavirus and Polyomavirus Capsids. In *J. Mol. Biol* (Vol. 259, p. 249-263).

Bennett, S. M., Zhao, L., Bosard, C., & Imperiale, M. J. (2015). Role of a nuclear localization signal on the minor capsid Proteins VP2 and VP3 in BKPyV nuclear entry. *Virology*, *474*, 110-116. https://doi.org/10.1016/j.virol.2014.10.013

Berger, J. R., & Khalili, K. (2011). The Pathogenesis of Progressive Multifocal Leukoencephalopathy. *Discovery Medicine*, *12*(67), 495-503.

Berger, J. R., Pall, L., Lanska, D., & Whiteman, M. (1998). Progressive multifocal leukoencephalopathy in patients with HIV infection. *Journal of Neurovirology*, *4*(1), 59-68. https://doi.org/10.3109/13550289809113482

Bergh, J., Marklund, I., Gustavsson, C., Wiklund, F., Grönberg, H., Allard, A., Alexeyev, O., & Elgh, F. (2007). No link between viral findings in the prostate and subsequent cancer development. *British Journal of Cancer*, *96*(1), 137-139. https://doi.org/10.1038/sj.bjc.6603480

Bernard-Valnet, R., Koralnik, I. J., & Du Pasquier, R. (2021). Advances in Treatment of Progressive Multifocal Leukoencephalopathy. *Annals of Neurology*, *90*(6), 865-873. https://doi.org/10.1002/ana.26198

Bethge, T., Hachemi, H. A., Manzetti, J., Gosert, R., Schaffner, W., & Hirsch, H. H. (2015). Sp1 Sites in the Noncoding Control Region of BK Polyomavirus Are Key Regulators of Bidirectional Viral Early and Late Gene Expression. *Journal of Virology*, *89*(6), 3396-3411. https://doi.org/10.1128/JVI.03625-14

Blake, K., Pillay, D., Knowles, W., Brown, D. W., Griffiths, P. D., & Taylor, B. (1992). JC virus associated meningoencephalitis in an immunocompetent girl. *Archives of Disease in Childhood*, *67*(7), 956-957. https://doi.org/10.1136/adc.67.7.956

Bodary, S. C., & McLean, J. W. (1990). The integrin beta 1 subunit associates with the vitronectin receptor alpha v subunit to form a novel vitronectin receptor in a human embryonic kidney cell line. *Journal of Biological Chemistry*, *265*(11), 5938-5941. https://doi.org/10.1016/S0021-9258(19)39269-5

Bofill-Mas, S., Pina, S., & Girones, R. (2000). Documenting the Epidemiologic Patterns of Polyomaviruses in Human Populations by Studying Their Presence in Urban Sewage. *Applied and Environmental Microbiology*, *66*(1), 238-245.

Bohl, D. L., Brennan, D. C., Ryschkewitsch, C., Gaudreault-Keener, M., Major, E. O., & Storch, G. A. (2008). BK virus antibody titers and intensity of infections after renal transplantation. *Journal of clinical virology : the official publication of the Pan American Society for Clinical Virology*, *43*(2), 184-189. https://doi.org/10.1016/j.jcv.2008.06.009

Boldorini, R., Allegrini, S., Miglio, U., Paganotti, A., Cocca, N., Zaffaroni, M., Riboni, F., Monga, G., & Viscidi, R. (2011). Serological evidence of vertical transmission of JC and BK polyomaviruses in humans. *Journal of General Virology*, *92*(5), 1044-1050. https://doi.org/10.1099/vir.0.028571-0

Bollag, B., Hofstetter, C. A., Reviriego-Mendoza, M. M., & Frisque, R. J. (2010). JC virus small t antigen binds phosphatase PP2A and Rb family proteins and is required for efficient viral DNA replication activity. *PLoS ONE*, *5*(5). https://doi.org/10.1371/journal.pone.0010606

Bouvard, V., Baan, R. A., Grosse, Y., Lauby-Secretan, B., El Ghissassi, F., Benbrahim-Tallaa, L., Guha, N., & Straif, K. (2012). Carcinogenicity of malaria and of some polyomaviruses. *The Lancet Oncology*, *13*(4), 339-340. https://doi.org/10.1016/S1470-2045(12)70125-0

Brickelmaier, M., Lugovskoy, A., Kartikeyan, R., Reviriego-Mendoza, M. M., Allaire, N., Simon, K., Frisque, R. J., & Gorelik, L. (2009). Identification and Characterization of Mefloquine Efficacy against JC Virus In Vitro. *Antimicrobial Agents and Chemotherapy*, *53*(5), 1840. https://doi.org/10.1128/AAC.01614-08

Broekema, N. M., & Imperiale, M. J. (2013). MiRNA regulation of BK polyomavirus replication during early infection. *Proceedings of the National Academy of Sciences of the United States of America*, *110*(20), 8200-8205. https://doi.org/10.1073/pnas.1301907110

Buck, C. B., Phan, G. Q., Raiji, M. T., Murphy, P. M., McDermott, D. H., & McBride, A. A. (2012). Complete Genome Sequence of a Tenth Human Polyomavirus. *Journal of Virology*, *86*(19), 10887-10887. https://doi.org/10.1128/jvi.01690-12

Burger-Calderon, R., Madden, V., Hallett, R. A., Gingerich, A. D., Nickeleit, V., & Webster-Cyriaque, J. (2014). Replication of Oral BK Virus in Human Salivary Gland Cells. *Journal of Virology*, *88*(1), 559-573. https://doi.org/10.1128/JVI.02777-13

Calvignac-Spencer, S., Feltkamp, M. C. W., Daugherty, M. D., Moens, U., Ramqvist, T., Johne, R., & Ehlers, B. (2016). A taxonomy update for the family Polyomaviridae. *Archives of Virology*, *161*(6), 1739-1750. https://doi.org/10.1007/s00705-016-2794-y

Carr, M. J., McCormack, G. P., Mutton, K. J., & Crowley, B. (2006). Unique BK virus non-coding control region (NCCR) variants in hematopoietic stem cell transplant recipients with and without hemorrhagic cystitis. *Journal of Medical Virology*, *78*(4), 485-493. https://doi.org/10.1002/jmv.20566

Caruso, M., Belloni, L., Sthandier, O., Amati, P., & Garcia, M.-I. (2003). A4β1 Integrin Acts as a Cell Receptor for Murine Polyomavirus at the Postattachment Level. *Journal of Virology*, *77*(7), 3913-3921. https://doi.org/10.1128/JVI.77.7.3913-3921.2003

Cettomai, D., & McArthur, J. C. (2009). Mirtazapine Use in Human Immunodeficiency Virus–Infected Patients With Progressive Multifocal Leukoencephalopathy. *Archives of Neurology*, *66*(2), 255-258. https://doi.org/10.1001/archneurol.2008.557

Chan, B. D., Wong, G., Jiang, Q., Lee, M. M.-L., Wong, W.-Y., Chen, F., Wong, W.-T., Zhu, L., Wong, F. K.-M., & Tai, W. C.-S. (2020). Longitudinal study of BK Polyomavirus outcomes, risk factors, and kinetics in renal transplantation patients. *Microbial Pathogenesis*, *142*, 104036. https://doi.org/10.1016/j.micpath.2020.104036

Chen, P.-L., Wang, M., Ou, W.-C., Lii, C.-K., Chen, L.-S., & Chang, D. (2001). *Disulﹷde bonds stabilize JC virus capsid-like structure by protecting calcium ions from chelation*.

Chesters, P. M., Heritage, J., & McCance, D. J. (s. d.). *Persistence of DNA Sequences of OK Virus and JC Virus in Normal Human Tissues and in Diseased Tissues*. 9.

Chiang, C., Dvorkin, S., Chiang, J. J., Potter, R. B., & Gack, M. U. (2021). The Small t Antigen of JC Virus Antagonizes RIG-I-Mediated Innate Immunity by Inhibiting TRIM25's RNA Binding Ability. *mBio*, *12*(2), e00620-21. https://doi.org/10.1128/mBio.00620-21

Christensen, K. L. Y., Holman, R. C., Hammett, T. A., Belay, E. D., & Schonberger, L. B. (2010). Progressive Multifocal Leukoencephalopathy Deaths in the USA, 1979–2005. *Neuroepidemiology*, *35*(3), 178-184. https://doi.org/10.1159/000311014

Clifford, D. B., Nath, A., Cinque, P., Brew, B. J., Zivadinov, R., Gorelik, L., Zhao, Z., & Duda, P. (2013). A study of mefloquine treatment for progressive multifocal leukoencephalopathy : Results and exploration of predictors of PML outcomes. *Journal of Neurovirology*, *19*(4), 351-358. https://doi.org/10.1007/s13365-013-0173-y

Co, J. K. G., Verma, S., Gurjav, U., Sumibcay, L., & Nerurkar, V. R. (2007). Interferon-α and -β Restrict Polyomavirus JC Replication in Primary Human Fetal Glial Cells : Implications for Progressive Multifocal Leukoencephalopathy Therapy. *The Journal of Infectious Diseases*, *196*(5), 712-718. https://doi.org/10.1086/520518

Coleman, D. V., Gardner, S. D., & Field, A. M. (1973). Human Polyomavirus Infection in Renal Allograft Recipients. *British Medical Journal*, *3*(5876), 371-375. https://doi.org/10.1136/bmj.3.5876.371

Comar, M., Zanotta, N., Bovenzi, M., & Campello, C. (2010). JCV/BKV and SV40 viral load in lymphoid tissues of young immunocompetent children from an area of North-East Italy. *Journal of Medical Virology*, *82*(7), 1236-1240. https://doi.org/10.1002/jmv.21786

Cubukcu-Dimopulo, O., Greco, A., Kumar, A., Karluk, D., Mittal, K., & Jagirdar, J. (2000). BK Virus Infection in AIDS. *The American Journal of Surgical Pathology*, *24*(1), 145.

Dalianis, T., & Hirsch, H. H. (2013). Human polyomaviruses in disease and cancer. *Virology*, *437*(2), 63-72. https://doi.org/10.1016/j.virol.2012.12.015

De Luca, A., Ammassari, A., Pezzotti, P., Cinque, P., Gasnault, J., Berenguer, J., Di Giambenedetto, S., Cingolani, A., Taoufik, Y., Miralles, P., Marra, C. M., Antinori, A., & for Gesida 9/99, I. (2008). Cidofovir in addition to antiretroviral treatment is not effective for AIDS-associated progressive multifocal leukoencephalopathy : A multicohort analysis. *AIDS*, *22*(14), 1759-1767. https://doi.org/10.1097/QAD.0b013e32830a5043

De Luca, A., Giancola, M. L., Ammassari, A., Grisetti, S., Cingolani, A., Larussa, D., Alba, L., Murri, R., Ippolito, G., Cauda, R., Monforte, A., & Antinori, A. (2001). Potent anti-retroviral therapy with or without cidofovir for AIDS-associated progressive multifocal leukoencephalopathy : Extended follow-up of an observational study. *Journal of Neurovirology*, *7*(4), 364-368. https://doi.org/10.1080/13550280152537256

De Luca, A., Giancola, M. L., Cingolani, A., Ammassari, A., Gillini, L., Murri, R., & Antinori, A. (1999). Clinical and Virological Monitoring During Treatment with Intrathecal Cytarabine in Patients with AIDS-Associated Progressive Multifocal Leukoencephalopathy. *Clinical Infectious Diseases*, *28*(3), 624-628. https://doi.org/10.1086/515153

Decaprio, J. A., & Garcea, R. L. (2013). A cornucopia of human polyomaviruses. In *Nature Reviews Microbiology* (Vol. 11, Numéro 4, p. 264-276). https://doi.org/10.1038/nrmicro2992

Dechecchi, M. C., Tamanini, A., Bonizzato, A., & Cabrini, G. (2000). Heparan Sulfate Glycosaminoglycans Are Involved in Adenovirus Type 5 and 2-Host Cell Interactions. *Virology*, *268*(2), 382-390. https://doi.org/10.1006/viro.1999.0171

de Kort, H., Heutinck, K. M., Ruben, J. M., Ede V. Silva, A., Wolthers, K. C., Hamann, J., & ten Berge, I. J. M. (2017). Primary Human Renal-Derived Tubular Epithelial Cells Fail to Recognize and Suppress BK Virus Infection. *Transplantation*, *101*(8), 1820-1829. https://doi.org/10.1097/TP.0000000000001521

Di Taranto, C., Pietropaolo, V., Orsi, G. B., Lin, L., Sinibaldi, L., & Degener, A. M. (1997). Detection of BK polyomavirus genotypes in healthy and HIV-positive children. *European Journal of Epidemiology*, *13*(6), 653-657. https://doi.org/10.1023/A:1007371320999

Domingo-Calap, P., Schubert, B., Joly, M., Solis, M., Untrau, M., Carapito, R., Georgel, P., Caillard, S., Fafi-Kremer, S., Paul, N., Kohlbacher, O., González-Candelas, F., & Bahram, S. (2018). An unusually high substitution rate in transplant-associated BK polyomavirus in vivo is further concentrated in HLA-C-bound viral peptides. *PLoS Pathogens*, *14*(10), e1007368. https://doi.org/10.1371/journal.ppat.1007368

Drachenberg, C. B., Hirsch, H. H., Papadimitriou, J. C., Gosert, R., Wali, R. K., Munivenkatappa, R., Nogueira, J., Cangro, C. B., Haririan, A., Mendley, S., & Ramos, E. (2007). Polyomavirus BK Versus JC Replication and Nephropathy in Renal Transplant Recipients : A Prospective Evaluation. *Transplantation*, *84*(3), 323-330. https://doi.org/10.1097/01.tp.0000269706.59977.a5

Drachenberg, C. B., Papadimitriou, J. C., Hirsch, H. H., Wali, R., Crowder, C., Nogueira, J., Cangro, C. B., Mendley, S., Mian, A., & Ramos, E. (2004). Histological Patterns of Polyomavirus Nephropathy : Correlation with Graft Outcome and Viral Load. *American Journal of Transplantation*, *4*(12), 2082-2092. https://doi.org/10.1046/j.1600-6143.2004.00603.x

Dropulic, L. K., & Jones, R. J. (2008). Polyomavirus BK infection in blood and marrow transplant recipients. *Bone Marrow Transplantation*, *41*(1), Art. 1. https://doi.org/10.1038/sj.bmt.1705886

Dugan, A. S., Eash, S., & Atwood, W. J. (2005). An N-linked glycoprotein with alpha(2,3)-linked sialic acid is a receptor for BK virus. *Journal of Virology*, *79*(22), 14442-14445. https://doi.org/10.1128/jvi.79.22.14442-14445.2005

DuShane, J. K., Wilczek, M. P., Mayberry, C. L., & Maginnis, M. S. (2018). ERK Is a Critical Regulator of JC Polyomavirus Infection. *Journal of Virology*, *92*(7), e01529-17. https://doi.org/10.1128/JVI.01529-17

Eash, S., Querbes, W., & Atwood, W. J. (2004). Infection of Vero Cells by BK Virus Is Dependent on Caveolae. *Journal of Virology*, *78*(21), 11583-11590. https://doi.org/10.1128/jvi.78.21.11583-11590.2004

Egli, A., Infanti, L., Dumoulin, A., Buser, A., Samaridis, J., Stebler, C., Gosert, R., & Hirsch, H. H. (2009). Prevalence of polyomavirus BK and JC infection and replication in 400 healthy blood donors. *The Journal of Infectious Diseases*, *199*(6), 837-846. https://doi.org/10.1086/597126

Elphick, G. F. (2004). The Human Polyomavirus, JCV, Uses Serotonin Receptors to Infect Cells. *Science*, *306*(5700), 1380-1383. https://doi.org/10.1126/science.1103492

Erickson, K. D., Garcea, R. L., & Tsai, B. (2009). Ganglioside GT1b Is a Putative Host Cell Receptor for the Merkel Cell Polyomavirus. *Journal of Virology*, *83*(19), 10275-10279. https://doi.org/10.1128/jvi.00949-09

Evans, G. L., Caller, L. G., Foster, V., & Crump, C. M. (2015). Anion homeostasis is important for non-lytic release of BK polyomavirus from infected cells. *Open Biology*, *5*(8). https://doi.org/10.1098/rsob.150041

Fahsbender, E., Altan, E., Estrada, M., Seguin, M. A., Young, P., Leutenegger, C. M., & Delwart, E. (2019). *Lyon-IARC Polyomavirus DNA in Feces of Diarrheic Cats*. https://doi.org/10.1128/MRA

Feng, H., Shuda, M., Chang, Y., & Moore, P. S. (2008). Clonal integration of a polyomavirus in human Merkel cell carcinoma. *Science*, *319*(5866), 1096-1100. https://doi.org/10.1126/science.1152586

Ferenczy, M. W., Marshall, L. J., Nelson, C. D. S., Atwood, W. J., Nath, A., Khalili, K., & Major, E. O. (2012). Molecular Biology, Epidemiology, and Pathogenesis of Progressive Multifocal Leukoencephalopathy, the JC Virus-Induced Demyelinating Disease of the Human Brain. *Clinical Microbiology Reviews*, *25*(3), 471-506. https://doi.org/10.1128/CMR.05031-11

Fiore, T., Martin, E., Descamps, V., Brochot, E., Morel, V., Handala, L., Dakroub, F., Castelain, S., Duverlie, G., Helle, F., & François, C. (2020). Indoleamine 2,3-Dioxygenase Is Involved in Interferon Gamma's Anti-BKPyV Activity in Renal Cells. *Viruses*, *12*(8), 865. https://doi.org/10.3390/v12080865

Forni, D., Cagliani, R., Clerici, M., Pozzoli, U., & Sironi, M. (2020). You Will Never Walk Alone : Codispersal of JC Polyomavirus with Human Populations. *Molecular Biology and Evolution*, *37*(2), 442-454. https://doi.org/10.1093/molbev/msz227

Foulongne, V., Sauvage, V., Hebert, C., Dereure, O., Cheval, J., Gouilh, M. A., Pariente, K., Segondy, M., Burguière, A., Manuguerra, J. C., Caro, V., & Eloit, M. (2012). Human skin Microbiota : High diversity of DNA viruses identified on the human skin by high throughput sequencing. *PLoS ONE*, *7*(6). https://doi.org/10.1371/journal.pone.0038499

Furmaga, J., Kowalczyk, M., Zapolski, T., Furmaga, O., Krakowski, L., Rudzki, G., Jaroszyński, A., & Jakubczak, A. (2021). BK Polyomavirus—Biology, Genomic Variation and Diagnosis. *Viruses*, *13*(8), Art. 8. https://doi.org/10.3390/v13081502

Gandhi, N. S., & Mancera, R. L. (2008). The Structure of Glycosaminoglycans and their Interactions with Proteins. *Chemical Biology & Drug Design*, *72*(6), 455-482. https://doi.org/10.1111/j.1747-0285.2008.00741.x

Gardner, S. D. (1973). Prevalence in England of Antibody to Human Polyomavirus (B.K.). *British Medical Journal*, *1*(5845), 77-78.

Gasnault, J., Kahraman, M., de Goër de Herve, M. G., Durali, D., Delfraissy, J.-F., & Taoufik, Y. (2003). Critical role of JC virus-specific CD4 T-cell responses in preventing progressive multifocal leukoencephalopathy. *AIDS*, *17*(10), 1443-1449.

Gasnault, J., Kousignian, P., Kahraman, M., Rahoiljaon, J., Matheron, S., Delfraissy, J. F., & Taoufik, Y. (2001). Cidofovir in AIDS-associated progressive multifocal leukoencephalopathy : A monocenter observational study with clinical and JC virus load monitoring. *Journal of Neurovirology*, *7*(4), 375-381. https://doi.org/10.1080/13550280152537274

Gaynor, A. M., Nissen, M. D., Whiley, D. M., Mackay, I. M., Lambert, S. B., Wu, G., Brennan, D. C., Storch, G. A., Sloots, T. P., & Wang, D. (2007). Identification of a novel polyomavirus from patients with acute respiratory tract infections. *PLoS Pathogens*, *3*(5), 0595-0604. https://doi.org/10.1371/journal.ppat.0030064

Gedvilaite, A., Tryland, M., Ulrich, R. G., Schneider, J., Kurmauskaite, V., Moens, U., Preugschas, H., Calvignac-Spencer, S., & Ehlers, B. (2017). Novel polyomaviruses in shrews (Soricidae) with close similarity to human polyomavirus 12. *Journal of General Virology*, *98*(12), 3060-3067. https://doi.org/10.1099/jgv.0.000948

Geoghegan, E. M., Pastrana, D. V., Schowalter, R. M., Ray, U., Gao, W., Ho, M., Pauly, G. T., Sigano, D. M., Kaynor, C., Cahir-McFarland, E., Combaluzier, B., Grimm, J., & Buck, C. B. (2017). Infectious Entry and Neutralization of Pathogenic JC Polyomaviruses. *Cell Reports*, *21*(5), 1169-1179. https://doi.org/10.1016/j.celrep.2017.10.027

Gheit, T., Dutta, S., Oliver, J., Robitaille, A., Hampras, S., Combes, J. D., McKay-Chopin, S., Le Calvez-Kelm, F., Fenske, N., Cherpelis, B., Giuliano, A. R., Franceschi, S., McKay, J., Rollison, D. E., & Tommasino, M. (2017). Isolation and characterization of a novel putative human polyomavirus. *Virology*, *506*, 45-54. https://doi.org/10.1016/j.virol.2017.03.007

Gheuens, S., Pierone, G., Peeters, P., & Koralnik, I. J. (2010). Progressive multifocal leukoencephalopathy in individuals with minimal or occult immunosuppression. *Journal of Neurology, Neurosurgery & Psychiatry*, *81*(3), 247-254. https://doi.org/10.1136/jnnp.2009.187666

Gilbert, J., & Benjamin, T. (2004). Uptake Pathway of Polyomavirus via Ganglioside GD1a. *JOURNAL OF VIROLOGY*, *78*(22), 12259-12267. https://doi.org/10.1128/JVI.78.21.12259-12267.2004

Giroglou, T., Florin, L., Schäfer, F., Streeck, R. E., & Sapp, M. (2001). Human Papillomavirus Infection Requires Cell Surface Heparan Sulfate. *Journal of Virology*, *75*(3), 1565-1570. https://doi.org/10.1128/JVI.75.3.1565-1570.2001

Giudici, B., Vaz, B., Bossolasco, S., Casari, S., Brambilla, A. M., Lüke, W., Lazzarin, A., Weber, T., & Cinque, P. (2000). Highly Active Antiretroviral Therapy and Progressive Multifocal Leukoencephalopathy : Effects on Cerebrospinal Fluid Markers of JC Virus Replication and Immune Response. *Clinical Infectious Diseases*, *30*(1), 95-99. https://doi.org/10.1086/313598

Goodfellow, I. G., Sioofy, A. B., Powell, R. M., & Evans, D. J. (2001). Echoviruses Bind Heparan Sulfate at the Cell Surface. *Journal of Virology*, *75*(10), 4918-4921. https://doi.org/10.1128/JVI.75.10.4918-4921.2001

Gosert, R., Rinaldo, C. H., Funk, G. A., Egli, A., Ramos, E., Drachenberg, C. B., & Hirsch, H. H. (2008). Polyomavirus BK with rearranged noncoding control region emerge in vivo in renal transplant patients and increase viral replication and cytopathology. *Journal of Experimental Medicine*, *205*(4), 841-852. https://doi.org/10.1084/jem.20072097

Goudsmit, J., Dillen, P. W., van Strien, A., & van der Noordaa, J. (1982). The role of BK virus in acute respiratory tract disease and the presence of BKV DNA in tonsils. *Journal of Medical Virology*, *10*(2), 91-99. https://doi.org/10.1002/jmv.1890100203

Granot, R., Lawrence, R., Barnett, M., Masters, L., Rodriguez, M., Theocharous, C., Pamphlett, R., & Hersch, M. (2009). What lies beneath the tent? JC-virus cerebellar granule cell neuronopathy complicating sarcoidosis. *Journal of Clinical Neuroscience*, *16*(8), 1091-1092. https://doi.org/10.1016/j.jocn.2008.07.091

Gross, L. (1951). « Spontaneous » leukemia developing in C3H mice following inoculation in infancy, with AK-leukemic extracts, or AK-embrvos. *Proceedings of the Society for Experimental Biology and Medicine. Society for Experimental Biology and Medicine (New York, N.Y.)*, *76*(1), 27-32.

Guo, J., Kitamura, T., Ebihara, H., Sugimoto, C., Kunitake, T., Takehisa, J., Na, Y. Q., Al-Ahdal, M. N., Hallin, A., Kawabe, K., Taguchi, F., & Yogo, Y. (1996). Geographical distribution of the human polyomavirus JC virus types A and B and isolation of a new type from Ghana. *Journal of General Virology*, *77*(5), 919-927. https://doi.org/10.1099/0022-1317-77-5-919

Haghighi, M. F., Seyyedi, N., Farhadi, A., Zare, F., Kasraian, L., Refiei Dehbidi, G. R., Ranjbaran, R., & Behzad-Behbahani, A. (2019). Polyomaviruses BK and JC DNA infection in peripheral blood cells from blood donors. *The Brazilian Journal of Infectious Diseases*, *23*(1), 22-26. https://doi.org/10.1016/j.bjid.2019.01.005

Hall, C. D., Dafni, U., Simpson, D., Clifford, D., Wetherill, P. E., Cohen, B., McArthur, J., Hollander, H., Yainnoutsos, C., Major, E., Millar, L., & Timpone, J. (1998). Failure of Cytarabine in Progressive Multifocal Leukoencephalopathy Associated with Human Immunodeficiency Virus Infection. *New England Journal of Medicine*, *338*(19), 1345-1351. https://doi.org/10.1056/NEJM199805073381903

Handala, L., Blanchard, E., Raynal, P.-I., Roingeard, P., Morel, V., Descamps, V., Castelain, S., Francois, C., Duverlie, G., Brochot, E., & Helle, F. (2020). BK Polyomavirus Hijacks Extracellular Vesicles for En Bloc Transmission. *Journal of Virology*, *94*(6), e01834-19. https://doi.org/10.1128/JVI.01834-19

Harris, K. F., Christensen, J. B., & Imperiale, M. J. (1996). BK Virus Large T Antigen : Interactions with the Retinoblastoma Family of Tumor Suppressor Proteins and Effects on Cellular Growth Control. In *JOURNAL OF VIROLOGY* (N° 4; Vol. 70, p. 2378-2386).

Harris, K. F., Christensen, J. B., Radany, E. H., Imperiale, M. J., & Biology, M. (1998). Novel Mechanisms of E2F Induction by BK Virus Large-T Antigen : Requirement of Both the pRb-Binding and the J Domains. In *MOLECULAR AND CELLULAR BIOLOGY* (N° 3; Vol. 18, p. 1746-1756).

Harrison, C. J., Meinke, G., Kwun, H. J., Rogalin, H., Phelan, P. J., Bullock, P. A., Chang, Y., Moore, P. S., & Bohm, A. (2011). Asymmetric assembly of merkel cell polyomavirus large T-antigen origin binding domains at the viral origin. *Journal of Molecular Biology*, *409*(4), 529-542. https://doi.org/10.1016/j.jmb.2011.03.051

Harypursat, V., Zhou, Y., Tang, S., & Chen, Y. (2020). JC Polyomavirus, progressive multifocal leukoencephalopathy and immune reconstitution inflammatory syndrome : A review. *AIDS Research and Therapy*, *17*(1), 37. https://doi.org/10.1186/s12981-020-00293-0

Haynes, J. I., Chang, D., & Consigli, R. A. (1993). Mutations in the Putative Calcium-Binding Domain of Polyomavirus VP1 Affect Capsid Assemblyt. In *JOURNAL OF VIROLOGY* (p. 2486-2495).

Hecht, J. H., Glenn, O. A., Wara, D. W., & Wu, Y. W. (2007). JC Virus Granule Cell Neuronopathy in a Child With CD40 Ligand Deficiency. *Pediatric Neurology*, *36*(3), 186-189. https://doi.org/10.1016/j.pediatrneurol.2006.10.007

Hedquist, B. G., Bratt, G., Hammarin, A.-L., Grandien, M., Nennesmo, I., Sundelin, B., & Seregard, S. (1999). Identification of BK virus in a patient with acquired immune deficiency syndrome and bilateral atypical retinitis. *Ophthalmology*, *106*(1), 129-132. https://doi.org/10.1016/S0161-6420(99)90014-3

Helle, F., Brochot, E., Handala, L., Martin, E., Castelain, S., Francois, C., & Duverlie, G. (2017). Biology of the BKPyV : An Update. *Viruses*, *9*(11), 327. https://doi.org/10.3390/v9110327

Heritage, J., Chesters, P. M., & McCance, D. J. (1981). The persistence of papovavirus BK DNA sequences in normal human renal tissue. *Journal of Medical Virology*, *8*(2), 143-150. https://doi.org/10.1002/jmv.1890080208

Hirsch, H. H. (2002). Polyomavirus BK Nephropathy : A (Re-)emerging Complication in Renal Transplantation. *American Journal of Transplantation*, *2*, 25-30.

Hirsch, H. H., Kardas, P., Kranz, D., & Leboeuf, C. (2013a). The human JC polyomavirus (JCPyV) : Virological background and clinical implications. *APMIS*, *121*(8), 685-727. https://doi.org/10.1111/apm.12128

Hirsch, H. H., Randhawa, P., & the AST Infectious Diseases Community of Practice. (2013b). BK Polyomavirus in Solid Organ Transplantation : BK Polyomavirus in Solid Organ Transplantation. *American Journal of Transplantation*, *13*(s4), 179-188. https://doi.org/10.1111/ajt.12110

Hirsch, H. H., & Steiger, J. (2003). Polyomavirus BK. *The Lancet Infectious Diseases*, *3*(10), 611-623. https://doi.org/10.1016/S1473-3099(03)00770-9

Hix, J. K., Braun, W. E., & Isada, C. M. (2004). Delirium in a Renal Transplant Recipient Associated with BK Virus in the Cerebrospinal Fluid. *Transplantation*, *78*(9), 1407-1408. https://doi.org/10.1097/01.TP.0000137106.09925.8B

Holman, R. C., Török, T. J., Belay, E. D., Janssen, R. S., & Schonberger, L. B. (1998). Progressive multifocal leukoencephalopathy in the United States, 1979-1994 : Increased mortality associated with HIV infection. *Neuroepidemiology*, *17*(6), 303-309. https://doi.org/10.1159/000026184

Hou, J., & Major, E. O. (1998). The efficacy of nucleoside analogs against JC virus multiplication in a persistently infected human fetal brain cell line. *Journal of Neurovirology*, *4*(4), 451-456. https://doi.org/10.3109/13550289809114545

Huang, L.-Y., Halder, S., & Agbandje-McKenna, M. (2014). Parvovirus glycan interactions. *Current Opinion in Virology*, *7*, 108-118. https://doi.org/10.1016/j.coviro.2014.05.007

Hurdiss, D. L., Frank, M., Snowden, J. S., Macdonald, A., & Ranson, N. A. (2018). The Structure of an Infectious Human Polyomavirus and Its Interactions with Cellular Receptors. *Structure*, *26*(6), 839-847.e3. https://doi.org/10.1016/j.str.2018.03.019

Ikegaya, H., Saukko, P. J., Tertti, R., Metsärinne, K. P., Carr, M. J., Crowley, B., Sakurada, K., Zheng, H.-Y., Kitamura, T., & Yogo, Y. (2006). Identification of a genomic subgroup of BK polyomavirus spread in European populations. *Journal of General Virology*, *87*(11), 3201-3208. https://doi.org/10.1099/vir.0.82266-0

Inoue, T., & Tsai, B. (2013). How viruses use the endoplasmic reticulum for entry, replication, and assembly. In *Cold Spring Harbor Perspectives in Biology* (Vol. 5, Numéro 1). https://doi.org/10.1101/cshperspect.a013250

Jamshad, M., Charlton, J., Lin, Y.-P., Routledge, S. J., Bawa, Z., Knowles, T. J., Overduin, M., Dekker, N., Dafforn, T. R., Bill, R. M., Poyner, D. R., & Wheatley, M. (2015). G-protein coupled receptor solubilization and purification for biophysical analysis and functional studies, in the total absence of detergent. *Bioscience Reports*, *35*(2), e00188. https://doi.org/10.1042/BSR20140171

Jeffers, L. K., Madden, V., & Webster-Cyriaque, J. (2009). BK virus has tropism for human salivary gland cells in vitro : Implications for transmission. *Virology*, *394*(2), 183-193. https://doi.org/10.1016/j.virol.2009.07.022

Jeffers, L., & Webster-Cyriaque, J. Y. (2011). Viruses and Salivary Gland Disease (SGD). *Advances in Dental Research*, *23*(1), 79-83. https://doi.org/10.1177/0022034510396882

Jelcic, I., Jelcic, I., Kempf, C., Largey, F., Planas, R., Schippling, S., Budka, H., Sospedra, M., & Martin, R. (2016). Mechanisms of immune escape in central nervous system infection with neurotropic JC virus variant : Neurotropic JCV. *Annals of Neurology*, *79*(3), 404-418. https://doi.org/10.1002/ana.24574

Jiang, M., Abend, J. R., Tsai, B., & Imperiale, M. J. (2009). Early Events during BK Virus Entry and Disassembly. *Journal of Virology*, *83*(3), 1350-1358. https://doi.org/10.1128/jvi.02169-08

Jin, L. (1993). Rapid genomic typing of BK virus directly from clinical specimens. *Molecular and Cellular Probes*, *7*(4), 331-334. https://doi.org/10.1006/mcpr.1993.1047

Jin, L., Gibson, P. E., Knowles, W. A., & Clewley, J. P. (1993a). BK virus antigenic variants : Sequence analysis within the capsid VP1 epitope. *Journal of Medical Virology*, *39*(1), 50-56. https://doi.org/10.1002/jmv.1890390110

Jin, L., Gibson, P. E., Booth, J. C., & Clewley, J. P. (1993b). Genomic typing of BK virus in clinical specimens by direct sequencing of polymerase chain reaction products. *Journal of Medical Virology*, *41*(1), 11-17. https://doi.org/10.1002/jmv.1890410104

Jin, L., Pietropaolo, V., Booth, J. C., Ward, K. H., & Brown, D. W. (1995). Prevalence and distribution of BK virus subtypes in healthy people and immunocompromised patients detected by PCR-restriction enzyme analysis. *Clinical and Diagnostic Virology*, *3*(3), 285-295. https://doi.org/10.1016/S0928-0197(94)00044-1

Jobes, D. V., Friedlaender, J. S., Mgone, C. S., Agostini, H. T., Koki, G., Yanagihara, R., Ng, T. C. N., Chima, S. C., Ryschkewitsch, C. F., & Stoner, G. L. (2001). New JC virus (JCV) genotypes from Papua New Guinea and Micronesia (Type 8 and Type 2E) and evolutionary analysis of 32 complete JCV genomes. *Archives of Virology*, *146*(11), 2097-2113. https://doi.org/10.1007/s007050170023

Kable, K., Davies, C. D., O'connell, P. J., Chapman, J. R., & Nankivell, B. J. (2017). Clearance of BK Virus Nephropathy by Combination Antiviral Therapy With Intravenous Immunoglobulin. *Transplantation Direct*, *3*(4), e142. https://doi.org/10.1097/TXD.0000000000000641

Kamminga, S., van der Meijden, E., de Brouwer, C., Feltkamp, M., & Zaaijer, H. (2019). Prevalence of DNA of fourteen human polyomaviruses determined in blood donors. *Transfusion*, *59*(12), 3689-3697. https://doi.org/10.1111/trf.15557

Khalili, K., Sariyer, I. K., & Safak, M. (2008). Small tumor antigen of polyomaviruses : Role in viral life cycle and cell transformation. In *Journal of Cellular Physiology* (Vol. 215, Numéro 2, p. 309-319). https://doi.org/10.1002/jcp.21326

Khan, Z. M., Liu, Y., Neu, U., Gilbert, M., Ehlers, B., Feizi, T., & Stehle, T. (2014). Crystallographic and Glycan Microarray Analysis of Human Polyomavirus 9 VP1 Identifies N-Glycolyl Neuraminic Acid as a Receptor Candidate. *Journal of Virology*, *88*(11), 6100-6111. https://doi.org/10.1128/JVI.03455-13

Knoll, G. A., Humar, A., Fergusson, D., Johnston, O., House, A. A., Kim, S. J., Ramsay, T., Chassé, M., Pang, X., Zaltzman, J., Cockfield, S., Cantarovich, M., Karpinski, M., Lebel, L., & Gill, J. S. (2014). Levofloxacin for BK Virus Prophylaxis Following Kidney Transplantation : A Randomized Clinical Trial. *JAMA*, *312*(20), 2106-2114. https://doi.org/10.1001/jama.2014.14721

Knowles, W. A. (2001). The Epidemiology of BK Virus and the Occurrence of Antigenic and Genomic Subtypes. In *Human Polyomaviruses* (p. 527-559). John Wiley & Sons, Ltd. https://doi.org/10.1002/0471221945.ch19

Knowles, W. A., Gibson, P. E., & Gardner, S. D. (1989). Serological typing scheme for bk-like isolates of human polyomavirus. *Journal of Medical Virology*, *28*(2), 118-123. https://doi.org/10.1002/jmv.1890280212

Knowles, W. A., Pipkin, P., Andrews, N., Vyse, A., Minor, P., Brown, D. W. G., & Miller, E. (2003). Population-based study of antibody to the human polyomaviruses BKV and JCV and the simian polyomavirus SV40. *Journal of Medical Virology*, *71*(1), 115-123. https://doi.org/10.1002/jmv.10450

Kolter, T. (2012). Ganglioside Biochemistry. *ISRN Biochemistry*, *2012*, 1-36. https://doi.org/10.5402/2012/506160

Koralnik, I. J. (2006). Progressive multifocal leukoencephalopathy revisited : Has the disease outgrown its name? *Annals of Neurology*, *60*(2), 162-173. https://doi.org/10.1002/ana.20933

Koralnik, I. J., Wüthrich, C., Dang, X., Rottnek, M., Gurtman, A., Simpson, D., & Morgello, S. (2005). JC virus granule cell neuronopathy : A novel clinical syndrome distinct from progressive multifocal leukoencephalopathy. *Annals of Neurology*, *57*(4), 576-580. https://doi.org/10.1002/ana.20431

Korup, S., Rietscher, J., Calvignac-Spencer, S., Trusch, F., Hofmann, J., Moens, U., Sauer, I., Voigt, S., Schmuck, R., & Ehlers, B. (2013). Identification of a Novel Human Polyomavirus in Organs of the Gastrointestinal Tract. *PLoS ONE*, *8*(3). https://doi.org/10.1371/journal.pone.0058021

Krymskaya, L., Sharma, M. C., Martinez, J., Haq, W., Huang, E. C., Limaye, A. P., Diamond, D. J., & Lacey, S. F. (2005). Cross-Reactivity of T Lymphocytes Recognizing a Human Cytotoxic T-Lymphocyte Epitope within BK and JC Virus VP1 Polypeptides. *Journal of Virology*, *79*(17), 11170-11178. https://doi.org/10.1128/JVI.79.17.11170-11178.2005

Lee, B. T., Gabardi, S., Grafals, M., Hofmann, R. M., Akalin, E., Aljanabi, A., Mandelbrot, D. A., Adey, D. B., Heher, E., Fan, P.-Y., Conte, S., Dyer-Ward, C., & Chandraker, A. (2014). Efficacy of Levofloxacin in the Treatment of BK Viremia : A Multicenter, Double-Blinded, Randomized, Placebo-Controlled Trial. *Clinical Journal of the American Society of Nephrology : CJASN*, *9*(3), 583-589. https://doi.org/10.2215/CJN.04230413

Lee, S., Paulson, K. G., Murchison, E. P., Afanasiev, O. K., Alkan, C., Leonard, J. H., Byrd, D. R., Hannon, G. J., & Nghiem, P. (2011). Identification and validation of a novel mature microRNA encoded by the Merkel cell polyomavirus in human Merkel cell carcinomas. *Journal of Clinical Virology*, *52*(3), 272-275. https://doi.org/10.1016/j.jcv.2011.08.012

Leung, A. Y. H., Yuen, K.-Y., & Kwong, Y.-L. (2005). Polyoma BK virus and haemorrhagic cystitis in haematopoietic stem cell transplantation : A changing paradigm. *Bone Marrow Transplantation*, *36*(11), 929-937. https://doi.org/10.1038/sj.bmt.1705139

Leuzinger, K., Kaur, A., Wilhelm, M., & Hirsch, H. H. (2020). Variations in BK Polyomavirus Immunodominant Large Tumor Antigen-Specific 9mer CD8 T-Cell Epitopes Predict Altered HLA-Presentation and Immune Failure. *Viruses*, *12*(12), 1476. https://doi.org/10.3390/v12121476

Levican, J., Acevedo, M., León, O., Gaggero, A., & Aguayo, F. (2018). Role of BK human polyomavirus in cancer. *Infectious Agents and Cancer*, *13*(1), 12. https://doi.org/10.1186/s13027-018-0182-9

Li, E., Brown, S. L., Stupack, D. G., Puente, X. S., Cheresh, D. A., & Nemerow, G. R. (2001). Integrin αvβ1 Is an Adenovirus Coreceptor. *Journal of Virology*, *75*(11), 5405-5409. https://doi.org/10.1128/JVI.75.11.5405-5409.2001

Li, Y., Huang, H., Lan, T., Wang, W., Zhang, J., Zheng, M., Cao, L., Sun, W., & Lu, H. (2021). First detection and complete genome analysis of the Lyon IARC polyomavirus in China from samples of diarrheic cats. *Virus Genes*, *57*(3), 284-288. https://doi.org/10.1007/s11262-021-01840-1

Liddington, R. C., Yan, Y., Moulaitt, J., Sahli, R., Benjamin, T. L., & Harrison, S. C. (1991). *Structure of simian virus 40 at 0 3.8-A resolution*.

Lim, E. S., Reyes, A., Antonio, M., Saha, D., Ikumapayi, U. N., Adeyemi, M., Stine, O. C., Skelton, R., Brennan, D. C., Mkakosya, R. S., Manary, M. J., Gordon, J. I., & Wang, D. (2013). Discovery of STL polyomavirus, a polyomavirus of ancestral recombinant origin that encodes a unique T antigen by alternative splicing. *Virology*, *436*(2), 295-303. https://doi.org/10.1016/j.virol.2012.12.005

Limaye, A. P., Smith, K. D., Cook, L., Groom, D. A., Hunt, N. C., Jerome, K. R., & Boeckh, M. (2005). Polyomavirus Nephropathy in Native Kidneys of Non-Renal Transplant Recipients. *American Journal of Transplantation*, *5*(3), 614-620. https://doi.org/10.1034/j.1600-6143.2003.00126.x-i1

Lindner, J. M., Cornacchione, V., Sathe, A., Be, C., Srinivas, H., Riquet, E., Leber, X.-C., Hein, A., Wrobel, M. B., Scharenberg, M., Pietzonka, T., Wiesmann, C., Abend, J., & Traggiai, E. (2019). Human Memory B Cells Harbor Diverse Cross-Neutralizing Antibodies against BK and JC Polyomaviruses. *Immunity*, *50*(3), 668-676.e5. https://doi.org/10.1016/j.immuni.2019.02.003

Loria, S. J., Siddiqui, N. N., Gary, J. M., Bhatnagar, J., Bollweg, B. C., Ahmed, B., & Berenson, C. S. (2022). BK virus associated with small cell carcinoma of bladder in a patient with renal transplant. *BMJ Case Reports CP*, *15*(3), e244740. https://doi.org/10.1136/bcr-2021-244740

Low, J. A., Magnuson, B., Tsai, B., & Imperiale, M. J. (2006). Identification of Gangliosides GD1b and GT1b as Receptors for BK Virus. *Journal of Virology*, *80*(3), 1361-1366. https://doi.org/10.1128/JVI.80.3.1361-1366.2006

Low, J., Humes, H. D., Szczypka, M., & Imperiale, M. (2004). BKV and SV40 infection of human kidney tubular epithelial cells in vitro. *Virology*, *323*(2), 182-188. https://doi.org/10.1016/j.virol.2004.03.027

Luo, C., Bueno, M., Kant, J., Martinson, J., & Randhawa, P. (2009). Genotyping Schemes for Polyomavirus BK, Using Gene-Specific Phylogenetic Trees and Single Nucleotide Polymorphism Analysis. *Journal of Virology*, *83*(5), 2285-2297. https://doi.org/10.1128/JVI.02180-08

Maginnis, M. S., & Atwood, W. J. (2009). JC Virus : An oncogenic virus in animals and humans? In *Seminars in Cancer Biology* (Vol. 19, Numéro 4, p. 261-269). https://doi.org/10.1016/j.semcancer.2009.02.013

Mäntyjärvi, R. A., Meurman, O. H., Vihma, L., & Berglund, B. (1973). A human papovavirus (B.K.), biological properties and seroepidemiology. *Annals of Clinical Research*, *5*(5), 283-287.

Martinez-Fierro, M. L., Leach, R. J., Gomez-Guerra, L. S., Garza-Guajardo, R., Johnson-Pais, T., Beuten, J., Morales-Rodriguez, I. B., Hernandez-Ordoñez, M. A., Calderon-Cardenas, G., Ortiz-Lopez, R., Rivas-Estilla, A. M., Ancer-Rodriguez, J., & Rojas-Martinez, A. (2010). Identification of viral infections in the prostate and evaluation of their association with cancer. *BMC Cancer*, *10*, 326. https://doi.org/10.1186/1471-2407-10-326

Marzocchetti, A., Tompkins, T., Clifford, D. B., Gandhi, R. T., Kesari, S., Berger, J. R., Simpson, D. M., Prosperi, M., De Luca, A., & Koralnik, I. J. (2009). Determinants of survival in progressive multifocal leukoencephalopathy. *Neurology*, *73*(19), 1551-1558. https://doi.org/10.1212/WNL.0b013e3181c0d4a1

Mayberry, C. L., Soucy, A. N., Lajoie, C. R., DuShane, J. K., & Maginnis, M. S. (2019). JC Polyomavirus Entry by Clathrin-Mediated Endocytosis Is Driven by β-Arrestin. *Journal of Virology*, *93*(8), e01948-18. https://doi.org/10.1128/JVI.01948-18

Mayberry, C. L., Wilczek, M. P., Fong, T. M., Nichols, S. L., & Maginnis, M. S. (2021). GRK2 Mediates β-Arrestin Interactions with 5-HT2 Receptors for JC Polyomavirus Endocytosis. *Journal of Virology*, *95*(7), e02139-20. https://doi.org/10.1128/JVI.02139-20

Mazalrey, S., McIlroy, D., & Bressollette-Bodin, C. (2015). *BK polyomavirus : Virus-cell interactions, host immune response, and viral pathogenesis*. *19*, 17.

McIlroy, D., Hönemann, M., Nguyen, N.-K., Barbier, P., Peltier, C., Rodallec, A., Halary, F., Przyrowski, E., Liebert, U., Hourmant, M., & Bressollette-Bodin, C. (2020). Persistent BK Polyomavirus Viruria Is Associated with Accumulation of VP1 Mutations and Neutralization Escape. *Viruses*, *12*(8), 824. https://doi.org/10.3390/v12080824

Mengel, M. (2017). BK Virus Nephropathy Revisited. *American Journal of Transplantation*, *17*(8), 1972-1973. https://doi.org/10.1111/ajt.14358

Mills, E. A., & Mao-Draayer, Y. (2018). Understanding Progressive Multifocal Leukoencephalopathy Risk in Multiple Sclerosis Patients Treated with Immunomodulatory Therapies : A Bird's Eye View. *Frontiers in Immunology*, *9*, 138. https://doi.org/10.3389/fimmu.2018.00138

Minic, J., Grosclaude, J., Aioun, J., Persuy, M.-A., Gorojankina, T., Salesse, R., Pajot-Augy, E., Hou, Y., Helali, S., Jaffrezic-Renault, N., Bessueille, F., Errachid, A., Gomila, G., Ruiz, O., & Samitier, J. (2005). Immobilization of native membrane-bound rhodopsin on biosensor surfaces. *Biochimica et Biophysica Acta (BBA) - General Subjects*, *1724*(3), 324-332. https://doi.org/10.1016/j.bbagen.2005.04.017

Mishra, N., Pereira, M., Rhodes, R. H., An, P., Pipas, J. M., Jain, K., Kapoor, A., Briese, T., Faust, P. L., & Ian Lipkin, W. (2014). Identification of a novel Polyomavirus in a pancreatic transplant recipient with retinal blindness and Vasculitic Myopathy. *Journal of Infectious Diseases*, *210*(10), 1595-1599. https://doi.org/10.1093/infdis/jiu250

Monaco, M. C. G., Jensen, P. N., Hou, J., Durham, L. C., & Major, E. O. (1998). Detection of JC Virus DNA in Human Tonsil Tissue : Evidence for Site of Initial Viral Infection. *Journal of Virology*, *72*(12), 9918-9923.

Morris-Love, J., Gee, G. V., O'Hara, B. A., Assetta, B., Atkinson, A. L., Dugan, A. S., Haley, S. A., & Atwood, W. J. (2019). JC Polyomavirus Uses Extracellular Vesicles To Infect Target Cells. *mBio*, *10*(2), e00379-19. https://doi.org/10.1128/mBio.00379-19

Nelson, A. S., Yalamarthi, N., Yong, M. K., & Blyth, E. (2021). Beyond antivirals : Virus-specific T-cell immunotherapy for BK virus haemorrhagic cystitis and JC virus progressive multifocal leukoencephalopathy. *Current Opinion in Infectious Diseases*, *34*(6), 627-634. https://doi.org/10.1097/QCO.0000000000000794

Nelson, C. D. S., Carney, D. W., Derdowski, A., Lipovsky, A., Gee, G. V., O'Hara, B., Williard, P., Dimaio, D., Sello, J. K., & Atwood, W. J. (2013). A retrograde trafficking inhibitor of ricin and Shiga-like toxins inhibits infection of cells by human and monkey polyomaviruses. *mBio*, *4*(6). https://doi.org/10.1128/mBio.00729-13

Nelson, C. D. S., Derdowski, A., Maginnis, M. S., O'Hara, B. A., & Atwood, W. J. (2012). The VP1 subunit of JC polyomavirus recapitulates early events in viral trafficking and is a novel tool to study polyomavirus entry. *Virology*, *428*(1), 30-40. https://doi.org/10.1016/j.virol.2012.03.014

Neu, U., Allen, S. A., Blaum, B. S., Liu, Y., Frank, M., Palma, A. S., Ströh, L. J., Feizi, T., Peters, T., Atwood, W. J., & Stehle, T. (2013). A Structure-Guided Mutation in the Major Capsid Protein Retargets BK Polyomavirus. *PLoS Pathogens*, *9*(10), e1003688. https://doi.org/10.1371/journal.ppat.1003688

Neu, U., Hengel, H., Blaum, B. S., Schowalter, R. M., Macejak, D., Gilbert, M., Wakarchuk, W. W., Imamura, A., Ando, H., Kiso, M., Arnberg, N., Garcea, R. L., Peters, T., Buck, C. B., & Stehle, T. (2012). Structures of Merkel Cell Polyomavirus VP1 Complexes Define a Sialic Acid Binding Site Required for Infection. *PLoS Pathogens*, *8*(7), e1002738. https://doi.org/10.1371/journal.ppat.1002738

Neu, U., Maginnis, M. S., Palma, A. S., Ströh, L. J., Nelson, C. D. S., Feizi, T., Atwood, W. J., & Stehle, T. (2010). Structure-function analysis of the human JC polyomavirus establishes the LSTc pentasaccharide as a functional receptor motif. *Cell Host and Microbe*, *8*(4), 309-319. https://doi.org/10.1016/j.chom.2010.09.004

Nickeleit, V., Davis, V. G., Thompson, B., & Singh, H. K. (2021a). The Urinary Polyomavirus-Haufen Test : A Highly Predictive Non-Invasive Biomarker to Distinguish « Presumptive » from « Definitive » Polyomavirus Nephropathy: How to Use It-When to Use It-How Does It Compare to PCR Based Assays? *Viruses*, *13*(1), 135. https://doi.org/10.3390/v13010135

Nickeleit, V., Singh, H. K., Dadhania, D., Cornea, V., El-Husseini, A., Castellanos, A., Davis, V. G., Waid, T., & Seshan, S. V. (2021b). The 2018 Banff Working Group classification of definitive polyomavirus nephropathy : A multicenter validation study in the modern era. *American Journal of Transplantation*, *21*(2), 669-680. https://doi.org/10.1111/ajt.16189

Nickeleit, V., Singh, H. K., Randhawa, P., Drachenberg, C. B., Bhatnagar, R., Bracamonte, E., Chang, A., Chon, W. J., Dadhania, D., Davis, V. G., Hopfer, H., Mihatsch, M. J., Papadimitriou, J. C., Schaub, S., Stokes, M. B., Tungekar, M. F., & Seshan, S. V. (2018). The Banff Working Group Classification of Definitive Polyomavirus Nephropathy : Morphologic Definitions and Clinical Correlations. *Journal of the American Society of Nephrology*, *29*(2), 680-693. https://doi.org/10.1681/ASN.2017050477

Nishimoto, Y., Takasaka, T., Hasegawa, M., Zheng, H.-Y., Chen, Q., Sugimoto, C., Kitamura, T., & Yogo, Y. (2006). Evolution of BK Virus Based on Complete Genome Data. *Journal of Molecular Evolution*, *63*(3), 341-352. https://doi.org/10.1007/s00239-005-0092-5

Nishimoto, Y., Zheng, H.-Y., Zhong, S., Ikegaya, H., Chen, Q., Sugimoto, C., Kitamura, T., & Yogo, Y. (2007). An Asian Origin for Subtype IV BK Virus Based on Phylogenetic Analysis. *Journal of Molecular Evolution*, *65*(1), 103-111. https://doi.org/10.1007/s00239-006-0269-6

Okada, Y., Endo, S., Takahashi, H., Sawa, H., Umemura, T., & Nagashima, K. (2001). Basic Science and Immunobiology Report Distribution and function of JCV agnoprotein. In *Journal of NeuroVirology* (Vol. 7, p. 302-306).

Padgett, BillieL., Zurhein, GabrieleM., Walker, DuardL., Eckroade, RobertJ., & Dessel, BertH. (1971). CULTIVATION OF PAPOVA-LIKE VIRUS FROM HUMAN BRAIN WITH PROGRESSIVE MULTIFOCAL LEUCOENCEPHALOPATHY. *The Lancet*, *297*(7712), 1257-1260. https://doi.org/10.1016/S0140-6736(71)91777-6

Panou, M. M., Prescott, E. L., Hurdiss, D. L., Swinscoe, G., Hollinshead, M., Caller, L. G., Morgan, E. L., Carlisle, L., Müller, M., Antoni, M., Kealy, D., Ranson, N. A., Crump, C. M., & Macdonald, A. (2018). Agnoprotein is an essential egress factor during BK Polyomavirus infection. *International Journal of Molecular Sciences*, *19*(3). https://doi.org/10.3390/ijms19030902

Papadimitriou, J. C., Randhawa, P., Rinaldo, C. H., Drachenberg, C. B., Alexiev, B., & Hirsch, H. H. (2016). BK Polyomavirus Infection and Renourinary Tumorigenesis. *American Journal of Transplantation*, *16*(2), 398-406. https://doi.org/10.1111/ajt.13550
Pasquier, R. A. D., Corey, S., Margolin, D. H., Williams, K., Pfister, L.-A., Girolami, U. D., Key, J. J. M., Wüthrich, C., Joseph, J. T., & Koralnik, I. J. (2003). Productive infection of cerebellar granule cell neurons by JC virus in an HIV+ individual. *Neurology*, *61*(6), 775-782. https://doi.org/10.1212/01.WNL.0000081306.86961.33

Pastrana, D. V., Brennan, D. C., Çuburu, N., Storch, G. A., Viscidi, R. P., Randhawa, P. S., & Buck, C. B. (2012). Neutralization Serotyping of BK Polyomavirus Infection in Kidney Transplant Recipients. *PLoS Pathogens*, *8*(4), e1002650. https://doi.org/10.1371/journal.ppat.1002650

Pastrana, D. V., Ray, U., Magaldi, T. G., Schowalter, R. M., Cuburu, N., & Buck, C. B. (2013). BK Polyomavirus Genotypes Represent Distinct Serotypes with Distinct Entry Tropism. *Journal of Virology*, *87*(18), 10105-10113. https://doi.org/10.1128/JVI.01189-13

Peretti, A., Geoghegan, E. M., Pastrana, D. V., Smola, S., Feld, P., Sauter, M., Lohse, S., Ramesh, M., Lim, E. S., Wang, D., Borgogna, C., FitzGerald, P. C., Bliskovsky, V., Starrett, G. J., Law, E. K., Harris, R. S., Killian, J. K., Zhu, J., Pineda, M., … Buck, C. B. (2018). Characterization of BK Polyomaviruses from Kidney Transplant Recipients Suggests a Role for APOBEC3 in Driving In-Host Virus Evolution. *Cell Host & Microbe*, *23*(5), 628-635.e7. https://doi.org/10.1016/j.chom.2018.04.005

Perez-Liz, G., Del Valle, L., Gentilella, A., Croul, S., & Khalili, K. (2008). Detection of JC Virus DNA Fragments but Not Proteins in Normal Brain Tissue. *Annals of neurology*, *64*(4), 379-387. https://doi.org/10.1002/ana.21443

Pho, M. T., Ashok, A., & Atwood, W. J. (2000). JC Virus Enters Human Glial Cells by Clathrin-Dependent Receptor-Mediated Endocytosis. In *JOURNAL OF VIROLOGY* (Nº 5; Vol. 74, p. 2288-2292).

Pillay, S., Meyer, N. L., Puschnik, A. S., Davulcu, O., Diep, J., Ishikawa, Y., Jae, L. T., Wosen, J. E., Nagamine, C. M., Chapman, M. S., & Carette, J. E. (2016). An essential receptor for adeno-associated virus infection. *Nature*, *530*(7588), 108-112. https://doi.org/10.1038/nature16465

Polo, C., Pérez, J. L., Mielnichuck, A., Fedele, C. G., Niubo, J., & Tenorio, A. (2004). Prevalence and patterns of polyomavirus urinary excretion in immunocompetent adults and children. *Clinical Microbiology and Infection*, *10*(7), 640-644. https://doi.org/10.1111/j.1469-0691.2004.00882.x

Qian, M., Cai, D., Verhey, K. J., & Tsai, B. (2009). A lipid receptor sorts polyomavirus from the endolysosome to the endoplasmic reticulum to cause infection. *PLoS Pathogens*, *5*(6). https://doi.org/10.1371/journal.ppat.1000465

Qu, Q., Sawa, H., Suzuki, T., Semba, S., Henmi, C., Okada, Y., Tsuda, M., Tanaka, S., Atwood, W. J., & Nagashima, K. (2004). Nuclear entry mechanism of the human polyomavirus JC virus-like particle : Role of importins and the nuclear pore complex. *Journal of Biological Chemistry*, *279*(26), 27735-27742. https://doi.org/10.1074/jbc.M310827200

Querbes, W., O'Hara, B. A., Williams, G., & Atwood, W. J. (2006). Invasion of Host Cells by JC Virus Identifies a Novel Role for Caveolae in EndosomalSorting of Noncaveolar Ligands. *Journal of Virology*, *80*(19), 9402-9413. https://doi.org/10.1128/jvi.01086-06

Rajan, A., Palm, E., Trulsson, F., Mundigl, S., Becker, M., Persson, B. D., Frängsmyr, L., & Lenman, A. (2021). Heparan Sulfate Is a Cellular Receptor for Enteric Human Adenoviruses. *Viruses*, *13*(2), Art. 2. https://doi.org/10.3390/v13020298

Ramos, E., Drachenberg, C. B., Papadimitriou, J. C., Hamze, O., Fink, J. C., Klassen, D. K., Drachenberg, R. C., Wiland, A., Wali, R., Cangro, C. B., Schweitzer, E., Bartlett, S. T., & Weir, M. R. (2002). Clinical course of polyoma virus nephropathy in 67 renal transplant patients. *Journal of the American Society of Nephrology: JASN*, *13*(8), 2145-2151. https://doi.org/10.1097/01.asn.0000023435.07320.81

Randhawa, P., Ho, A., Shapiro, R., Vats, A., Swalsky, P., Finkelstein, S., Uhrmacher, J., & Weck, K. (2004). Correlates of quantitative measurement of BK polyomavirus (BKV) DNA with clinical course of BKV infection in renal transplant patients. *Journal of Clinical Microbiology*, *42*(3), 1176-1180. https://doi.org/10.1128/JCM.42.3.1176-1180.2004

Randhawa, P. S., Finkelstein, S., Scantlebury, V., Shapiro, R., Vivas, C., Jordan, M., Picken, M. M., & Demetris, A. J. (1999). HUMAN POLYOMA VIRUS-ASSOCIATED INTERSTITIAL NEPHRITIS IN THE ALLOGRAFT KIDNEY1. *Transplantation*, *67*(1), 103-109.

Ray, U., Cinque, P., Gerevini, S., Longo, V., Lazzarin, A., Schippling, S., Martin, R., Buck, C. B., & Pastrana, D. V. (2015). JC Polyomavirus Mutants Escape Antibody-Mediated Neutralization. *Science translational medicine*, *7*(306), 306ra151. https://doi.org/10.1126/scitranslmed.aab1720

Richards, K. F., Bienkowska-Haba, M., Dasgupta, J., Chen, X. S., & Sapp, M. (2013). Multiple Heparan Sulfate Binding Site Engagements Are Required for the Infectious Entry of Human Papillomavirus Type 16. *Journal of Virology*, *87*(21), 11426-11437. https://doi.org/10.1128/JVI.01721-13

Richardson, E. P., & Webster, H. D. (1983). Progressive multifocal leukoencephalopathy : Its pathological features. *Progress in Clinical and Biological Research*, *105*, 191-203.

Rinaldo, C. H., Traavik, T., & Hey, A. (1998). The Agnogene of the Human Polyomavirus BK Is Expressed. In *JOURNAL OF VIROLOGY* (N° 7; Vol. 72, p. 6233-6236).

Rollison, D. E. M., Utaipat, U., Ryschkewitsch, C., Hou, J., Goldthwaite, P., Daniel, R., Helzlsouer, K. J., Burger, P. C., Shah, K. V., & Major, E. O. (2005). Investigation of human brain tumors for the presence of polyomavirus genome sequences by two independent laboratories. *International Journal of Cancer*, *113*(5), 769-774. https://doi.org/10.1002/ijc.20641

Ryschkewitsch, C. F., Friedlaender, J. S., Mgone, C. S., Jobes, D. V., Agostini, H. T., Chima, S. C., Alpers, M. P., Koki, G., Yanagihara, R., & Stoner, G. L. (2000). Human polyomavirus JC variants in Papua New Guinea and Guam reflect ancient population settlement and viral evolution. *Microbes and Infection*, *2*(9), 987-996. https://doi.org/10.1016/S1286-4579(00)01252-1

Sariyer, I. K., Khalili, K., & Safak, M. (2008). Dephosphorylation of JC virus agnoprotein by protein phosphatase 2A: Inhibition by small t antigen. *Virology*, *375*(2), 464-479. https://doi.org/10.1016/j.virol.2008.02.020

Sarvari, J., Mahmoudvand, S., Pirbonyeh, N., Safaei, A., & Hosseini, S. Y. (2018). The Very Low Frequency of Epstein-Barr JC and BK Viruses DNA in Colorectal Cancer Tissues in Shiraz, Southwest Iran. *Polish Journal of Microbiology*, *67*(1), 73-79. https://doi.org/10.5604/01.3001.0011.6146

Schowalter, R. M., Pastrana, D. V., & Buck, C. B. (2011). Glycosaminoglycans and Sialylated Glycans Sequentially Facilitate Merkel Cell Polyomavirus Infectious Entry. *PLoS Pathogens*, *7*(7), e1002161. https://doi.org/10.1371/journal.ppat.1002161

Schowalter, R. M., Pastrana, D. V., Pumphrey, K. A., Moyer, A. L., & Buck, C. B. (2010). Merkel cell polyomavirus and two previously unknown polyomaviruses are chronically shed from human skin. *Cell Host and Microbe*, *7*(6), 509-515. https://doi.org/10.1016/j.chom.2010.05.006

Scuda, N., Hofmann, J., Calvignac-Spencer, S., Ruprecht, K., Liman, P., Kühn, J., Hengel, H., & Ehlers, B. (2011). A Novel Human Polyomavirus Closely Related to the African Green Monkey-Derived Lymphotropic Polyomavirus. *Journal of Virology*, *85*(9), 4586-4590. https://doi.org/10.1128/jvi.02602-10

Seamone, M. E., Wang, W., Acott, P., Beck, P. L., Tibbles, L. A., & Muruve, D. A. (2010). MAP kinase activation increases BK polyomavirus replication and facilitates viral propagation in vitro. *Journal of Virological Methods*, *170*(1-2), 21-29. https://doi.org/10.1016/j.jviromet.2010.08.014

Seemayer, C. A., Seemayer, N. H., Dürmüller, U., Gudat, F., Schaub, S., Hirsch, H. H., & Mihatsch, M. J. (2008). BK virus large T and VP-1 expression in infected human renal allografts. *Nephrology Dialysis Transplantation*, *23*(12), 3752-3761. https://doi.org/10.1093/ndt/gfn470

Seo, G. J., Chen, C. J., & Sullivan, C. S. (2009). Merkel cell polyomavirus encodes a microRNA with the ability to autoregulate viral gene expression. *Virology*, *383*(2), 183-187. https://doi.org/10.1016/j.virol.2008.11.001

Seo, G. J., Fink, L. H. L., O'Hara, B., Atwood, W. J., & Sullivan, C. S. (2008). Evolutionarily Conserved Function of a Viral MicroRNA. *Journal of Virology*, *82*(20), 9823-9828. https://doi.org/10.1128/jvi.01144-08

Shah, K. V., Daniel, R. W., & Warszawski, R. M. (1973). High Prevalence of Antibodies to BK Virus, an SV40-related Papovavirus, in Residents of Maryland. *Journal of Infectious Diseases*, *128*(6), 784-787. https://doi.org/10.1093/infdis/128.6.784

Sharma, R., & Zachariah, M. (2020). BK Virus Nephropathy : Prevalence, Impact and Management Strategies . *International Journal of Nephrology and Renovascular Disease*, *13*, 187-192. https://doi.org/10.2147/IJNRD.S236556

Shen, C., Tung, C., Chao, C., Jou, Y., Huang, S., Meng, M., Chang, D., & Chen, P. (2021). The differential presence of human polyomaviruses, JCPyV and BKPyV, in prostate cancer and benign prostate hypertrophy tissues. *BMC Cancer*, *21*(1), 1141. https://doi.org/10.1186/s12885-021-08862-w

Shishido-Hara, Y., Hara, Y., Larson, T., Yasui, K., Nagashima, K., & Stoner, G. L. (2000). Analysis of Capsid Formation of Human Polyomavirus JC (Tokyo-1 Strain) by a Eukaryotic Expression System : Splicing of Late RNAs, Translation and Nuclear Transport of Major Capsid Protein VP1, and Capsid Assembly. In *JOURNAL OF VIROLOGY* (N° 4; Vol. 74, p. 1840-1853).

Shuda, M., Kwun, H. J., Feng, H., Chang, Y., & Moore, P. S. (2011). Human Merkel cell polyomavirus small T antigen is an oncoprotein targeting the 4E-BP1 translation regulator. *Journal of Clinical Investigation*, *121*(9), 3623-3634. https://doi.org/10.1172/JCI46323

Siebrasse, E. A., Reyes, A., Lim, E. S., Zhao, G., Mkakosya, R. S., Manary, M. J., Gordon, J. I., & Wang, D. (2012). Identification of MW Polyomavirus, a Novel Polyomavirus in Human Stool. *Journal of Virology*, *86*(19), 10321-10326. https://doi.org/10.1128/jvi.01210-12

Sikorski, M., Coulon, F., Peltier, C., Braudeau, C., Garcia, A., Giraud, M., Renaudin, K., Kandel-Aznar, C., Nedellec, S., Hulin, P., Branchereau, J., Véziers, J., Gaboriaud, P., Touzé, A., Burlaud-Gaillard, J., Josien, R., McIlroy, D., Bressollette-Bodin, C., & Halary, F. (2021). Non-permissive human conventional CD1c+ dendritic cells enable trans-infection of human primary renal tubular epithelial cells and protect BK polyomavirus from neutralization. *PLoS Pathogens*, *17*(2), e1009042. https://doi.org/10.1371/journal.ppat.1009042

Silin, V. I., Karlik, E. A., Ridge, K. D., & Vanderah, D. J. (2006). Development of surface-based assays for transmembrane proteins : Selective immobilization of functional CCR5, a G protein-coupled receptor. *Analytical Biochemistry*, *349*(2), 247-253. https://doi.org/10.1016/j.ab.2005.10.025

Singh, H. K., Andreoni, K. A., Madden, V., True, K., Detwiler, R., Weck, K., & Nickeleit, V. (2009). Presence of Urinary Haufen Accurately Predicts Polyomavirus Nephropathy. *Journal of the American Society of Nephrology : JASN*, *20*(2), 416-427. https://doi.org/10.1681/ASN.2008010117

Solis, M., Velay, A., Porcher, R., Domingo-Calap, P., Soulier, E., Joly, M., Meddeb, M., Kack-Kack, W., Moulin, B., Bahram, S., Stoll-Keller, F., Barth, H., Caillard, S., & Fafi-Kremer, S. (2018). Neutralizing Antibody–Mediated Response and Risk of BK Virus–Associated Nephropathy. *Journal of the American Society of Nephrology*, *29*(1), 326-334. https://doi.org/10.1681/ASN.2017050532

Sorin, M. N., Kuhn, J., Stasiak, A. C., & Stehle, T. (2021). Structural insight into non-enveloped virus binding to glycosaminoglycan receptors : A review. In *Viruses* (Vol. 13, Numéro 5). MDPI AG. https://doi.org/10.3390/v13050800

Sospedra, M., Schippling, S., Yousef, S., Jelcic, I., Bofill-Mas, S., Planas, R., Stellmann, J.-P., Demina, V., Cinque, P., Garcea, R., Croughs, T., Girones, R., & Martin, R. (2014). Treating Progressive Multifocal Leukoencephalopathy With Interleukin 7 and Vaccination With JC Virus Capsid Protein VP1. *Clinical Infectious Diseases: An Official Publication of the Infectious Diseases Society of America*, *59*(11), 1588-1592. https://doi.org/10.1093/cid/ciu682

Stehle, T. (1997). High-resolution structure of a polyomavirus VP1-oligosaccharide complex : Implications for assembly and receptor binding. *The EMBO Journal*, *16*(16), 5139-5148. https://doi.org/10.1093/emboj/16.16.5139

Stehle, T., Gamblin, S. J., Yan, Y., & Harrison, S. C. (1996). The structure of simian virus 40 refined at 3.1 A resolution. *Structure (London, England: 1993)*, *4*(2), 165-182. https://doi.org/10.1016/s0969-2126(96)00020-2

Stewart, S. E., Eddy, B. E., & Borgese, N. (s. d.). *Neoplasms in Mice Inoculated with a Tumor Agent Carried in Tissue Cul-ture*. https://academic.oup.com/jnci/article-abstract/20/6/1223/1014185

Ströh, L. J., Maginnis, M. S., Blaum, B. S., Nelson, C. D. S., Neu, U., Gee, G. V., O'Hara, B. A., Motamedi, N., DiMaio, D., Atwood, W. J., & Stehle, T. (2015). The Greater Affinity of JC Polyomavirus Capsid for α2,6-Linked Lactoseries Tetrasaccharide c than for Other Sialylated Glycans Is a Major Determinant of Infectivity. *Journal of Virology*, *89*(12), 6364-6375. https://doi.org/10.1128/JVI.00489-15

Stroh, L. J., Neu, U., Blaum, B. S., Buch, M. H. C., Garcea, R. L., & Stehle, T. (2014). Structure Analysis of the Major Capsid Proteins of Human Polyomaviruses 6 and 7 Reveals an Obstructed Sialic Acid Binding Site. *Journal of Virology*, *88*(18), 10831-10839. https://doi.org/10.1128/jvi.01084-14

Ströh, L. J., Rustmeier, N. H., Blaum, B. S., Botsch, J., Rößler, P., Wedekink, F., Lipkin, W. I., Mishra, N., & Stehle, T. (2020). Structural Basis and Evolution of Glycan Receptor Specificities within the Polyomavirus Family. *MBio*, *11*(4), e00745-20, /mbio/11/4/mBio.00745-20.atom. https://doi.org/10.1128/mBio.00745-20

Sugimoto, C., Hasegawa, M., Kato, A., Zheng, H.-Y., Ebihara, H., Taguchi, F., Kitamura, T., & Yogo, Y. (2002). Evolution of Human Polyomavirus JC : Implications for the Population History of Humans. *Journal of Molecular Evolution*, *54*(3), 285-297. https://doi.org/10.1007/s00239-001-0009-x

Sugimoto, C., Kitamura, T., Guo, J., Al-Ahdal, M. N., Shchelkunov, S. N., Otova, B., Ondrejka, P., Chollet, J.-Y., El-Safi, S., Ettayebi, M., Grésenguet, G., Kocagöz, T., Chaiyarasamee, S., Thant, K. Z., Thein, S., Moe, K., Kobayashi, N., Taguchi, F., & Yogo, Y. (1997). Typing of urinary JC virus DNA offers a novel means of tracing human migrations. *Proceedings of the National Academy of Sciences*, *94*(17), 9191-9196. https://doi.org/10.1073/pnas.94.17.9191

Suzuki, T., Orba, Y., Okada, Y., Sunden, Y., Kimura, T., Tanaka, S., Nagashima, K., Hall, W. W., & Sawa, H. (2010). The human polyoma JC virus agnoprotein acts as a viroporin. *PLoS Pathogens*, *6*(3). https://doi.org/10.1371/journal.ppat.1000801

Suzuki, T., Semba, S., Sunden, Y., Orba, Y., Kobayashi, S., Nagashima, K., Kimura, T., Hasegawa, H., & Sawa, H. (2012). Role of JC virus agnoprotein in virion formation. *Microbiology and Immunology*, *56*(9), 639-646. https://doi.org/10.1111/j.1348-0421.2012.00484.x

Svennerholm, L. (s. d.). *The gangliosides*.

Sweet, B. H., & Hilleman, M. R. (1960). The vacuolating virus, S.V. 40. *Proceedings of the Society for Experimental Biology and Medicine. Society for Experimental Biology and Medicine (New York, N.Y.)*, *105*, 420-427. https://doi.org/10.3181/00379727-105-26128

Swenson, J. J., Trowbridge, P. W., & Frisque, R. J. (1996). Replication activity of JC virus large T antigen phosphorylation and zinc finger domain mutants. In *Journal of NeuroVirology* (Vol. 2, p. 78-86).

Takasaka, T., Goya, N., Tokumoto, T., Tanabe, K., Toma, H., Ogawa, Y., Hokama, S., Momose, A., Funyu, T., Fujioka, T., Omori, S., Akiyama, H., Chen, Q., Zheng, H.-Y., Ohta, N., Kitamura, T., & Yogo, Y. (2004). Subtypes of BK virus prevalent in Japan and variation in their transcriptional control region. *Journal of General Virology*, *85*(10), 2821-2827. https://doi.org/10.1099/vir.0.80363-0

Tan, C. S., Dezube, B. J., Bhargava, P., Autissier, P., Wüthrich, C., Miller, J., & Koralnik, I. J. (2009). Detection of JC Virus DNA and Proteins in the Bone Marrow of HIV-Positive and HIV-Negative Patients : Implications for Viral Latency and Neurotropic Transformation. *The Journal of Infectious Diseases*, *199*(6), 881-888. https://doi.org/10.1086/597117

Tan, C. S., & Koralnik, I. J. (2010). Beyond progressive multifocal leukoencephalopathy : Expanded pathogenesis of JC virus infection in the central nervous system. *Lancet neurology*, *9*(4), 425-437. https://doi.org/10.1016/S1474-4422(10)70040-5

Tan, S. K., Huang, C., Sahoo, M. K., Weber, J., Kurzer, J., Stedman, M. R., Concepcion, W., Gallo, A. E., Alonso, D., Srinivas, T., Storch, G. A., Subramanian, A. K., Tan, J. C., & Pinsky, B. A. (2019). Impact of Pretransplant Donor BK Viruria in Kidney Transplant Recipients. *The Journal of Infectious Diseases*, *220*(3), 370-376. https://doi.org/10.1093/infdis/jiz114

Thongprayoon, C., Khoury, N. J., Bathini, T., Aeddula, N. R., Boonpheng, B., Leeaphorn, N., Ungprasert, P., Bruminhent, J., Lertjitbanjong, P., Watthanasuntorn, K., Chesdachai, S., Mao, M. A., & Cheungpasitporn, W. (2019). BK polyomavirus genotypes in renal transplant recipients in the United States : A meta-analysis. *Journal of Evidence-Based Medicine*, *12*(4), 291-299. https://doi.org/10.1111/jebm.12366

Tian, Y. C., Li, Y. J., Chen, H. C., Wu, H. H., Weng, C. H., Chen, Y. C., Lee, C. C., Chang, M. Y., Hsu, H. H., Yen, T. H., Hung, C. C., & Yang, C. W. (2014). Polyomavirus BK-encoded microRNA suppresses autoregulation of viral replication. *Biochemical and Biophysical Research Communications*, *447*(3), 543-549. https://doi.org/10.1016/j.bbrc.2014.04.030

Tikhanovich, I., & Nasheuer, H. P. (2010). Host-Specific Replication of BK Virus DNA in Mouse Cell Extracts Is Independently Controlled by DNA Polymerase α-Primase and Inhibitory Activities. *Journal of Virology*, *84*(13), 6636-6644. https://doi.org/10.1128/JVI.00527-10

Toppinen, M., Sajantila, A., Pratas, D., Hedman, K., & Perdomo, M. F. (2021). The Human Bone Marrow Is Host to the DNAs of Several Viruses. *Frontiers in Cellular and Infection Microbiology*, *11*, 657245. https://doi.org/10.3389/fcimb.2021.657245

Toscano, M. G., & de Haan, P. (2018). How Simian Virus 40 Hijacks the Intracellular Protein Trafficking Pathway to Its Own Benefit … and Ours. *Frontiers in Immunology*, *9*. https://www.frontiersin.org/article/10.3389/fimmu.2018.01160

Trydzenskaya, H., Sattler, A., Müller, K., Schachtner, T., Dang-Heine, C., Friedrich, P., Nickel, P., Hoerstrup, J., Schindler, R., Thiel, A., Melzig, M. F., Reinke, P., & Babel, N. (2011). Novel Approach for Improved Assessment of Phenotypic and Functional Characteristics of BKV-Specific T-Cell Immunity. *Transplantation*, *92*(11), 1269-1277. https://doi.org/10.1097/TP.0b013e318234e0e5

Tuve, S., Wang, H., Jacobs, J. D., Yumul, R. C., Smith, D. F., & Lieber, A. (2008). Role of Cellular Heparan Sulfate Proteoglycans in Infection of Human Adenovirus Serotype 3 and 35. *PLOS Pathogens*, *4*(10), e1000189. https://doi.org/10.1371/journal.ppat.1000189

Tyagarajan, S. K., & Frisque, R. J. (2006). Stability and Function of JC Virus Large T Antigen and T′ Proteins Are Altered by Mutation of Their Phosphorylated Threonine 125 Residues. *Journal of Virology*, *80*(5), 2083-2091. https://doi.org/10.1128/jvi.80.5.2083-2091.2006

Tyler, K. L. (2003). The uninvited guest : JC virus infection of neurons in PML. *Neurology*, *61*(6), 734-735. https://doi.org/10.1212/WNL.61.6.734

Vallbracht, A., Löhler, J., Gossmann, J., Glück, T., Petersen, D., Gerth, H. J., Gencic, M., & Dörries, K. (1993). Disseminated BK type polyomavirus infection in an AIDS patient associated with central nervous system disease. *The American Journal of Pathology*, *143*(1), 29-39.

van der Meijden, E., Janssens, R. W. A., Lauber, C., Bavinck, J. N. B., Gorbalenya, A. E., & Feltkamp, M. C. W. (2010). Discovery of a new human polyomavirus associated with Trichodysplasia Spinulosa in an immunocompromized patient. *PLoS Pathogens*, *6*(7), 1-10. https://doi.org/10.1371/journal.ppat.1001024

Verma, S., Cikurel, K., Koralnik, I. J., Morgello, S., Cunningham-Rundles, C., Weinstein, Z. R., Bergmann, C., & Simpson, D. M. (2007). Mirtazapine in Progressive Multifocal Leukoencephalopathy Associated with Polycythemia Vera. *The Journal of Infectious Diseases*, *196*(5), 709-711. https://doi.org/10.1086/520514

Verma, S., Ziegler, K., Ananthula, P., Co, J. K. G., Frisque, R. J., Yanagihara, R., & Nerurkar, V. R. (2006). JC virus induces altered patterns of cellular gene expression : Interferon-inducible genes as major transcriptional targets. *Virology*, *345*(2), 457-467. https://doi.org/10.1016/j.virol.2005.10.012

Viallard, J.-F., Ellie, E., Lazaro, E., Lafon, M.-E., & Pellegrin, J.-L. (2005). JC virus meningitis in a patient with systemic lupus erythematosus. *Lupus*, *14*(12), 964-966. https://doi.org/10.1191/0961203305lu2229cr

Vu, D., Shah, T., Ansari, J., Naraghi, R., & Min, D. (2015). Efficacy of Intravenous Immunoglobulin in the Treatment of Persistent BK Viremia and BK Virus Nephropathy in Renal Transplant Recipients. *Transplantation Proceedings*, *47*(2), 394-398. https://doi.org/10.1016/j.transproceed.2015.01.012

Wacker, D., Wang, S., McCorvy, J. D., Betz, R. M., Venkatakrishnan, A. J., Levit, A., Lansu, K., Schools, Z. L., Che, T., Nichols, D. E., Shoichet, B. K., Dror, R. O., & Roth, B. L. (2017). Crystal Structure of an LSD-Bound Human Serotonin Receptor. *Cell*, *168*(3), 377-389.e12. https://doi.org/10.1016/j.cell.2016.12.033

Wadei, H. M., Rule, A. D., Lewin, M., Mahale, A. S., Khamash, H. A., Schwab, T. R., Gloor, J. M., Textor, S. C., Fidler, M. E., Lager, D. J., Larson, T. S., Stegall, M. D., Cosio, F. G., & Griffin, M. D. (2006). Kidney Transplant Function and Histological Clearance of Virus Following Diagnosis of Polyomavirus-Associated Nephropathy (PVAN). *American Journal of Transplantation*, *6*(5p1), 1025-1032. https://doi.org/10.1111/j.1600-6143.2006.01296.x

Walker, F. (1986). The biology and molecular biology of JC virus. *The Papovaviridae*, 327-377.

Wang, X., Li, J., Schowalter, R. M., Jiao, J., Buck, C. B., & You, J. (2012). Bromodomain Protein Brd4 Plays a Key Role in Merkel Cell Polyomavirus DNA Replication. *PLoS Pathogens*, *8*(11). https://doi.org/10.1371/journal.ppat.1003021

Weber, F., Goldmann, C., Krämer, M., Kaup, F. J., Pickhardt, M., Young, P., Petry, H., Weber, T., & Lüke, W. (2001). Cellular and humoral immune response in progressive multifocal leukoencephalopathy. *Annals of Neurology*, *49*(5), 636-642. https://doi.org/10.1002/ana.1004

Weigel-Kelley, K. A., Yoder, M. C., & Srivastava, A. (2003). α5β1 integrin as a cellular coreceptor for human parvovirus B19 : Requirement of functional activation of β1 integrin for viral entry. *Blood*, *102*(12), 3927-3933. https://doi.org/10.1182/blood-2003-05-1522

Weist, B. J. D., Schmueck, M., Fuehrer, H., Sattler, A., Reinke, P., & Babel, N. (2014). The role of CD4+ T cells in BKV-specific T cell immunity. *Medical Microbiology and Immunology*, *203*(6), 395-408. https://doi.org/10.1007/s00430-014-0348-z

Weist, B. J. D., Wehler, P., El Ahmad, L., Schmueck-Henneresse, M., Millward, J. M., Nienen, M., Neumann, A. U., Reinke, P., & Babel, N. (2015). A revised strategy for monitoring BKV-specific cellular immunity in kidney transplant patients. *Kidney International*, *88*(6), 1293-1303. https://doi.org/10.1038/ki.2015.215

Wilson, J. J., Lin, E., Pack, C. D., Frost, E. L., Hadley, A., Swimm, A. I., Wang, J., Dong, Y., Breeden, C. P., Kalman, D., Newell, K. A., & Lukacher, A. E. (2011). Gamma Interferon Controls Mouse Polyomavirus Infection In Vivo ▿. *Journal of Virology*, *85*(19), 10126-10134. https://doi.org/10.1128/JVI.00761-11

Wollebo, H. S., White, M. K., Gordon, J., Berger, J. R., & Khalili, K. (2015). Persistence and pathogenesis of the neurotropic polyomavirus JC. *Annals of Neurology*, *77*(4), 560-570. https://doi.org/10.1002/ana.24371

Wunderink, H. F., De Brouwer, C. S., Gard, L., De Fijter, J. W., Kroes, A. C. M., Rotmans, J. I., & Feltkamp, M. C. W. (2019). Source and Relevance of the BK Polyomavirus Genotype for Infection After Kidney Transplantation. *Open Forum Infectious Diseases*, *6*(3), ofz078. https://doi.org/10.1093/ofid/ofz078

Wunderink, H. F., van der Meijden, E., van der Blij-de Brouwer, C. S., Mallat, M. J. K., Haasnoot, G. W., van Zwet, E. W., Claas, E. C. J., de Fijter, J. W., Kroes, A. C. M., Arnold, F., Touzé, A., Claas, F. H. J., Rotmans, J. I., & Feltkamp, M. C. W. (2017). Pretransplantation Donor–Recipient Pair Seroreactivity Against BK Polyomavirus Predicts Viremia and Nephropathy After Kidney Transplantation. *American Journal of Transplantation*, *17*(1), 161-172. https://doi.org/10.1111/ajt.13880

Wüthrich, C., Dang, X., Westmoreland, S., McKay, J., Maheshwari, A., Anderson, M. P., Ropper, A. H., Viscidi, R. P., & Koralnik, I. J. (2009). Fulminant JC virus encephalopathy with productive infection of cortical pyramidal neurons. *Annals of neurology*, *65*(6), 742-748. https://doi.org/10.1002/ana.21619

Yanagihara, R., Nerurkar, V. R., Scheirich, I., Agostini, H. T., Mgone, C. S., Cui, X., Jobes, D. V., Cubitt, C. L., Ryschkewitsch, C. F., Hrdy, D. B., Friedlaender, J. S., & Stoner, G. L. (2002). JC Virus Genotypes in the Western Pacific Suggest Asian Mainland Relationships and Virus Association with Early Population Movements. *Human Biology*, *74*(3), 473-488. https://doi.org/10.1353/hub.2002.0037

Yang, J. F., & You, J. (2020). Regulation of Polyomavirus Transcription by Viral and Cellular Factors. *Viruses*, *12*(10), 1072. https://doi.org/10.3390/v12101072

Yogo, Y., Iida, T., Taguchi, F., Kitamura, T., & Aso, Y. (1991). Typing of human polyomavirus JC virus on the basis of restriction fragment length polymorphisms. *Journal of Clinical Microbiology*, *29*(10), 2130-2138.

Yogo, Y., Sugimoto, C., Zheng, H.-Y., Ikegaya, H., Takasaka, T., & Kitamura, T. (2004). JC virus genotyping offers a new paradigm in the study of human populations. *Reviews in Medical Virology*, *14*(3), 179-191. https://doi.org/10.1002/rmv.428

Zhao, L., Marciano, A. T., Rivet, C. R., & Imperiale, M. J. (2016). Caveolin- and clathrin-independent entry of BKPyV into primary human proximal tubule epithelial cells. *Virology*, *492*, 66-72. https://doi.org/10.1016/j.virol.2016.02.007

Zheng, H.-Y., Nishimoto, Y., Chen, Q., Hasegawa, M., Zhong, S., Ikegaya, H., Ohno, N., Sugimoto, C., Takasaka, T., Kitamura, T., & Yogo, Y. (2007). Relationships between BK virus lineages and human populations. *Microbes and Infection*, *9*(2), 204-213. https://doi.org/10.1016/j.micinf.2006.11.008

Zhong, S., Randhawa, P. S., Ikegaya, H., Chen, Q., Zheng, H.-Y., Suzuki, M., Takeuchi, T., Shibuya, A., Kitamura, T., & Yogo, Y. (2009). Distribution patterns of BK polyomavirus (BKV) subtypes and subgroups in American, European and Asian populations suggest co-migration of BKV and the human race. *Journal of General Virology*, *90*(1), 144-152. https://doi.org/10.1099/vir.0.83611-0

Zou, W., & Imperiale, M. J. (2021). Biology of Polyomavirus miRNA. In *Frontiers in Microbiology* (Vol. 12). Frontiers Media S.A. https://doi.org/10.3389/fmicb.2021.662892

zur Hausen, H. (2008). Novel human polyomaviruses—Re-emergence of a well known virus family as possible human carcinogens. *International Journal of Cancer*, *123*(2), 247-250. https://doi.org/10.1002/ijc.23620

Figure design:

- Biorender.com
- Schrödinger, L., & DeLano, W. (2020). PyMOL. Retrieved from http://www.pymol.org/pymol
- GraphPad Prism 8; www.graphpad.com
- FlowJo™ Software Windows: FlowJo Version X. Ashland, OR: Becton, Dickinson and Company; 2021

Figures 14 and 16 were generated by the Glycoscience Laboratory of Imperial college.
Figures 28 and 29 were generated by the plateform IMPACT.

Résumé

Les polyomavirus BK (BKPyV) et JC (JCPyV) sont des virus infectant l'Homme, d'un diamètre de 40-45 nm et composés d'un génome circulaire d'ADN double brin. Leur capside est composée de 72 pentamères de protéines VP1 associés à des protéines VP2 ou VP3 en interne. Ce sont, via les protéines VP1, que les polyomavirus interagissent avec leur hôte. Cette protéine possède de nombreuses boucles en surface, dont la boucle BC, qui permettent l'interaction avec les récepteurs de type glycanes sialylés. En effet, le BKPyV interagit avec les gangliosides de la série b, notamment GT1b et GD1b alors que le JCPyV interagit avec l'oligosaccharide de la lacto-série c, LSTc. Les interactions se font au niveau de la partie sialylée : le motif di-sialylé des gangliosides de la série b pour le BKPyV et l'acide sialique en α2-6 pour de LSTc pour le JCPyV. Ce dernier a aussi été décrit pour interagir avec les récepteurs de la sérotonine 5-HT2 pour entrer dans les cellules, utilisant ainsi LSTc comme récepteur d'attachement.

Ces virus sont des virus opportunistes dont l'infection se produit de façon asymptomatique durant l'enfance. Plus de 80% de la population mondiale est séropositive pour le BKPyV et entre 30-70% pour le JCPyV. Malgré une infection asymptomatique, ces virus restent latents dans les individus sains, surtout au niveau de l'appareil urinaire et rénal mais aussi au niveau du cerveau et des tissus lymphoïdes pour le JCPyV. Ce sont dans des contextes d'immunosuppression que la réactivation de ces virus peut avoir lieu causant différentes pathologies. La réactivation du BKPyV est fréquente pour les patients transplantés du rein dûe à la prise d'immunosuppresseurs, causant ainsi des néphropathies ou plus rarement des sténoses urétérales. Les néphropathies associées au BKPyV (BKPyVAN) sont initialement soupçonnées par la présence d'une virurie et virémie élevée et uniquement le diagnostic par biopsie permet un diagnostic définitif. Dans certains cas, la réactivation du BKPyV peut aller jusqu'à un dysfonctionnement sérieux du greffon voire la perte de celui-ci. La stratégie thérapeutique est de rétablir l'immunité en modulant le traitement immunosuppresseur du patient. Dans un contexte de transplantation de cellules hématopoïétiques, la réactivation du BKPyV a aussi été associée au développement de cystite hémorragique. Dans un contexte du syndrome d'immunodéficience acquise (SIDA), de thérapies immunomodulatrices impliquant des anticorps monoclonaux, de troubles lymphoprolifératifs ou encore de transplantation rénale, le JCPyV peut causer plusieurs pathologies, dont principalement la leuco-encéphalopathie multifocale progressive (LMP). Cette pathologie affecte le cerveau

en induisant la démyélinisation de la substance blancheet peut induire de sérieuses séquelles ou même être fatale. D'autres pathologies affectant le cerveau comme la neuronopathie des cellules granulaires, des encéphalites ou des méningites ont également été associées à la réactivation du JCPyV. Dans de plus rares cas, le JCPyV peut induire lui aussi des néphropathies.

L'objectif principal de cette thèse est d'étudier les interactions entre les virus BKPyV et JCPyV et leurs récepteurs en combinant des études fonctionnelles et structurales. Trois projets ont été réalisés au cours de cette thèse : le premier se concentre sur l'étude du tropisme et de la structure de variants du BKPyV observés chez des patients transplantés rénaux ayant des infections persistantes, le deuxième consiste en l'étude encore une fois du tropisme et de la structure des quatre génotypes du BKPyV, et pour finir, le troisième projet a pour objectif de caractériser l'interaction entre le JCPyV et le récepteur de la sérotonine 5HT2RB.

Projet A : Étude du tropisme et de la structure de variant du BKPyV provenant de patients transplantés rénaux.

Au CHU de Nantes, nous disposons d'une cohorte de patients transplantés rénaux. Certains de ces patients ont des réactivations du BKPyV et parmi ceux-ci certains présentent des infections persistantes malgré la modulation du traitement immunosuppresseur. Chez ces patients, il a été observé une accumulation de mutations dans la protéine de capside VP1, en particulier au niveau de la boucle BC impliquée dans l'interaction avec les récepteurs. Des études préliminaires sur ces variants ont montré qu'ils avaient des profils infectieux divers sur deux lignées cellulaires rénales : les cellules rénales embryonnaires 293TT, et les cellules épithéliales rénales du tubule proximal immortalisées de la lignée RS. L'objectif de ce projet était donc de comprendre comment les mutations dans la protéine VP1 pouvaient influencer les interactions entre la capside et les gangliosides ainsi que d'observer au niveau moléculaire l'influence des mutations sur la structure de la protéine VP1.

Plusieurs variants ont été étudiés, en particulier les variants : E73Q, E73A, VQQ et N-Q du sous-type Ib2. Leurs profils infectieux ont révélé que les pseudovirus E73Q infecte autant que le WT les cellules 293TT alors que dans les cellules RS, ce variant infecte environ 10 fois mieux. En revanche pour N-Q, on observe une

diminution de l'infection dans les 293TT et une quasi-absence d'infection des cellules RS. Pour VQQ, on observe aussi une quasi-absence d'infection mais dans les cellules 293TT et une infection similaire à celle du WT est observée dans les RS. Pour E73A, l'infection est plus faible dans les 293TT et similaire au WT dans les RS. Afin de mieux comprendre les différents profils infectieux observés, nous avons effectué de la spectrométrie de masse sur les membranes des deux lignées cellulaires afin de connaître leur composition en gangliosides. Cette expérience, effectuée en collaboration avec l'Université de Lilles par Dr. Delannoy et Prof. Guerardel, a montré que les 293TT sont composés des gangliosides de la série a : GM2 et GM3 alors que les cellules RS ont en plus, le GD1a et des gangliosides de la série b : GD2 et GD3. De plus, ces différents profils infectieux nous ont amené(s) à tester si ces différents variants maintenaient leur capacité à interagir avec les acides sialiques, partie avec laquelle le virus WT interagit sur les gangliosides de la série b. Pour cela, j'ai effectué des expériences d'infections avec des pseudovirus sur les cellules 293TT ou RS traitées ou non avec la neuraminidase. Alors que les variants E73A, E73Q et VQQ se sont montrés assez dépendant de la présence d'acides sialiques pour une infection efficace, le variant N-Q semble ne pas avoir besoin d'acide sialique, en infectant correctement voire mieux les cellules 293TT en leur absence. Ceci indique donc la présence d'un autre récepteur sur ces cellules capable de supporter l'infection par le variant N-Q. Suite à ce résultat, nous avons quand tout de même étudié les interactions de ces variants avec les glycanes en particulier les gangliosides. Pour cela, nous avons étudié la fixation à ces composés de deux façons : par glycan array screening et expérience de fixation avec des Virus-like Particles (VLPs). Pour le glycan array screening, j'ai exprimé et purifié les différents pentamères de VP1 variants et WT avec leur histidine tag. Ensuite, j'ai envoyé ces pentamères au Glycoscience laboratory de Imperial Collège à Londres où une équipe dirigée par le Dr. Liu et le Prof. Feizi, ont analysé la fixation des différents pentamères de VP1 sur un array composé de plusieurs sondes représentant les différents gangliosides. Chaque variant a été incubé avec cet array et la fixation a été quantifiée via la fluorescence des anticorps ciblant les His tag des pentamères. Les résultats ont montré un profil attendu pour le WT avec fixation aux gangliosides GT1b et GD1b. En revanche pour les variants E73Q, E73A et VQQ, un profil de fixation plus large a été observé avec toujours une fixation aux gangliosides de la série b dont GT1b et GD1bmais aussi la fixation à des gangliosides de la série a : GD1a et GT1a. Pour le variant N-Q, aucune

fixation a aucun ganglioside n'a été observée confirmant ainsi nos observations faites via l'expérience d'infection en présence de neuraminidase. Cette technique étant assez artificielle, j'ai fait des expériences de fixation complémentaire afin de confirmer ces résultats. J'ai utilisé la lignée cellulaire LNCaP, dépourvue de gangliosides, à laquelle j'ai supplémenté différents gangliosides (GM1, GD3, GD1b, GT1b, GD1a ou GT1a). Ensuite, j'ai testé la fixation de VLPs fluorescentes via cytométrie en flux. Cette expérience faite avec des VLPs WT, VQQ et N-Q a permis de confirmer les résultats du glycan array screening. L'attachement d'un virus à un récepteur ne veut pas nécessairement dire que ce récepteur induit l'entrée du virus dans la cellule, c'est donc pour cela que j'ai aussi effectué des expériences d'infection,avec des PSVs, en utilisant le même principe du supplémentation de gangliosides surdeux lignées cellulaires : LNCaP et GM95 qui sont des cellules dépourvues de glycosphingolipides. Les résultats sont identiques dans les deux lignées cellulaires avec une meilleure infection dans les cellules GM95. Nous avons pu voir que le WT, E73Q et E73A sont capables d'infecter les cellules via GD1b. De plus, parmi les troisvariants capables d'interagir avec les gangliosides de la série a, seule E73Q semble infecter les cellules via GD1a, ce qui expliquerait donc sa capacité plus élevée à infecter les cellules RS exprimant à leur surface ce ganglioside. Le variant VQQ, malgré sa capacité à fixer multiples gangliosides de la série a et b, ne semble pas pouvoir infecter les cellules via ceux-ci. Pour le variant N-Q, nous avons pu confirmerencore une fois qu'aucune infection n'est induite via les gangliosides.

Après ces résultats fonctionnels, nous nous sommes intéressés à la structure de ces différents variants. Pour cela, j'ai résolu la structure des pentamères de VP1 par cristallographie à rayon X. La structure du variant E73Q ne présente aucune modification structurale comparée à celle du WT. En revanche, pour le variant E73A deux monomères de VP1 sur cinq présentent une conformation différente de la deuxième partie de la boucle BC là où la mutation est présente. Cette conformation est aussi observée pour tous les monomères de VP1 du variant VQQ, indiquant que l'acide aminé 73 est assez déterminant de l'orientation de la boucle BC, surtout si une mutation en position 72 est associée à la mutation de l'acide aminé 73. Cependant, ces changements structuraux sont situés assez loin du site de fixation des acides sialiques ce qui reste cohérent avec nos observations puisque ces variants maintiennent leur capacité de fixation aux gangliosides. Pour la structure du variant N-Q, aucun changement de conformation majeur n'est observable. Cependant, la

mutation de l'acide aminé 69 de la lysine à l'asparagine semble induire un encombrement stérique pouvant expliquer la perte d'interaction avec les acides sialiques observée chez le variant N-Q.

Cette étude nous a permis d'observer que les mutations dans la boucle BC peuvent avoir différents impacts sur le virus. Le variant N-Q a perdu la capacité d'interagir avec les acides sialiques à cause de la mutation de l'acide aminé 69 en asparagine. Cependant ce variant est toujours capable d'infecter les cellules 293TT indiquant donc qu'un autre récepteur est utilisé par ce variant. Pour ce qui est des autres variants, nous avons observé que E73A et VQQ avaient un changement de conformation de la boucle BC suite aux mutations et que ses deux variants étaient moins infectieux dans les cellules 293TT alors que le variant E73Q, qui n'a pas ce changement de conformation, infecte bien ces cellules. Donc, nous en avons déduit que le changement de conformation pourrait avoir un impact sur l'interaction des deux variants avec le potentiel récepteur inconnu ciblé par le variant N-Q, réduisant ainsi leur capacité d'infection dans les 293TT. En revanche pour E73Q, la mutation apporte une perte de charge qui semble induire un profil de fixation et d'infection plus large et nous avons donc pu conclure que la capacité d'infection de ce mutant supérieure à celle du WT dans les cellules RS est dû à son interaction avec le ganglioside GD1a présent sur ces cellules. Pour le variant VQQ, nous avons aussi pu observer qu'il garde sa capacité d'interagir avec les acides sialiques et nous avons même vu qu'il a un profil de fixation plus large que la WT. En revanche, ce variant ne semble pas pouvoir infecter les cellules via une interaction seulement avec les gangliosides.

J'ai aussi étudié, mais moins en détail, d'autres variants du gIb2 du virus ainsi que du gIVc2. Dans ces cas-là aussi, les mutations influencent le profil de fixation aux gangliosides avec des profils plus larges pour la plupart ou pour le cas de la mutation E73K que l'on trouve dans le gI et gIVc2. Ce variant présente un profil de fixation restreint au ganglioside GT1b ce qui pourrait être expliqué par le remplacement de la charge négative par une charge positive qui ainsi réduirait la spécificité de fixation de ce variant.

Projet B : Étude de tropisme et de la structure des différents génotypes du BKPyV

Le BKPyV est divisé en quatre génotypes : I, II, III et IV. Le génotype I étant, suivi du génotype IV, le plus représenté dans la population mondiale, alors que les

génotypes II et III sont retrouvés plus rarement. Ces génotypes se différencient surtout au niveau de leurs séquences au niveau de la boucle BC. Pour ce projet, que je réalise en collaboration avec Jasmine Freytag (IFIB, Tübingen), les objectifs étaient de voir si les différents génotypes ont un tropisme différent ainsi que de résoudre leur structure. Pour cela j'ai effectué des expériences similaires à celle du projet précédent, notamment, en utilisant la neuraminidase pour déterminer si les différents génotypes étaient dépendant ou non de la présence d'acide sialique pour l'infection. Alors que les génotypes I, II et III se sont révélés très dépendant de la présence d'acides sialiques à la surface des 293TT pour la fixation et l'infection, le génotype IV maintient 50% d'infection en l'absence d'acides sialiques, indiquant donc l'utilisation d'un autre récepteur pour induire supporter l'infection. J'ai aussi pu résoudre la structure de la protéine VP1 du génotype IV qui, en comparaison à la structure du génotype I, reste très similaire. L'ensemble du projet est encore en cours avec pour objectif d'effectuer aussi des analyses de la fixation au gangliosides via glycan array screening et d'obtenir les structures des deux autres génotypes.

Projet C : Caractérisation de l'interaction entre JCPyV et le récepteur de la sérotonine 5HT2RB.

Le JCPyV infecte les oligodendrocytes via la LSTc qui sert de récepteur d'attachement, et via les récepteurs de la sérotonine : 5HT2RA, B ou C, qui servent de récepteur d'entrée. L'objectif de ce projet était de caractériser l'interaction entre le virus et le récepteur 5HT2RB au travers d'expériences de fixation et d'études structurales. Afin de caractériser si le virus interagit via le pentamère de VP1 uniquement ou si l'interaction avec le récepteur nécessite l'interface de plusieurs pentamères, j'ai d'abord exprimé et purifié des pentamères de VP1 et des VLPs du JCPyV. Dans un premier temps, j'ai effectué des expériences d'ELISA afin de tester la fixation des pentamères et VLPs à des peptides synthétisés pour représenter les boucles extracellulaires du récepteur 5HTR2RB. Cependant, ces expériences n'ont pas été concluantes, sûrement parce que les peptides n'adoptent pas la même conformation que les boucles dans le récepteur et aussi peut-être parce que l'interaction requièrent plusieurs boucles. J'ai donc ensuite travaillé sur le récepteur entier. J'ai exprimé et purifié ce récepteur membranaire en faible quantité, cependant, je n'ai pas eu le temps de bien caractériser sa conformation et sa stabilité. Malgré

cela, des expériences de résonance plasmon de surface ont été tentées afin de quantifier une constante de dissociation entre le récepteur et le virus, soit sous forme de pentamère ou sous forme de VLPs. Cependant, ces expériences n'ont pas fonctionné sûrement à cause la qualité du récepteur. Ce projet avait pour but, après avoir montré comment le virus interagissait avec le récepteur, d'aboutir à une étude structurale afin de caractériser les acides aminés impliqués dans l'interaction. Si le pentamère était suffisant pour l'interaction avec le récepteur, nous aurions pu tenter de cristalliser le récepteur en phase lipidique cubique en interaction avec le pentamère de VP1. En revanche, si l'intégralité de la capside était nécessaire à l'interaction, nous aurions tenté de résoudre la structure du complexe par cryo-microscopie électronique.

Zusammenfassung

The following abstract was written with the help of Anne Beschorner.

BK- und JC-Polyomaviren sind doppelsträngig, zirkuläre DNA-Viren mit einem ikosaedrischen Kapsid, das hauptsächlich aus Pentameren des VP1-Proteins besteht. Diese opportunistischen Viren können unter immunsuppressiven Bedingungen reaktiviert werden und verursachen hauptsächlich BKPyV-assoziierte Nephropathie bei Nierentransplantationen oder progressive multifokale Leukoenzephalopathie im Falle einer JCPyV-Reaktivierung. Diese Arbeit konzentriert sich auf die Untersuchung der Interaktionen zwischen dem Virus und seinen Wirtsrezeptoren. Das erste Projekt zielt darauf ab, zu verstehen, wie Mutationen im VP1-Protein, die bei Empfängern von Nierentransplantaten während einer persistierenden BKPyV-Infektion häufig auftreten, die Struktur und den Tropismus des Virus beeinflussen. Durch funktionelle und strukturelle Studien konnten wir zwei unterschiedliche Funktionsmuster aufzeigen. Die N-Q-Variante verliert durch die Mutation der Aminosäure 69 die Fähigkeit, mit Sialinsäure zu interagieren, was darauf hindeutet, dass ein anderer Rezeptor verwendet wird, um die Infektion dieser Variante in 293TT-Zellen zu unterstützen. Andererseits weist die VQQ-Variante einen Loop-Switch auf, der durch Mutationen der Aminosäuren 72 und 73 verursacht wird, was uns zu der Annahme veranlasst, dass diese Variante die Interaktion mit dem unbekannten Rezeptor verliert und somit ihre schwache Infektiosität in 293TT-Zellen erklärt. Obwohl diese Variante ein breiteres Gangliosid-Bindungsprofil aufweist, infiziert sie nicht über die Ganglioside. Es wurden weitere Varianten untersucht, die ebenfalls unterschiedliche Gangliosid-Bindungsprofile und strukturelle Veränderungen aufweisen. Das zweite Projekt dieser Arbeit zielt ebenfalls auf die Untersuchung des Tropismus und der Struktur ab, in diesem Fall jedoch der verschiedenen Genotypen von BKPyV. Funktionelle Tests haben gezeigt, dass gI, II und III für die Infektion stark von Sialinsäuren abhängig sind, während 50 % der Infektion bei gIV verbleiben, was auch in diesem Fall darauf hindeutet, dass ein anderer Rezeptor für die Infektion verwendet wird. Die Strukturstudie des gIV-VP1-Pentamers ergab keine wesentlichen strukturellen Unterschiede im Vergleich zur gI-Struktur. Das dritte Projekt konzentrierte sich auf die Charakterisierung der Interaktion zwischen JCPyV und einem seiner Eintrittsrezeptoren: dem Serotoninrezeptor 5HTRB. JCPyV VP1-Pentamere und VLPs wurden exprimiert und gereinigt, ebenso wie 5HT2RB. Ziel war es, durch SPR-Messungen herauszufinden, ob das Virus nur über ein Pentamer mit dem Rezeptor interagiert oder die Schnittstelle mehrerer Pentamere benötigt. Die SPR-Messungen waren jedoch nicht schlüssig.

Annex - Review

viruses

MDPI

Review

Structural Insight into Non-Enveloped Virus Binding to Glycosaminoglycan Receptors: A Review

Marie N. Sorin [1,2,†], Jasmin Kuhn [1,†], Aleksandra C. Stasiak [1,†] and Thilo Stehle [1,3,*]

[1] Interfaculty Institute of Biochemistry, University of Tuebingen, 72076 Tuebingen, Germany; marie.sorin@univ-nantes.fr (M.N.S.); jasmin.kuhn@uni-tuebingen.de (J.K.); aleksandra.stasiak@uni-tuebingen.de (A.C.S.)
[2] Faculté de Médecine, Université de Nantes, Inserm, Centre de Recherche en Transplantation et Immunologie, UMR 1064, ITUN, F-44000 Nantes, France
[3] Department of Pediatrics, Vanderbilt University School of Medicine, Nashville, TN 37232, USA
* Correspondence: thilo.stehle@uni-tuebingen.de
† These authors contributed equally.

Abstract: Viruses are infectious agents that hijack the host cell machinery in order to replicate and generate progeny. Viral infection is initiated by attachment to host cell receptors, and typical viral receptors are cell-surface-borne molecules such as proteins or glycan structures. Sialylated glycans (glycans bearing sialic acids) and glycosaminoglycans (GAGs) represent major classes of carbohydrate receptors and have been implicated in facilitating viral entry for many viruses. As interactions between viruses and sialic acids have been extensively reviewed in the past, this review provides an overview of the current state of structural knowledge about interactions between non-enveloped human viruses and GAGs. We focus here on adeno-associated viruses, human papilloma viruses (HPVs), and polyomaviruses, as at least some structural information about the interactions of these viruses with GAGs is available. We also discuss the multivalent potential for GAG binding, highlighting the importance of charged interactions and positively charged amino acids at the binding sites, and point out challenges that remain in the f eld.

Keywords: viruses; glycans; glycosaminoglycans; glycovirology; non-enveloped viruses; structural biology

Citation: Sorin, M.N.; Kuhn, J.; Stasiak, A.C.; Stehle, T. Structural Insight into Non-Enveloped Virus Binding to Glycosaminoglycan Receptors: A Review. Viruses **2021**, 13, 800. https:/ / doi.org/ 10.3390/ v13050800

Academic Editor: Jacques Le Pendu

Received: 14 April 2021
Accepted: 26 April 2021
Published: 29 April 2021

1. Introduction

Viruses are infectious entities that require a living organism, a host, to support their replication. They can target any kind of organism, ranging from complex hosts such as animals or plants to microorganisms such as bacteria or archaea. Until now, more than 6500 types of viruses have been discovered, and more than 260 of these can infect humans [1]. Viruses are encoded by DNA or RNA genomes, which are packaged into and protected by a protein capsid. Enveloped viruses additionally contain a lipid bilayer shell that is derived from the host cell membrane, while non-enveloped viruses lack such a membrane envelope and are encased in a capsid protein shell.

In order to infect a host organism and replicate, specif c virus proteins interact with receptor molecules on the host cell surface. Among these receptors, carbohydrate-based structures, or glycans, are used by many viruses to infect cells [2]. Such glycans can be grouped into three major groups: structures that terminate in sialic acids (sialylated glycans), neutral structures that are based on histo-blood group antigens (HBGAs), and structures known as glycosaminoglycans (GAGs). These GAGs are long, linear, negatively charged polysaccharides with molecular weights ranging from 10 to 100 kilodaltons (kDa), and they can be divided into two main types: sulfated GAGs, including heparan sulfate (HS), heparin, chondroitin sulfate (CH), and dermatan sulfate (DS); and non-sulfated GAGs, including hyaluronic acid [3].

HS and heparin are both linear polysaccharides composed of repeating units of uronic acid linked to D-glucosamine. HS is ubiquitously found on the cell surface or on mammalian extracellular matrix proteins, where it is involved in multiple biological processes, while heparin is secreted by mast cells and is medically used as an anticoagulant. HS and heparin share the same backbone, which is comprised of uronic acid and D-glucosamine, where the uronic acid moiety can either be α-L-iduronic acid (IdoA) or β-D-glucuronic acid (GlcA). Both components of the polysaccharide can be modif ed by sulfatation, deacetylation, and epimerization during biosynthesis [4]. There are three main differences between heparin and HS: (i) The uronic acid in heparin is predominantly IdoA, while it is GlcA in HS. (ii) D-glucosamine is mainly N-sulfated in heparin, while it is N-acetylated in HS. (iii) Heparin is composed of at least 70–80% of Ido(2S)-(1→ 4)-GlcNS(6S) disaccharides, while in HS 40–60% of the disaccharide units are GlcA-(1→ 4)-D-glucosamine, either N-acetylated or N-sulfated. Taken together, these differences indicate that heparin carries more sulfatation, and therefore has a higher overall negative charge compared to HS [5]. Chondroitin sulfate is also a linear polysaccharide composed of repeated units of uronic acid and N-acetylgalactosamine (GalNAc). Similar to HS, CS is found on the cell surface and in the extracellular matrix, and is involved in diverse physiological processes [6]. Dermatan sulfate, also known as chondroitin sulfate B, is the main GAG expressed in skin tissue. DS is structurally close to CH because it is composed of GalNAc, but also to HS and heparin because of the presence of IdoA in the disaccharide repeating unit [7].

While several non-enveloped viruses have been found to use GAGs as their receptors (e.g., adenoviruses [8] and rhinoviruses [9]), these results have not necessarily been verif ed in vivo, and it remains unclear whether the reported receptor specif city is the result of cell culture adaptation or is also present in nature [10]. This review aims to provide an update on the structural work characterizing the interaction of non-enveloped viruses with sulfated glycosaminoglycans, especially heparin. Among the structural studies that will be discussed, only structures with a resolution better than 4 Å will be considered in detail, and primarily only ones where electron density maps for the ligands are publicly available and can be inspected to assess the quality of the ligand f tting.

2. Adeno-Associated Virus

Adeno-associated viruses (AAVs) are single-stranded DNA viruses, members of the family Parvoviridae, with a small genome of about 4.5 kilobases. They require the host cell to be infected by another virus, typically an adenovirus, for productive replication, and they are not associated with human pathology. Their signif cance in research is connected to their potential as gene delivery vectors, associated with, among others, their ability to transduce non-dividing cells and lack of pathogenicity. The AAV capsid is about 26 nm in diameter, composed of 60 subunits, and has T = 1 icosahedral symmetry (see Figure 1a) [11]. The three capsid proteins, VP1, VP2, and VP3, all share most of the C-terminal sequence. Compared with the other two proteins, about ten times more copies of VP3 are found in the capsid. All three proteins consist of a jelly roll β-barrel fold, with loops between the barrel strands containing most of the sequences that differ among AAV strains and that are mainly responsible for receptor binding [11]. The loops form the triple-capsomer peaks close to the threefold symmetry axis (Figure 1b)—a location where multiple residues associated with heparin binding cluster [12–14].

While heparan sulfate was long considered to be the primary receptor for AAVs, recent research suggests that this role is in fact performed by the adeno-associated virus receptor [15], with GAGs serving as lower-aff nity co-receptors of signif cance for attachment. Structural studies of GAG binding to AAV generally have suffered from diff culties in obtaining well-diffracting crystals of the virus–receptor complex, either by co-crystallization or soaking [16]. These diff culties have excluded X-ray crystallography as a method for the structural analysis of AAV–GAG complexes, and led to efforts of obtaining cryoelectron microscopy (cryoEM) structures instead.

Among the f rst structures of AAV–GAG complexes are two examples that were solved before the cryoEM "resolution revolution" [17], at lower resolutions of 18 Å [18] and 8 Å [19]. Both reports examined the structures of AAV type 2 in complex with heparin, and came to opposite conclusions, with the lower-resolution analysis postulating signif cant conformational shifts on GAG binding that were not observed in the higher-resolution structure. Additional studies of complexes of AAV-DJ (a mutant strain selected for resistance to most common human neutralizing antibodies, with a high capsid sequence similarity to AAV-2) at 5 Å [16] and 2.8 Å resolution [20] provided data that argue against a large conformational shift. In these cases, heparin analogues were used to mitigate the issues caused by multiple-site, asymmetric binding of the physiological ligand and to provide a clearer view of binding.

While the use of smaller, shorter GAG analogues such as fondaparinux (f ve sugar moieties) or sucrose octasulfate (SOS) is a promising approach to the problem of averaging out the non-icosahedral ligand density, the resulting structures do not provide high-resolution information on GAG binding to AAV. In the lower-resolution structure at 5 Å, the level of molecular details is low (as expected at this resolution), and while electron density for the ligand is visible, this density is largely globular and does not allow the assignment of specif c contacts. Unfortunately, this situation is not improved for the 2.8 Å structure, probably due to low occupancy of the ligand. The viral capsid density allows for a clear delineation of the main chain and most side chains of the amino acids, but the ligand electron density is not detailed enough to reliably place the ligand or to deduce much information about its conformation (see Figure 1c).

The most detailed structural information on GAG binding to AAV is provided not through structural analyses but mutational studies. The residues identif ed by these studies as necessary (or of importance) for heparin binding can then be mapped onto the capsid or capsomer structures, where they do localize in the proximity of ligand densities from structural studies. Thus, positively charged residues at the threefold peak, primarily arginines (R587 and R590 from one capsomer and R486 and R489 from another—see Figure 1e; residue numbering according to AAV-DJ sequence), have been shown to play an important role in the cell binding of AAV-2, since a loss in infectivity was seen after their mutation [12]. These residues, along with others, form a positively-charged patch coming downwards from the peak (Figure 1d). GAG binding is often mediated by positive charges on the protein, with positively charged residues forming ionic interactions with the sulfur groups, and this is where the GAG density is found in the structures. Structural and mutational studies of AAV-6, a strain which binds both HS and sialic acid, have also highlighted the threefold peak as the location of an HS binding site [13,14]. Given that GAG molecules can achieve signif cant lengths, it is possible that one chain would engage multiple sites on a single capsid, winding in the clefts between the peaks. This would serve to increase the binding aff nity and enhance the strength of the interaction, increasing the chance of entry.

Structural studies of AAV binding to GAGs form an interesting example of the challenges encountered in this f eld, and of characterizing interactions despite the unavailability of a high-resolution structure of the complex. Combining the high-resolution apostructures of AAV with extensive mutational data, an overview of the binding site locations and their residues has been obtained. A recent cryo-EM structure of AAV-DJ at a resolution below 1.6 Å [21], and a continuing interest in AAV as a gene therapy vector [22], shows this is an active f eld, both in structural biology and applied medicine; therefore, elucidating the details of AAV–GAG interactions at atomic (or near atomic) resolution would be an important development.

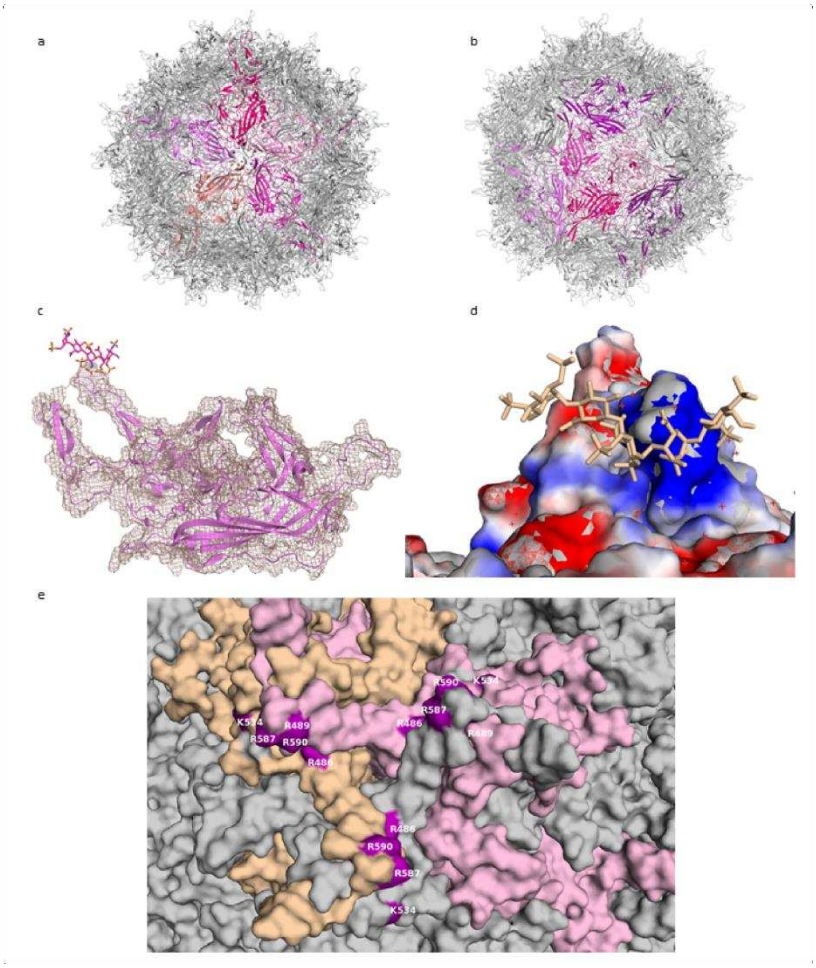

Figure 1. AAV-DJ capsid and its binding by GAG (PDB: 5UF6). (**a**) The viral capsid, with one constituting pentamer highlighted in shades of purple. (**b**) The viral capsid, with one constituting hexamer, and a threefold symmetry axis peak, highlighted in shades of purple. (**c**) A close-up of the density (salmon) for the structure at σ 1.5, showing that the capsid protein (purple) matches it closely and can be well resolved, while the ligand (raspberry) density is not visible at this level. (**d**) The charge distribution in the proximity of the threefold peak. Negatively charged residues are shown in red, positively charged in blue, ligand in wheat. (**e**) Close-up of the residues identif ed in mutational studies as contributing to binding HS, highlighted in purple. Capsomers in wheat, pink, and grey. Figures were created using PyMOL [23].

3. Human Papillomavirus

Human papillomaviruses (HPVs) are small, non-enveloped viruses containing a double-stranded DNA genome. Over 170 HPV types have been described, of which approximately 40 can be transmitted by sexual contacts, making HPV the most common sexually transmitted infection (STI) [24]. It is estimated that more than 80% of the world's population has at one point been in contact with HPV, although 90% of infections spontaneously resolve within the f rst two years and are often asymptomatic. However, some strains can cause warts or precancerous lesions (progressing to cancer), mainly of the genital or oropharyngeal tract. Strains HPV6 and HPV11 are the most common cause of genital warts, while 70% of cervical cancers are associated with HPV16 or HPV18 [25,26].

The HPV capsid is comprised of 360 copies of the major capsid protein L1 arranged in 72 capsomers of L1 pentamers, forming an icosahedral T = 7d geometry (Figure 2a,b). The minor capsid protein L2 is incorporated into the viral capsid in a not fully understood manner. The cell entry of HPV is mediated by binding of the viral capsid to cell surface proteoglycans as the primary receptors [27–29].

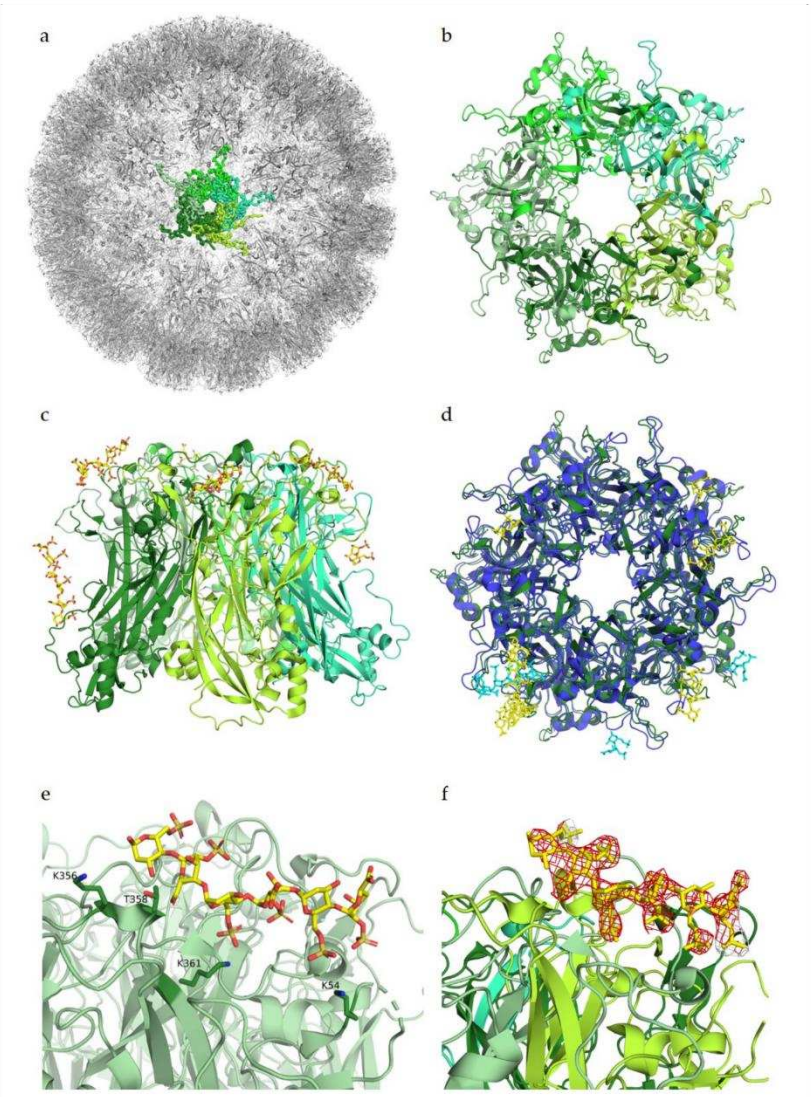

Figure 2. Glycan engagement of HPV16. (**a**) Capsid structure of HPV16 L1 pentamers (PDB ID 5KEP). L1 subunits of one pentamer are displayed in different shades of green. The highlighted pentamer is represented as a ribbon, the remaining capsid is depicted as cartoons. (**b**) Top view of a HPV16 L1 pentamer (PDB ID 5W1O). Subunits are displayed in cartoon representation and colored in different shades of green. (**c**) Side view of the pentamer. The heparin ligand is colored by atom type and represented with sticks in yellow. (**d**) Superposition of HPV16 L1 pentamer in green with its heparin ligand in yellow with HPV18 L1 pentamer (PDB ID 5W1X) in blue and its ligand in cyan. (**e**) Close-up view of one ligand binding site of HPV16. Ligand-binding residues K356, T358, K361, and K54 are represented as sticks. (**f**) Close-up view as in (**e**) of one ligand binding site with the negative F_o–F_c difference map of the ligand contoured at 3σ, colored in red. Figures were created using PyMOL [23].

Heparin binding assays identif ed largely positively charged peptide sequences at the C-terminus of L1, spanning amino acids G472 to L505, as the main interaction partners for GAGs [30]. Additional interaction studies determined similar residues of L1 as well as residues of L2 to bind to heparin, with binding constants in the high millimolar range [31]. However, both studies were only performed with small peptide fragments of both L1 and L2. Studies by Dasgupta et al. (2011) for the f rst time revealed structural details of the interactions between HPV and receptor candidates. Using co-crystallization experiments with heparin, these studies showed multiple heparan sulfate binding sites in the intact pentamers of both HPV16 and HPV18, demonstrating that these two strains display somewhat different oligosaccharide binding patterns (Figure 2d). The study identif ed key regions for ligand binding on surface loops (HI, FG, BC, EF, and a4) of the capsid protein L1, which are conserved between HPV16 and HPV18. These regions were determined to be located on the capsid-distal sides as well as on the capsid-proximal sides of the pentamer (Figure 2c). As more data are available for HPV16, we will mainly focus on HPV16 from here on. The crucial residues interacting with the negatively charged heparin in the HPV16 binding sites were identif ed as positively charged lysines that engage in charge–charge interactions with the sulfated groups of the receptors. These lysines form a mostly positively charged binding pocket in comparison to the highly negatively charged pore. For the two binding sites on the capsid-distal side of the pentamer, interaction partners were determined to be K54, K356, and K361 (Figure 2e), as well as K278 and N285 for a second binding site. Additionally, polar residues T358 and T266 were found to contact the glycan through polar interactions. To our knowledge, the characterized residues had not been identif ed before in binding assays as involved for glycan binding. Mutational experiments by Dasgupta et al. have conf rmed K278 and K361 as essential residues for HPV16 pseudoviral infection, while mutations of the other structurally identif ed binding partners did not signif cantly inf uence infectivity [32].

The structure of HPV16 in complex with heparin has a resolution of 2.8 Å, meaning that residues and ligands should be clearly visible in the electron density, as previously described for adeno-associated viruses. In the difference map (F_o–F_c map, from PDB ID 5W1O), no negative difference density can be observed for the L1 pentamers; however, for the complex structure, a large amount of negative electron density around the heparin ligand is visible (Figure 2f). This negative density indicates that the modelled ligand structure does not fully agree with the experimentally observed data, perhaps because of high f exibility of the glycan or low occupancy, as both would show density in the initial map but would display negative density after ref nement. Nevertheless, it is also possible that the glycan was placed incorrectly in the structure. Structural studies by Guan et al. (2017) identif ed a different heparan sulfate binding site, which overlaps with two of the previously identif ed binding sites [33]. However, no complex structure or difference maps are available for the newer study, and therefore cannot be considered for this review.

As already discussed for AAV complex structures, complex structures of HPV with heparin or HS published to date should be treated with caution, as the available electron density maps do not allow for unambiguous assignment of contacts between protein and ligand. It also becomes clear that f exibility and occupancy represent major challenges in structural elucidations of virus–GAG interactions.

4. Polyomavirus

The Polyomaviridae form a family of non-enveloped icosahedral dsDNA viruses. To date, fourteen human polyomaviruses have been identif ed. Infection mostly occurs during childhood, and the viruses typically persist in host cells asymptomatically. In the context of immunosuppression, polyomavirus family members can reactivate and lead to various diseases [34]. The BK (BKPyV) and JC (JCPyV) polyomaviruses were the f rst polyomaviruses to be discovered, and they induce polyomavirus-associated nephropathy and progressive multifocal leukoencephalopathy in immunocompromised patients, respectively [35,36]. The more recently discovered Merkel cell polyomavirus (MCPyV)

was found in Merkel cell carcinomas, and is the f rst conf rmed human oncovirus within the Polyomaviridae family [37]. Similar to papillomaviruses, polyomaviruses have a capsid composed of 72 pentameric capsomers (referred to as VP1 pentamers) with an icosahedral T = 7d symmetry. However, polyomaviruses are smaller, with a diameter of around 50 nanometers compared to 60 nanometers for papillomaviruses. Moreover, the structures of the L1 and VP1 differ signif cantly. VP1 capsomers have a barrel-shaped morphology while papillomavirus L1 capsomers are mushroom-like protrusions with star-shaped pentamers [38].

When initiating infection, many polyomaviruses use glycans terminating in the sialic acid N-acetyl neuraminic acid (Neu5Ac) as their receptors. Interactions are mediated through surface loops at the outer margin of the major capsid protein VP1, and structural information is available for many complexes of polyomavirus VP1 pentamers with their cognate receptors [39–45]. These analyses have revealed that polyomaviruses differ in their specif cities for sialylated glycan structures. For example, BKPyV binds to cells via sialylated structures found in b-series gangliosides, which carry two sialic acids on the inner galactose (Neu5Acα2-8Neu5Acα2-3Gal) (Figure 3b) [41]. On the other hand, JCPyV specif cally engages glycans carrying terminal α2,6-linked Neu5Ac in the context of the monosialylated lactoseries tetrasaccharide c (LSTc) glycan [45]. MCPyV binds to yet another type of sialylated glycan carrying a terminal Neu5Acα2-3Gal motif [40].

For some polyomaviruses, additional interactions with non-sialylated glycans have been reported to be required for cell entry. For example, MCPyV requires both GAGs and sialylated glycans for entry, and these interactions occur sequentially, with GAGs serving as the primary receptor [46]. BKPyV and JCPyV have also been proposed to bind GAGs [47]. This recent study showed only a small decrease in the cell attachment of wild-type JCPyV and BKPyV virus-like particles (VLPs) on cells producing non-sialylated or hyposialylated glycans [47]. This result indicates that these two viruses do not require sialylated glycans for initial binding to cells. Further work showed that simultaneous removal of GAGs and sialylated glycans drastically reduced the binding of those VLPs to cells. Taken together, the results of this study suggest that wild-type BK and JC viruses can interact with either GAGs or sialylated glycans for initial cell attachment [47].

In the case of BKPyV, a structural study has investigated interactions of this virus with GAGs, solving the structure of BKPyV virus-like particles via cryo-electron microscopy (cryoEM) at 3.8 Å resolution. As expected, the BKPyV capsid was found to consist of 72 pentamers of the major capsid protein VP1 arranged in T = 7d icosahedral symmetry (Figure 3a). Six distinct VP1 conformations, all sharing the β-sandwich jelly roll fold, were found within the asymmetric unit of the capsid. The C-terminal arms are well resolved, and the structure of the assembled VLP shows how they are extended into adjacent capsomers and maintain a stable capsid structure, similar to what has been observed for other polyomavirus family members [39,48]. A structure of BKPyV VLPs in complex with heparin was also determined at a resolution of 3.6 Å. No structural differences at the protein level were seen between this structure and the unliganded BKPyV structure, establishing that heparin binding does not induce a structural change of the capsid. However, electron density corresponding to heparin was not visible at high resolution, and difference maps calculated to identify potential binding sites had to be computed at lower resolution, yielding a rather imprecise representation of the BKPyV–heparin complex at only 8 Å resolution. Difference density was observed between capsomers as well as at the top of each capsomer (Figure 3c). Density in between pentamers cannot be associated with GAG binding with certainty. However, this site is positively charged, which would f t the observations made for other viruses where GAG binding sites are indeed positively charged. The density observed in the pore of the pentamers could be attributed to the effects of symmetry averaging, but the authors do not completely discount the idea of GAG binding to the pore [49].

A detailed study conducted in 2011 investigated MCPyV cellular tropism and found that this virus sequentially engages GAGs and sialylated glycans. Through multiple

binding and transduction assays, it was shown that the initial attachment of MCPyV to cells requires GAGs such as HS and CS. Particularly, N-sulfated and/ or 6-O-sulfated forms of HS are needed for infectious entry of the virus [46].

Structural information on GAG interactions with MCPyV is currently limited to a study by Bayer et al., which analyzed the binding of different GAGs to MCPyV particles and isolated VP1 capsomers with saturation transfer difference nuclear magnetic resonance spectroscopy (STD NMR). Interestingly, it was found that isolated, unassembled VP1 pentamers did not bind any of the tested GAGs, while the assembled virus capsid gave a strong binding signal. Isolated VP1 pentamers are thus not able to establish interactions with GAGs, in contrast to the interactions with sialylated glycans, which were analyzed using VP1 pentamers. Additional STD NMR experiments showed that MCPyV VLPs were able to bind HS-derived disaccharide, heparin-derived octosaccharide, DS-derived hexasaccharide, as well as the HS-derived pentasaccharide Arixtra(fondaparinux). Based on these observations, it is clear that MCPyV can bind a broad range of GAGs, and that the presence of sulfatation seems to be essential for interaction. Most importantly, GAG binding by MCPyV requires more than one VP1 pentamer, suggesting that the GAG binding sites most likely lie in the recessions that separate individual VP1 pentamers. However, attempts to visualize this interaction by solving the structure of MCPyV VLPs with GAGs through crystal soaking or cryoEM studies were not conclusive [50].

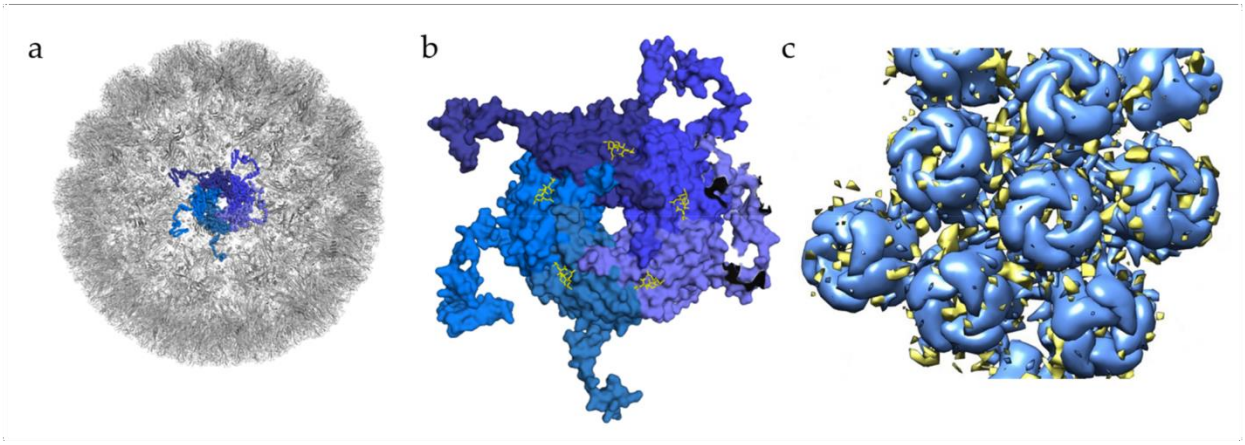

Figure 3. Glycan engagement of BKPyV. (**a**) Capsid structure of BKPyV (PDB ID 6ESB). The capsid is represented in the gray cartoon, except for the highlighted pentamer, where VP1 monomers are displayed as ribbons in different shades of blue. (**b**) Top view of BKPyV VP1 pentamers in interaction with GT1b. The pentamer is displayed as a surface colored in different shades of blue for each subunit. The double sialic acid part of GT1b is represented as yellow sticks. (**c**) Surface representation of BKPyV VP1 pentamers, in blue, associated with the difference map for heparin, in yellow (generated through subtraction of the unliganded VLP map (EMD-3946) from the heparin-VLP map (EMD-3945)). Figures were created using PyMOL [23] and Chimera [51].

5. Conclusions

In this review, we surveyed the available structural data on the binding of GAGs to non-enveloped viruses. It is clear that GAGs are exceedingly important glycans that play key roles in the entry processes of many viruses, including several that are relevant to human health. However, reliable and detailed structural information about contacts between GAGs and virus capsid proteins is essentially non-existent. More than anything, our review has therefore highlighted the challenges that hamper structural studies of GAG receptor binding to viruses. Crystallographic methods are in many cases unsuitable, primarily due to the diff culty of obtaining crystals—particularly with asymmetric, heterogeneous molecules such as HS. This moves the focus to cryo-EM. While it is developing rapidly, this method does not yet necessarily match crystallography's resolution and suffers from

a paucity of reliable metrics for assessing structure quality, particularly because of the variety of workf ows applied for data processing, which can signif cantly inf uence the result. Perhaps more importantly, in the case of virus–GAG interactions, the icosahedral symmetry imposed during processing can result in the averaging out or weakening of the signal of the non-icosahedrally symmetrical ligand. Issues with ligand heterogeneity, and ligand binding to multiple sites on the same capsid also increase this challenge, further lowering the level of detail that can be resolved.

With the continuously increasing quality of cryoEM data and the development of new approaches to data processing, particularly algorithms that allow for non-icosahedral symmetry within a primarily icosahedral structure [52], these challenges can be addressed in the future. Using this approach, one could, for example, visualize longer and heterogeneous ligands that do not adhere to the rules of icosahedral symmetry when binding to virus capsids. Any detailed structural information would drastically increase our understanding of structural mechanisms of virus–GAG binding—an aspect of glycovirology that remains to be more fully explored.

Author Contributions: Conceptualization, M.N.S., J.K., and A.C.S.; writing—original draft preparation, M.N.S., J.K., A.C.S., and T.S.; visualization, M.N.S., J.K., and A.C.S.; supervision, T.S. All authors have read and agreed to the published version of the manuscript.

Funding: M.N.S. was funded by Ministère Français de l'Enseignement Supérieur, de la Recherche et de l´Innovation through l´Université de Nantes as well as the Deutscher Akademischer Austauschdienst and Deutsch-Französische Hochschule; J.K. was funded by the German Research Foundation (Deutsche Forschungsgemeinschaft, DFG), grant number FOR2327; and A.C.S. was funded by Viral and Bacterial Adhesin Network Training Innovative Training Network, part of the European Union's Horizon 2020 Research and Innovation Programme under the Marie Skłodowska-Curie Grant Agreement No. 765042.

Acknowledgments: Molecular graphics and analyses were performed with UCSF Chimera, developed by the Resource for Biocomputing, Visualization, and Informatics at the University of California, San Francisco, with support from NIH P41-GM103311. We apologize to our many colleagues whose work could not be discussed or cited here.

Conf icts of Interest: The authors declare no conf ict of interest.

References

1. Lefkowitz, E.J.; Dempsey, D.M.; Hendrickson, R.C.; Orton, R.J.; Siddell, S.G.; Smith, D.B. Virus taxonomy: The database of the International Committee on Taxonomy of Viruses (ICTV). Nucleic Acids Res. **2018**, 46, D708–D717. [CrossRef] [PubMed]
2. Suenaga, T.; Arase, H. Viral Interactions with Glycans. Glycosci. Biol. Med. **2014**, 785, 785–794.
3. Gandhi, N.S.; Mancera, R.L. The Structure of Glycosaminoglycans and their Interactions with Proteins. Chem. Biol. Drug Des. **2008**, 72, 455–482. [CrossRef] [PubMed]
4. Rabenstein, D.L. Heparin and heparan sulfate: Structure and function. Nat. Prod. Rep. **2002**, 19, 312–331. [CrossRef]
5. Gallagher, J.T.; Walker, A. Molecular distinctions between heparan sulphate and heparin. Analysis of sulphation patterns indicates that heparan sulphate and heparin are separate families of N-sulphated polysaccharides. Biochem. J. **1985**, 230, 665–674. [CrossRef]
6. Mikami, T.; Kitagawa, H. Biosynthesis and function of chondroitin sulfate. Biochim. Biophys. Acta (BBA) Gen. Subj. **2013**, 1830, 4719–4733. [CrossRef]
7. Trowbridge, J.M.; Gallo, R.L. Dermatan sulfate: New functions from an old glycosaminoglycan. Glycobiology **2002**, 12, 117R–125R. [CrossRef]
8. Dechecchi, M.C.; Melotti, P.; Bonizzato, A.; Santacatterina, M.; Chilosi, M.; Cabrini, G. Heparan Sulfate Glycosaminoglycans Are Receptors Suff cient To Mediate the Initial Binding of Adenovirus Types 2 and 5. J. Virol. **2001**, 75, 8772–8780. [CrossRef]
9. Khan, A.G.; Pichler, J.; Rosemann, A.; Blaas, D. Human Rhinovirus Type 54 Infection via Heparan Sulfate Is Less Eff cient and Strictly Dependent on Low Endosomal pH. J. Virol. **2007**, 81, 4625–4632. [CrossRef]
10. Cagno, V.; Tseligka, E.D.; Jones, S.T.; Tapparel, C. Heparan Sulfate Proteoglycans and Viral Attachment: True Receptors or Adaptation Bias? Viruses **2019**, 11, 596. [CrossRef]
11. Xie, Q.; Bu, W.; Bhatia, S.; Hare, J.; Somasundaram, T.; Azzi, A.; Chapman, M.S. The atomic structure of adeno-associated virus (AAV-2), a vector for human gene therapy. Proc. Natl. Acad. Sci. USA **2002**, 99, 10405–10410. [CrossRef]
12. Kern, A.; Schmidt, K.; Leder, C.; Müller, O.J.; Wobus, C.E.; Bettinger, K.; Von Der Lieth, C.W.; King, J.A.; Kleinschmidt, J.A. Identif cation of a Heparin-Binding Motif on Adeno-Associated Virus Type 2 Capsids. J. Virol. **2003**, 77, 11072–11081. [CrossRef]

13. Ng, R.; Govindasamy, L.; Gurda, B.L.; McKenna, R.; Kozyreva, O.G.; Samulski, R.J.; Parent, K.N.; Baker, T.S.; Agbandje-McKenna, M. Structural Characterization of the Dual Glycan Binding Adeno-Associated Virus Serotype 6. J. Virol. **2010**, 84, 12945–12957. [CrossRef]
14. Xie, Q.; Lerch, T.F.; Meyer, N.L.; Chapman, M.S. Structure–function analysis of receptor-binding in adeno-associated virus serotype 6 (AAV-6). Virology **2011**, 420, 10–19. [CrossRef]
15. Pillay, S.; Meyer, N.L.; Puschnik, A.S.; Davulcu, O.; Diep, J.; Ishikawa, Y.; Jae, L.T.; Wosen, J.E.; Nagamine, C.M.; Chapman, M.S.; et al. An essential receptor for adeno-associated virus infection. Nat. Cell Biol. **2016**, 530, 108–112. [CrossRef]
16. Xie, Q.; Spilman, M.; Meyer, N.L.; Lerch, T.F.; Stagg, S.M.; Chapman, M.S. Electron microscopy analysis of a disaccharide analog complex reveals receptor interactions of adeno-associated virus. J. Struct. Biol. **2013**, 184, 129–135. [CrossRef]
17. Hurtley, S.M. Continuing the resolution revolution. Science **2018**, 360, 280–282. [CrossRef]
18. Levy, H.C.; Bowman, V.D.; Govindasamy, L.; McKenna, R.; Nash, K.; Warrington, K.; Chen, W.; Muzyczka, N.; Yan, X.; Baker, T.S.; et al. Heparin binding induces conformational changes in Adeno-associated virus serotype 2. J. Struct. Biol. **2009**, 165, 146–156. [CrossRef]
19. O'Donnell, J.; Taylor, K.A.; Chapman, M.S. Adeno-associated virus-2 and its primary cellular receptor—Cryo-EM structure of a heparin complex. Virology **2009**, 385, 434–443. [CrossRef]
20. Xie, Q.; Spear, J.M.; Noble, A.J.; Sousa, D.R.; Meyer, N.L.; Davulcu, O.; Zhang, F.; Linhardt, R.J.; Stagg, S.M.; Chapman, M.S. The 2.8 Å Electron Microscopy Structure of Adeno-Associated Virus-DJ Bound by a Heparinoid Pentasaccharide. Mol. Ther. Methods Clin. Dev. **2017**, 5, 1–12. [CrossRef]
21. Xie, Q.; Yoshioka, C.K.; Chapman, M.S. Adeno-Associated Virus (AAV-DJ)—Cryo-EM Structure at 1.56 Å Resolution. Viruses **2020**, 12, 1194. [CrossRef] [PubMed]
22. Wang, D.; Tai, P.W.L.; Gao, G. Adeno-associated virus vector as a platform for gene therapy delivery. Nat. Rev. Drug Discov. **2019**, 18, 358–378. [CrossRef] [PubMed]
23. Schrödinger, L.L.C. The {PyMOL} Molecular Graphics System, Version~1.8. 2015. Available online: https:/ / pymol.org/ 2/ (accessed on 14 April 2021).
24. Bzhalava, D.; Guan, P.; Franceschi, S.; Dillner, J.; Clifford, G. A systematic review of the prevalence of mucosal and cutaneous human papillomavirus types. Virology **2013**, 445, 224–231. [CrossRef]
25. Lei, J.; Ploner, A.; Elfström, K.M.; Wang, J.; Roth, A.; Fang, F.; Sundström, K.; Dillner, J.; Sparén, P. HPV Vaccination and the Risk of Invasive Cervical Cancer. N. Engl. J. Med. **2020**, 383, 1340–1348. [CrossRef]
26. Crosbie, E.J.; Einstein, M.H.; Franceschi, S.; Kitchener, H.C. Human papillomavirus and cervical cancer. Lancet **2013**, 382, 889–899. [CrossRef]
27. Shafti-Keramat, S.; Handisurya, A.; Kriehuber, E.; Meneguzzi, G.; Slupetzky, K.; Kirnbauer, R. Different Heparan Sulfate Proteoglycans Serve asCellular Receptors for HumanPapillomaviruses. J. Virol. **2003**, 77, 13125–13135. [CrossRef]
28. Buck, C.B.; Thompson, C.D.; Roberts, J.N.; Müller, M.; Lowy, D.R.; Schiller, J.T. Carrageenan Is a Potent Inhibitor of Papillomavirus Infection. PLOS Pathog. **2006**, 2, e69. [CrossRef] [PubMed]
29. Rommel, O.; Dillner, J.; Fligge, C.; Bergsdorf, C.; Wang, X.; Selinka, H.-C.; Sapp, M. Heparan sulfate proteoglycans interact exclusively with conformationally intact HPV L1 assemblies: Basis for a virus-like particle ELISA. J. Med. Virol. **2005**, 75, 114–121. [CrossRef]
30. Bousarghin, L.; Touzé, A.; Combita-Rojas, A.-L.; Coursaget, P. Positively charged sequences of human papillomavirus type 16 capsid proteins are suff cient to mediate gene transfer into target cells via the heparan sulfate receptor. J. Gen. Virol. **2003**, 84, 157–164. [CrossRef]
31. Sun, J.; Yu, J.S.; Jin, S.; Zha, X.; Wu, Y.; Yu, Z. Interaction of synthetic HPV-16 capsid peptides with heparin: Thermodynamic parameters and binding mechanism. J. Phys. Chem. B **2010**, 114, 9854–9861. [CrossRef]
32. Dasgupta, J.; Bienkowska-Haba, M.; Ortega, M.E.; Patel, H.D.; Bodevin, S.; Spillmann, D.; Bishop, B.; Sapp, M.; Chen, X.S. Structural Basis of Oligosaccharide Receptor Recognition by Human Papillomavirus. J. Biol. Chem. **2011**, 286, 2617–2624. [CrossRef]
33. Guan, J.; Bywaters, S.M.; Brendle, S.A.; Ashley, R.E.; Makhov, A.M.; Conway, J.F.; Christensen, N.D.; Hafenstein, S. Cryoelectron Microscopy Maps of Human Papillomavirus 16 Reveal L2 Densities and Heparin Binding Site. Structure **2017**, 25, 253–263. [CrossRef]
34. Maginnis, M.S. Human Polyomaviruses (Papillomaviridae). In Encyclopedia of Virology, 4th ed.; Bamford, D.H., Zuckerman, M., Eds.; Academic Press: Oxford, UK, 2021; pp. 518–527.
35. Hirsch, H.H. Polyomavirus BK nephropathy: A (re-)emerging complication in renal transplantation. Am. J. Transplant. **2002**, 2, 25–30. [CrossRef]
36. Padgett, B.L.; Walker, D.L.; ZuRhein, G.M.; Eckroade, R.J.; Dessel, B.H. Cultivation of papova-like virus from human brain with progressive multifocal leucoencephalopathy. Lancet **1971**, 1, 1257–1260. [CrossRef]
37. Feng, H.; Shuda, M.; Chang, Y.; Moore, P.S. Clonal Integration of a Polyomavirus in Human Merkel Cell Carcinoma. Science **2008**, 319, 1096–1100. [CrossRef]
38. Belnap, D.M.; Olson, N.H.; Cladel, N.M.; Newcomb, W.W.; Brown, J.C.; Kreider, J.W.; Christensen, N.D.; Baker, T.S. Conserved Features in Papillomavirus and Polyomavirus Capsids. J. Mol. Biol. **1996**, 259, 249–263. [CrossRef]

39. Stehle, T.; Yan, Y.; Benjamin, T.L.; Harrison, S.C. Structure of murine polyomavirus complexed with an oligosaccharide receptor fragment. Nat. Cell Biol. **1994**, 369, 160–163. [CrossRef]
40. Neu, U.; Hengel, H.; Blaum, B.S.; Schowalter, R.M.; Macejak, D.; Gilbert, M.; Wakarchuk, W.W.; Imamura, A.; Ando, H.; Kiso, M.; et al. Structures of Merkel Cell Polyomavirus VP1 Complexes Def ne a Sialic Acid Binding Site Required for Infection. PLOS Pathog. **2012**, 8, e1002738. [CrossRef]
41. Neu, U.; Allen, S.-A.A.; Blaum, B.S.; Liu, Y.; Frank, M.; Palma, A.S.; Ströh, L.J.; Feizi, T.; Peters, T.; Atwood, W.J.; et al. A Structure-Guided Mutation in the Major Capsid Protein Retargets BK Polyomavirus. PLoS Pathog. **2013**, 9, e1003688. [CrossRef]
42. Khan, Z.M.; Liu, Y.; Neu, U.; Gilbert, M.; Ehlers, B.; Feizi, T.; Stehle, T. Crystallographic and glycan microarray analysis of human polyomavirus 9 VP1 identif es N-glycolyl neuraminic acid as a receptor candidate. J. Virol. **2014**, 88, 6100–6111. [CrossRef]
43. Ströh, L.J.; Gee, G.V.; Blaum, B.S.; Dugan, A.S.; Feltkamp, M.C.W.; Atwood, W.J.; Stehle, T. Trichodysplasia spinulosa-Associated Polyomavirus Uses a Displaced Binding Site on VP1 to Engage Sialylated Glycolipids. PLoS Pathog. **2015**, 11, e1005112. [CrossRef] [PubMed]
44. Ströh, L.J.; Rustmeier, N.H.; Blaum, B.S.; Botsch, J.; Rößler, P.; Wedekink, F.; Lipkin, W.I.; Mishra, N.; Stehle, T. Structural Basis and Evolution of Glycan Receptor Specif cities within the Polyomavirus Family. mBio **2020**, 11. [CrossRef] [PubMed]
45. Neu, U.; Maginnis, M.S.; Palma, A.S.; Ströh, L.J.; Nelson, C.D.; Feizi, T.; Atwood, W.J.; Stehle, T. Structure-Function Analysis of the Human JC Polyomavirus Establishes the LSTc Pentasaccharide as a Functional Receptor Motif. Cell Host Microbe **2010**, 8, 309–319. [CrossRef] [PubMed]
46. Schowalter, R.M.; Pastrana, D.V.; Buck, C.B. Glycosaminoglycans and sialylated glycans sequentially facilitate Merkel cell polyomavirus infectious entry. PLoS Pathog. **2011**, 7, e1002161. [CrossRef] [PubMed]
47. Geoghegan, E.M.; Pastrana, D.V.; Schowalter, R.M.; Ray, U.; Gao, W.; Ho, M.; Pauly, G.T.; Sigano, D.M.; Kaynor, C.; Cahir-McFarland, E.; et al. Infectious Entry and Neutralization of Pathogenic JC Polyomaviruses. Cell Rep. **2017**, 21, 1169–1179. [CrossRef]
48. Liddington, R.C.; Yan, Y.; Moulai, J.; Sahli, R.; Benjamin, T.L.; Harrison, S.C. Structure of simian virus 40 at 3.8-A resolution. Nature **1991**, 354, 278–284. [CrossRef] [PubMed]
49. Hurdiss, D.L.; Frank, M.; Snowden, J.S.; Macdonald, A.; Ranson, N.A. The Structure of an Infectious Human Polyomavirus and Its Interactions with Cellular Receptors. Structure **2018**, 26, 839–847. [CrossRef]
50. Bayer, N.J.; Januliene, D.; Zocher, G.; Stehle, T.; Moeller, A.; Blaum, B.S. Structure of Merkel Cell Polyomavirus Capsid and Interaction with Its Glycosaminoglycan Attachment Receptor. J. Virol. **2020**, 94, 1–17. [CrossRef]
51. Pettersen, E.F.; Goddard, T.D.; Huang, C.C.; Couch, G.S.; Greenblatt, D.M.; Meng, E.C.; Ferrin, T.E. UCSF Chimera—A visualization system for exploratory research and analysis. J. Comput. Chem. **2004**, 25, 1605–1612. [CrossRef]
52. Ilca, S.L.; Kotecha, A.; Sun, X.; Poranen, M.M.; Stuart, D.I.; Huiskonen, J.T. Localized reconstruction of subunits from electron cryomicroscopy images of macromolecular complexes. Nat. Commun. **2015**, 6, 4–11. [CrossRef] [PubMed]

DOCTORAT BIOLOGIE BRETAGNE SANTE LOIRE

Nantes Université

EBERHARD KARLS UNIVERSITÄT TÜBINGEN

Titre : Etudes structurales des interactions des Polyomavirus BK et JC avec leurs récepteurs

Mots clés : Polyomavirus, interaction, récepteurs, VP1, structure

Résumé : Les polyomavirus BK et JC sont des virus à ADN double brin circulaire dont la capside en forme d'icosaèdre est composée de pentamères de la protéine VP1. Ces virus opportunistes peuvent se réactiver dans des contextes d'immunosuppression et peuvent causer principalement, pour le BKPyV, des néphropathies chez les greffés du rein, et, pour JCPyV, la leuco-encéphalopathie multifocale progressive. Cette thèse a pour but d'étudier les interactions entre ces virus et leurs récepteurs. Le premier projet a pour but de comprendre comment les mutations dans la protéine VP1 du BKPyV, fréquemment observées chez des greffés du rein, influencent le tropisme et la structure du virus. Grâce à des études fonctionnelles et structurales, nous avons pu mettre en évidence deux fonctionnements différents pour deux variants. Le variant N-Q a perdu sa capacité à se fixer aux gangliosides à cause de la mutation de l'acide aminé 69, suggérant que ce variant utilise un autre récepteur pour infecter les cellules 293TT. En revanche, le variant VQQ a un changement de conformation au niveau de la boucle BC et des acides aminés 72 et 73 et, malgré sa capacité à fixer de nombreux gangliosides, ce variant n'est presque pas capable d'infecter les cellules 293TT. Ceci suggère donc que VQQ n'interagit pas avec le récepteur inconnu ciblé par le variant N-Q. De plus, malgré sa fixation à de nombreux gangliosides, le variant VQQ ne semble pas pouvoir infecter efficacement les cellules LNCaP ou GM95 supplémentées. Le deuxième projet de cette thèse a pour but d'étudier le tropisme et la structure des différents génotypes du BKPyV. Les études fonctionnelles ont permis de montrer que les génotypes I, II et III étaient assez dépendent des acides sialiques pour l'infection alors que le génotype IV maintient une capacité d'infection de 50% malgré l'absence d'acide sialiques, indiquant donc qu'un autre récepteur semble être utilisé pour l'infection. La structure du pentamère de VP1 du gIV ne révèle aucun changement majeur dans sa conformation comparé au gI. Enfin, le troisième projet se focalise sur la caractérisation de l'interaction entre le JCPyV et un de ses récepteurs d'entrée : le récepteur de la sérotonine 5HT2RB. Les pentamères de VP1 et des VLPs du JCPyV ont été purifiés ainsi que le récepteur 5HT2RB. L'objectif a ensuite été de faire du SPR afin de tester si le virus interagissait avec le récepteur via un pentamère uniquement ou à l'interface de multiples pentamères. Cependant, les résultats n'ont pas été concluants.

Title: Structural studies of BK and JC Polyomaviruses interactions with their receptors

Keywords: Polyomavirus, interaction, receptors, VP1, structure

Abstract: BK and JC Polyomaviruses are double-stranded DNA viruses with an icosahedral capsid mainly composed of pentamers of VP1 protein. These opportunistic viruses can reactivate in immunosuppressive contexts and mainly cause BKPyV associated nephropathy after kidney transplantation or progressive multifocal leukoencephalopathy in case of JCPyV reactivation. This thesis focuses on the study of interactions between the virus and its host receptors. The first project aimed to understand how mutations in the VP1 protein, frequently occurring in kidney graft recipients during persistent BKPyV infection, influence the structure and tropism of the virus. Through functional and structural studies, we were able to highlight two different functional patterns. The N-Q variant lost the ability to interact with sialic acid due to mutation of amino acid 69, but retained significant infectivity in 293TT cells, indicating that a currently unknown sialic acid-independent entry receptor is present on 293TT cells. On the other hand, the VQQ variant had an altered conformation of the BC2 loop caused by mutations of amino acids 72 and 73, and although it had broadened specificity for gangliosides, it was almost non-infectious in 293TT cells. This raises the possibility that VQQ does not interact with the putative sialic acid-independent entry receptor.
Moreover, despite displaying a broader ganglioside binding profile, the VQQ variant was not able to infect ganglioside-supplemented GM95 or LNCaP cells. Other variants were also studied, showing also different ganglioside binding profiles and structural changes.
The second project of the thesis aimed to study the tropism and the structure of the different BKPyV genotypes. Functional assays highlighted that gI, II and III are highly dependent on sialic acids for infection while 50% of infection remains for gIV, indicating once again that another receptor can be used for infection. Structural study of gIV VP1 pentamer revealed no major structural differences compared to gI. Finally, the third project focused on characterising the interaction between JCPyV and one of its entry receptors: the serotonin receptor 5HTRB. JCPyV VP1 pentamers and VLPs were expressed and purified as well as 5HT2RB. The aim was to perform SPR measurement to know whether the virus interacts with the receptor through a pentamer only or needs the interface of multiple pentamers. However, SPR measurements were not conclusive.